GUIDELINES FOR THE STABILIZATION OF BANKS USING THE FUNCTIONAL TRAITS OF ROOTS

Megan Carene van der Haar

A research report submitted to the Faculty of Engineering and the Built Environment, University of the Witwatersrand, in partial fulfilment of the requirements for the degree of Master of Science in Engineering.

Johannesburg, 2018

DECLARATION

I declare that this thesis is my own unaided work. It is being submitted to the Degree of Master of Science to the University of the Witwatersrand, Johannesburg. It has not been submitted before for any degree or examination to any other University.

………………………………………………

..28…day of ..August…., ..2018...

ABSTRACT

A decrease in riverbank stability results in accelerated changes in channel morphology, a loss of agricultural and natural lands, reduced water quality, possible movement of sediments and/or contaminants from surrounding lands into the river, and potential damage to property. Vegetation plays a critical role in stabilizing natural slopes. The purpose of this study was to determine the applicability of vegetation roots for the stabilization of South African riverbanks and quantify the effect of root reinforcement, specifically by means of root functional traits. The study focuses on South African riverbanks as there are limited studies on soil bioengineering for the South African environment. Further, there is a growing concern of riverbank failure in South Africa as expressed by the Water Research Commission. Numerical modelling using geotechnical software formed the method of research. A table was developed to provide scoping level guidance on the suitability of vegetation stabilization for various soil types, bank angles and bank heights for various flood conditions.

Results from transient finite element seepage analyses show that the input parameters are reliable within realistic ranges, but the saturated volumetric water content should be identified with accuracy in order for the guidelines presented to be used with greater confidence.

This report includes a thorough review of existing models that account for the effects of vegetation on bank stability. A limit equilibrium based model that accounts for the enhanced cohesion due to the presence of roots was proposed. A sensitivity analysis together with literature indicated that the most significant root functional traits are: root diameter, root density and root length. Results pertaining to the root functional traits that were able to stabilize appropriate banks were presented and the use demonstrated through hypothetical examples.

It was concluded that bank geometry, material permeability and material strength perform a significant role in riverbank stability and as a result loamy sand and gravel riverbanks are more suitable for vegetation stabilization.

DEDICATION

I dedicate this work and give special thanks to Michael Schrenk for supporting me throughout the past years and for providing the inspiration to finish the work.

ACKNOWLEDGEMENTS

"Those who hope in the Lord will renew their strength. They will soar on wings like eagles; they will run and not grow weary, they will walk and not be faint."

~ Isaiah 40:31

Gratitude is expressed to Doctor Liz Day for initiating the research problem and to the Water Research Commission for funding part of the study from which this thesis stemmed. Thanks to Anton Kirsten for providing guidance from the onset of this research and for arranging use of the SRK library. Alexia Stokes, Joanne Norris and Slobodan Mickovski are sincerely thanked for their enthusiastic responses to my persistent queries regarding SLIP4EX. Thanks also go to Doctor Rens van Beek for providing me with the SLIP4EX program. A great number of other individuals provided literature on the subject matter and helped refine my understanding of soil bioengineering. Although not specifically mentioned their contributions are greatly appreciated.

I would also like to acknowledge and thank my supervisors, Professor Chris James and Dr. Charles MacRobert for their guidance, patience and encouragement throughout my research.

Finally I thank my mother Carol-Ann Russon for her continuous support and encouragement.

CONTENTS

LIST OF FIGURES

LIST OF TABLES

LIST OF SYMBOLS

A	Area of soil occupied by roots, m^2
α	Inclination of the base of the soil slice to the horizontal, degrees
α_i	Root cross-sectional area, m^2
A_r	Total cross-sectional area of roots intersecting a soil profile, mm^2
a_{AEV}	Approximately the air-entry value of the soil, kPa
b	Width of soil slice
C	Soil cohesion, kPa
c'	Effective cohesion at the base of a slice of soil, kN/m^2
C_r	Increase in shear strength due to roots/root cohesion, kPa
C_T	Lag coefficient
C'_r	Effective cohesion at the base of a slice of soil with vegetation, kN/m^2
D	Mean root diameter, mm
D	Depth, m
D_{10}	Particle size below which 10% by mass are smaller in size, mm
D_{60}	Particle size below which 60% by mass are smaller in size, mm
D_w	Wind force, kN
F_f	Factor of safety with respect to force equilibrium
F_m	Factor of safety with respect to moment equilibrium
F_{max}	Maximum force needed to break the root, N
h	Hour
$H_{0.1L}$	Elevation height at 10% of the length of the watercourse, m
$H_{0.85L}$	Elevation height at 85% of the length of the watercourse, m
i	Root diameter class
K	Factor accounting for the decomposition of root tensile strength
km	Kilometre, $\mathrm{m} \times 10^3$
K_U	Factor for appropraite veld type
l	Length of the slip surface, m
L	Length of the longest stream to the catchment boundary, km
L_C	Length from the centroid of the catchment area to the catchment boundary, km
L_f	Length of the critical slip surface along the bank
L_i	Length of the *i*th soil slice
m	Parameter that is related to the residual water content
M	Metre

m^2	Square metres
m^3	Cubed metres
mm	Millimetre, $\mathrm{m} \times 10^{-3}$
m_v	Coefficient of volume compressibility
n	Parameter that controls the slope at the inflection point in the VWC function
N	Number of roots per square metre
n_i	Number of roots in a diameter class
Q	Discharge, m^3/s
Q_P	Peak discharge, m^3/s
RL	Total root length per soil depth class, m
S	Average slope of the longest stream
t	Time, hours
T	Available root force acting on the base of each slice of soil, kN
T_i	Root tensile strength in a root diameter class, MPa
T_L	Lag time, hours
T_n	Normal component of the root tensile strength, MPa
t_R	Mobilized tensile stress of root fibers per unit area of soil
T_r	Root tensile strength, MPa
T_{rd}	Available root force per square metre of soil, kN
T_{ru}	Ultimate root force per square metre across the slip plane,
T_t	Tangential component of the root tensile strength, MPa
u	Average water pressure on the base of a slice, kN/m^2
U_1	Water force on the left side of a slice, kN
U_2	Water force on the right side of a slice, kN
W	Total weight of a soil slice, kN
W_v	Total weight of a soil slice with vegetation, kN
X	Shear displacement, mm
α	Scale factor
β	Rate of strength decrease

β_w	Angle between the wind direction and the horizontal, degrees
τ	Soil shear strength, kPa
τ_P	Shear stress acting on the shear plane, kPa
τ_r	Shear strength of the soil reinforced by root, kPa
σ_n	Effective normal stress on the shear plane, MPa
σ_{rf}	Tensile strength at failure, MPa
σ_{rt}	Tensile strength of a root segment, MPa
Δh_w	Increase in average piezometric head at base of a slice, m
Δu_v	Change in water pressure due to vegetation, kN/m^2
ΔU_{1v}	Change in water force on the left side of a slice due to vegetation, kN
ΔU_{2v}	Change in water force on the right side of a slice due to vegetation, kN
θ	Angle of shear distortion in the shear zone, degrees
θ_r	Residual water content
θ_s	Saturated volumetric water content
θ_w	Volumetric water content
Φ'	Effective angle of friction at the base of a slice, degrees
Φ	Angle of internal friction, degrees
Φ_b	Angle of increase in strength due to the negative pore-water pressure, degrees
Ψ	Negative pore-water pressure, kPa

LIST OF ABBREVIATIONS

AEV	Air-Entry Value
CSRA	Committee of State Road Authorities
DWAF	Department of Water Affairs and Forestry
FBM	Fiber Bundle Model
FOS	Factor of safety
HRU	Hydrological Research Unit
KF	Hydraulic Conductivity Function
NSV	No suitability for vegetation stabilization
NV	No vegetation stabilization is required
RAR	Root Area Ratio
SDSS	Slope Decision Support System
SWCC	Soil-Water Characteristic Curve
UV	Use vegetation to stabilize bank
VWC	Volumetric Water Content

Chapter 1 Introduction

The loss of soil as a result of bank failure is one of the greatest environmental concerns affecting both agricultural and natural lands worldwide (Burylo et al., 2012; Abernethy and Rutherfurd, 1999). Riverbank failure occurs both naturally and through human impact. The natural process of riverbank failure may have favorable outcomes such as the formation of productive floodplains and alluvial terraces. Slope failure occurring on unstable rivers is of concern as it may lead to undesirable consequences such as a loss of agricultural and natural lands, reduced water quality, possible movement of sediments and/or contaminants from surrounding lands into the river, and potential damage to property.

Chen and Huang (2011) and Oya et al. (2015) identify the rapid drawdown of bank phreatic surfaces following flooding as one of the main potential causes of riverbank failure. Flood events may sustain high water levels in rivers for long periods of time. When water levels subsequently reduce rapidly and the pore pressure within the soil remains high, there is a decrease in the effective shear strength of the soil which may result in bank failure (Simon et al., 2000). Factors influencing this behaviour include the geometry of the riverbank, initial location of the phreatic surface, permeability of the material, duration of the flood and the rate of drawdown (Budhu and Gobin, 1995; Green, 1999; Garcia, 2004).

The two main classifications given to the structural measures of riverbank stabilization are soft engineering and hard engineering. Soft engineering approaches use vegetation or artificial material. Soft engineering may provide a natural, effective, visually appealing, inexpensive and environmentally beneficial solution to stabilizing riverbanks that have been degraded by soil erosion. Vegetation is environmentally suitable as it increases the site's biodiversity and acts as a filtration system that purifies runoff water. Hard engineering makes use of rubble, stone or concrete. These engineering solutions are the most expensive in riverbank protection design, but they have a low risk of failure (Kosiw et al., 2008). The wide range of advantages in the use of vegetation makes it a preferable option for bank stabilization. However, vegetation is not as much of a reliable solution to bank stabilization as hard engineering approaches as its impacts are complex and the risks implicit in its use are not fully understood (Wynn and Mostaghimi, 2006). It is important to decide which approach or combination of approaches would be the most effective for the site characteristics and realise that not all approaches are suitable for all failure states.

This study is focused on soft engineering through soil bioengineering (plant parts themselves serve as the main structural and mechanical elements in a slope protection system). Soil bioengineering is now an established practice in many parts of the world and it is a practical alternative to the more traditional soil stabilization methods such as geosynthetic reinforcement (Norris and Greenwood, 2006).

Burylo et al. (2012) highlight the use of vegetation in influencing the erosion rate of unstable slopes. Vegetation has been used since the 1960s in ecological restoration operations on degraded land. The approaches in planting or preserving vegetation for the purpose of erosion control have mainly focused on the effects of the above-ground biomass, whereas the effects of the below-ground biomass is often neglected or underestimated (De Baets et al., 2008). Slope vegetation reduces stream bank erosion above ground as shoots bend and cover the surface and reduce the velocity at the soil/water interface, and below ground, the roots mechanically restrain or hold soil particles in place (Gray and Sotir, 1996). Further, it is argued that root reinforcement is the most significant property for vegetation stabilization. This study focuses on the functional traits of root systems, particularly pertaining to the prevention of slip failure in river banks. The term ‘functional traits’ refers to the traits of roots and root systems that have a particular function with regards to their ability to stabilise soil and soil particles and thus enhance the stability of a river bank. The term will be widely used within this report to serve as the main descriptor for how the roots will be scientifically analysed for their ability to stabilize soils.”

1.1 The research problem

It has been shown that vegetation significantly contributes to bank stabilization. However, the effects are not fully understood as much of the information remains qualitative and more quantitative findings are necessary in order to allow slope stabilization by vegetation to be a more reliable option that can be argued as a viable alternative to hard engineering in some circumstances. There is a need to develop a guideline for decision makers pertaining to the stabilization of South African riverbanks and to establish the conditions under which vegetation would be appropriate and which species would be most suitable for the failure mechanism taking place.

1.2 The purpose and objectives of the study

The purpose of this study was to identify the circumstances whereby vegetation roots would be an appropriate bank stabilization method by analyzing how the various factors, including geometry of the riverbank, initial location of the phreatic surface, permeability of the material, duration of the flood and the rate of drawdown, affect the stability of riverbanks. The intention was to characterize the functional traits of roots in terms of analogous soil characteristics in slope stability modelling. The research was aimed at producing slope stability results that express the effect of vegetation root characteristics on the Factor of Safety against slip failures, thereby providing some guidance on which root functional traits or combination of root functional traits would be most suitable in preventing failure across a plane, following flooding and rapid drawdown at a particular site.

The decision-maker can then match plant species to the suitable functional traits that would mitigate slip failure on that plane.

The results produced, together with a thorough literature review on previously developed models and guidelines, were used to develop a guideline for the stabilizing of South African riverbanks using vegetation. The results of this research also contributed to a broader project developed by the Water Research Commission (WRC), published as "The Development of a Comprehensive Manual for River Rehabilitation in South Africa". The project was undertaken for the purpose of assisting land-users, communities and environmental protection practitioners in the practical rehabilitation of rivers in South Africa. Other important aspects of bank failure, such as bank undercutting and surface erosion, are addressed in this broader WRC document and these aspects are described in the background section of this report. Hypothetical examples are included in the study for the purpose of demonstrating how the guidelines could be used in determining the suitability of vegetation roots with regards to the stabilizing of South African river banks. In section 5.2 several sensitivity analyses were performed using GeoStudio programs, by varying the most significant seepage parameters used in the study and comparing the resultant factor of safety, thus adding to the reliability of the guidelines.

In order to use the guideline effectively, the decision maker requires a significant amount of information including soil strength criteria, soil permeability criteria, riverbank geometries, flood conditions, root functional traits and root strength properties. The quality of the results is directly dependent on the quality of the data used. Methods of obtaining the data are suggested in the methods and procedures of research as well as in the recommendations section of this report. Due to the complexity of obtaining certain parameters, further research would need to be carried out so that the data can be more readily available. The proposed research is defined in the recommendations section.

The resource costs associated with obtaining this data are validated due to the fact that there is significant value that lies in preserving river bank stability, as well as preserving bank stability using soft engineering approaches over harder approaches. Preserving bank stability and mitigating erosion is an important engineering consideration because of the fact that there are human and infrastructure risks that come about, in addition to the environmental degradation concerns which include the loss of arable land and the decline of water quality due to the ingress of contaminants. A brief review of the literature reveals that there are recent case studies in both India and South Africa which detail the risks that are present due to the ongoing recession of river banks. In 2014 an article was published by Das et al. (2014) describing in detail the detrimental effects that the erosion of the Brahmaputra, Ganges, Ghaghara, and Mahanadi river banks has been having on both the social and economic sectors of India. Das et al. (2014) highlights the fact that the foremost issue is the exacerbation of poverty due to the loss of land causing homelessness. Articles published in 2017 relevant to Randburg, South Africa, reveal that the constant erosion of suburban river banks threatens the structure of landowners' boundary walls and thus residents safety and security, as well as the safety of the public and children using the surrounding parks (Sonwabile, 2017, p. 3) and (Sonwabile, 2017, p. 1).

The social and economic impacts described above are likely to be most severe in developing countries, where the economic structure of the country is inferior to that of a developed country. These developing countries may not have sufficient budgets to tend to the widespread risks brought about by poor river and ecosystem management, and a larger portion of the population may be at risk of homelessness brought about by land erosion. It is due to this reasoning that the utilization of soft engineering approaches which are largely reliant on the implementation of readily available natural infrastructure such as grasses, trees and small plants, presents a significant opportunity. Once the complexity related to the analysis and obtaining of the data can be overcome, applying the techniques outlined within this report means that there may be an affordable and easily implementable solution available for developing countries. Enabling them to address river bank erosion and the risks that it brings about in a more rapid and sustainable manner.

1.3 Structure of report

This research report is structured into seven chapters, each along with several sections and subsections. The first chapter covers the purpose and scope of the study. The background to the study follows in the second chapter. This chapter shows the current level of understanding regarding bank failure mechanisms and how soil characteristics affect bank stability. The second chapter also defines functional root traits, outlines the effect of functional root traits on soils, and gives a brief description of how various models account for the effect of vegetation on slope stability. Chapter 3 focuses on the determination of the most significant root functional traits for the purpose of slope stability. Foremost, a case study was used to determine whether the results obtained from a previously developed program (SLIP4EX), to determine the stability from root functional traits, agrees with the results of a more robust program (SLOPE/W). The plant root functional traits from the case study were used as the control model for a sensitivity analysis using SLIP4EX, where each plant root functional trait was individually varied within reasonable ranges, obtained from literature, to determine which root functional traits contribute more significantly to slope stability. Chapter 4 covers the methods and procedures of the research, which includes how the significant root functional traits were modelled and analysed as well as how flood conditions for South African rivers were accounted for and analysed in the models. The results and analysis of the data is presented in Chapter 5 along with a sensitivity analysis of the soil-water parameters that were used in modelling the flood conditions, as a means of providing a level of measurable reliability of the program used and results obtained. Chapter 6 concludes the research and summarizes the main findings. Finally, chapter 7 presents potential future work and recommendations for researchers. A list of references is included and is followed by nine Appendices.

Chapter 2 Background

2.1 Bank failure

Bank retreat usually occurs from a combination of three processes: subaerial processes (processes occurring or forming on the earth's surface, this includes erosion), failure mechanisms, and other weakening processes (such as undercutting, which are not considered within the scope of this research) (Wynn and Mostaghimi, 2006; Thorne et al., 1996).

Subaerial processes reduce soil strength which may result in direct erosion (erosion processes that occur due to direct influences of weather and climate, such as rain and wind; this differs from fluvial erosion whereby fluvial refers specifically to processes within the river) and an increase in the banks vulnerability to fluvial erosion (removal of soil particles from the riverbed or bank toe by streamflow). Thorne et al. (1996) identify a range of erosion processes, where fluvial entrainment by water flowing parallel to the bank is considered to be the most significant. This category of erosion occurs when the water velocity is such that the shear stress applied on the bank is greater than the shear resistance of the bank material.

Failure mechanisms result in the collapse of part of, or the entire bank. The mechanisms responsible for bank collapse are shallow sliding, rotational slipping, slab failure, cantilever failure, dry granular flow and wet earth flow. Slip failure, a type of mass failure, is the failure mechanism of interest in this study. This type of failure is characterized by a slope movement in which a shear failure occurs along a specific surface or combination of surfaces in the failure mass. Slip failure may be analyzed by making use of limiting force equilibrium and limit analysis (Gray and Sotir, 1996).

Weakening processes reduce the erosion resistance and the geotechnical stability of banks by leaching, trampling by people or animals, destruction of riparian vegetation, mechanical damage, pore water pressure increases and desiccation.

2.1.1 Soil characteristics that affect bank stability against slope failure

The cohesion and friction angle material parameters are most commonly used to describe the shear strength of geotechnical materials and are defined in the Mohr-Coulomb failure criterion (Geo-Slope, 2007). The Mohr-Coulomb envelope is represented as a straight line on a shear strength versus normal strength plot of stresses on a failure plane (Fig. 2.1), where the intercept on the shear strength axis is the cohesion (c), the slope of the line is the angle of internal friction (Φ), and σ_n is the normal stress on the shear plane.

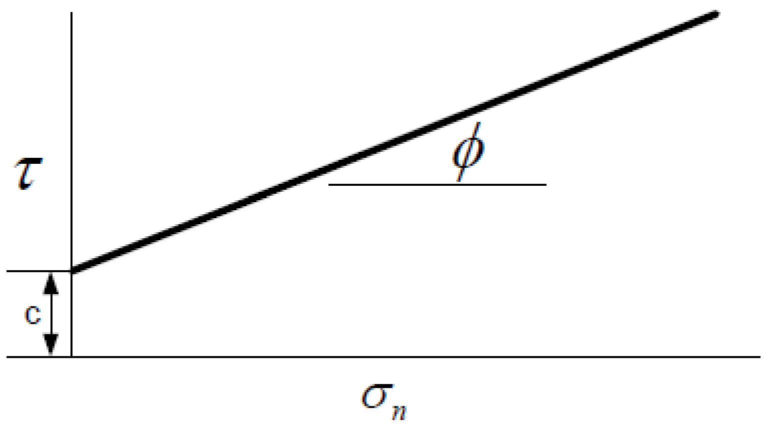

Figure 2.1: Graphical representation of the Mohr-Coulomb envelope

The angle of internal friction is the shear strength parameter used to describe the friction shear resistance of soils generated by the normal effective stress. For an infinite slope of cohesionless soil the stability of the slope can be described by the angle of internal friction where the slope is stable as long as the slope angle is equal to or less than the angle of internal friction (Palanikumar, 2013).

In natural soils, cohesion is a result of electrostatic bonds between clay or silt particles. Soils that do not contain clay or silt lack cohesive strength other than that due to the capillary forces arising when internal air is present and water forms bridges between sand grains, resulting in negative pore pressure (Blasio, 2011). Dietrich and Montgomery (1998) explain that in slope stability modelling, setting cohesion to zero maximizes the possibility of instability across the slope.

Various processes may lead to the reduction in the shear strength of the soil mass such as increased pore pressure, cracking, swelling, creep under sustained load, leaching, strain softening, weathering and cyclic loading. Further, an increase in loading at the top of the bank, increase in water pressure in cracks at the top of the slope, increase in soil weight, excavation at the bottom of the bank, and earthquakes, would increase shear stresses of the soil and thus reduce stability (Geotechnical Design Manual, 2015).

2.1.2 Types of slope stability analysis

The factor of safety provides a numerical estimate of the stability of a slope. Unstable situations are therefore represented by a number between 0 and 1 whereas stable conditions are represented by a value greater than 1. The Factor of Safety (FOS) against failure is expressed by:

$$FOS = \frac{shear\ resistance}{shear\ force\ rquired\ for\ equilibrium} = \frac{restoring\ force}{disturbing\ force} \tag{2.1}$$

For stability to be maintained the available shear strength must exceed the disturbing forces (Norris et al., 2008; Naghdi et al, 2013). SLOPE/W is one of the products from a range of geotechnical products in the GeoStudio product suite. The program is commercially available for analyzing slope stability. The software computes the factor of safety by making use of limit equilibrium techniques based on the method of slices (SLOPE/W, 2007). Through the years various solution techniques for the method of slices have been developed. The differences between the methods depends on which equations of static equilibrium are included and satisfied, which inter-slice forces are included, and the assumed relationship between the inter-slice shear and normal forces. The approach of the method of slices is to divide the soil mass into vertical slices as illustrated in Figure 2.2, and then consider the forces acting on each slice including normal and shear forces on the slice base and slice sides.

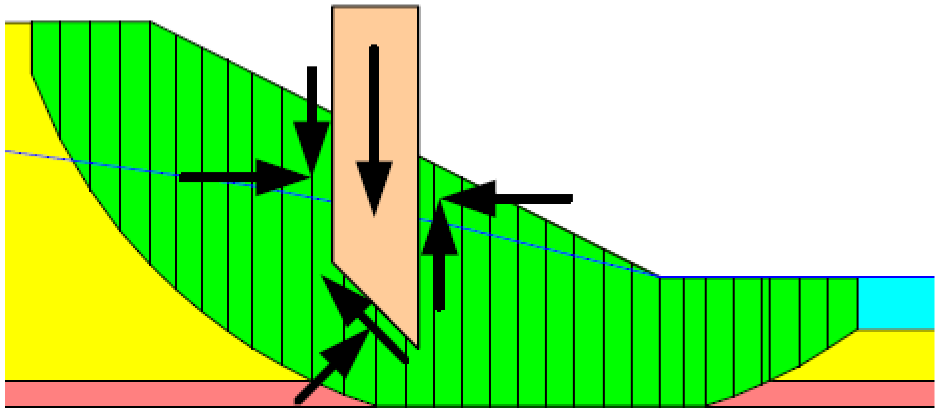

Figure 2.2: Forces acting on soil slice in a sliding mass (after SLOPE/W, 2007)

A number of solution methods are available in SLOPE/W, including the Ordinary or Fellenius method, the Bishop's Simplified method, the Janbu's Simplified method, the Spencer method, the Morgenstern-Price method, the Corps of Engineers method, the Lowe-Karafiath method, the Janubu Generalized method, and the Sarma method. Table 2.1 describes how the inter-slice forces are considered and what assumptions are made in computing the factor of safety for the most commonly used limit equilibrium methods in SLOPE/W. The limit equilibrium methods do not consider the stress-deformation properties of the soil and should thus not be used to calculate the stress distributions along the slip surface but should rather be limited to providing an indicator of the overall stability of the slope.

SLOPE/W includes a range of tools that assist in obtaining a level of reliability in the results, such as a tool that allows the user to graph a list of different variables along the slip surface or display detailed forces on each slice. The program is more robust when used together with other GeoStudio products such as SEEP/W, SIGMA/W, QUAKE/W, TEMP/W, CTRAN/W, AIR/W and VADOSE/W. SIGMA/W performs stress and deformation analyses, specifically for civil and mining problems. Further, SIGMA/W enables the modelling of pore-water pressure generation and dissipation with surcharge loads (SIGMA/W, 2013).

Table 2.1: Various limit equilibrium methods

Method	**Conditions of static equilibrium**	**Preferred use**	**How are inter-slice forces considered**
1. General limit equilibrium method	F_m and F_f(vertical and horizontal). Subscripts refer to moment equilibrium and force equilibrium respectively.	The method may be used to analyze circular and non-circular slip surfaces (Geo-Slope, 2007).	The approach of the general limit equilibrium method is to divide the soil mass into vertical slices, and consider the forces acting on each individual slice to ensure the equilibrium of each slice and the soil mass as a whole.
2. Bishop's Simplified method	F_m and F_f (only vertical)	The simplified Bishop method is the simplest of all the methods and is only applicable to circular slip surfaces.	The primary assumptions of the method are: it ignores inter-slice shear forces, and satisfies only moment equilibrium (Bishop, 1955).
3. Janbu's Simplified method	F_f (vertical and horizontal)	The method is only applicable to non-circular failure surfaces (Janbu, 1973).	Jandu's method also ignores inter-slice shear forces.
4. Spencer method	Satisfies both F_m and F_f	Applicable for any shape of failure surface (Spencer, 1967).	It assumes a constant inter-slice force function and considers both shear and normal inter-slice forces (Geo-Slope, 2007).
5. Morgenstern-Price method	Satisfies all of the equilibrium conditions	The failure surface may be of any shape, and it can be used for any geometry and/or soil type (Geo-Slope, 2007).	Similar to the Spencer method, but allows for various user-specific inter-slice force functions (Morgenstern and Price, 1965).
6. Ordinary method of slices (also referred to as the Fellenius method or the Swedish method of slices)	F_m and F_f (only vertical)	The simplicity of the method makes it possible to compute the factor of safety using hand calculations but does not achieve force equilibrium and hence should not be used in practice because it is subject to unrealistic factors of safety (Geo-Slope, 2007).	The method ignores all inter-slice forces, and the slice weight is resolved into forces parallel and perpendicular to the slice base (Fellenius, 1936).

QUAKE/W can be used for the dynamic analysis of earth structures when exposed to earthquakes or impact loads. It is used to determine the movement and excess pore-water pressure from shaking. TEMP/W is used to analyse thermal changes in the ground due to environmental factors or construction (QUAKE/W, 2014). CTRAN/W is used to model the movement of contaminants through soil or rock (CTRAN/2012). AIR/W is used to model the interaction between groundwater and air in soil and rock. It can be coupled with TEMP/W to analyse acid rock drainage and gas transfer (AIR/W, 2012). VADOSE/W is used to analyse the interaction between the soil profile, vegetation, and the atmosphere. It is typically used to analyse and design land reclamation, mine closure and waste contamination projects (VADOSE/W, 2014). SEEP/W analyses groundwater flow in porous materials such as soil and rock. It can be used to model steady-state problems as well as saturated/unsaturated time dependent geotechnical problems (SEEP/W, 2007).

The pore-water pressure significantly influences the shear strength and volume change behavior of soil. Thus, modeling groundwater conditions in SEEP/W provides more realistic results in a slope stability model. The SEEP/W product in GeoStudio is a finite element numerical model that can mathematically simulate the physical process of water flowing through a porous medium such as soil and rock (SEEP/W, 2007). The model accounts for the flow of water through saturated soil using Darcy's Law. The approach is to divide the entire soil mass into smaller sections and the process is called discretization or meshing as illustrated in Fig.2.3. SEEP/W uses the contributing area that surrounds each node of the discretized mass to calculate the corresponding flow rate. The elevation of the phreatic surface at each discretized section is calculated. A transient analysis may be done by changing the water table position over time.

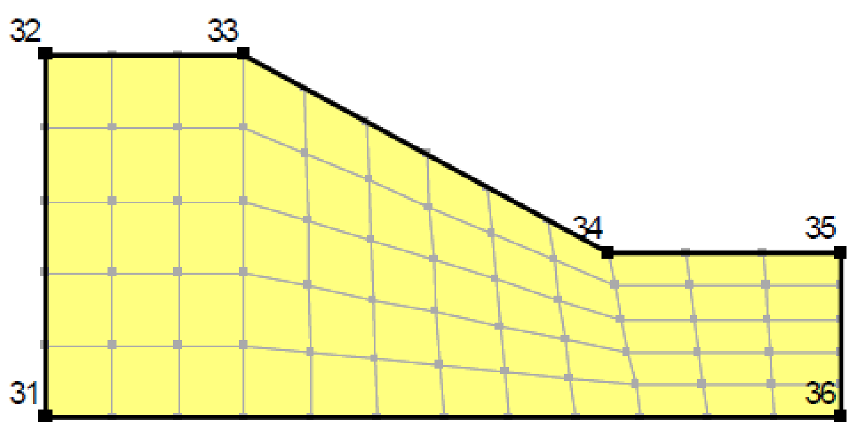

Figure 2.3: Region meshed with rectangular grid pattern (after SEEP/W, 2007)

SEEP/W has limitations with regards to not allowing for moisture to leave the system at the ground surface. Further, it does not account for temperature changes, volume changes and chemical changes, as the mathematics involved in these extended considerations is too complex.

2.1.3 Soil types

Natural characteristics such as physiography, climate, geology, soils and vegetation vary within different river ecoregions of South Africa. According to the State of Rivers Report (2001) riverbanks located in the Central Highlands consist of mainly sandy to sandy loam soils in the upper regions and clayey soils in the lower region, whereas rivers located in the Lowveld consist mainly of sandy, clayey and sandy loam soils. Gravel and cobble banks are predominant in the Western and Eastern Cape of South Africa (Sieben, 2000). The resistance of a bank to failure is determined by the shear strength of the soil along a potential failure surface. The shear strength is governed by the cohesion, which is related to the clay content, and internal friction resistance, which is a result of the soil's density, particle size, and particle shape (Rinaldi and Darby, 2008).

2.2 Functional root traits and their effects on soils

A thorough understanding of the effects of vegetation on the processes involved in riverbank retreat is required for improved bank stabilization purposes (Abernethy and Rutherfurd, 1998).

A trait is defined as a distinct, quantitative property of organisms and is used comparatively across species. McGill et al. (2006) define a functional trait as one that strongly influences organismal performance. The concept of identifying functional root traits to enable the prediction of the ability of plant species to aid in bank stability was investigated by Burylo et al. (2012). The functional root traits identified are root density (root mass per unit volume of soil), root length density (root length per unit volume of soil), specific root length (the ratio of root length to dry mass of fine roots), root system type (heart versus tap root system), root surface area density (root surface per unit volume of soil), root area ratio (the fraction of the soil cross sectional area occupied by the roots), percentage of fine roots (fibrous roots less than 0.5 mm in diameter), mean root diameter, root to shoot biomass ratio, root tissue density, root volume and external root surface. Figure 2.4 shows the three main root system types: plate, heart and tap (Norris and Greenwood, 2006). Plate root systems are classified as having large lateral roots and smaller vertical sinker roots, heart root systems have a number of diagonal and vertical roots, and tap root systems have one major central root and smaller horizontal and vertical roots. Several plant species have a mixture of root system types.

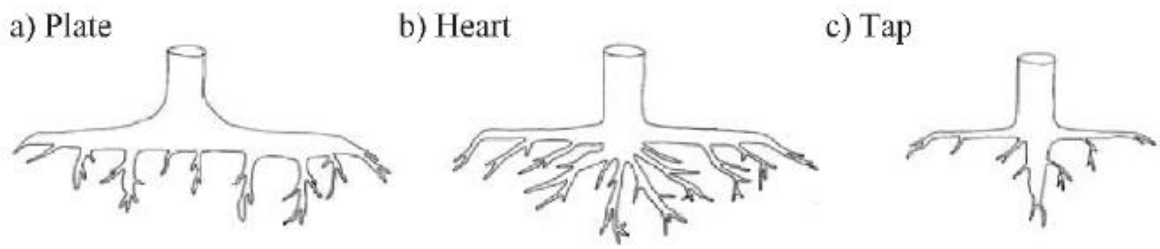

Figure 2.4: Main root system types (after Stokes and Mattheck, 1996 (in Norris and Greenwood (2006))

2.2.1 Root characteristics and functions

The use of root reinforcement for the purpose of slope stabilization requires an understanding of root functions, as well as the factors that influence these functions. A brief description of root systems, their development, functions and characteristics is contained in the following paragraphs.

2.2.2 Classification of root systems

Root systems grow by a branching process, with laterals emerging from the main roots. There are two basic types of root systems. A taproot system has one main root, which is the longest and thickest root in the root system of a plant. Thinner and shorter roots branch from the tap root. Fibrous root systems are a type of heart root system that consist of several large roots that are similar in size. Fibrous root systems are extensively branched with growth extending into a large volume of soil. Beck et al. (1988) (in Waisel et al. (1991)) found that roots consisting of well-developed laterals (crown roots) exhibit higher tensile strength and a greater pullout resistance, in their study of different types of maize roots. The multidirectional growth pattern of root systems has also proven to contribute to the pullout resistance of the plant and hence increases the stability of the plant.

The different root classes are mainly identified by the shape of the root systems of mature plants. Surface roots are defined as lateral roots that grow from the upper part of a taproot system, are uniform in both length and diameter, and exhibit high tensile strength (Kobayashi, 1977).

Root tensile strength is also affected by the age of the root system. In a root system, the main roots usually survive throughout the plant's lifetime, lateral roots however have a shorter life span. In some plant species, shedding of old roots or roots that have developed into unfavorable conditions may contribute to the life span of the root system as a whole (Caldwell, 1979).

2.2.3 Functions of root systems

The two basic functions performed by the root system of plants are the absorption of soil-based resources (such as water and dissolved ions) and anchorage (Waisel et al. 1991). It is acknowledged that the different features of root systems (diameter, colour, surface texture and root distribution) are related to variations in the root environment such as soil moisture, microsite relations, nutrients and soil temperatures (Adhikari et al. 2013).

Root diameter is of great interest in this context since it is defined as one of the functional traits of a root system. It is a feature that differs broadly within and between species. Waisel et al. (1991) suggest that in vegetation species such as grasses, rushes and sedges, the roots narrow in diameter until they reach an effective minimum diameter which allows for transport of water and ions to and from the root tip, and to the absorbing cells. Other species such as *Alliaceae*, *Magnoliaceae*, and a vast number of trees, generally have coarse terminal roots (0.5-1.0 mm in diameter). Root diameter is directly linked to the length of root that a plant can produce. Typically trees grown in soil containing ectomycorrhizal fungi have thick roots and low root densities resulting in low total lengths of roots per unit soil volume. Where nutrient supply rates are low, plants will usually produce finer roots. Goss (1977) (summarized in Waisel et al.

(1991)) suggests that thicker roots may be able to exert greater forces on soil and thereby have a greater ability to penetrate compact soil. Thicker roots are able to penetrate soils more successfully, contributing to a more developed roots system by effectively branching out underground. The texture of roots is governed by the number, size and density of root hairs.

2.2.4 The growth and form of root systems

The ideal conditions for root growth vary with the time of the year and local soil conditions, and at any one time may vary between different depths in the soil. The ability of the root system to develop and support the plant in the period in which it is most stressed, determines the productivity of plants. This suggests, for example, that a plant subject to dry conditions shortly after it has been planted would require rapid development of the root system in order for adequate lateral roots to develop and thus allow for sufficient nutrients and water to be absorbed (Russel, 1977). Weaver (1926) (described in Russel (1977)) illustrates how plants which are dependent on regular rain will develop a shallow root system when irrigation does not penetrate deeply into the soil, compared to irrigation that provides water to an extensive depth. In other cases where water supply is more constantly available at a considerable depth, a smaller portion of the total root system may be found in the surface soil during dry periods when the water supply in the surface soil is limited.

Pinthus (1967) emphasizes the important effect the spatial orientation of the root system has on the soil exploited, the local depletion of water, the ability of the root system to retain the plant in an upright position, and subsequently the stability and resistance of the plant to uprooting. The orientation of the roots is influenced by their proximity to the roots of other plants. Raper and Barber (1970) (described in Russel (1977)) found this 'exclusion' mechanism in their work with soy bean plants. When the plants were grown in isolation the lateral roots extended horizontally, and in contrast, they turned downwards and away when they approached adjacent plants of the same species. This mechanism is attributed to the competitive nature that the roots display concerning the withdrawal of water or nutrients from the soil. However, in practice adjacent roots often become closely interlaced (Mitchell, 1969;

Baldwin and Tinker, 1972). Nonetheless, the sizes of root systems are commonly reduced when they are grown in competition with other plants.

2.2.5 Factors affecting plant root systems

The growth of plants is largely determined by the balance of functions between roots and shoots. Roots are dependent on shoots for carbohydrates, growth regulators and some organic compounds.

The effects of environmental factors on plant root systems may vary even for a single species within a single stage of development. Environmental factors influence the distribution between roots and shoots. The environmental variables including light intensity, nutrient supply, temperature and water supply, are the main factors that are practically considered in the influence of the distribution between roots and shoots (Russel, 1977).

In general, a decrease of light intensity will in turn decrease the ratio of roots to shoots and an increased supply of nitrogen may result in greater growth, increasing the weight of the roots and more so the weight of the shoots. Davidson (1969b) (summarized in Russel (1977)) found that when an increased supply of phosphate leads to increased growth, the root/shoot ratio usually decreases.

The effect of temperature variation is more complex than the other environmental factors since within the root system itself substantial differences in temperature can occur; temperature variation affects roots and shoots where each experience different temperature regimes. Walker (1969) (as noted in Russel (1977)) showed the clear sensitivity of root systems to changes in temperature. The root system is sensitive to a degree such that an increase of 1°C in soil temperature would greatly influence the effects on growth and nutrient uptake. Brouwer (1964), Neilson and Cunningham (1964), Kleinendorst and Brouwer (1965) and Davidson (1969a) have developed a clear relation of the effects of variation in root temperature on shoot growth. In some cases a decrease of root temperature which in turn restricts shoot growth may increase the total weight of the roots.

2.2.6 Soil characteristics that influence plant growth

The principal factors affecting root growth include soil moisture content, soil temperature, pores in the soil, strength and compressibility of the soil, oxygen supply, the density of toxins and pathogens in the soil and nutrient supply.

The clay content is an important indicator of pore sizes. In clay soils there are very few pores larger than 30-60 µm and there are more commonly pores less than 0.2 µm. The rate at which roots extend is reduced if the roots require small pressures to enlarge pores smaller than the roots themselves. Soils with a high clay content compress under wet conditions which may result in unfavourable conditions for root growth and distribution. Roots rarely occupy more than 5% of the soil volume; the percentage occupancy is greater in sands than in clay based soils.

2.3 Modelling

A range of methods and models have been developed to account for the stabilizing effect of vegetation. The applicability of a model depends on the level of site information available and the degree of accuracy required in order to implement bank stabilization.

2.3.1 The contribution of vegetation roots to slope stability

It is understood that roots can withstand high tension while soils, on the other hand, are strong in compression and weak in tension (Adhikari et al. 2013). This supports that roots developing into soil result in a reinforced soil structure with increased soil shear strength (De Baets et al. 2008). Gray and Sotir (1996) reason that roots should penetrate across the failure surface to have a significant effect. Furthermore, roots penetrating into fractures or fissures in the underlying bedrock are most effective in providing restraint against shallow slip failure.

Swanston (1970), Wu et al. (1979) and Burroughs and Thomas (1977), found that small flexible roots with a high root surface area and high tensile strength are widely suitable in soil stabilization. These results suggest that a large number of fine roots will contribute more to soil reinforcement than a small number of thick roots. Reubens et al. (2007) (summarized in Burylo et al. (2012)), attribute the effectiveness of using plant species with small flexible root systems to their ability to lower porewater pressure, increase surface roughness of the soil mass (from vegetation cover including plant stems and roots) and provide additional soil cohesion through root reinforcement. Abernethy and Rutherfurd (2001) argue that interspecies differences in root distribution is a more significant characteristic in bank stability than interspecies differences in tensile strength. However, studies by Simon et al. (2006) indicate that the hydrological effects of roots (such as the removal of water by transpiration) contribute less to stream bank stability than the mechanical effects. It is important to note that there is a limited understanding regarding the influence of vegetation on soil pore water pressure, and this poses a challenge in quantifying the mechanical and hydrological effect of vegetation on soil stabilization. In their study Burylo et al. (2012) conclude that the root length density, external root surface and specific root length imply greater fine root content and hence more soil-root contact. In addition, De Baets et al. (2008) show that roots may affect the infiltration rate, moisture content, shear strength and organic matter content of a soil; all of which have critical relevance to slope stability in that these affect the ability of a soil to resist stresses.

The root area ratio is recognized as an important functional root trait in estimating the root contribution to soil strength. In the investigation carried out by De Baets et al. (2008), the root length density and root diameter were used to determine the root area ratio. De Baets et al. (2008) developed a detailed relationship for the root area ratio of grasses and shrubs in their publication and this methodology is outlined on page 38.

It has been postulated (Weaver and Clements, 1938) that a high root area ratio at greater soil depths is a result of deep nutrient soil layers. Although the reinforcing capability of roots may decrease with an increasing soil depth, the ability of roots to improve soil cohesion may intensify locally with an increased root area ratio that comes with an increasing depth.

Identifying situations where vegetation, specifically root reinforcement, can be used for active bank management or stabilization, and the selection of appropriate species, requires understanding the ways in which root systems can fail, and their causes. In pull-out tests, Wu

(2013) observed that in situations where a tensile force is applied to the exposed end of a root, in situ failure can occur by tension failure of the main root, progressive failure in the branch roots, shear failure between the roots and soil, or through a combination of these failure modes.

Additional advantages of root reinforcement include: a substantial increase in the shear strength of soil including roots, as the tensile strengths of roots may reach 100 MPa, root systems are self-rectifying and able to maximise root extent under changing hydrological and topographical conditions, and roots do not corrode but rather they are self-repairing and regenerative (Coppin et al., 1990).

2.3.2 Qualitative models that account for the effect of vegetation on bank stability

Guidelines for stabilizing stream banks with riparian vegetation have been developed by Abernethy and Rutherfurd (1999) for Australian rivers. The tool proposed in the guideline is to assess the vegetation condition according to a 'traffic light' classification: green, yellow and red for riparian vegetation in good, intermediate and poor conditions. The main aspect in the guideline is adequately assessing the dominant erosion process. The guideline includes a decision tree for determining the minimum riparian zone widths for bank stability. The guideline also encourages a thorough assessment of the existing riparian condition in terms of historical channel change, channel hydraulics and channel form.

Thorne et al. (1996) provides a framework for the selection of the appropriate types of river bank protective solutions based on the various types of bank erosion and instability processes.

Hey et al. (1991) (cited in Calow and Petts (1994)) established flowcharts to enable selection of the most environmentally acceptable method (hard and soft stabilizing measures) to stabilize a particular erosion problem along a bank. The selection is based on flow velocity, bank slope, soil type, water level drawdown rate, rate of bank retreat and failure mode.

2.3.3 Advanced models that account for the effect of vegetation on bank stability

The model presented by Wu et al. (1979) uses root tensile strength and root distribution to estimate the increase in soil shear strength. The model assumes that all roots grow vertically and that tension is transferred to the roots as the soil is sheared. Moreover, the model accounts for the soil binding effect of the roots by introducing an additional cohesion effect.

Waldron (1977) and Wu et al. (1979) (cited in Adhikari et al. (2013)) developed a theoretical model to express the increase in shear strength due to the presence of roots.

$$C_r = t_R(sin\theta + cos\theta tan\Phi) \quad (2.2)$$

where, C_r is the increase in shear strength due to the presence of roots, θ is the angle of shear distortion (the angle of the root relative to the vertical after shear distortion as shown in Figure 2.5), Φ is the soil friction angle, and t_R is the total mobilized tensile stress of root fibres and is defined by Wu et al. (1979) as:

$$t_R = \sum T_{ri}/A \quad (2.3)$$

where $\sum T_{ri}$ is the total force in the roots per unit of soil area *A*.

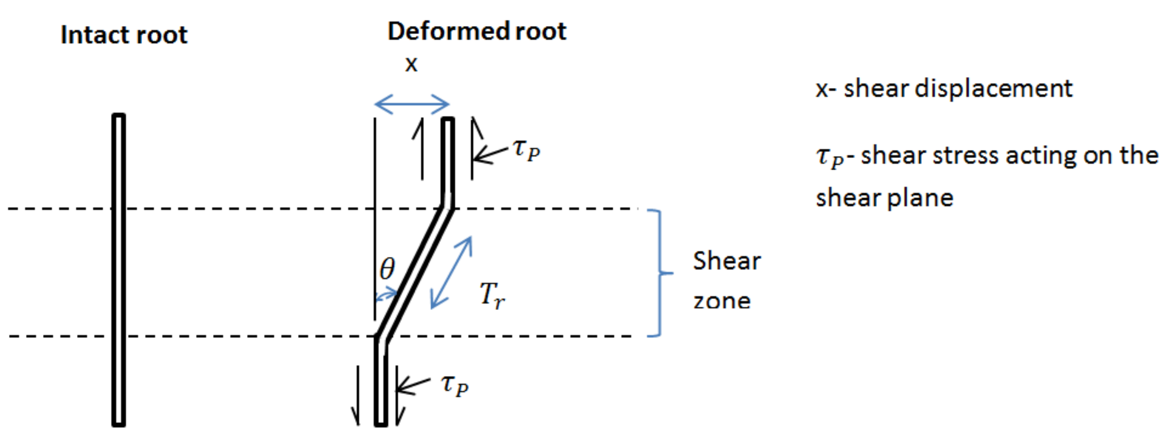

Figure 2.5: Root reinforcement models (after Waldron, 1977)

The expression for the additional cohesion due to the presence of roots may be further simplified for sandy soils for a friction angle of 27° according to Thomas and Pollen-Bankhead (2010) and an angle of shear distortion assumed to be 45° (Adhikari et al, 2013), i.e.

$$C_r = 1.06\frac{\Sigma T_i n_i \alpha_i}{A} \tag{2.4}$$

where T_i is root tensile strength (MPa), n_i is the number of roots in a diameter class, i is the root diameter class, α_i is the root cross-sectional area (m^2) and A is the reference area of soil occupied by roots (m^2).

The additional cohesion in silt loam soils for a friction angle of 25° as suggested by Pollen and Simon (2005) and an assumed angle of shear distortion of 45° is presented by De Baets et al. (2008), i.e.

$$C_r = 1.04\frac{\Sigma T_i n_i \alpha_i}{A} \tag{2.5}$$

The model assumes that all roots reach ultimate tensile strength simultaneously during shearing of the soil. This assumption has been shown by Docker and Hubble (2008) and Mickovski et al. (2011) to be flawed and it tends to overestimate additional root cohesion (defined by the variable C_r above) as shown by Pollen and Simon (2005) and Docker and Hubble (2008) since in practice. It is suggested by Adhikari et al. (2013) that Wu's model is only useful to rank species according to their soil reinforcement potential. De Baets et al. (2008) used Wu's model to rank 25 Mediterranean plant species according to their suitability for slope stabilization as they reason that additional root cohesion values alone could be used to rank plant species for their potential pertaining to slope stabilization.

Wu (2013) distinguishes between the tensile strength of a root segment, σ_{rt}, from the strength at failure, σ_{rf}. The tensile strength of a root is determined through simple tension tests on a root segment and is dependent on the species, diameter and location along the bank, whereas the tensile resistance or the strength at failure is measured by pull-out tests. Burroughs and Thomas (1977), Greenway (1987), Nilaweera (1994), Gray and Sotir (1996) and Norris and Greenwood (2000) (in Wu (2013)) found that the tensile strengths of roots of various diameters from different species range between 5 and 60 MPa. Greenwood et al. (2004) carried out laboratory tests to compare the root tensile strength and root pull out resistance. The results showed that the root pull out resistance is significantly lower than the tensile strength of the roots. Norris and Greenwood (2006) confirmed this finding in field experiments and estimates the root pull-out strength to be 50-70% of the tensile strength.

De Baets et al. (2008) made use of a standard stress formula for the determination of root tensile strength,

$$T_{r=\frac{F_{max}}{\pi(\frac{D^2}{4})}} \tag{2.6}$$

where F_{max} is the maximum force (N) needed to break the root and D is the mean root diameter (mm) close to the point of rupture before stretching. Equations (2.6), (2.7) and (2.8) assume that all roots have a circular cross section.

The tests done by De Baets et al. (2008) accounted for the root area ratio (*RAR*) in ranking 25 Mediterranean plant species for their suitability in bank stabilization. For grasses, the *RAR* was calculated using the equation

$$RAR_{grass} = \frac{\frac{RL}{0.1}\alpha_i}{A} \tag{2.7}$$

where RL is the total root length per soil depth class (the class designation assigned to sequential groups of depths that roots reach for each species, in this case referring to plant roots sampled from every 0.10 m of soil depth), α_i is the mean root cross-sectional area of the root and A is the reference area (m^2).

For shrubs, the total length of roots having a similar diameter was found by dividing the total lengths per diameter class by 0.10 m to obtain the number of 10 cm long roots for all roots having similar diameter. The *RAR* for the shrubs was calculated at different soil depths by the following equation:

$$RAR = \frac{\sum_i^n n_i \alpha_i}{A} \tag{2.8}$$

where n_i is the number of 10 cm long roots in each root diameter class and α_i is mean root cross-sectional area of a root diameter class (m^2).

The mean *RAR* for the 25 Mediterranean plant species with their corresponding standard errors is well documented by De Baets et al. (2008). Further, De Baets et al. (2008) list the diameter range with the associated standard error and relate the tensile strength to diameter. The additional cohesion due to vegetation with depth below the ground surface is plotted for herbs, reeds, rush, trees and grasses.

Pollen and Simon (2005) (reviewed by Adhikari et al. (2013)) describe how the Fiber Bundle Model (FBM) overcomes the overestimation of additional root cohesion in Wu's model by accounting for the different maximum strengths of the roots in the soil. The FBM is used to estimate additional cohesion due to the roots as it further redistributes the load from the broken roots (broken during shearing) to the remaining intact roots crossing the shear surface.

In response to the flaws of Wu's model, RipRoot was developed (Pollen and Simon, 2005). The model, similar to the Fiber Bundle Model, incrementally applies load onto the root-soil system. It thereby accounts for the breakage and redistribution of loads from the broken roots to the remaining intact roots in the soil matrix. Pollen and Simon (2005) describe how RipRoot allows for more realistic estimations of root reinforcement compared to Wu's perpendicular model.

Operstein and Frydman (2000) accounted for the overestimation in additional root cohesion values of Wu's model by applying the following equation for the increase in soil shear strength (C_r) due to the presence of plant roots:

$$C_r = 0.25t_R \tag{2.9}$$

where t_R is the total mobilized tensile strength of the root fibres per unit area of soil. It accounts for the average tensile strength per average root cross-sectional area and assumes that all the tensile strength of the roots is mobilized instantaneously at the moment of slope failure.

An Excel program presented by Greenwood (2006), SLIP4EX is able to combine the mechanical and hydrological effects of vegetation on slope stability in terms of enhanced cohesion, changed water pressures and root reinforcement forces. Greenwood expressed the ultimate root force per square metre across the slip plane, T_{ru}, as a function of the number of roots, the diameter of the roots, and the pull out resistance of the roots. The method makes use of the general limit equilibrium methods, specifically Bishop, Janbu, Fellenius, Simple, Swedish and Greenwood method (as defined in Table 2.1) to determine the Factor of Safety of the slip surface of a vegetated slope. The program determines the available root reinforcement force acting on each soil slice as expressed in Equation (2.10),

$$T = T_{rd} \times l \tag{2.10}$$

where T is the available root force acting on the base of each slice (in the direction of the bank, at an effective angle of 45° between the roots crossing the slip surface, and the slip surface itself), T_{rd} is the available root force per square metre of soil and l is the length of the slip surface.

T_{rd} is calculated as follows

$$T_{rd} = \frac{T_{ru}}{partial\ factor\ of\ safety} \tag{2.11}$$

The partial factor of safety is applied to allow for the uncertainty in root distribution and the availability of adequate additional root cohesion. T_{ru} from Equation (2.11) is the ultimate root force per square metre perpendicular the slip plane (kN/m^2) which is expressed as

$$T_{ru} = NA\sigma_{rt} \tag{2.12}$$

where N is the number of roots per square metre, A is the area of roots per metre (m^2) and σ_{rt} is the ultimate pull out resistance per root per square metre across the slip plane (kN/m^2).

The additional tensile root reinforcing force (T), assumed to act at the base of each slice, is included in the slope stability analysis by adding the forces to the Greenwood General, Greenwood Simple (equation 2.13 and equation 2.15 below, respectively) and Swedish equations (point 6 in Table 2.1 on page 26). Greenwood reasons that the general limit equilibrium equation compared to the methods (Bishop and Janbu, points 2 and 3 on page 26 respectively) gives a more suitable estimate of the Factor of Safety for all slope and hydrological conditions. The author suggests that Greenwood's SLIP4EX program be used as an independent check to other commercial programs which are used to locate the slip surface, as this is a limitation in SLIP4EX.

Greenwood et al. (2004) adapted the General equation

$$F = \frac{\sum[c'l + (W cos\alpha - ul - (U_2 - U_1) sin\alpha) tan\emptyset']}{\sum W sin\alpha} \quad (2.13)$$

in order to include the reinforcement and hydrological effects of vegetation, i.e.

$$F = (\sum[c' + c'_v)l + (W + W_v)cos\alpha - (u - \Delta u_v)l - \big((U_2 + \Delta U_{2v}) - (U_1 + \Delta U_{1v})\big)sin\alpha \quad (2.14)$$

$$-(-D_w \sin(\alpha - \beta_w) + T sin\theta) tan\emptyset']) / (\sum[(W + W_v) sin\alpha + D_w \cos(\alpha - \beta_w) - T cos\theta])$$

The Greenwood Simple equation (Greenwood, 1985) is derived from equation 2.13 but it is based on the assumption that there is a consistent horizontal water surface across the soil slice ($U_2 - U_1 = -ubtan\alpha$), i.e. the difference in the interslice water forces on the left and right hand side of the soil slice results in a consistent horizontal water surface across the soil slice, and:

$$F = \frac{\sum[c'l + (W - ub) cos\alpha] tan\emptyset'}{\sum W sin\alpha} \quad (2.15)$$

where c' is the effective cohesion at the base of a slice (kN/m^2), b is the width of the soil slice, W is the total weight of a soil slice (kN), u is the average water pressure on the base of a slice (kN/m^2), U_2 is the water force on the right side of a slice, U_1 is the water force on the left side of a slice, α is the inclination of the base of the soil slice to the horizontal, $\emptyset'$ is the effective angle of friction at the base of a slice, β_w is the angle between the wind direction and the horizontal, D_w is the wind force and the subscript 'v' denotes the inclusion of vegetation on these parameters. The method accounts for the influence of the vegetation on the soil suction as a result of a changing pore water pressure (Δu_v) by altering the water table levels (as the effective interslice forces and water forces on the sides of the slice are taken into account thus producing a continuous phreatic surface representative of the actual water surface), since moisture content and soil water pressures are related (Norris and Greenwood, 2006).

There is a wide range of soil-vegetation interaction models available such as: models that represent reinforcement as flexible cables (Wu, 2007); models that represent reinforcement as a beam (Stokes et al., 2009) or pile (Burylo et al., 2010); those analyzing forces on the slip surface (Norris and Greenwood, 2006); those analyzing axial forces and bending in reinforcement (Wu, 2007); and the finite element method (Mao et al., 2014 and Manoli et al., 2014). Wu (2013) has reviewed these soil-interaction models. Comparison of the predictions made by the analytical models to laboratory and in situ tests allowed Wu to conclude that for soil reinforced by vegetation roots, the most important plant material properties are Young's Modulus and tensile strength. As previously mentioned Wu (2013) also found that the tensile strengths of roots of various diameters from different species range between 5 and 60 MPa.

Simple methods are easy to use and suitable when data are limited, however they are found to be inaccurate and only useful for order-of-magnitude estimates. The finite element method is more accurate but requires extensive input data.

ECO-SLOPES was a multi-disciplinary project that involved a variety of specialists in developing techniques for improving slope stability and controlling erosion across Europe (Mickovski and van Beek, 2006). The ECO-SLOPES project prompted the development of a decision support system for the purpose of assisting decision makers on the applicability and selection of bio-engineering solutions for protection against erosion and mass movement on sloping ground. The slope decision support system (SDSS) which is presented as a computer program is founded on a knowledge-based framework, Confound , which uses a simple rule-based approach to provide advice on the suitability of each of the eco-engineering choices based on project specific information provided by the user (Toll and Barr, 2001). The system's knowledge base consists of the most common stability problems occurring on slopes, which are generally slope instability and erosion problems. The program is designed in such a manner as to permit the user to input as much information (such as ground conditions, nature of the slope, condition of the vegetation, land use and climate) as is available on the specific project location (Norris and Greenwood, 2006).

The level of information that the user enters into the SDSS has a bearing on the quality of the assessment – the greater the detail of information provided by the user, the more thorough and specific are the proposed eco-engineering methods generated. Once the information is supplied by the user, the system provides assistance in the form of commentary and or recommendations for eco-engineering measures and strategies for stabilization and land reclamation. The system is able to use incomplete information and displays "confidence levels" to ensure that the user is made aware of the credibility of the returned comments. The multidisciplinary nature of SDSS makes it a most valuable tool during the initial stages of an eco-engineering project when various eco-engineering strategies are considered (Mickovski and van Beek, 2006). The system is not designed to provide the user with a final decision but rather it affords guidance by suggesting important considerations to be taken into account. Mickovski and van Beek (2006) carried out four case studies on the SDSS using data from literature. The strategies suggested by the SDSS proved to stabilize the soil against erosion and shallow mass movement in all the case studies. The SDSS is currently not available since it was developed for Windows XP which is no longer supported. There are plans to upgrade the SDSS and make it available to the public.

Conclusions from the advanced models and proposal for further advancement

It is acknowledged that plant roots provide the soil with mechanical reinforcement against shallow slip failure. A range of methods and models, which include both qualitative and advanced approaches, have been developed to describe the mechanical reinforcement provided by roots. In most of these approaches the mechanical reinforcement of the soil by the roots was modelled as an increase in shear strength from additional cohesion.

However, there were no studies in literature that were found to provide a guideline as to which functional root traits are required to stabilize riverbanks that differ in slope angle, soil type and flood condition. In this study the additional cohesion due to the presence of roots is related to measurable properties (root tensile strength, root diameter, root length, root area ratio, and number of roots per square metre) so as to recommend which measurable root properties would be suitable to stabilize a bank.

First, the study aims to identify when vegetation would be an appropriate bank stabilization technique. Secondly, this study aims at quantifying the roots' contribution to soil strength as a function of root functional traits for a range of soil types, bank slopes, bank heights and hydrological conditions.

Chapter 3 Sensitivity analysis for determining significant root functional traits

In this chapter, the example given by Norris and Greenwood (2006) that makes use of SLIP4EX to assess the effect of plant roots on slope stability is used as a case study to provide a general indication as to which root functional traits contribute most to slope stability. Furthermore, the FOS results from the proposed software (SLOPE/W) are verified against those using SLIP4EX, since they both make use of limit equilibrium methods. However, SLOPE/W is the preferred software in this study as it is capable of running the same analysis as SLIP4EX but may be coupled with SEEP/W to allow for a transient analysis to be done, which enables hydrological conditions to be accounted for. Further, SLOPE/W is less tedious in the process of building riverbank models and provides the slip surface, whereas the slip surface needs to be specified in SLIP4EX.

3.1 Case study

The case study carried out by Norris and Greenwood (2006) using SLIP4EX to determine the effects of the presence of roots on the Factor of Safety (hereafter FOS) of London Clay slopes, situated on the M25 at Passingford Bridge, was used as the "control model" for the sensitivity analysis. Hawthorn (*Crataegus monogyna*) in its mature state was the plant species used in the analysis of this case study.

Table 3.1 provides a summary of the soil and root characteristics that were used in the case study by Norris and Greenwood (2006), where the contribution of the roots was estimated. The program allows for a partial factor of safety to be applied to the root strength to account for uncertainties in the assumed root distribution with depth and the availability of adequate additional root cohesion. In section 3.2, the FOS results from SLOPE/W are compared to the FOS results from SLIP4EX for the case of no vegetation. In the sections that follow, the root strength properties and root functional traits from Table 3.1 were then accounted for in SLOPE/W and compared to the results from SLIP4EX.

Table 3.1: Soil and root characteristics for the M25 site

Slope Characteristics without vegetation	
Slope angle (°)	26
Effective cohesion c' (kN/m^2)	7
Effective friction angle Φ' (°)	20
Unit weight of the soil γ (kN/m^3)	19
Location of the water table	At ground surface (along the slope)
Slope characteristics with vegetation	
Angle at which the roots intersect the slip plane (°)	45
Effective cohesion due to the roots C'_r (kN/m^2)	3
Typical ultimate root strength (kN/m^2)	8300
Typical root diameter (mm)	12
Typical number of roots per square metre	4
Partial factor of safety on root strength	8

3.2 Case study modeled in SLOPE/W for the case of no vegetation

The characteristics listed in Table 3.1 were used to model the slope in SLOPE/W. The bank height for the M25 site varied between 3 and 11 m according to Joanne Norris (personal communication). The bank was remodeled in SLOPE/W using an assumed bank height of 7 m. The number of soil slices analyzed in SLIP4EX was not mentioned in the case study and subsequently 15 slices were used in the SLOPE/W analysis. The grid and radius method of specifying trial slip surfaces was used in the SLOPE/W model in order to locate the critical slip surface with the lowest FOS. A schematic of the slope setup in SLOPE/W is provided in Fig. 3.1. In this method, the trial slip surface is represented by the arc of a circle where the arc is the portion of a circle that cuts through the slope. Since a circle can be defined by specifying the x-y coordinate of the centre and the radius, a wide range of trial slip surfaces can be specified with a defined grid of circle centres and a range of defined radii (Geo-Slope, 2007). The points above the modelled slope in Fig. 3.1 represent the grid of rotation centres where each grid point is the circle centre for the trial slip surfaces.

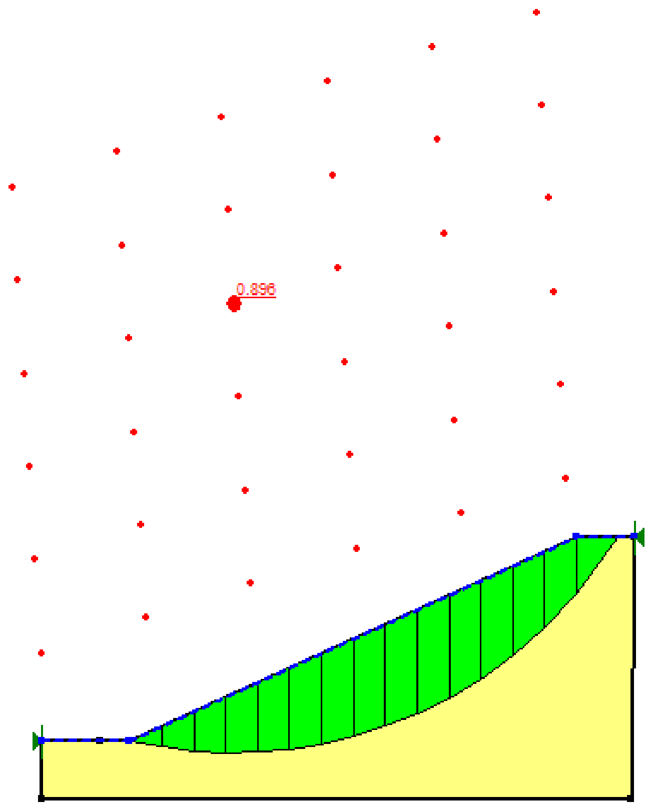

Figure 3.1: Critical slip surface and Factor of Safety by the Bishop method in SLOPE/W for the case of no vegetation

The resulting FOS from SLOPE/W was 0.896 using the Bishop method of analysis. The documented FOS using SLIP4EX is 0.88 (Norris and Greenwood, 2006) which is 1.6% less than that obtained from SLOPE/W. The difference may be attributed to the assumed slope height and number of slices analyzed.

3.3 Sensitivity study of plant root functional traits and root strength properties using SLIP4EX

Since SLIP4EX is not able to determine the location of the critical slip surface, the critical slip surface obtained using the grid and radius method in SLOPE/W was input into the SLIP4EX program together with the previously mentioned root and soil characteristics from Table 3.1. The resulting FOS was 0.90 by the Bishop method of analysis which is 2% greater than the 0.88 FOS as reported in the case study that was conducted in section 3.1 and 3.2 above. The difference may be attributed to the specified critical slip surface from SLOPE/W as well as the assumed slope height and selection of the number of slices analyzed. This data (the soil and plant root characteristics in Table 3.1 as well as the location of the critical slip surface from SLOPE/W) in SLIP4EX was used as the "control model" for the sensitivity analysis to follow.

In order to carry out the sensitivity analysis for the parameters required in the SLIP4EX program, a range of plant root functional traits together with root strength properties were sought from previous literature studies. The parameters were each individually varied in turn while all the other variables in the control model remained constant. Table 3.2 provides the range of values for the plant root functional traits and root strength properties used in the sensitivity analysis.

The graphical representation and discussion of the sensitivity for each root functional trait and root strength property is provided in Appendix A (Figure A1-A8). For each input variable the FOS is determined using both the Greenwood Simple Method (equation 2.15 on page 41) and the Greenwood General Method (equation 2.13 on page 41).

Figure 3.2 shows how the slices are taken as a proportion of the length of the critical slip surface along the bank, in order to clarify in which section along the bank the vegetation was positioned in the investigation. This is an important consideration because vegetation position is one of the variables that are altered in the sensitivity analysis that follows, and as Table 3.2 shows, the vegetation position covers three different slices for each run of the analysis. The figure also illustrates the increased depth of the piezometric head below the ground surface.

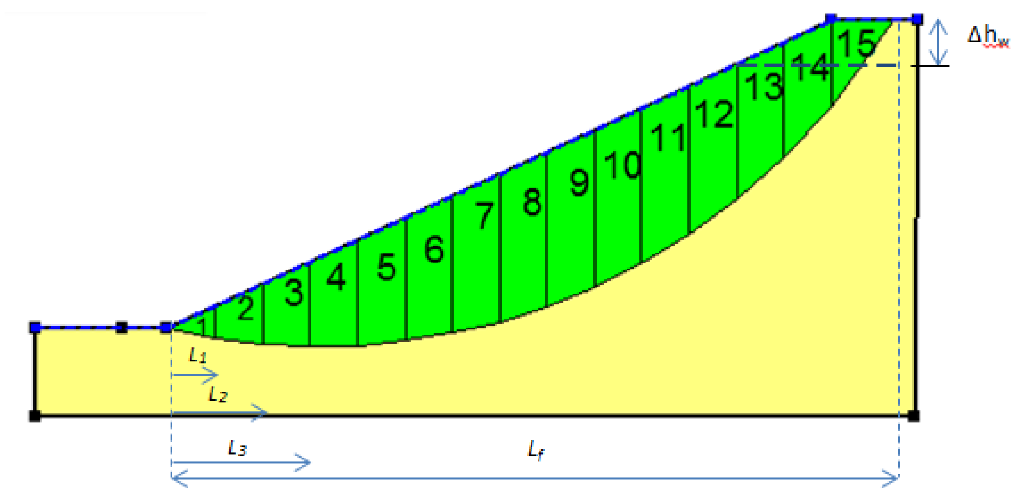

Figure 3.2: Slices are proportioned from the toe of the bank to the bank crest

In Fig.3.2, L_f is the length of the critical slip surface along the bank which is 17 m for this example. The soil slices are equally divided into 1.13 m each.

Table 3.2: Range of values for the plant root functional traits and root strength properties used in the sensitivity analysis

Plant root functional traits and root strength properties	Range of values	Increment	Source
Root diameter	Fine roots: 0.5-2 mm Coarse roots: >2 mm	0.2 mm	Adhikari et at. (2013)
	D<25 mm		The maximum root diameter reported by Riestenberg and Sovonick-Dunford (1983)(in Wu (2013)) for sugar maple (*Acer saccharum*).
***Pull out strength**	2.5-42 MPa	2.5 MPa	Norris and Greenwood (2006) found the range of tensile strength for various plant species to lie between 5-60 MPa and the pull-out strength (MPa) within 50-70% of the tensile strength.
***Additional cohesion due to roots (to depth of slip surface)**	2-12 kN/m^2	2 kN/m^2	Varies depending on vegetation, soil type and location. Range for silt loam soils under alder (*Alnus*) in a Japan nursery is used from Endo and Tsuruta (1969) (cited in Norris and Greenwood (2006)).
Number of roots per square metre	2-15	1 root	This parameter is not well documented. Norris and Greenwood (2006) use 2 and 4 for hawthorn roots. Habibah et al. (2013) tested roots from a 50 cm square trench and accounted for up to 140 roots.
Angle between root and slip surface	30°-45°	2°	Mattia et al. (2005)(in De Baets et al. (2008))
***Influence of the vegetation on pore water pressure**	0-0.2 m reduction due to vegetation	0.02 m	The influence of vegetation on the soil suction is not well documented (Ridley et al., 2003).
Surcharge load due to weight of vegetation (from roots and above ground biomass)	0-5 kN/m	0.5 kN/m	A rough estimation for different species (Tiwari et al., 2011).
Vegetation's position along the bank (Slices are numbered from the toe of the bank to the bank crest as shown in Fig. 3.2)	1-15 slices	3 slices	Vegetation positioning is critical in bank stabilization (Van De Wiel and Darby, 2007).

*Root strength properties

3.4 Deductions from the sensitivity analysis

For all of the sensitivity plots (Figure A1-A8 in Appendix A), except Fig. A7, the results obtained from the Greenwood General Methods produce the same trend as the Greenwood Simple method but with lower FOS values. A comparison of the methods suggests that the Greenwood General method is more conservative than the Greenwood Simple method. Greenwood (2006) reasons that the Greenwood General equation is more suitable since it results in practical estimates of the FOS for all slope and hydrological conditions and it may easily account for vegetation and reinforcement forces. The Greenwood General Method assumes that the phreatic surface is parallel to the slip surface, and no alternative scenario was investigated in this study. The results from the Greenwood General Method in Appendix A are used to plot the Tornado chart in Fig. 3.3, because the general equation is reported as being more suitable than the simple equation. The base case is taken as the FOS obtained in the control model, using the Greenwood General Method which corresponds to a FOS of 1.04. The parameters compared below are plotted around their respective relationship to the base case and its resultant FOS value. Other than this, the parameters do not have any commonality besides that they are all root functional traits and root strength properties and they may be plotted to the same scale due to the fact that each parameter is only varied within its respective range that is deemed most practical from the literature. Because they are each varied within their most practical ranges, the comparison is relevant and the resulting FOS values may be compared to one another for sensitivity purposes.

The Tornado plot clearly illustrates to which input parameters the FOS is most sensitive. However, the individual sensitivity plots in Appendix A indicate the change in magnitude of the FOS as the input parameters increase. The SLIP4EX program is more sensitive to pull out strength and number of roots per square metre of soil for large root diameters, and less sensitive to finer roots as shown in the sensitivity study presented in Appendix A.

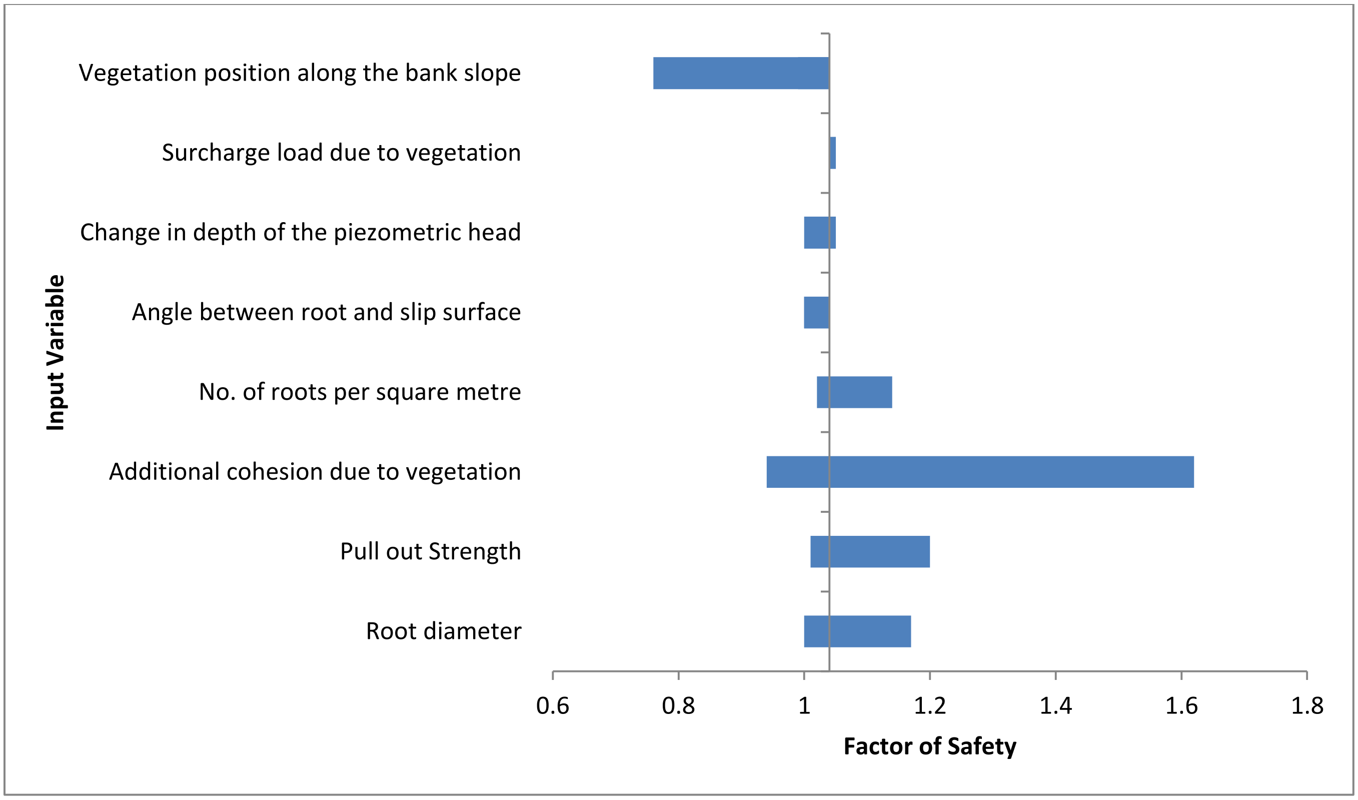

Figure 3.3: Tornado chart to illustrate the sensitivity of FOS to the input parameters

The most influential factor was identified as the additional effective cohesion. The increase in average piezometric head at the base of the slice was also found to significantly influence the stability of the slope as indicated by the FOS. The limited understanding of the influence of vegetation on soil pore water pressure poses a challenge in quantifying the mechanical and hydrological effect of vegetation on soil stabilization. The angle between the roots and the slip surface is insensitive for the range of angles investigated and suggests that an angle of 45° is an adequate approximation.

3.5 Further observations from the SLIP4EX program

Determination of the critical slip surface using SLIP4EX is time consuming as the user is required to input the slice information (slice height, slice width and base angle) for each trial slip surface investigated before the critical slip surface with the lowest FOS is identified. The process would be repeated for changing bank properties such as bank height, bank angle and soil properties. The program assumes that the mechanical and hydrological effects of the vegetation are effective to the depth of the specified critical slip surface without accounting for the length of the plant roots.

The shortcomings of SLIP4EX suggest that it cannot be used alone for the purpose of this study. This investigation will incorporate the methodology from SLIP4EX from the manner that it was utilised throughout the sensitivity analysis, but will use commercially available geotechnical software to uniquely implement these principles in accounting for the root functional traits along a riverbank.

Chapter 4 Methods and procedures of research

This investigation, concerning the effect of plant root functional traits on the stability of banks, centered on the increase in cohesive strength due to root reinforcement. Simulations for different soil types, bank slopes, bank heights and hydrological conditions and were first assessed for stability without the effect of vegetation. The focus was on slopes prone to shallow mass movement as a result of natural events such as storms.

In this study the two influential factors that limit the suitability of vegetation as a stabilizing method are: the depth of the critical slip surface, and the ability of vegetation to increase the stability of the bank to a factor of safety that represents stable conditions. It was identified from the deductions made from Figure 3.3 of section 3.4 as well as in the literature review in chapter 2, that the most significant factors are the pull out strength, the root diameter, the root density, the root length and the additional effective cohesion. The selection of the particular root functional traits required to achieve stabilization for certain riverbank scenarios are included in this chapter.

Numerical modeling using commercially available geotechnical software was used to conduct the methods and procedures as outlined below, and although the concepts are similar to recent research (the Fiber Bundle Model, RipRoot and SLIP4EX) the software is more easily accessible than those more advanced modelling procedures. Furthermore there are limited models that consider vegetated slopes through a multidisciplinary approach (Stokes et al., 2009). This investigation looks into the stability of vegetated slopes by considering the interaction between soil, water, and plants. The procedure outlining how the features in the geotechnical software were used to include the reinforcing effect of vegetation roots is described in this chapter.

Furthermore, the procedure used to obtain the flood conditions for South African rivers using the method developed by the Hydrological Research Unit is outlined in this chapter.

4.1 Experimental justification

The commercially available computer programs SLOPE/W (2007) and SEEP/W (2007) were used to model the riverbanks. Although more advanced computer programs have recently been developed to model the effects of vegetation, as summarized in section 2.8, these programs are only available in the research arena and not yet available to practitioners. Furthermore, since these computer programs have only recently been developed, their limitations are not yet fully understood. This investigation aims to use existing and easily available technology to account for the effect of root reinforcement on riverbanks.

In SLOPE/W, the geometry of the riverbanks was modeled and the soil strength criteria were defined as cohesion, unit weight, and friction angle for each soil type considered. SLOPE/W also allowed for the effect of vegetation to be incorporated into the riverbanks through its ability to adjust the soil cohesion at specified regions within the bank. The stability of the banks was assessed using the Morgenstern-Price limit-equilibrium formulation, since the method accounts for both force and moment equilibrium which improves the accuracy of the FOS calculation and it allows for various user-specific inter-slice force functions, with and without the effects of vegetation and various flood conditions. The critical slip surface and the factor of safety at each stage of the analysis were obtained using the auto-locate function in SLOPE/W. The auto-locate function provides a reasonable result since 1000 trial slip surfaces are generated in SLOPE/W to locate the most probable minimum FOS slip surface before further optimization is performed (SLOPE/W, 2007). For each analysis, a reference value of 30 slices was specified for systematic convergence purposes, since a greater number of slices creates an excessive amount of unnecessary data without a significant improvement in the safety factor accuracy.

SLOPE/W was coupled with a SEEP/W, transient seepage analysis to determine how the phreatic surface would change during flood events. SEEP/W was used to investigate the effect of both flood duration and river drawdown on bank stability in terms of the factor of safety. The results were used to develop a preliminary design-aid to facilitate the assessment of the risk and provide a recommendation as to when vegetation would be a suitable stabilizing technique. The preliminary design aid is presented in chapter 5.

4.2 Specific aspects examined

The objective was to consider riverbank stabilization for the South African environment in terms of typical soil types, hydrological conditions, bank heights and bank angles for South African riverbanks.

4.2.1 Material parameters

Although riverbanks may consist of various soil types, only homogeneous banks were considered in this investigation. The practitioners using the guideline provided in chapter 5 would need to establish which soil type is most prominent for the problem site and use that soil in the decision making process. Four conceptual soil types were considered in this study, where their D10 and D60 values are presented in Table 5.2 and Table 5.3 respectively, and the liquid limit for each soil type is also detailed in Table 5.3 in section 5.2.1. These parameters were chosen to represent four broad groups of soil: a clay soil, a silt loam soil, a loamy sand and a gravel, since they encompass the main soil types across the country (State of Rivers Report, 2001 and Sieben, 2000). The strength of these soils was defined by the Mohr-Coulomb criteria as summarized in Table 4.1.

Table 4.1: Soil strength criteria

Property	**Soils**			
	Clay	**Silt loam**	**Loamy sand**	**Gravel**
Cohesion (kPa)	15	7.5	1	0
Friction Angle (°)	23	30	25.5	32
Unit Weight (kN/m^3)	21	16	19	25.5

After Vandamme and Zou (2013) and Geotechdata.info (2013)

SEEP/W requires the definition of a volumetric water content function (VWC) and a hydraulic conductivity function (KF) to model transient seepage. SEEP/W (2007) describes the VWC function as the volume of the voids that remain water-filled as the soil drains and the KF function as the ability of a soil to convey water under both saturated and unsaturated conditions. The VWC for the silt loam and loamy sand were estimated using the modified

Kovacs formulation within SEEP/W using the parameters given in Table 4.2 (SEEP/W, 2007). The VWC for the clay and gravel soils was estimated using the sample functions in SEEP/W and the parameters in Table 4.2. To obtain the KF the van-Genuchten formulation in SEEP/W was used. The coefficient of permeability or hydraulic conductivity influences the amount of water passing through the soil and hence is a function of the negative pore-water pressure in the soil. This relationship exists since the coefficient of permeability (which influences water movement through a soil mass) is affected by the state of the soil particles within a soil mass, and this in turn is affected by the state of the negative pore water pressures. The coefficient of volume compressibility (m_v) describes how much a saturated soil volume will swell or shrink for a given change in pore-pressure, and was assumed to be 1e-5 /kPa for all soils. This value is recommended in the SEEP/W Users Guide (Geo-Slope, 2007) for unsaturated soil seepage problems, since the value is only sensitive to analyses involving coupled stress and pore-pressure systems, which not done in this study was. This involves consolidation type simulations in which the stresses and resulting strains of material are calculated based on the geotechnical properties of the slope and the movement of pore water pressure analyses.

Table 4.2: Soil permeability criteria

Property	**Soils**			
	Clay	**Silt loam**	**Loamy sand**	**Gravel**
Saturated Volumetric Water Content (m^3/m^3)	0.5	0.5	0.4	0.4
Residual Water Content (m^3/m^3)	0.07	0.02	0.04	0.04
Saturated Permeability (m/s)	1.7e-7	1.9e-6	1.7e-5	0.01
D_{10} (mm)	-	0.0017	0.041	-
D_{60} (mm)	-	0.028	0.47	-
Liquid limit (%)	-	25	27	-

After, Rawls et al. (1982), Thoma et al. (2013), Gurdal et al. (2003), Sivakugan (2000), Ward (2007) and Bowerman (1999).

4.2.2 Riverbank geometries

Riverbank angles of 1:1 and 1:2 (vertical:horizontal) were analysed for all soil types, and under all drawdown conditions. In addition, a 2:1 slope was analysed for the clay and silt loam soils, and a 1:3 slope was analysed for the loamy sand and gravel. Bank heights ranging from 1.0 m to 10.0 m were investigated.

4.2.3 Flood events

In order to evaluate the effect of flood conditions on the stability of a riverbank, flood conditions were modelled in SEEP/W as hydraulic boundary conditions in terms of change in stage (the height of the water level against the river bank) per unit time. The initial water level, for each riverbank, was assumed to be one-third from the bottom of the bank height. Furthermore, the initial phreatic surface within the bank was assumed to be level with the river. Three flood duration conditions and three drawdown rates were considered. This resulted in nine different combinations of flood duration and drawdown rate. Each flood event was simulated by raising the water level from the initial level to full bank height, maintaining it at this level and then lowering it to the initial water level. A short flood was defined as an increase of stage (rate at which water elevation increases) of 0.890 m/h, a medium flood by an increase of stage of 0.224 m/h and a long flood by an increase of stage of 0.023 m/h. It is noted that the units of m/h used here refers to metre per hour. The river's water level was then kept at the full bank level for a period equal to that required to reach this level. Drawdown rates considered (drawdown of the river level, or stage) were 0.380 m/h, 0.224 m/h and 0.023m/h for rapid, medium and slow drawdown rates respectively. These flood durations and drawdown rates were based on measured hydrographs from the Klip River (CSRA, 1994 and SANRAL, 2006) and the Berg River (DWAF, 2007). The nine combinations of flood duration and drawdown rates, for bank heights between 1.0 m to 10.0 m, are included in Appendix B. The change in the phreatic surface was simulated in SEEP/W, providing the pore-water pressure conditions at various points in time. The subsequent changes in stability from the time-varying pore-water pressure results in SEEP/W were analysed in SLOPE/W.

4.2.4 Failure mechanisms

Slip failure, a type of mass failure, is the failure mechanism of interest in this study (Fig. 4.1). Mass failure is the general term that is used to define the slope failure mechanism that arises when any occurrence leads to the weight of the bank producing cumulative stresses that are greater than the overall shear strength of the soil along a particular critical surface within the bank (Jaksa et al., 2013). Thorne (1990) noted that mass failure depends on the bank geometry, the soil type, and the type and density of the vegetation. Furthermore, mass failures often occur following floods. Hydrological conditions that result in overbank flooding, followed by a rapid drawdown, contribute to bank failure (Morgenstern and Price, 1965).

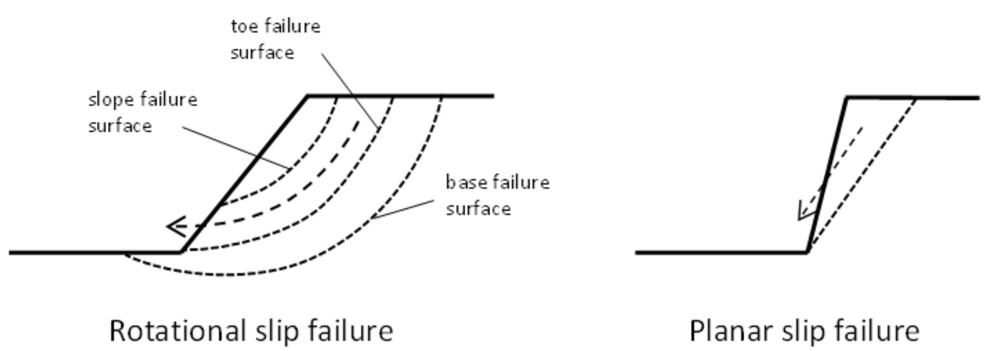

Figure 4.1: Cohesive bank failure mechanisms (after ASCE Task Committee on Hydraulics, Bank Mechanics, and Modeling of River Width Adjustment, 1998)

Vegetation is unlikely to have a significant effect on slope stability for deep-seated slip planes, due to the shallow rooting nature of many plant species. The study is limited to shallow translational slide failure (which is indicated as the slope failure surface in Figure 4.1) since deep rotational slips at depths greater than 2.0–3.0 m would be out of the zone of influence of many plant roots (Norris et al., 2008). Thus, banks which resulted in failure with deep rotational slips were considered unsuitable for root stabilization.

4.2.5 Bank stability without vegetation

The stability of the banks was defined by the guideline developed by Hubble (2010) given in Table 4.3. A factor of safety of less than 1.3 was used as an indicator of an unstable slope

(Hubble, 2010; Mulder, 1991). The methodological approach was to determine the factor of safety for each slope under the initial conditions, then at each stage of a flood event. The lowest FOS determined was then recorded. For each slope, at the time step of the lowest FOS, the maximum depth from the bank surface to the critical slip surface was recorded and is given in Appendix C. Illustrations of this depth variable are provided in the results section, chapter 5 (Figure 5.2), of this report. The recording of this depth is important to determine if the bank meets one of the minimum requirements, that of limiting depth, in order to assess the appropriateness of vegetation roots as a stabilizing method, this assessment is detailed in section 4.3.2.

Table 4.3: A suggested guideline for describing the slope stability of river banks (Hubble, 2010)

Factor of Safety	Probable Bank Stability Condition
Greater than 2.00	Stable
1.51 to 2.00	Probably Stable
1.31 to 1.50	Moderately Stable
1.10 to 1.30	Conditionally Stable
1.00 to 1.10	Critically Stable
0.91 to 0.99	Unstable
0.71 to 0.90	Very Unstable
0.50 to 0.70	Highly Unstable
Less than 0.50	Extremely Unstable

4.3 The contribution of vegetation roots to slope stability

For the cases where vegetation stabilization is an appropriate bank stabilization technique, the influence of vegetation was applied to the various models to determine which combination of root reinforcing properties is required to stabilize the banks. From the sensitivity analysis in chapter 3 and the literature review in chapter 2, it is clear that the most significant root functional traits are: root diameter, root density (number of roots per square metre of soil), and root length. Other important properties are the pull out strength or root tensile strength and the additional effective cohesion.

4.3.1 Simulation of vegetation stabilization

The root functional traits were taken into account by introducing additional cohesion provided by the roots into the slopes. The standard geotechnical strength parameters in SLOPE/W allowed for the cohesive strength to be modified simulating the effect of plant roots, where the properties of the roots were represented by the region of enhanced cohesion. The concept is supported by Gray and Leiser (1982) suggesting that intermingled roots of plants tend to bind the soil together in an apparent cohesion. However, because of their random orientation, the roots have a negligible influence on the frictional component of soil strength (Gray and Leiser, 1982).

4.3.2 Depth of root reinforcement

Waldron and Dakessian (1982) found that both thick and fine roots act in tension during slope failure, and provide a significant contribution to slope stability when they cross the slip surface. The regions of enhanced cohesion (as mentioned in section 4.3.1) were selected so as to penetrate below the critical slip zone in order to achieve adequate anchorage, through the additional cohesion provided, as would be the requirement for roots according to Gray and Sotir (1996).

This study is limited to shallow slip failure. A maximum depth of slip failure of 2.0 m was considered as the limiting depth to which vegetation roots are an appropriate stabilizing method, since roots rarely penetrate beyond a 2.5 m depth (Watson and Loughlin, 1990; Stokes et al., 2009; Price and Lovett, 2002; Norris et al., 2008). Hence, for slip surfaces greater than 2.0m, vegetation stabilization alone is not a recommended bank stabilizing technique. This is an applicable limitation since Perry (1989) determined that for many cut-slopes and embankments, the slip surface is most likely to be circular and at a depth of 1.5-2.0 m. In this study, the root functional traits, in terms of additional cohesion, were modeled to just cross the critical slip surface and the depth was increased in 0.1 m increments (but no further than a depth of 2.5 m) until the factor of safety that represents stable conditions (that is 1.3) was reached.

It has been shown by Steele et al. (2004) that the planting technique may greatly influence the rooting depth and further that it is possible to manipulate the depth at which rooting occurs. For example, where traditional planting methods would not normally reach a depth of 2.0 m below the surface, live willow stakes can be planted at this depth provided that anaerobic conditions are not present.

4.3.3 Stability analysis

Literature was studied to determine the maximum recorded increase in the FOS with the introduction of vegetation. Simon et al. (2002) determined a maximum increase in the FOS from 0.98 to 2.01 for *river birch*, in their experiment of the hydrological and mechanical effects of four riparian tree species and grasses on bank stability. This relates to a multiplication factor increase of 2.05 that vegetation may contribute to bank stability in terms of the factor of safety, calculated by dividing the factor of safety of the bank with vegetation by the factor of safety of the bank without vegetation as recorded by Simon et al. (2002). The limiting FOS to which vegetation roots are an appropriate stabilizing method was determined by reverse calculation, dividing 1.3 (the FOS that represents stable conditions) by 2.05 (the maximum increase factor). Thus, in this study, a limiting FOS of 0.63 was considered as the minimum FOS to which root reinforcement may be considered an appropriate bank stabilizing method.

The limiting depth of slip failure of 2.0 m and the limiting FOS of 0.63, to which vegetation stabilization was considered an appropriate stabilizing technique, were both applied as limiting considerations to the established boundary values in section 4.2.5 and Appendix C. This was in turn used to develop the design-aid for determining the feasibility of using vegetation for bank stabilization, which is included in chapter 5.

4.3.4 Root orientation

From the sensitivity analysis in chapter 3, it was found that the orientation of the roots to the slip surface was not influential on the FOS for the range of angles investigated. In the SLOPE/W models that include the effect of vegetation, the zone of increased cohesion due to root reinforcement was orientated perpendicular to the slope face since it has been shown that a perpendicular orientation of the roots to the shear surface is a good average of all possible orientations (Gray and Ohashi, 1983). This was done by defining points below the slope, perpendicular and to the depth of influence of the roots, using the KeyIn Points function in SLOPE/W and using those points to create a new region of enhanced soil cohesion due to the vegetation (an example and illustration is provided in section 5.3).

4.3.5 Enhanced cohesion due to vegetation

In the simulations, which are included on a CD-ROM in Appendix D, where vegetation stabilization was found to be an appropriate bank stabilization technique, additional cohesion values were added to the cohesion of the soil in the SLOPE/W model to the depth below the critical slip surface to account for the soil binding effect of the roots. Root cohesion is a function of depth and reduces significantly with increased depth below the soil surface (De Baets et al., 2008). For critical slip surfaces greater than 2 m in depth, the effect of additional cohesion was not considered in this study.

In SLOPE/W, the shear strength of the non-rooted soil was defined by the Mohr-Coulomb equation:

$$\tau = c + \sigma_n tan\Phi \quad (4.1)$$

where τ is the soil shear strength, c is the soil cohesion, σ_n is the normal stress on the shear plane and Φ is the angle of internal friction of the soil (Geo-Slope, 2007).

When the soil is rooted, the increased shear strength is expressed as an additional cohesion (Wu et al., 1979):

$$\tau_r = \tau + C_r \quad (4.2)$$

where τ_r is the shear strength of the soil reinforced by roots and C_r is the increase of shear strength due to the presence of roots (or root cohesion).

In this study, the additional root cohesion is determined using the model developed by Wu (1979) and extended by Waldron (1977),

$$C_r = RAR \times T_r \times K \tag{4.3}$$

where RAR (%) is the root area ratio (for all soil planes), T_r is the root tensile strength and K is the factor accounting for the decomposition of T_r according to the normal and tangential component on the shear plane (Hudek, 2013) as shown in Figure 4.2.

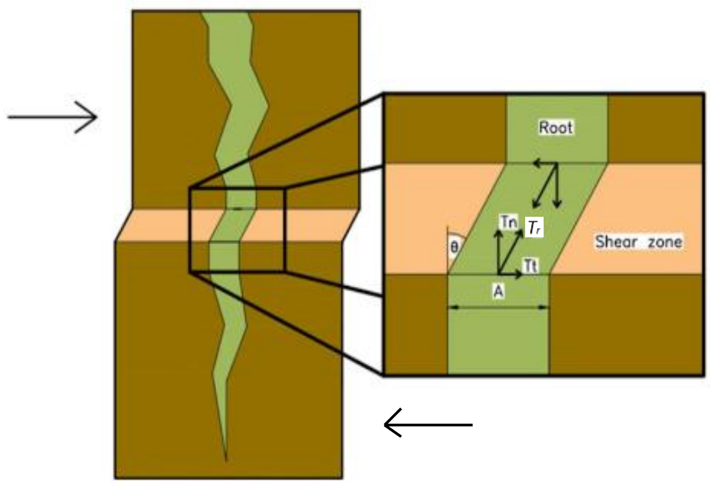

T_n- normal component

T_t- tangential component

Figure 4.2: Stresses in the root during shear (after Dias et al., 2017)

Although it was identified that pull out strength is one of the most significant root functional traits, the tensile strength of a root is a reasonable indicator of the maximum pull out resistance available (Norris, 2005a). Furthermore, the pull out strength may be estimated as 40% of the tensile strength, as found in field experiments by Norris and Greenwood (2006). The pull out strength can be obtained in the field by attaching a loading rig to the in situ root and measuring the vertical displacement, using a dial gauge, while a pull out force is applied to the root at a constant rate until failure of the root system (Osman et al., 2011). In the laboratory, root tensile strength can be determined by clamping the root using wedge grips or similar equipment, at each end of the root and using a test rig such as the Hounsfield Tensometer Apparatus (Nyambane and Mwea, 2011) or the Universal Testing Machine (Osman et al., 2011) to apply a load at a constant rate, whilst measuring and recording the force and extension at failure as well as the initial length of the exposed root.

The expression for the variable K as used in equation 4.3 above is given as:

$$K = \sin\theta + \cos\theta \tan\Phi \tag{4.4}$$

where θ is the angle of root distortion (shown above in Figure 4.2) in the shear zone. In this study θ is taken as 45° as it was found by Waldron (1977) to vary between 40° and 50° for various root-permeated soils.

The K values that were used to determine the cohesion in the four soil types are summarized in Table 4.4.

Table 4.4: *K* values for the various soils

Soils	***K***
Clay	1.01
Silt loam	1.12
Loamy sand	1.04
Gravel	1.15

The *K* values are in the range of 1.0 to 1.3 as found by Gray and Barker (2004).

The root area ratio (*RAR*) was calculated using equation:

$$\text{RAR} = \sum \frac{A_r}{A} \tag{4.5}$$

where A_r (mm^2) is the total cross-sectional area of roots intersecting a soil profile and A (mm^2) is the total cross-sectional area of the soil profile (Hudek, 2013, Naghdi et al., 2013). The full range of RAR for *Alnus* roots was found to be 0.0002% to 0.488% (Naghdi et al., 2013).

According to Gray and Sotir (1996), Norris (2005b), Mattia et al. (2005) and numerous other authors, the root tensile strength T_r decreases with increasing root diameter (*D*), following a power law equation:

$$T_R = \alpha . D^{\beta} \tag{4.6}$$

where α is a scale factor and β is the rate of strength decrease depending on the type of plant species.

The T_R-*D* relationships developed by Operstein and Frydman (2000), Nyambane and Mwea (2011), De Baets et al. (2008), Mattia et al. (2005), Naghdi et al. (2013), Preti and Giadrossich (2009), Danjon et al. (2008), Hengchaovanich and Nilaweera (1996) and Ghestem et al. (2014)

were used to estimate values of tensile strength for the diameter range applicable to the various models, as presented in Appendix G.

The methodological approach used in modeling the effect of plant roots in bank stability is summarized as follows:

a) A trial and error approach was adopted, where initially the depth of the roots was assumed to be just below the maximum depth to the critical slip surface (as determined for a slope with no root reinforcement).
b) For the length of root estimated in (a), an estimate of the diameter of the roots and the number of roots (root density) was made using the guideline presented in Appendix G. The number of roots was estimated from what was reported from various studies (reference numbers 26-28 in Appendix G) which provided an indication of realistic root density ranges.
c) The *RAR* was calculated using equation 4.5 and the root diameter and number of roots per square metre of soil as estimated in (b). A result of *RAR* was considered acceptable if it lay in the full range from 0.0002% to 0.488% as found by Naghdi et al. (2013) in the study of *Alnus* roots.
d) The tensile strength was then calculated using the assumed root diameter in (b), which is based on a reasonable estimate and not on any one specific value in Appendix G, and the applicable T_R-*D* relationships in Appendix G for that estimated root diameter and corresponding root depth. The guideline in Appendix G was used to check that the tensile strength values calculated corresponded to actual values as found in the literature for plant species in the diameter range assumed.
e) The additional root cohesion was then determined using equation 4.3 and *K* values in Table 4.4. The additional root cohesion calculated was compared to that found in literature, from the corresponding T_R-*D* model, as summarized in Appendix G.
f) The additional root cohesion was then added to the cohesion of the soil to the depth of the roots as assumed in (a).

g) The FOS was then determined for the new worst case critical slip surface, based on the new soil properties due to the additional cohesion. If the resulting FOS was equal to or above the stable FOS of 1.3, then the root functional traits and root strength properties were considered suitable for bank stabilization. However, if the resulting FOS was below 1.3 then a new diameter and/number of roots was chosen such that the root-soil cohesion was greater than the previously calculated additional root cohesion (this is achieved by decreasing the root diameter estimate and increasing the root density, by conservative amounts relative to the overall limits presented in the literature) and the process from (b) to (g) was repeated until the FOS representing stable conditions was reached or maximum additional cohesion for that root depth and root diameter was reached (according to the guideline in Appendix G, and in this case, specific to the additional cohesion values reported in the literature).

h) If the maximum additional cohesion was reached for the root depth considered in (b) by appropriately varying the root diameter and number of roots (*RAR*) but the bank FOS failed to reach the 1.3 stable condition, the root length was increased in increments of 0.1 m to a maximum depth of 2.5 m until stability was reached. And the entire process repeated.

In this study, it is the tensile strength of the roots that is determined using the root functional traits and T_R-*D* relationships developed in literature. The additional cohesion due to vegetation is then calculated (using equation 4.3) based on the tensile strength and additional root functional traits. Hence, in the study one root strength property (additional cohesion due to roots) is determined using the other (tensile strength) and only one is simulated (additional cohesion due to roots) to account for the effect of vegetation.

The results are tabulated in chapter 5 and represent the minimum requirements of the root functional traits that are required to stabilize the banks. Plant species that provide a greater number of roots with a smaller root diameter at the same depth or at a greater depth, than the values determined in Appendix H, would further enhance cohesion and increase bank stability. The models that account for the effect of vegetation roots by enhanced cohesion for the various bank types and flood conditions, that are suitable for bank stabilization, are attached in Appendix E. It must be noted that the type of plant species used, soil type, and rooting depth all influence anchorage (Nicoll et al., 2006 in Norris and Greenwood, 2006).

4.3.6 The effect of surcharge weight, wind forces and transpiration due to vegetation

The effect of the weight of the vegetation on the stability of the bank is not taken into account in the investigation as it is understood that the effect is negligible for grass, herbs and shrub vegetation (Norris et al., 2008). The surcharge weight of vegetation may cause instability problems for trees that are greater than 30 m in height with a total mass in the order of 2 kN/m2, according to Coppin et al. (1990) (in Norris and Greenwood (2006)). Furthermore, the analysis does not include wind forces, since these parameters cannot be determined from the root functional traits alone and above ground biomass would need to be considered. In addition, the transfer of water from the soil to the atmosphere by vegetation is not accounted for in the analysis since studies by Simon et al. (2006) indicate that the hydrological effects of roots (such as the removal of water by transpiration) contribute less to stream bank stability than the mechanical effects of roots.

4.4 Procedure to determine flood conditions for South African rivers

Two South African river systems were used to present a procedure for the evaluation of the potential use of vegetation to stabilise river banks. Due to the limited amount of relevant data available pertaining to river cross sections and rating curves, these aspects were approximated in the examples in section 5.3. The two river systems that were analysed are the Crocodile and Sabie-Sand River systems, both located in the north-eastern regions of South Africa.

The information required in order to adequately assess the applicability of vegetation use at a point in the river systems pertains to the design storm in the form of a direct runoff hydrograph for each section in the two rivers, which can then be paired with the assumed rating curve to determine the storm duration and maximum drawdown rate. The soil strata of the two river sections is also required for an accurate assessment to be performed.

In order to develop the necessary hydrographs, the storm rainfall hyetographs could be used for the two regions as well. There are processes available to design these hyetographs as presented by Smithers & Schulze (2002), and information on South African storm rainfall over a 24 hour period is also presented by Adamson (1981). Figure 4.3 outlines the numerous methods that may be used in design flood estimation. In the two examples that are presented in section 5.3 the Hydrological Research Unit (HRU) method was applied as developed by the Hydrological Research Unit (1972). The method involves the use of a synthesised unit hydrograph to develop a design storm for a catchment.

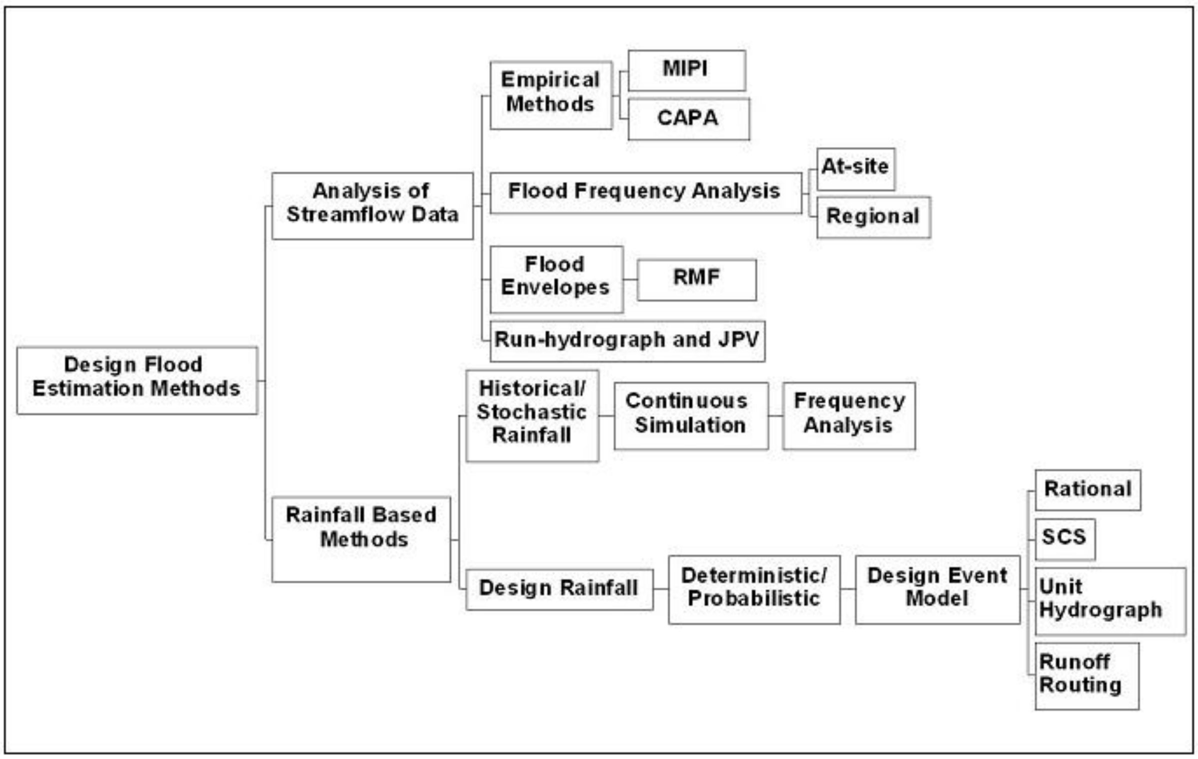

Figure 4.3: Approaches to design flood estimation in South Africa (after Smithers, 2012)

4.4.1 The HRU design storm method

The HRU method was applied to determine the peak discharge for a section in a river, as well as the flood hydrograph, pertaining to a certain recurrance interval. A synthesised unit hydrograph was coupled with excess storm rainfall in order to achieve this.

The methodological approach used to develop a synthetic unit hydrography (HRU method) is outlined below:

- Identify the zone for the required location using the diagram of generalised veld type zones in South Africa (Hydrological Research Unit, 1972).
- Obtain the dimensionless 1 hour unit hydrograph for the required zone from Regionally generalised dimensionelss 1-hour unit hydrographs (Hydrological Research Unit, 1972).
- Calculate the lag time (T_L) for the required catchment:

$$T_L = C_T \times (\frac{L \times L_C}{\sqrt{S}})^{0.36} \tag{4.7}$$

where T_L (hours) is the lag time, C_T is the lag coefficient from Hydrological Research Unit (1972), L (km) is the length of the longest stream to the catchment boundary, L_C (km) is the length from the centroid of the catchment area to the catchment boundary, following the longest stream and S is the average slope of the longest stream.

The average slope is calculated using the 10-85 method as developed by the US Geological Survey (SANRAL, 2013):

$$S = \frac{H_{0.85L} - H_{0.1L}}{0.75L} \tag{4.8}$$

where $H_{0.85L}$ (m) is the elevation height at 85% of the length of the watercourse, $H_{0.1L}$ (m) is the elevation height at 10% of the length of the watercourse and L (m) is the length of the watercourse.

- Calculate the peak discharge which is the peak of the unit hydrograph:

$$Q_P = K_U \times \frac{A}{T_L} \tag{4.9}$$

where Q_P (m^3/s) is the peak discharge, K_U is from the same table as C_T from Hydrological Research Unit (1972) and A (km^2) is the area of the catchment.

- Make the synthetic unit hydrograph dimensional:

Each x-ordinate: $(\frac{t}{T_L}) \times T_L$

Each y-ordinate: $(\frac{Q}{Q_P}) \times Q_P$

The above procedure produces a dimensional 1-hour unit hydrograph for the selected catchment.

The methodological approach used to develop a design storm (HRU method) is outlined:

- Choose a suitable recurrence interval.
- Choose a storm rainfall duration (hours).
- Use the coaxial plot in Figure 4.4, as presented by SANRAL (2013) to determine the point rainfall. From the storm duration select an inland or coastal region, then select the return period, then select the mean annual precipitation for the selected area, and then read off the amount of storm point rainfall in mm.

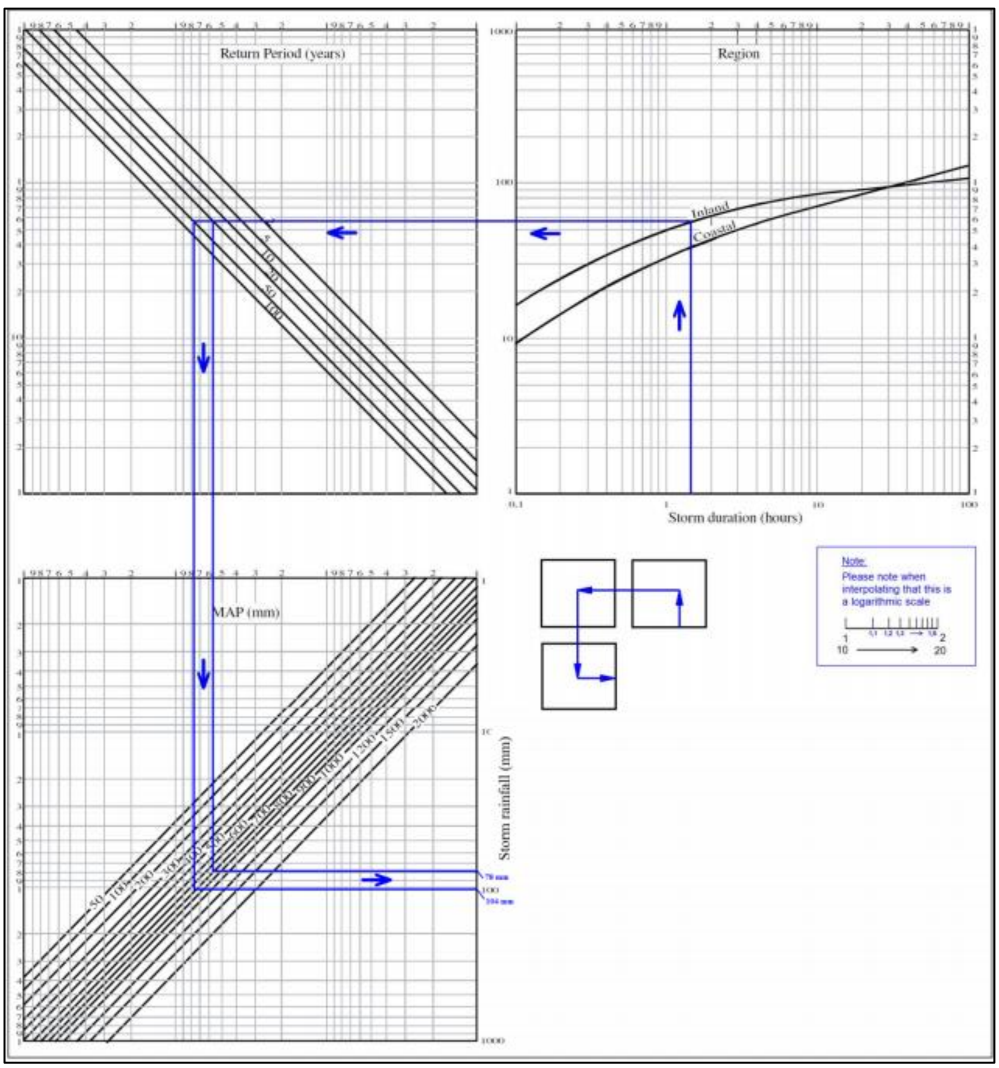

Figure 4.4: Depth-duration-frequency diagram to determine point rainfall (after SANRAL, 2013)

The mean annual precipitation may be approximated from Figure 4.5.

- The rainfall intensity is calculated as: the storm point rainfall divided by the storm duration (mm/hr)

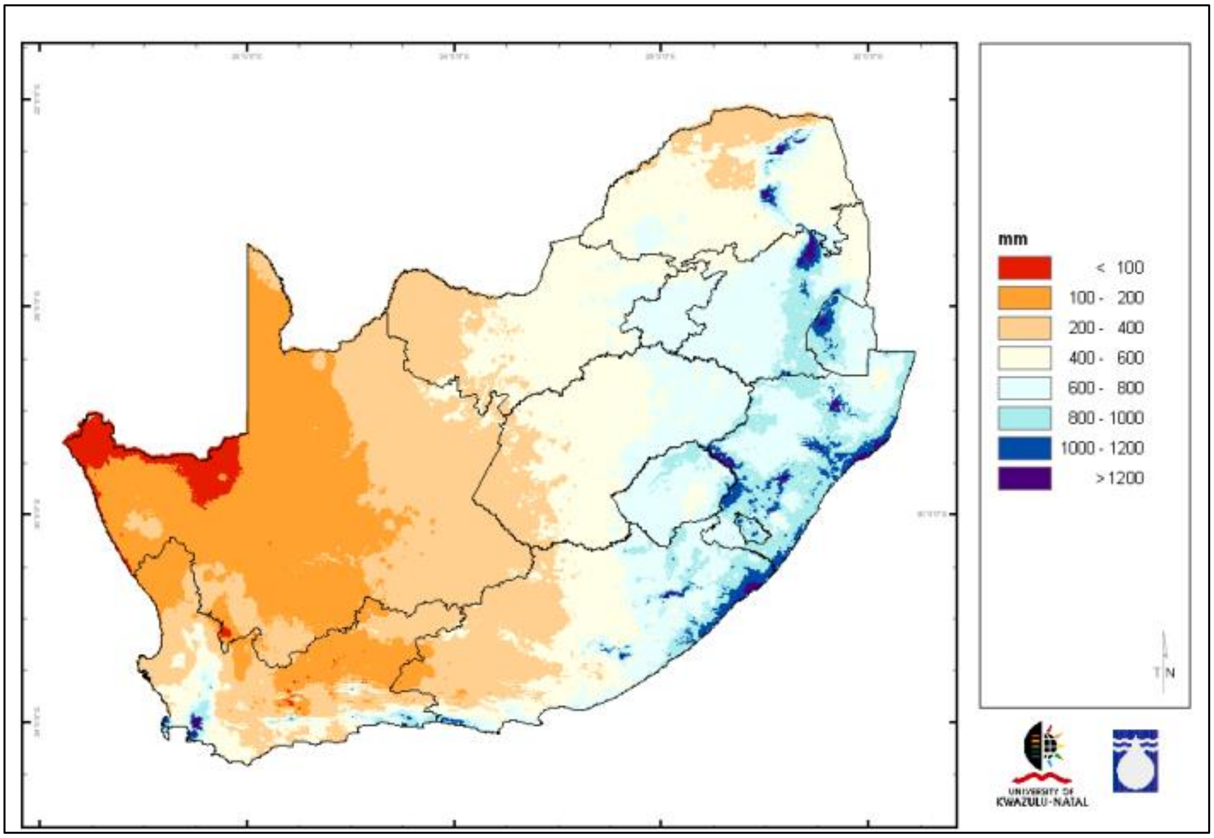

Figure 4.5: South African mean annual precipitation (after SANRAL, 2013)

- Apply the areal reduction factor using Figure 4.6. From the maximum point rainfall the average rainfall over the catchment is needed. Use the storm duration and the catchment area to determine the percentage of point rainfall to be applied, so that Areal rainfall is the areal reduction factor multiplied by the point rainfall amount (SANRAL, 2013).
- Account for rainfall losses over the catchment, since only the excess rainfall is required, by using Figure 4.7. Use the areal rainfall, the veld zone, and the catchment area to determine the percentage of storm runoff. The excess rainfall depth (direct runoff) is then the areal rainfall multiplied by the percentage of storm runoff (SANRAL, 2013).

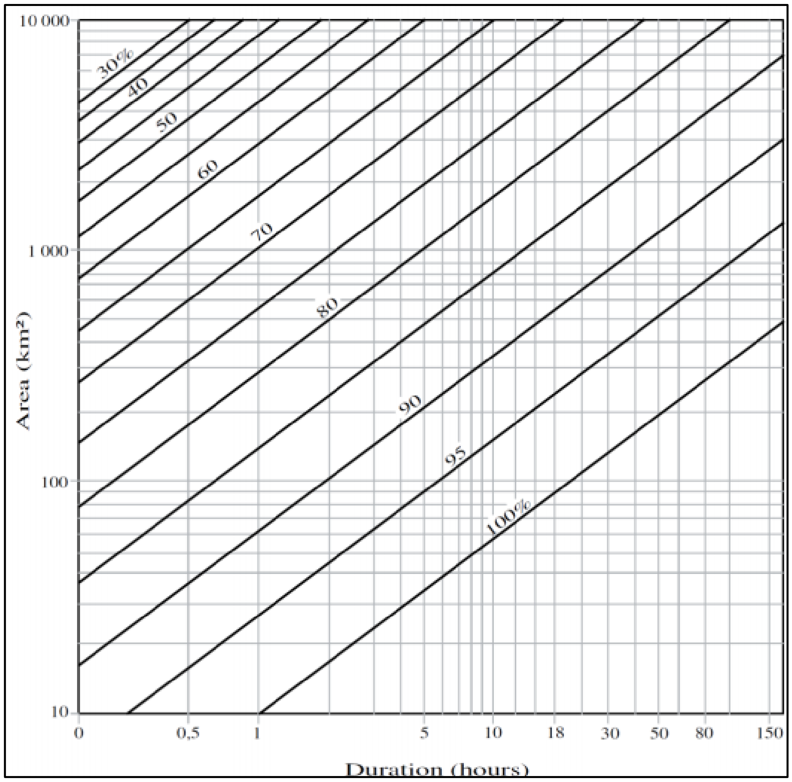

Figure 4.6: Area reduction factors (after SANRAL, 2013)

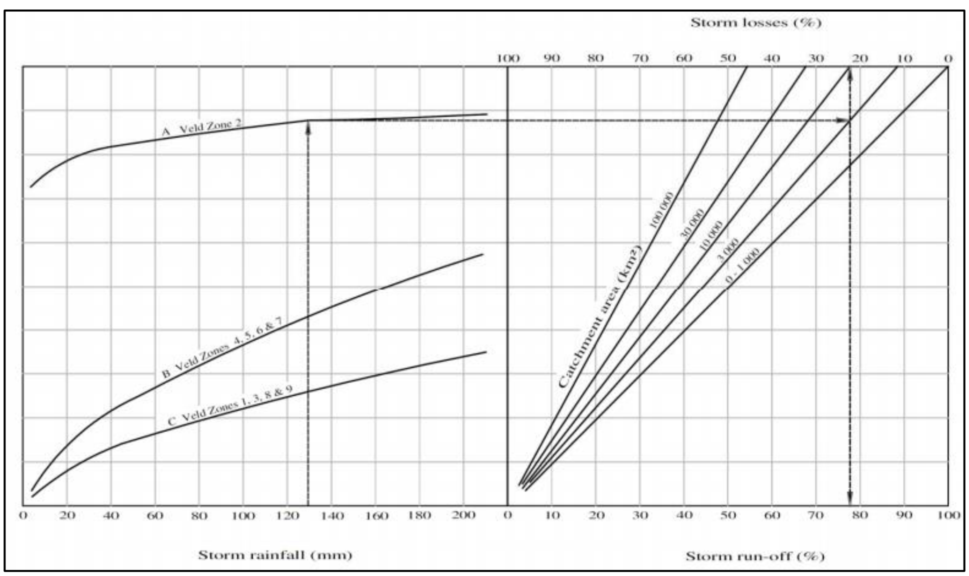

Figure 4.7: Average storm losses (after SANRAL, 2013)

- Obtain the 1-hour unit hydrograph for the catchment (procedure outlined above). The 1-hour unit hydrograph may be converted to the required storm duration hydrograph using the S-Curve technique as outlined by SANRAL (2013). However the hyetograph can be hourly in which case the 1-hour unit hydrograph can be applied to each hour of rainfall and then summed to form the total storm hydrograph.

- The flood hydrograph can then be drawn for the chosen return period and storm duration by applying the correct duration unit hydrograph to the correct duration excess rainfall intensity graph (hyetograph). The peak flood discharge (Q_P) is calculated as the unit hydrograph peak multiplied by the excess rainfall depth.
- In order to obtain the worst flood hydrograph for the chosen return period it is necessary to determine the corresponding storm duration. The above procedure is to be carried out at least three times for the same return period but for differing storm durations, and then a plot of Q_P versus duration of excess rainfall is developed and the peak of this plot corresponds to the corrected storm duration which is then used in the above procedure again to determine the corrected areal excess rainfall depth to be used with a corresponding unit hydrograph to obtain the worst flood hydrograph for the chosen area and return period.

A full description of the design storm method is outlined in section 3.1.1 of the 6th Edition of the SANRAL Drainage Manual (2013).

Flood routing methods may be used to determine the flood hydrograph for other sections of the river once the above method has been followed for a single section. Routing methods may be found in the 6th Edition of the SANRAL Drainage Manual, by SANRAL (2013).

Once the flood hydrograph is obtained, it can be used in conjunction with the rating curve for the same river section (a curve of stage versus discharge) to determine the rate of stage increase, and drawdown rate. The method is applied to two hypothetical examples for South African rivers included in chapter 5.

Chapter 5 Modelling outcome and results

5.1 Flood events and analysis of results, only considering when vegetation roots are a suitable bank stabilization technique

Figure 5.1 shows the results of a 3 m high, loamy sand riverbank with a bank angle of 1:3 under the initial conditions. It is clear from the displayed FOS value of 1.57 that the bank is stable under the initial conditions. Note that the dotted line denotes the initial water level at one-third from the bottom of the bank height. The water appears as a shaded region with water force arrows acting on the ground surface line.

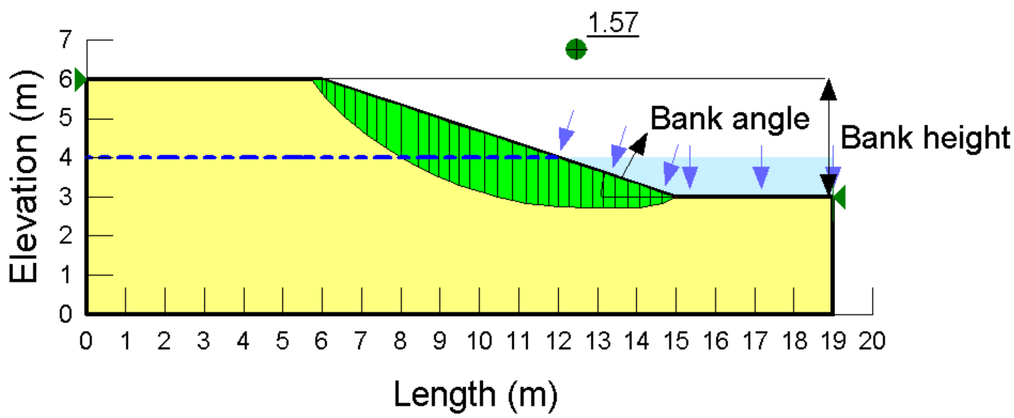

Figure 5.1: Example of initial slope stability analysis for a 3 m high 1:3 loamy sand riverbank

Figure 5.2 shows the same slope after a medium flood followed by rapid drawdown with a reduced FOS of 1.30. Although the FOS reduced significantly the riverbank remains stable.

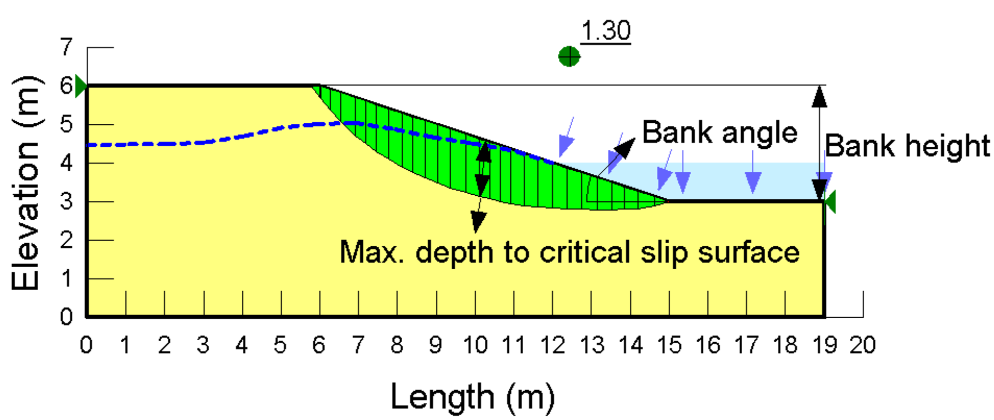

Figure 5.2: Result of medium duration flood followed by a rapid drawdown on the stability of a 3 m high 1:3 loamy sand riverbank

Figure 5.3 shows the same slope after a long flood followed by rapid drawdown. It is shown that the FOS reduced to 1.09. This flood event causes the riverbank to move from a stable condition to an unstable condition.

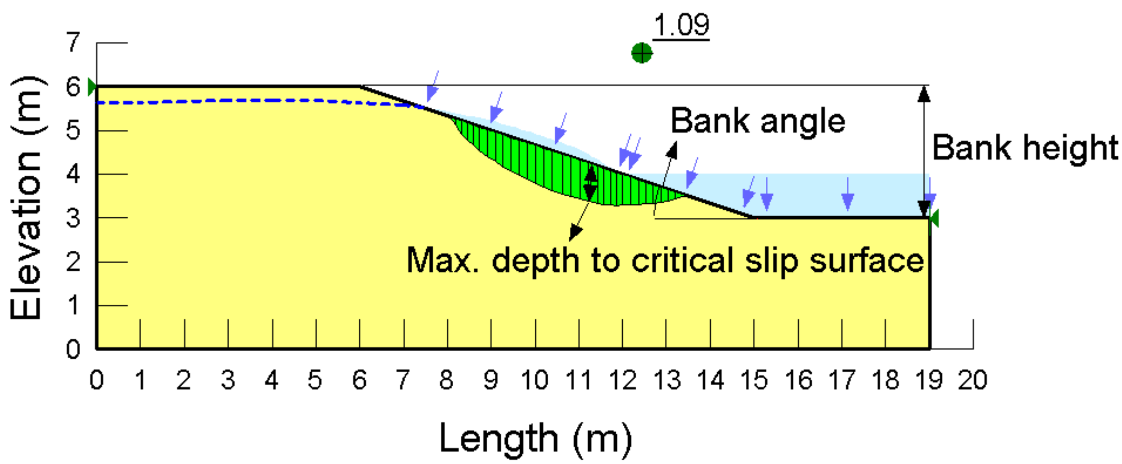

Figure 5.3: Result of long flood followed by rapid drawdown on the stability of a 3 m high 1:3 loamy sand riverbank

Figure 5.4 shows the Factor of Safety (FOS) results for the long duration flood followed by rapid drawdown for all soil types, bank angles and bank heights considered. This flood event was found to be the most critical with the lowest FOS. For FOS less than the limiting FOS of 0.63, the cases are ‘rejected’ i.e. root reinforcement should not be considered as an appropriate bank stabilizing method. For results with FOS between the limiting value of 0.63 and the stable FOS of 1.3, the scenarios satisfy the first limiting condition and ‘continue’ to the second limiting condition (check if the failure depth is in the zone of influence of plant roots to determine if root reinforcement is an appropriate bank stabilizing technique). For FOS results that are above the stable FOS of 1.3, the banks are ‘accepted’ i.e. the banks are considered stable and root reinforcement is not required.

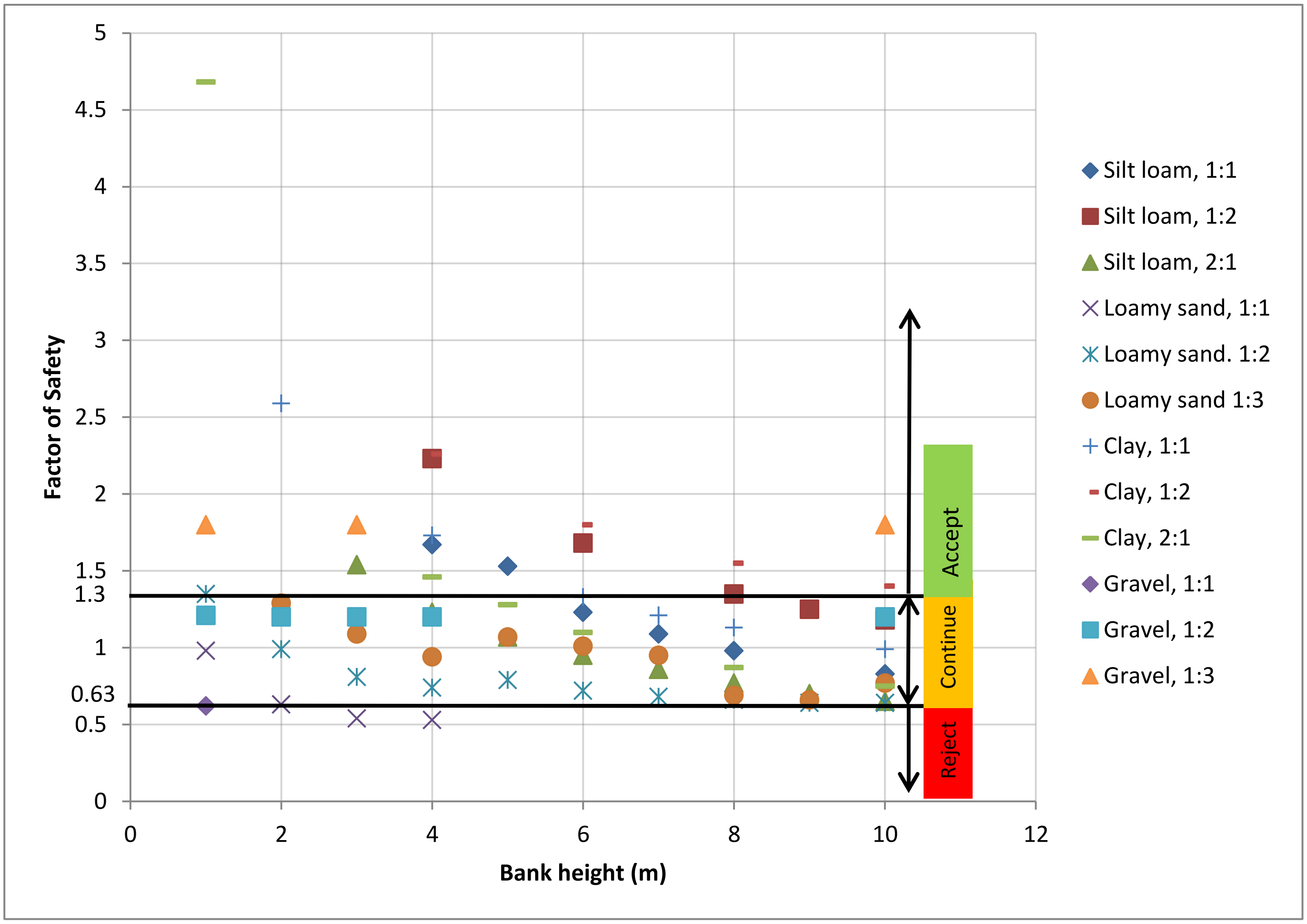

Figure 5.4: Factor of safety for various riverbank heights, soil types and bank angles (First limiting condition)

Figure 5.5 shows the results of the maximum depth from the bank surface to the critical slip surface for the long duration floods followed by rapid drawdown. These results are for the 'continue' scenarios from Figure 5.4 and are used to check the second limiting condition. For maximum depths less than the limiting depth of slip failure of 2.0 m, the failure depths are 'within the root reinforcement zone' and these scenarios are considered to be suitable for root stabilization. For maximum depths greater than the limiting depth of slip failure of 2.0 m, the failure depths are 'outside the root reinforcement zone' and these scenarios are considered unsuitable for root reinforcement alone to be used as a bank stabilization technique.

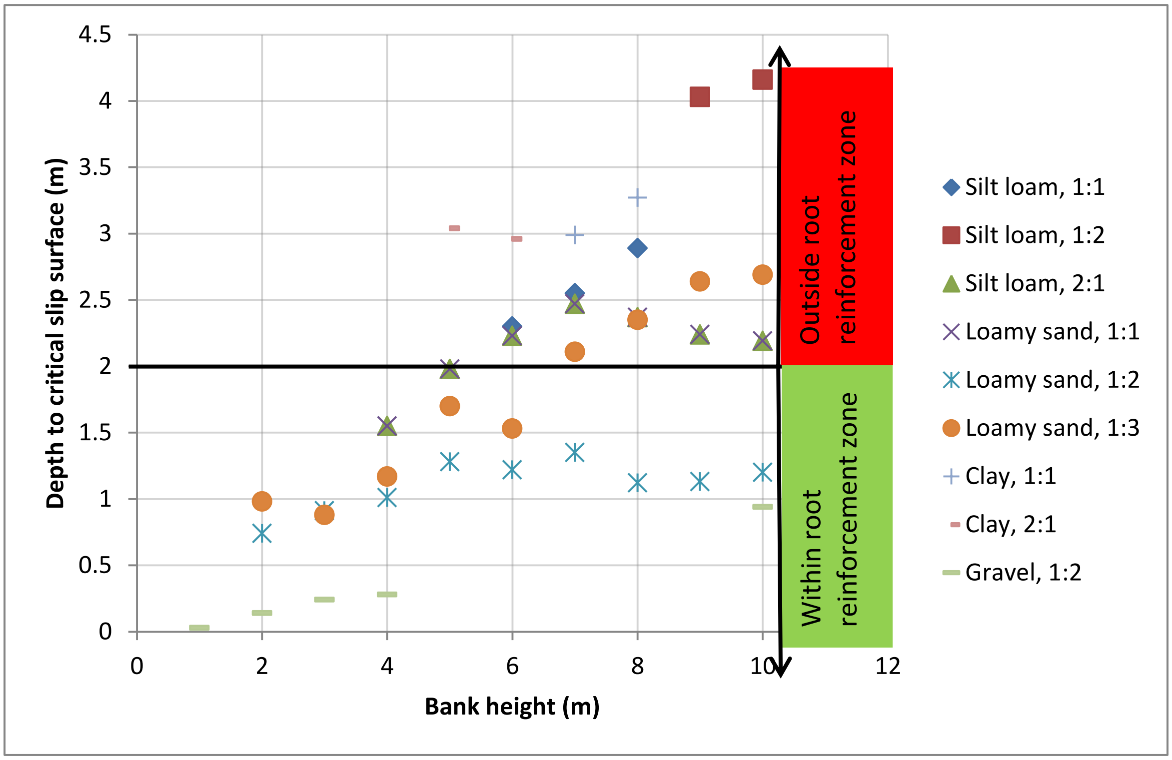

Figure 5.5: Depth to css for various riverbank heights, soil types and bank angle (Second limiting condition)

The Factor of Safety results for each slope under the initial conditions, as defined in section 4.2.3, and the lowest FOS at each stage of a flood event is recorded in Appendix C for all flood scenarios. The actual models are presented in Appendix D. Furthermore, the maximum depth from the bank surface to the critical slip surface for all flood events is recorded in Appendix C. These results are consolidated to produce the design-aid (Table 5.1) for determining the feasibility of using vegetation for bank stabilization.

Following is a summary of observations for all of the scenarios and a compilation of the design-aid. In all scenarios it is evident that a flood event may significantly reduce the stability of a riverbank but not all flood events cause the riverbank to move from a stable condition to an unstable condition.

5.1.1 Results of flood events in silt loam riverbanks

The following is evident for the 1:1 silt loam riverbanks (refer to Fig. 5.6):

- Bank heights less than 5 m remained stable under all flood conditions.
- From a bank height of 6 m, flood conditions started to compromise the stability of the banks. A 6 m high bank became unstable after long flood durations followed by rapid or medium drawdown rates.
- Bank heights between 7 and 10 m were unstable under all flood conditions.
- For all the bank heights that were unstable, the FOS was above the limiting FOS (a value of 0.63, determined using a multiplication factor which was based on the maximum increase in the FOS using vegetation, as reported in literature) but the failure depth was greater than the limiting depth of 2.0 m and as a result vegetation stabilization was not considered.

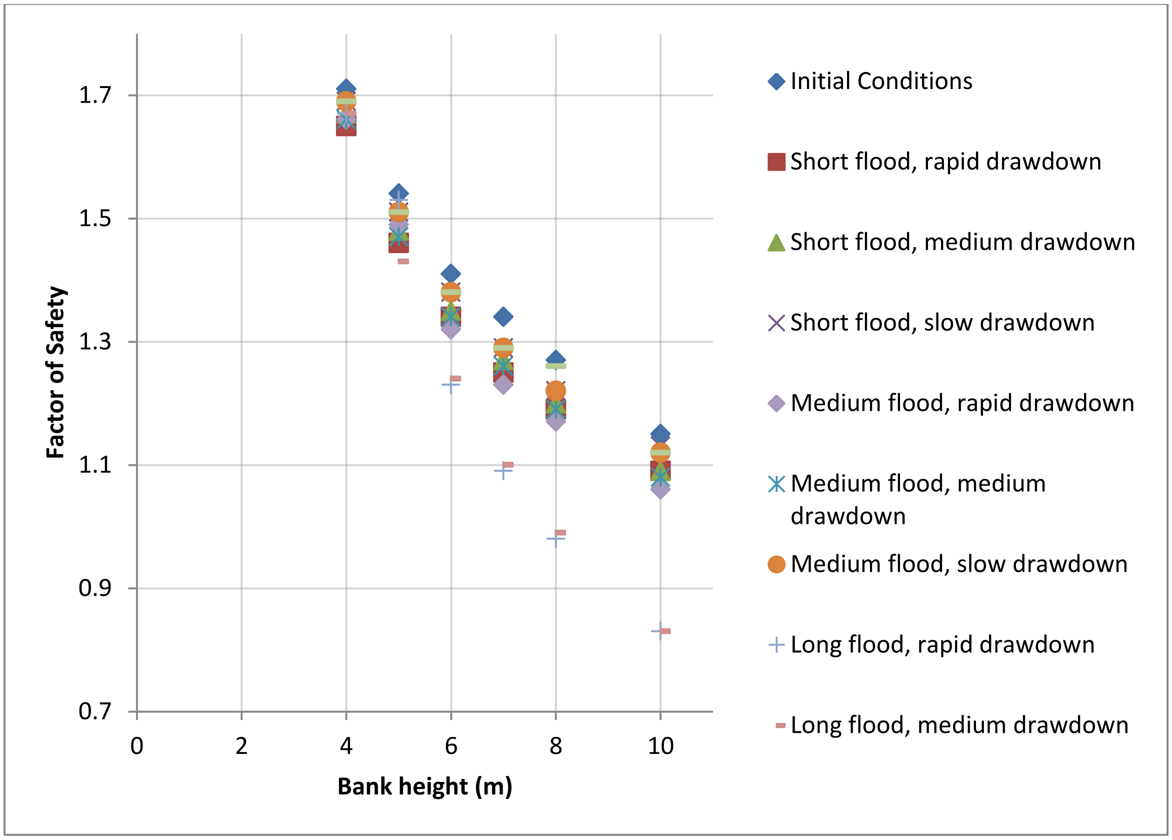

Figure 5.6: Factor of safety for 1:1 silt loam for various riverbank heights and flood conditions

The following is evident for the 1:2 silt loam riverbanks (refer to Fig. 5.7):

- All the slopes were stable, except the 9 and 10 m high banks, which were unstable after long duration floods followed by rapid or medium drawdown rates.
- For the cases whereby the flood conditions caused instability, the depth of failure was much greater than the limiting depth for root stabilization. For these cases the effect of vegetation roots was not considered.

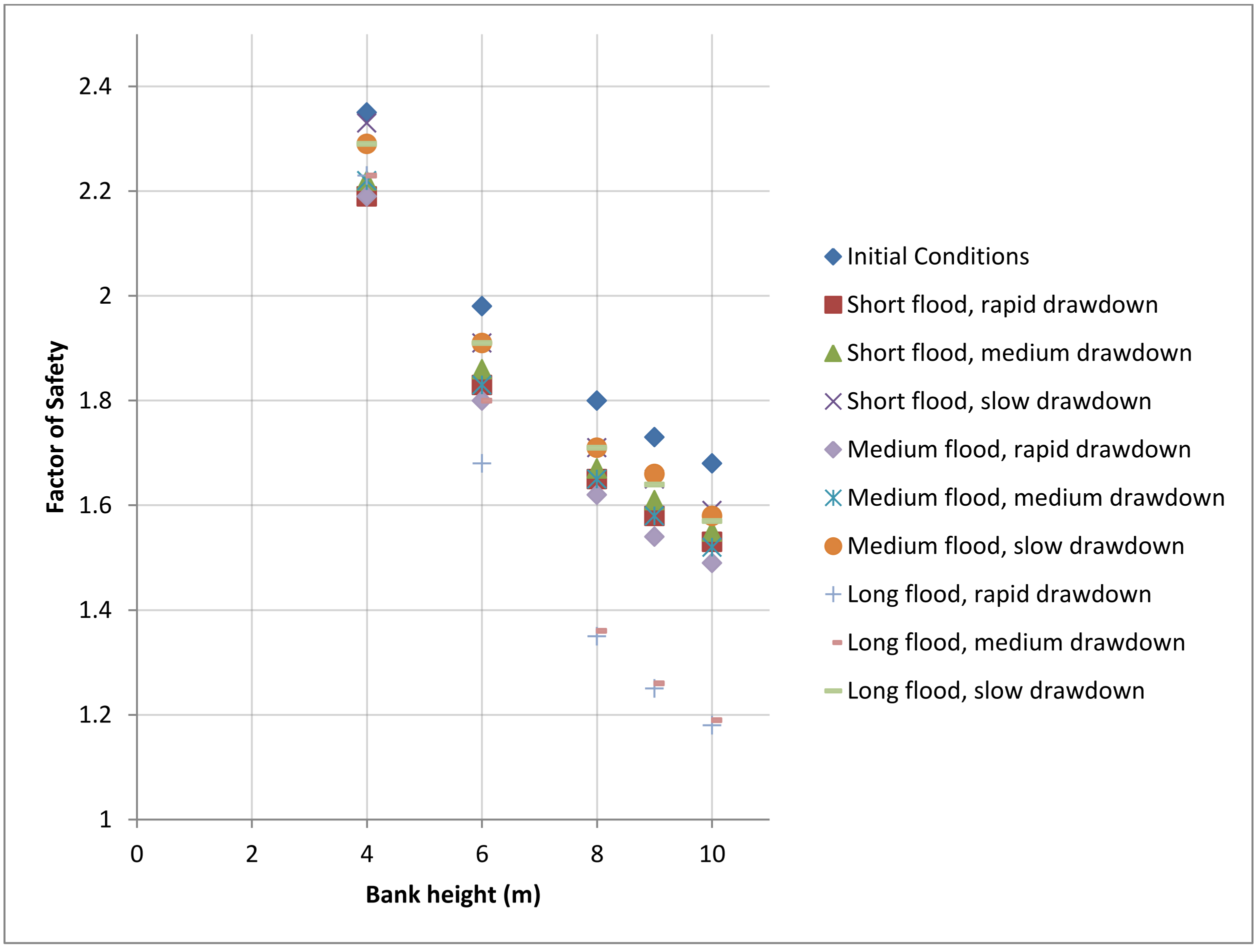

Figure 5.7: Factor of safety for 1:2 silt loam for various riverbank heights and flood conditions

The following is evident for the 2:1 silt loam riverbanks (refer to Fig. 5.8 and Fig. 5.9):

- Bank heights less than 3 m remained stable under all flood conditions.

- For bank heights between 4 and 10 m, the banks were unstable under the initial conditions as well as under all flood conditions. Thus, bank height was the main determining factor for stability with regards to this slope.
- For bank heights between 4 and 6 m under all flood conditions, except for long duration floods followed by rapid or medium drawdown for a 6 m high bank, vegetation stabilization is considered a possible stabilization technique since both FOS limitations and limitations of the depth to critical slip surface are satisfied.

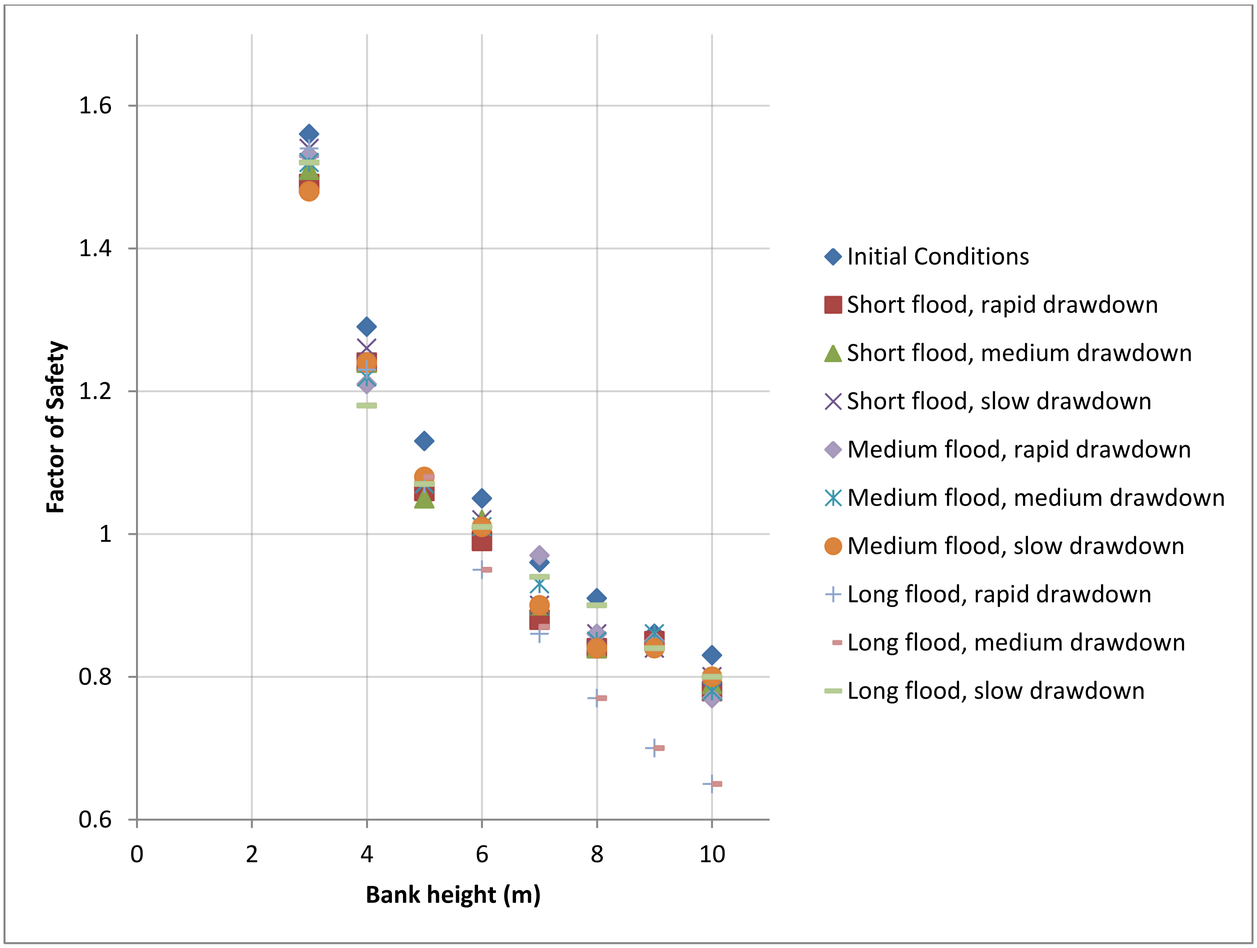

Figure 5.8: Factor of safety for 2:1 silt loam for various riverbank heights and flood conditions

5.1.2 Results of flood events in loamy sand riverbanks

The following is evident for the 1:1 loamy sand riverbanks (refer to Fig. 5.10):

- For all bank heights, the slopes were found to be unstable under the initial conditions as well as under all flood conditions.

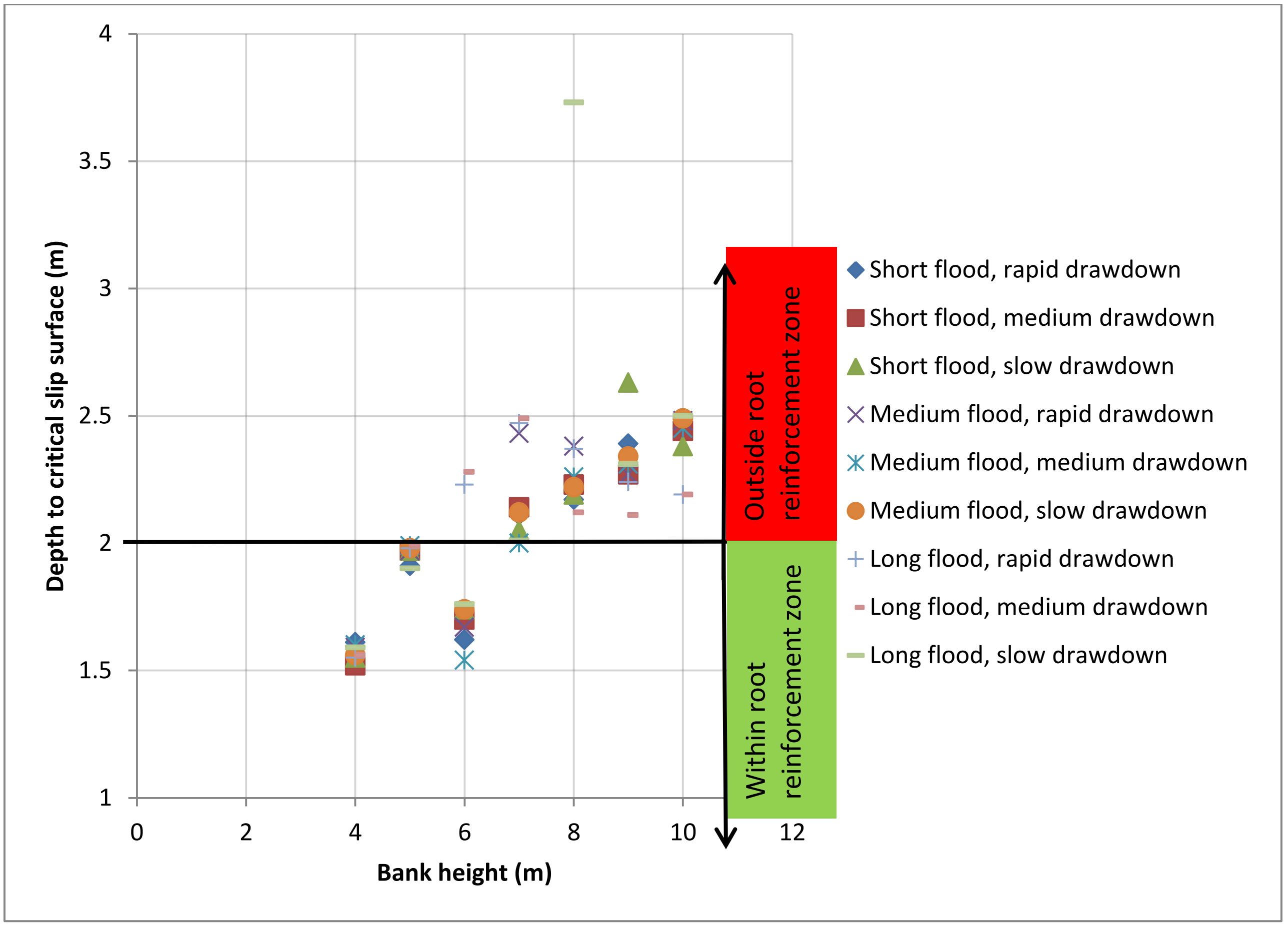

Figure 5.9: Depth to the css for 2:1 silt loam for various riverbank heights and flood conditions

- From a bank height of 4 m, the FOS values were below the limiting FOS to which vegetation roots are an appropriate stabilizing method. This was also the case for the 2 m high bank under a long flood duration and medium drawdown rate, and the 3 m high bank for the medium flood duration and rapid drawdown rate as well as for the long flood duration and both the rapid and medium drawdown rate. For these cases the limiting depth to the critical slip surface was satisfied but the minimum factor of safety requirements were not satisfied.

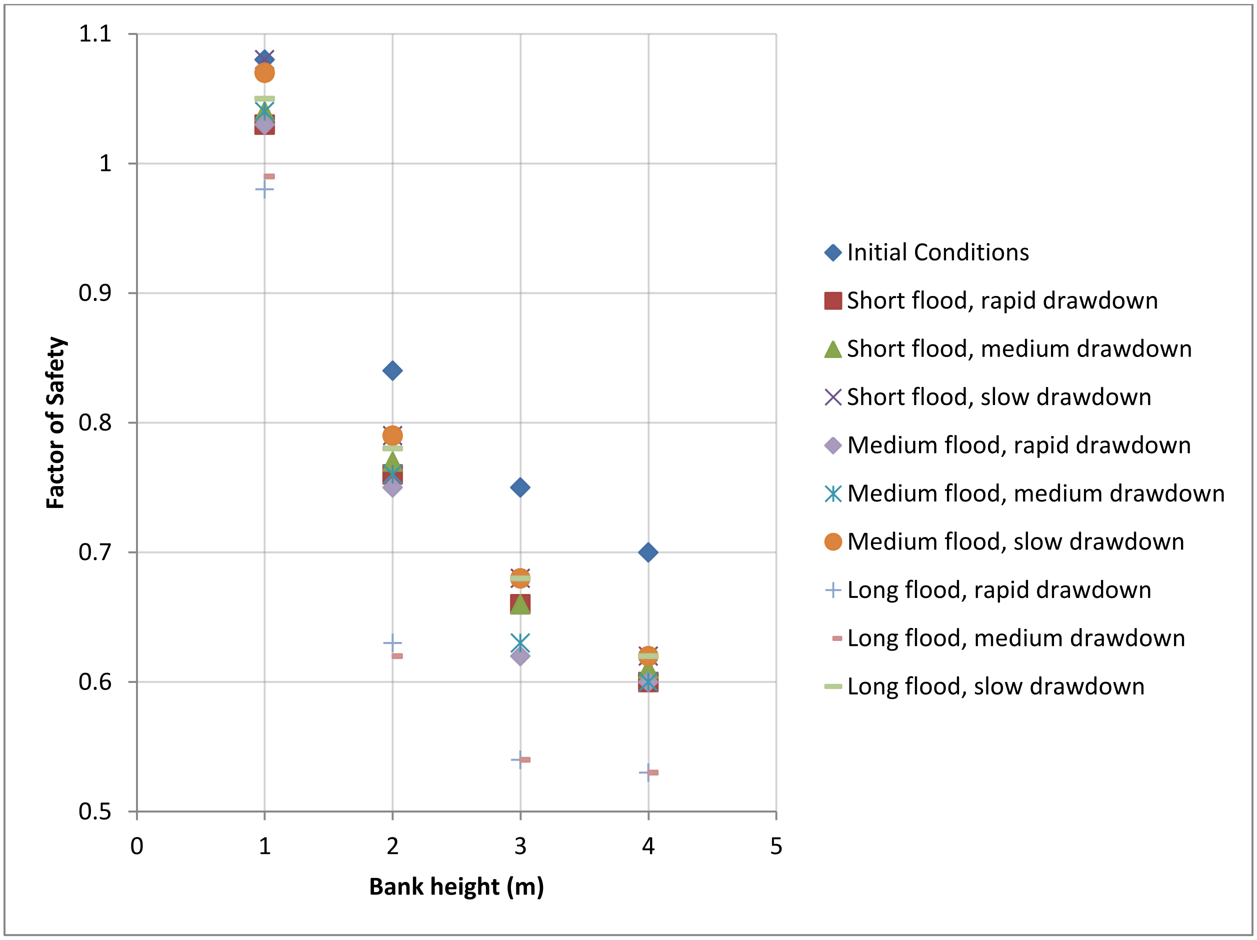

Figure 5.10: Factor of safety for 1:1 loamy sand for various riverbank heights and flood conditions

The following is evident for the 1:2 loamy sand riverbanks (refer to Fig. 5.11 and Fig. 5.12):

- The slopes were stable under all flood conditions for bank heights below 1 m but for bank heights between 2 and 10 m the slopes were unstable under the initial conditions as well as under all of the flood events.
- The FOS requirements for vegetation stabilization were satisfied for all bank heights between 2 and 10 m but the limitation on the depth to the critical slip surface was exceeded from the 7 m high bank for the flood conditions that were comprised of slow drawdown rates.

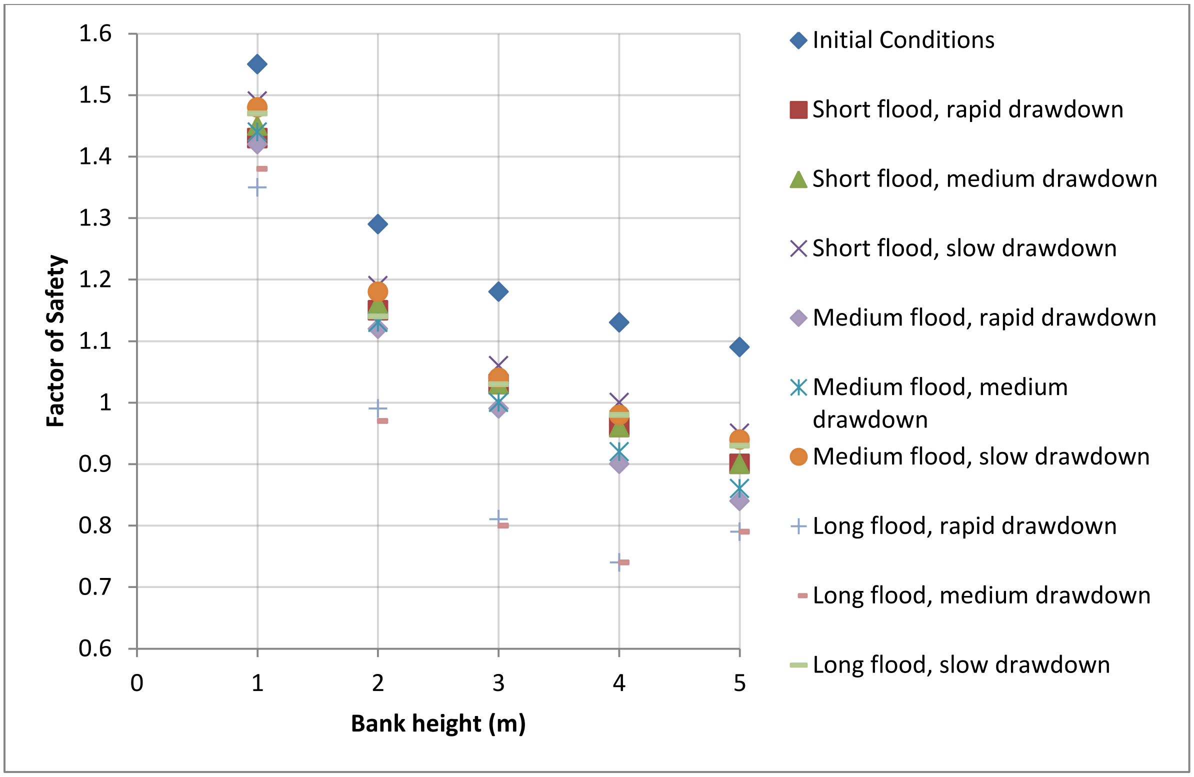

Figure 5.11: Factor of safety for 1:2 loamy sand for various riverbank heights and flood conditions

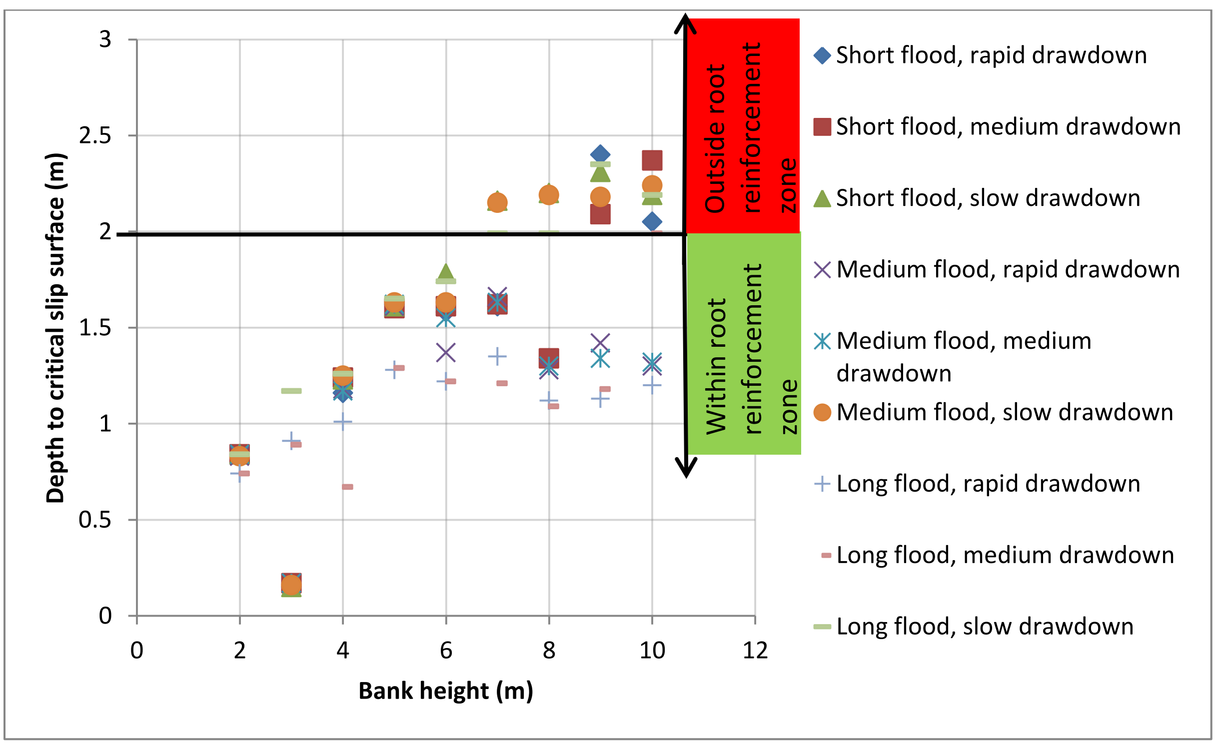

Figure 5.12: Depth to the css for 2:1 loamy sand for various riverbank heights and flood conditions

The following is evident for the 1:3 loamy sand riverbank (refer to Fig. 5.13 and 5.14):

- These riverbanks were most affected by flood events.
- The slopes were stable under all flood conditions for bank heights below 1 m.
- For bank heights between 2 and 3 m, long duration floods followed by either rapid or medium drawdown rates became unstable.
- For the 4 m high bank, the short duration flood followed by the slow drawdown rate and the medium flood duration followed by the slow drawdown rate remained stable while all other flood events resulted in unstable banks.
- Bank heights between 5 and 10 m resulted in instability for all flood events although the banks were stable under the initial conditions.
- The FOS for all flood conditions between the bank heights of 2 to 10 m satisfy the minimum limiting FOS to which vegetation stabilization is an appropriate stabilizing method, however, from a bank height of 5 m or more flood events result in a failure surface that is greater than the limiting depth of vegetation roots.

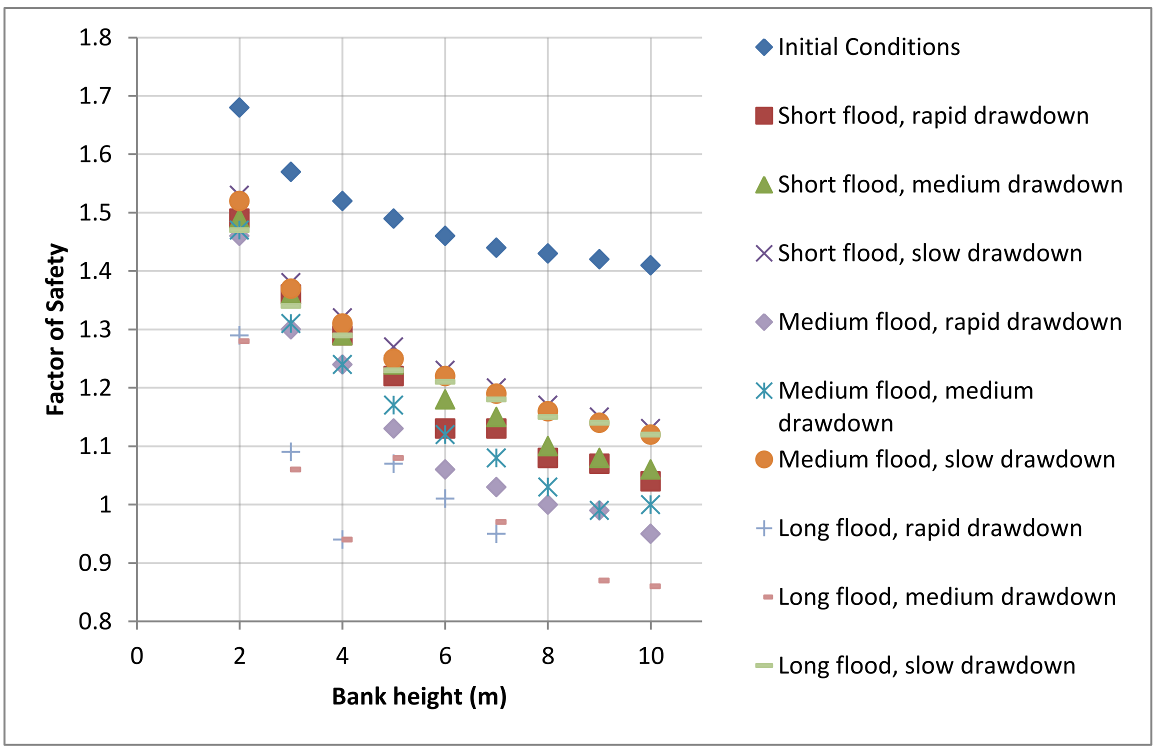

Figure 5.13: Factor of safety for 1:3 loamy sand for various riverbank heights and flood conditions

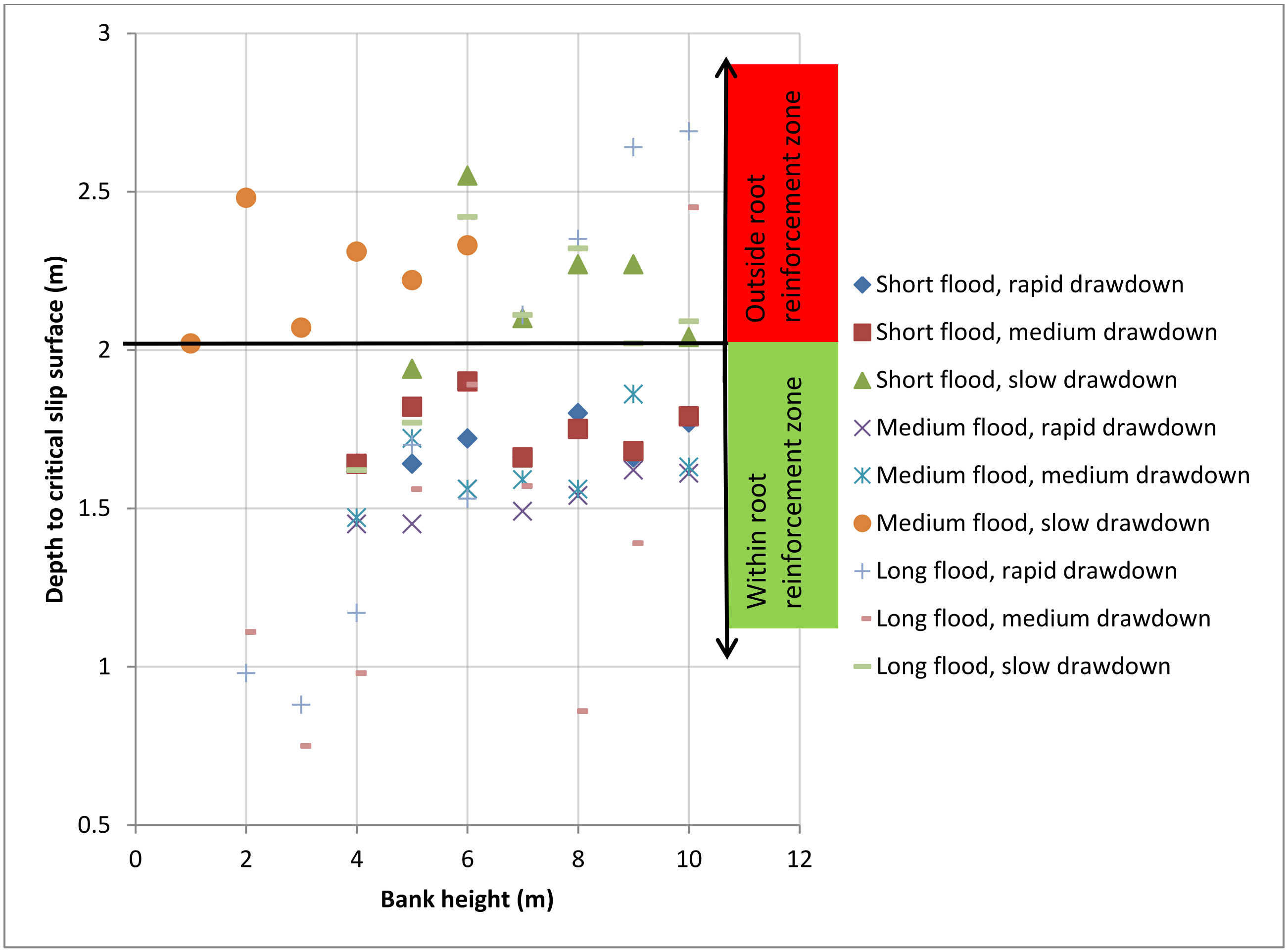

Figure 5.14: Depth to the css for 1:3 loamy sand for various riverbank heights and flood conditions

5.1.3 Results of flood events in clay riverbanks

The following is evident for the 1:1 clay riverbanks (refer to Fig. 5.15):

- Bank heights less than 6 m remained stable following all flood events.
- For bank heights between 6 and 10 m, all flood events resulted in unstable slopes except for the 7 m high bank that remained stable under the short duration flood followed by slow drawdown.
- For all bank heights that satisfy the limiting FOS for vegetation stabilization to be an appropriate stabilizing technique, the limiting depth of influence for vegetation roots was exceeded and hence vegetation stabilization was not considered.

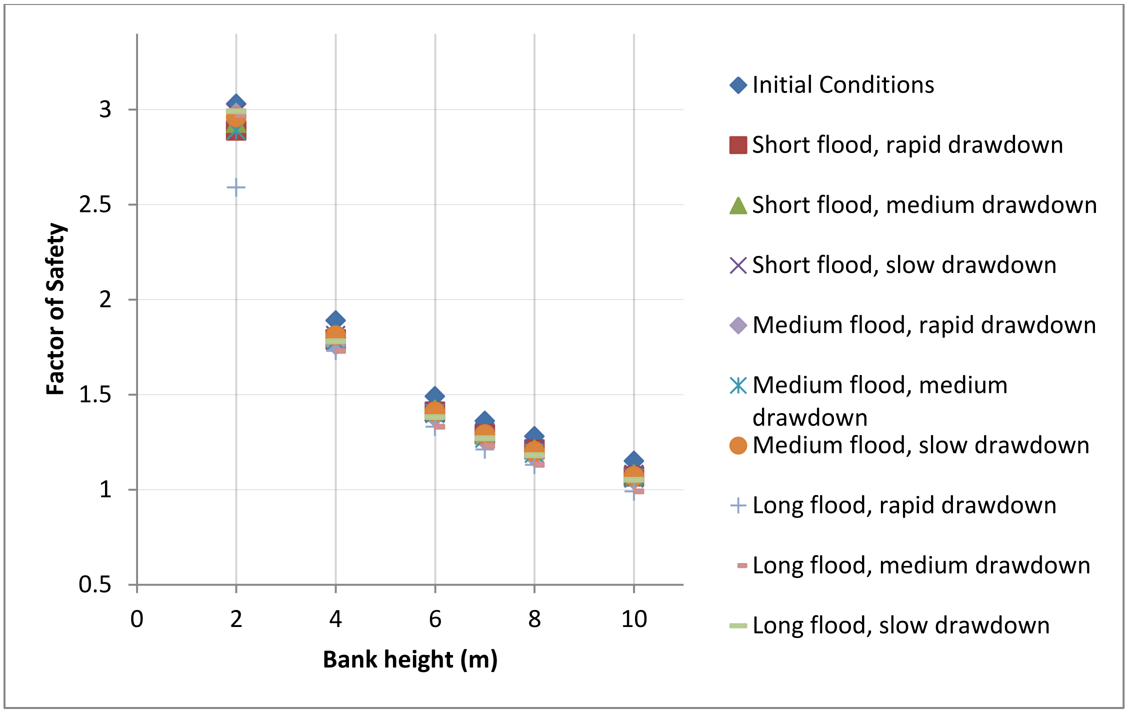

Figure 5.15: Factor of safety for 1:1 clay for various riverbank heights and flood conditions

The following is evident for the 1:2 clay riverbanks (refer to Fig. 5.16):

- The riverbanks were stable under all flood events and bank heights.

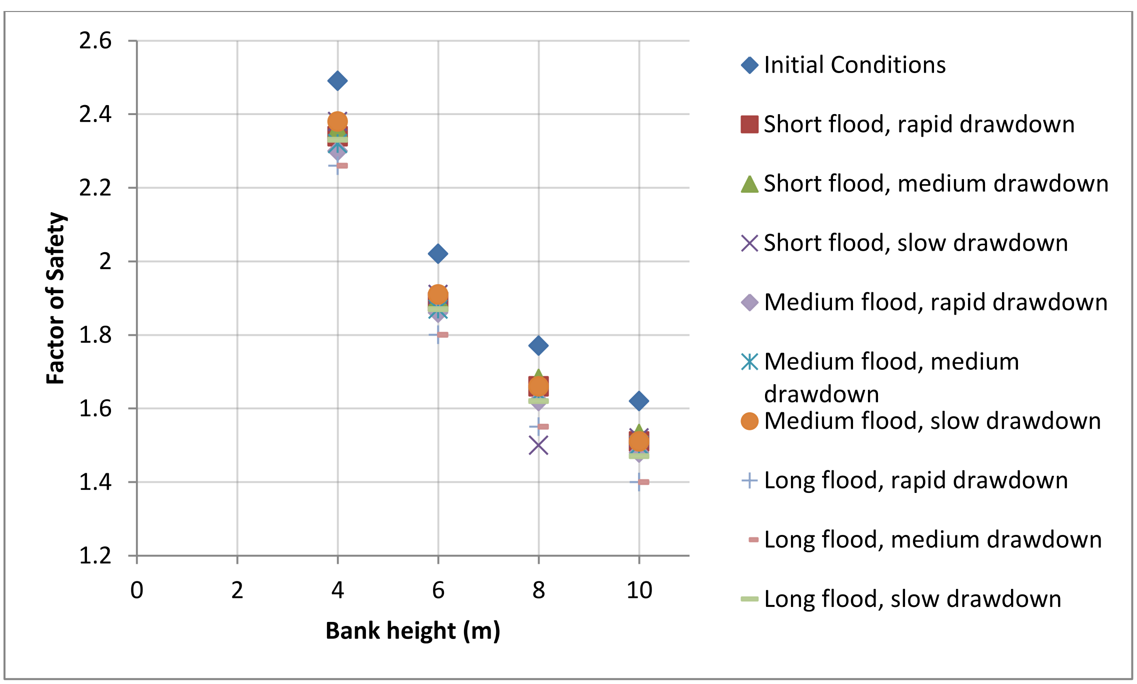

Figure 5.16: Factor of safety for 1:2 clay for various riverbank heights and flood conditions

The following is evident for the 2:1 clay riverbanks (refer to Fig. 5.17):

- The slopes were stable under all flood events when the bank height was less than 4 m but became unstable for bank heights between 5 and 10 m.
- For all bank heights that satisfy the limiting FOS for vegetation stabilization to be an appropriate stabilizing technique, the limiting depth of influence for vegetation roots was exceeded and hence vegetation stabilization was not considered for this slope.

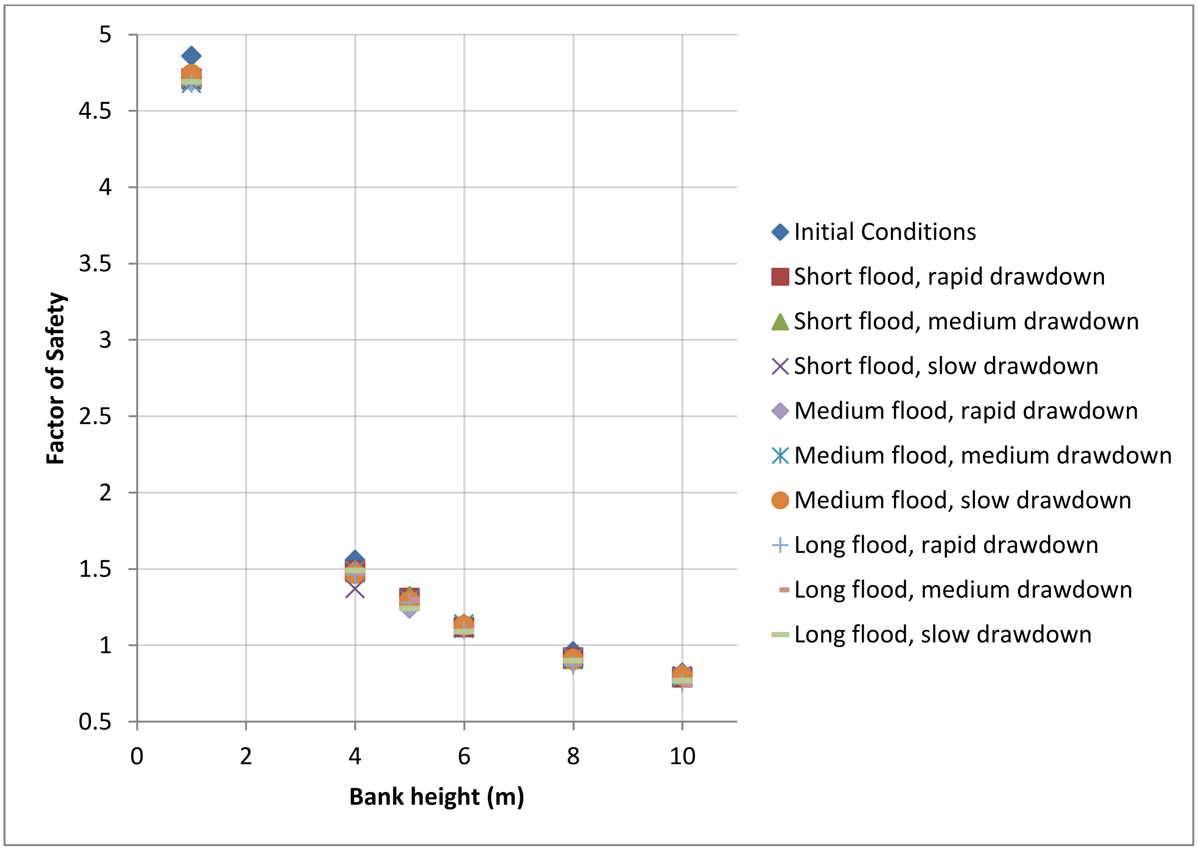

Figure 5.17: Factor of safety for 2:1 clay for various riverbank heights and flood conditions

5.1.4 Results of flood events in gravel riverbanks

The following is evident for the 1:1 gravel riverbanks:

- The riverbanks were unstable for all flood conditions and bank heights investigated.

- From a 1 m bank height under all flood conditions, the limiting FOS for vegetation stabilization was exceeded and thus vegetation stabilization was not considered for any of the scenarios.

The following is evident for the 1:2 gravel riverbanks (refer to Fig. 5.18 and Fig. 5.19):

- The riverbanks are unstable for all flood events and bank heights investigated.
- The stability of the slopes was governed by bank angle as the flood events did not significantly alter the FOS.
- For all bank heights and flood conditions, both the limiting FOS for vegetation stabilization and the limiting depth to the critical slip surface was satisfied. Thus, vegetation stabilization was considered an appropriate stabilizing technique for all the bank heights investigated.

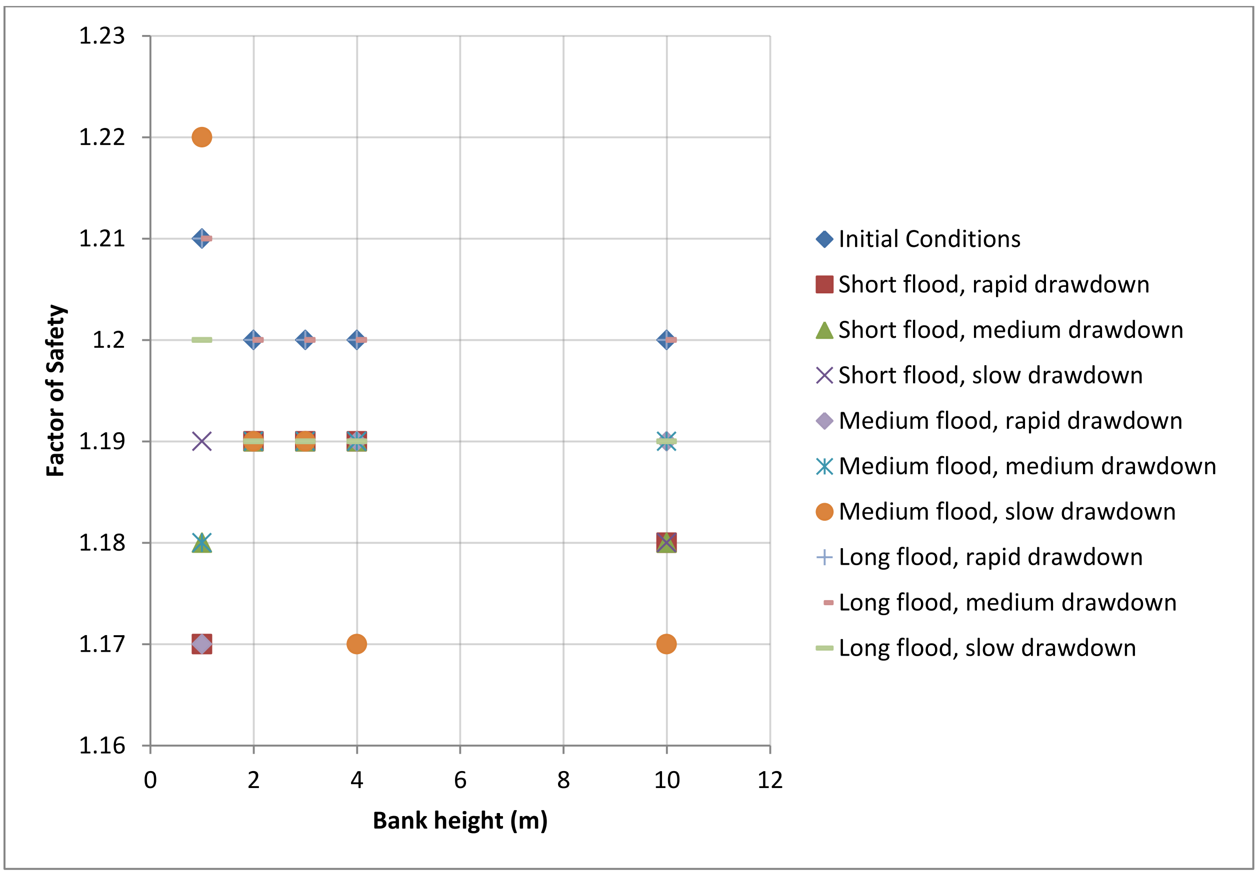

Figure 5.18: Factor of safety for 1:2 gravel for various riverbank heights and flood conditions

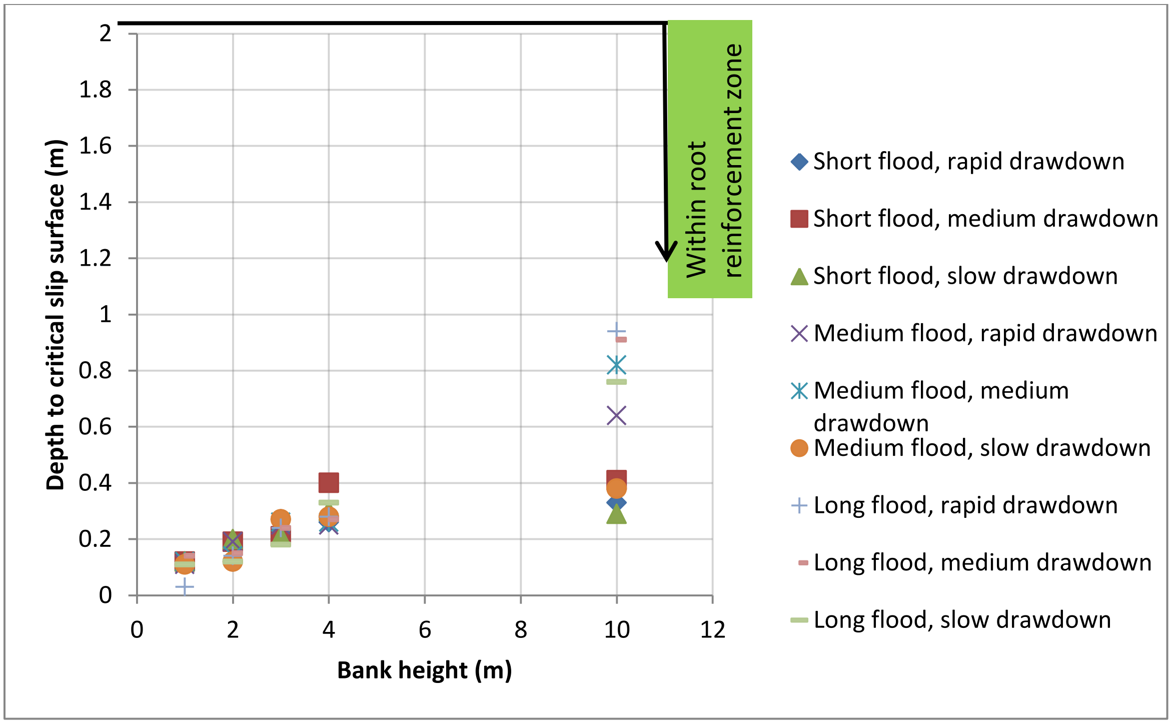

Figure 5.19: Depth to the css for 1:2 gravel for various riverbank heights and flood conditions

The following is evident for the 1:3 gravel riverbanks (refer to Fig. 5.10):

- The slopes were stable under all scenarios.

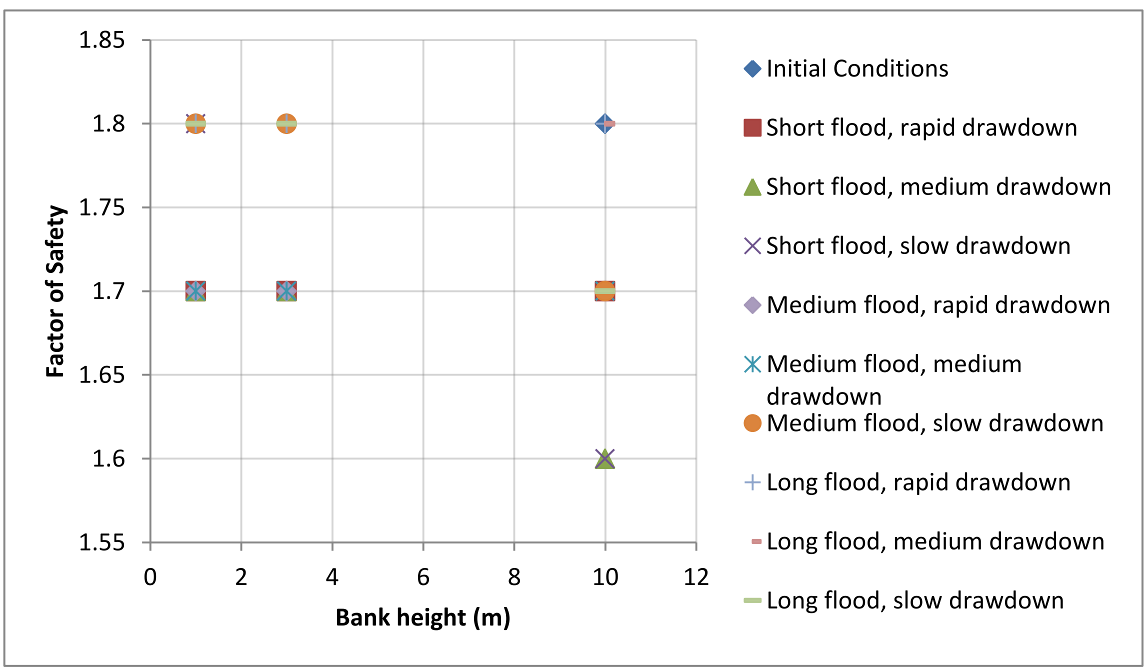

Figure 5.20: Factor of safety for 1:3 gravel for various riverbank heights and flood conditions

5.1.5 Analysis of flood events

Bank geometry and material permeability were found to play a significant role in bank stability following flood events for the range of bank heights investigated. The stability in gravel banks was not affected by the drawdown conditions due to the high permeability of the soil. The high permeability allowed the phreatic surface in the bank to recede with the flood for all drawdown rates investigated. The stability in low permeability soils, such as clays, was affected by flood events where steep bank angles were considered. The stability in soils of intermediate permeability, such as silt loam and loamy sands, was at a greater risk following the flood events, specifically in the flatter slopes where there are longer seepage surfaces.

Bank material strength was found to be an indicator of the type of failure. It was found that the failure depth is proportional to the cohesion. The high cohesive strength in clay and silt loam soils enabled banks of high elevation to remain stable for steep slopes over a range of flood conditions, but when failure occurred it was beyond the limiting 2m depth of influence for vegetation roots. For silt loam banks this failure depth ranged from 2m to 4 m and for clay banks this failure depth ranged from 2.18 m to 3.29 m. Thus, restricted opportunity was given to the use of vegetation as a stabilization method for these high cohesive soils. For clay banks there was no suitability for vegetation stabilization in all of the scenarios and for silt loam banks root reinforcement was limited to only steep slopes. The soils with low cohesive strength, such as loamy sand and gravel, became unstable at flatter slopes but generally failed at shallow depths. The failure depths recorded were shallower for gravel banks with a lower cohesive strength than for loamy sands with a slightly greater cohesive strength. These banks were more suitable for vegetation stabilization since vegetation roots contribute the greatest additional cohesion at shallow depths and the roots are able to anchor through the critical slip surface since the failure depths are shallower than the zone of influence of roots.

The results from this analysis were synthesized to develop the design-aid in Table 5.1 for determining the feasibility of vegetation use in bank stabilization. In this table, results from the stability analysis are summarised in the right hand columns. The columns coded NV indicate that the bank is in a stable state under the specified riverbank height and flood condition, columns coded UV indicate scenarios where vegetation can be used to stabilize the bank and columns coded NSV indicate that the banks do not meet the limiting criteria for vegetation roots alone to be used as a stabilization technique. An asterisk is used to indicate the flood conditions under which the limiting criteria for vegetation roots were suited but no realistic root functional traits from literature (using the guideline in Appendix G) was able to stabilize the bank for the limiting root depth of 2.5 m. Thus, these columns are in the same category as the columns coded NSV until a greater database of root functional traits is developed in which case it may become possible for the required additional cohesion at these greater depths to be reached using certain plant species. In the event that vegetation alone could not be a suitable stabilization technique, it is suggested that further guidance should be sought by geotechnical specialists. In such cases it may be recommended to first reduce the bank slope before vegetation may be considered as a suitable riverbank stabilization technique. Alternatively a combination of hard engineering and soft engineering techniques may be recommended, or it may be recommended to use hard engineering techniques alone to stabilize the bank.

Table 5.1: Design-aid for determining the feasibility of using vegetation for bank stabilization

<table>
<thead>
<tr><th rowspan="2">Soils</th><th rowspan="2">Bank angle</th><th rowspan="2">Height (m)</th><th>Flood duration:</th><th colspan="3">Short</th><th colspan="3">Medium</th><th colspan="3">Long</th></tr>
<tr><th>Drawdown rate:</th><th>Rapid</th><th>Medium</th><th>Slow</th><th>Rapid</th><th>Medium</th><th>Slow</th><th>Rapid</th><th>Medium</th><th>Slow</th></tr>
</thead>
<tbody>
<tr><td rowspan="9">Silt loam</td><td rowspan="3">1:1</td><td>≤ 4</td><td rowspan="39"></td><td colspan="9">NV</td></tr>
<tr><td>6</td><td colspan="6">NV</td><td colspan="2">NSV</td><td>NV</td></tr>
<tr><td>7-10</td><td colspan="9">NSV</td></tr>
<tr><td rowspan="2">1:2</td><td>≤ 8</td><td colspan="9">NV</td></tr>
<tr><td>9-10</td><td colspan="6">NV</td><td colspan="2">NSV</td><td>NV</td></tr>
<tr><td rowspan="4">2:1</td><td>≤ 3</td><td colspan="9">NV</td></tr>
<tr><td>4-5</td><td colspan="9">UV</td></tr>
<tr><td>6</td><td colspan="6">UV</td><td colspan="2">NSV</td><td>UV</td></tr>
<tr><td>7-10</td><td colspan="9">NSV</td></tr>
<tr><td rowspan="20">Loamy sand</td><td rowspan="4">1:1</td><td>≤ 1</td><td colspan="9">UV</td></tr>
<tr><td>2</td><td colspan="7">UV</td><td>NSV</td><td>UV</td></tr>
<tr><td>3</td><td colspan="3">UV</td><td>NSV</td><td colspan="2">UV</td><td colspan="2">NSV</td><td>UV</td></tr>
<tr><td>4-10</td><td colspan="9">NSV</td></tr>
<tr><td rowspan="6">1:2</td><td>≤ 1</td><td colspan="9">NV</td></tr>
<tr><td>2-3</td><td colspan="9">UV</td></tr>
<tr><td>4</td><td colspan="7">UV</td><td>*UV</td><td>UV</td></tr>
<tr><td>5-6</td><td colspan="9">*UV</td></tr>
<tr><td>7-8</td><td colspan="2">*UV</td><td>NSV</td><td colspan="2">*UV</td><td>NSV</td><td colspan="3">*UV</td></tr>
<tr><td>9-10</td><td colspan="3">NSV</td><td colspan="2">*UV</td><td>NSV</td><td colspan="2">*UV</td><td>NSV</td></tr>
<tr><td rowspan="10">1:3</td><td>≤ 1</td><td colspan="9">NV</td></tr>
<tr><td>2-3</td><td colspan="6">NV</td><td colspan="2">UV</td><td>NV</td></tr>
<tr><td>4</td><td colspan="2">UV</td><td>NV</td><td colspan="2">UV</td><td>NV</td><td colspan="3">UV</td></tr>
<tr><td>5</td><td colspan="5">UV</td><td>NSV</td><td colspan="3">UV</td></tr>
<tr><td>6</td><td colspan="2">UV</td><td>NSV</td><td colspan="2">UV</td><td>NSV</td><td colspan="2">*UV</td><td>NSV</td></tr>
<tr><td>7</td><td colspan="2">UV</td><td>NSV</td><td>*UV</td><td>UV</td><td colspan="2">NSV</td><td>*UV</td><td>NSV</td></tr>
<tr><td>8</td><td colspan="2">UV</td><td>NSV</td><td colspan="2">*UV</td><td colspan="2">NSV</td><td>*UV</td><td>NSV</td></tr>
<tr><td>9</td><td colspan="2">*UV</td><td>NSV</td><td colspan="2">*UV</td><td colspan="2">NSV</td><td>*UV</td><td>NSV</td></tr>
<tr><td>10</td><td colspan="2">*UV</td><td>NSV</td><td colspan="2">*UV</td><td colspan="4">NSV</td></tr>
<tr><td rowspan="7">Clay</td><td rowspan="3">1:1</td><td>≤ 6</td><td colspan="9">NV</td></tr>
<tr><td>7</td><td colspan="2">NSV</td><td>NV</td><td colspan="6">NSV</td></tr>
<tr><td>8-10</td><td colspan="9">NSV</td></tr>
<tr><td>1:2</td><td>≤ 10</td><td colspan="9">NV</td></tr>
<tr><td rowspan="3">2:1</td><td>≤ 4</td><td colspan="9">NV</td></tr>
<tr><td>5</td><td colspan="2">NV</td><td colspan="2">NSV</td><td>NV</td><td colspan="2">NSV</td><td>NV</td><td>NSV</td></tr>
<tr><td>6-10</td><td colspan="9">NSV</td></tr>
<tr><td rowspan="3">Gravel</td><td>1:1</td><td>≤ 10</td><td colspan="9">NSV</td></tr>
<tr><td>1:2</td><td>≤ 10</td><td colspan="9">UV</td></tr>
<tr><td>1:3</td><td>≤ 10</td><td colspan="9">NV</td></tr>
</tbody>
</table>

Key to table 5.1

NV (colour coded green) - the bank is in a stable state and vegetation is not necessary
UV (colour coded orange) - vegetation can be used to stabilize the bank
NSV (colour coded red) - vegetation alone is not a suitable bank stabilization technique

5.2 Sensitivity of the soil-water characteristic curves

The transient seepage analysis using SEEP/W required the definition of the soil-water characteristic curve (SWCC) for the soil types considered. The SWCCs, also referred to as soil-moisture retention curves, represent the relationship between water content and suction for a soil. The continuous sigmoidal function of the SWCC describes what portion or volume of the voids remains water-filled as the soil drains (Fuselier, 2006). Figure 5.21 shows a typical soil-water characteristic curve for a silty soil, along with some other important characteristics of the SWCC.

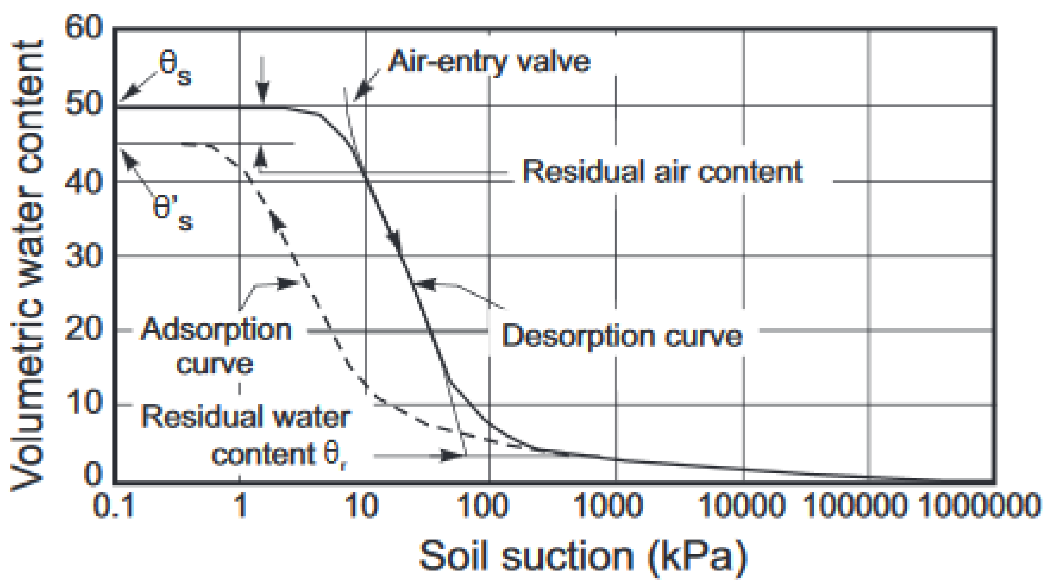

Figure 5.21: A typical soil-water characteristic curve for a silty soil (after Fredlund and XIng, 1994)

The SWCC generally depends on the grain size distribution, the pore-size distribution of the soil, the structure of the soils, and groundwater characteristics. The SWCC is used to predict other unsaturated soil parameters such as the permeability and shear-strength functions (Fredlund and Xing, 1994). In practice, the SWCC is typically obtained by drying or wetting a soil sample under a constant stress while monitoring the changes of water content in the soil. Heshmati and Motahari (2012) identify the soil-water characteristic curve as a fundamental property in soil physics and soil mechanics. It is therefore necessary to use reasonably accurate SWCCs.

This section investigates the sensitivity of the SWCCs to main input parameters. In SEEP/W (Geo-Slope, 2007), the three main features that characterize the SWCCs are: the air-entry value (the matric suction value from which air starts to enter into the soil), the slope of the function (the portion of the SWCC between the air-entry value and the residual water content), and the saturated volumetric water content (equivalent to soil porosity, which is the fraction of the volume of voids over the total volume). The air-entry value and the slope of the function depend on grain size data. The values of these input parameters are varied within reasonable ranges, as obtained from literature, through a series of transient analyses where only one parameter is changed at a time to clearly evaluate the influence of each parameter on the SWCCs and subsequently the factor of safety. The purpose is to provide an indication of how accurately these parameters need to be determined, as a means of providing a measure of the reliability of the design aid in section 5.1.

5.2.1 Riverbanks modeled, material parameters and flood conditions

The input parameters in Table 5.2 are varied for the following selected riverbanks:

- 4 m high, clay riverbank with a bank angle of 1:1
- 6 m high, silt loam riverbank with a bank angle of 1:1
- 1 m high, loamy sand riverbank with a bank angle of 1:1
- 1 m high, gravel riverbank with a bank angel of 1:3

Table 5.2: Soil permeability criteria for soil-water characteristic curve

Soil properties related to SWCC	**Range of values for soils:**				**Source**
	Clay	**Silt loam**	**Loamy sand**	**Gravel**	
(θ_s) Saturated Volumetric Water Content (m3/m3)	0.42-0.70	0.35-0.58	0.37-0.51	0.25-0.41	Rawls et al. (1982), Geotechdata.info (2013), Thoma et al. (2013) and Das (2008).
(AEV) Air-entry value (kPa)	>25	6.86-30	0.80-8.0	0.2-1.0	Aubertin et al. (1998), Fredlund et al. (2003) and Rawls et al. (1982).
D_{10} (mm)	1e-4- 0.001	0.0017- 0.047	0.0041-0.041	0.435-0.696	Hill (1941) and Kunberger (2007)

In assigning the soil strength criteria for the riverbank material, an advanced material property, Φ_b, was also required. Φ_b is related to the soil water characteristic curve, and is the angle that defines the increase in strength due to a negative pore-water pressure (Geo-Slope, 2007). Φ_b varies with the degree of saturation. As the degree of saturation increases there is a decrease in matric suction and consequently an increase in Φ_b. At high degrees of saturation, Φ_b approaches the effective angle of internal friction, Φ'. When the soil desaturates, Φ_b decreases (Vanapalli and Fredlund, 1997). SLOPE/W is limited to a constant value of Φ_b, and for practical purposes, Φ_b can be estimated as half the effective angle of internal friction (Geo-Slope, 2007; Rahardjo et al., 2014). In this study Φ_b was taken as 11.5°, 15°, 12.75° and 16° for clay, slit loam, loamy sand and gravel soils respectively.

For the purpose of determining the sensitivity in the grain size data (D_{10}), the volumetric water content function (VWC) for all soil types was estimated using the modified Kovacs formulation within SEEP/W, using the parameters in Table 5.3.

Table 5.3: Soil permeability criteria for estimation of the VWC using Kovacs formulation

Property	Soils				Source
	Clay	Silt loam	Loamy sand	Gravel	
D_{60} (mm)	0.0054	0.028	0.47	8	Li at al. (2014)
Liquid Limit (%)	34	25	27	0	White (1949) and Bowerman (1999).

For all of the selected riverbanks, a flood event of long duration and rapid drawdown as defined in section 4.2.3 was modeled in the sensitivity analysis, since this flood event was found to be the most critical with the lowest factor of safety.

5.2.2 Sensitivity of SWCC to the air-entry value

The air-entry value (AEV) of the soil is the matric suction value from which air starts to enter into the soil. The AEV is particularly important for partially saturated soils where the degree of saturation significantly decreases when the suction exceeds the AEV (Heshmati and Motahari, 2012). It is a function of the maximum pore size and the pore-size distribution in a soil. Typically, soils with large, uniformly shaped pores have relatively low AEV's (Geo-Slope, 2007).

The approach that was used to determine the sensitivity of the SWCCs to AEV was to fit graph data for the selected bank to the van Genuchten (1980) equation in SEEP/W, using the RETC code (van Genuchten et al. 1991). The RETC code is computer program which is publically available and may be used to analyse the soil water retention and hydraulic conductivity functions of unsaturated soils. The van Genuchten (1980) equation is as follows:

$$\theta_w = \theta_r + \frac{\theta_s - \theta_r}{\left[1+\left(\frac{\Psi}{a_{AEV}}\right)^n\right]^m} \tag{5.1}$$

where θ_w is the volumetric water content, θ_r is the residual water content, θ_s is the saturated volumetric water content, Ψ is the negative pore-water pressure, a_{AEV} is approximately the air-entry value of the soil, n is a parameter that controls the slope at the inflection point in the volumetric water content function and m is a parameter that is related to the residual water content.

The RETC code provided the curve fitting parameters *n* and *m*, which were the values that were kept constant in SEEP/W along with the coefficient of volume compressibility, saturated volumetric water content and residual water content. The parameters *n* and *m* obtained from the RETC code for the range of soils are summarised in Table 5.4.

Table 5.4: Parameters obtained from RETC code

Parameters	**Soils**			
	Clay	**Silt loam**	**Loamy sand**	**Gravel**
n	1.09	1.41	2.28	2.68
m	0.08	0.29	0.56	0.63

The van Genuchten type function in SEEP/W allowed for the air entry value to be changed while keeping the before-mentioned parameters constant, producing SWCCs and subsequently factors of safety for changing air-entry values for each soil type.

5.2.3 Deductions from the sensitivity analysis

The sensitivity plots of the SWCC for varying AEV, θ_s and D_{10} as well as for the sensitivity of the FOS with AEV, θ_s and D_{10} are presented in Appendix F. The sensitivity results of the FOS vary with the different input parameters (Figure F2, F4 and F6) and are used to plot the Tornado chart in Fig. 5.22. The FOS value of 1.14 was taken as the base case, merely for illustrative purposes, since it lies between the resultant FOS range for the range of D10, θ_s and AEV investigated. The low level of sensitivity suggests that the results presented in chapter 5.1 are reliable for a range of SWCCs within realistic ranges of AEV, grain size data and saturated volumetric water content. The sensitivity analysis as shown in the Tornado chart identifies the saturated volumetric water content as the most sensitive parameter in the SWCC, and may influence the stability results for lower permeability soils. Thus, this parameter should be identified with accuracy to increase the confidence level of the computed results in chapter 5.1.

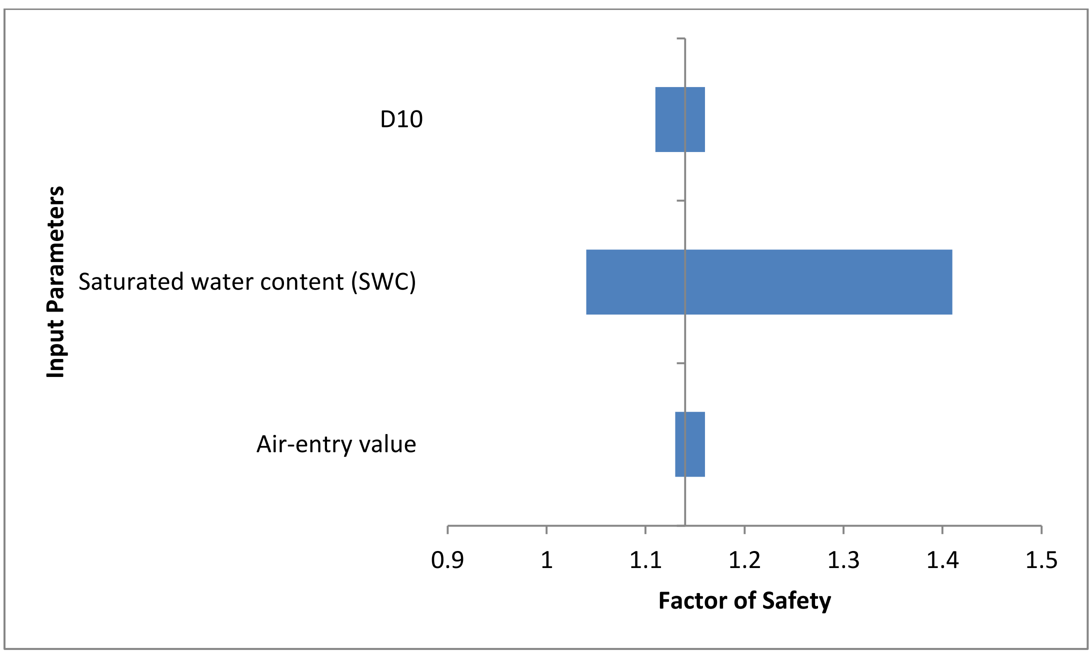

Figure 5.22: Tornado chart to illustrate the sensitivity of FOS with D10, θ_s and AEV

The Tornado plot clearly illustrates which input parameters are most sensitive. However, the individual sensitivity plots in Appendix F indicate the trend of FOS and SWCC to change in D10, θ_s and AEV.

5.3 Results and details of the root functional traits required to stabilize banks

Figure 5.23 shows an example of vegetation stabilization by enhanced soil cohesion of a 3 m high, loamy sand riverbank with a bank angle of 1:3 and a long flood followed by rapid drawdown. The region shaded in green is the zone of root reinforcement and in this example the lower limit of additional cohesion supplied by the plant roots was 4.54 kPa and was applied to a depth of 1 m below the slope face. This corresponded to the *Bauhinia championii* (denoted as *B. championii* in Appendix H) plant species from literature (Ghestem et al., 2014) for a 1.50 mm root diameter with 35 roots per sq. m. The T_R-*D* model (Ghestem et al., 2014) in Appendix G, resulted in a required root tensile strength of 20.10 MPa for the before-mentioned root functional traits of root diameter, root density, and root length as discussed in section 4.3.5.

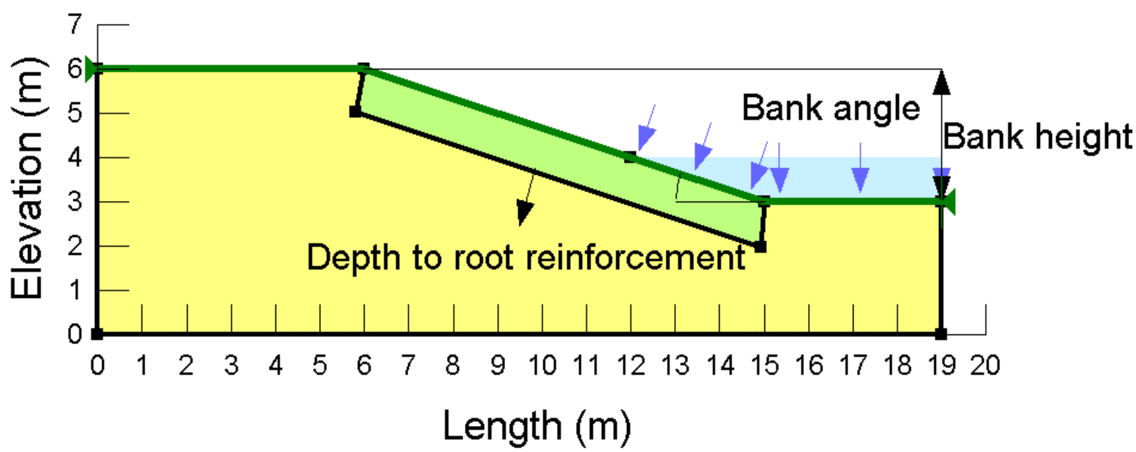

Figure 5.23: Increased soil cohesion due to vegetation stabilization for a long flood followed by rapid drawdown on a 3 m high 1:3 loamy sand riverbank

Figure 5.24 shows the stability of the same bank as a result of the vegetation stabilization by an increase in cohesion of 4.54 kPa (total soil cohesion of 5.54 kPa in root reinforcement zone). Without the influence of vegetation roots, the FOS was 1.09 and with vegetation roots, the FOS increased to 1.32. Thus, this riverbank moves from an unstable condition to a stable condition due to the influence of vegetation roots with the root functional traits described above.

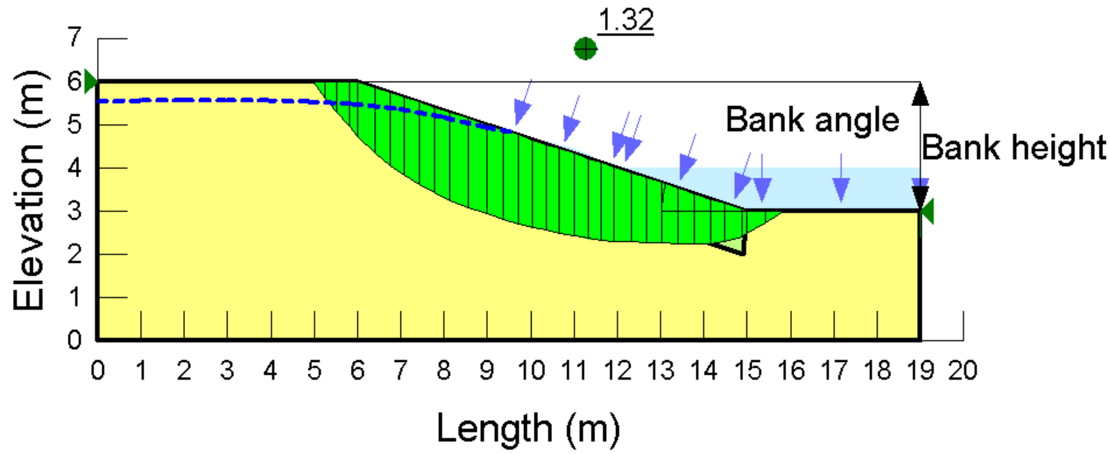

Figure 5.24: Result of increased cohesion due to vegetation stabilization on the stability of a 3 m high 1:3 loamy sand riverbank

The bank models that account for root reinforcement by additional soil cohesion for the range of banks found suitable in section 5.1 are attached in Appendix E.

The details of the root functional traits required to stabilize the suitable banks as described in section 4.3.5, coded UV in Table 5.1, are summarised in Table 5.5. The detailed results of vegetation type, root functional traits and root strength properties suitable to specific flood conditions are tabulated in Appendix H. The values of both the root strength properties and the root functional traits correspond to the mathematical models and values from the wide source of literature summarized in Appendix G. Table 5.5 was formulated by selecting (from the detailed list of results in Appendix H) the minimum *RAR* and root depth required for bank stabilization from all of the flood conditions for the bank heights, bank angles and soil types identified in Table 5.1 to be suitable for bank stabilization. The furthest right column in Table 5.5 lists the plant species that possess the functional root traits, commonly suitable to all of the flood conditions for the soil type, bank angles and bank heights specified in the left columns.

5.3.1 Qualitative aspects of results for root functional traits required to stabilize banks

This section gives observations noticed in the development of the guidelines in sections 5.1 and 5.3.

- Banks with low cohesive strength, such as gravel and loamy sand riverbanks, were most suited to vegetation stabilization because these banks tended to fail at shallow depths, where additional cohesion due to vegetation roots is high, and in the zone of influence of most plant species.
- Due to the absence of cohesive strength in gravel banks and consequently the shallow failure depths in these banks, there was a wide range of plant species with suitable root functional traits able to stabilize the banks. Thus suggesting that when these functional traits are matched to South African plant species, there should be a large variety of South African plant species that would be suitable to stabilize gravel banks.
- There were significantly fewer plant species listed to stabilize high banks since these banks had greater failure depths and there was a limited number of plant species obtained from literature that had roots able to penetrate below a depth of 0.5 m.
- The suitability of vegetation stabilization in gravel riverbanks was not dependent on flood conditions due to the high permeability of the soil, as discussed in section 5.1. The suitability of roots to stabilize the gravel banks was governed by bank height.
- For loamy sand soil at a bank angle of 1:2, and bank heights between 5 to 10 m, and for flood conditions that were within the limiting criteria of FOS and failure depth, there were no realistic root functional traits (from literature) that were able to stabilize the bank because the required root depth was greater than 2.5 m.
- For low permeability soils, flood conditions followed by rapid or medium drawdown rates required root functional traits that provided greater additional cohesion and/or root depth. These results correspond to section 5.1 where the effect of flood conditions was discussed.
- Root depth is considered a critical root functional trait. For banks with low FOS, there was a threshold in cohesion such that an increase in additional cohesion at the same depth had no influence on the FOS. In order to reach stability, the region of vegetation stabilization by additional cohesion had to increase in depth.

Table 5.5: Stabilizing root functional traits for scenarios where vegetation can be used to stabilize the bank

Soils	Bank angle	Bank height (m)	Flood condition	RAR (%)	Root Length (m)	Suitable vegetation type
Silt loam	**2:1**	**4**	All	0.0102	0.50	Grass, shrubs, *Lygeum spartum, Spanish Broom,* Vetiver grass roots
		5	All	0.0123	1.50	Vetiver grass roots
		6	All except for long duration floods followed by rapid drawdown and medium drawdown	0.0057	2.50	Vetiver grass roots
Loamy sand	**1:1**	**1**	All	0.0050	0.50	Shrubs: *Atriplex halimus*, *Salsola genistoides* and *Dorycnium pentaphyllum,* Vetiver grass roots
		2	All except for long duration floods followed by medium drawdown	0.0253	1.80	Vetiver grass roots
		3	All except for medium and long duration floods followed by rapid drawdown and long duration floods followed by medium drawdown	0.0052	2.50	Vetiver grass roots
	1:2	**2**	All	0.0165	1.00	Conifer and broadleaved species
		3	All	0.0050	2.00	Vetiver grass roots
		4	All except for long duration floods followed by medium drawdown	0.0067	2.50	Vetiver grass roots
		5-10	All	Note: There is no suitable model for tensile strength and additional cohesion from literature for a root reinforcing deeper than 2.5 m.		
	1:3	**2**	For only long duration floods followed by rapid drawdown and medium drawdown	0.0007	0.50	*Bauhinia championii* Shrubs: *Atriplex halimus, Salsola genistoides, Thymelaea hirsute, Artemisia barrelieri* and *Rosmarinus officinalis* Grass: *Stipa tenacissima* and *Lygeum spartum* Tree: *Tamarix canariensis* Rush: *Juncus acutus*
		3	For only long duration floods followed by rapid drawdown and medium drawdown	0.007	1.20	*B. championii,* vetiver grass, conifer and broadleaf species
		4	All except short duration and medium duration floods followed by slow drawdown	0.0029	2.00	Vetiver grass roots
		5	All except for medium duration floods followed by slow drawdown	0.0094	2.00	Vetiver grass roots
		6	For only short duration and medium duration floods followed by rapid and medium drawdown	0.0057	2.50	Vetiver grass roots
		7	For only short duration floods followed by rapid and medium drawdown and medium duration floods followed by medium drawdown	0.0067	2.50	Vetiver grass roots
		8	For only short duration floods followed by rapid and medium drawdown	0.0064	2.50	Vetiver grass roots
		9-10	All	Note: There is no suitable model for tensile strength and additional cohesion from literature for a root reinforcing deeper than 2.5 m.		
Gravel	**1:3**	**1-4**	All	0.0037	0.50	Shrubs: *Atriplex halimus* and *Salsola genistoides*
		5-10	All	0.0030	1.50	Vetiver grass roots

The results of root functional traits required to achieve bank stabilization is merely a guideline and represents the minimum requirements. The results were limited by the values and models found in literature. Plant species that have roots that provide greater additional cohesion at the minimum depths suggested, or are able to provide additional cohesion at greater depths than suggested, would further increase bank stability. Furthermore, in practical cases, riverbanks may not be homogeneous and soil strength criteria may differ from the criteria used in the models.

5.4 Hypothetical examples for South African rivers

This section includes a full assessment of two rivers within the Crocodile and Sabie-Sand River systems respectively, pertaining to the suitability of vegetation stabilization for the riverbanks. These are hypothetical examples for the purpose of demonstrating the necessary procedure required to identify when vegetation roots are a suitable bank stabilization technique and which root functional traits would be able to provide stabilization for the suitable cases. The actual applicability of these examples is subject to data acquisition of the soil strata, bank height and bank slope.

5.4.1 Crocodile River

Figure 5.25 shows the catchment outline for the Crocodile River, the point of interest as outlined refers to the location where the flow data was required and ultimately where the suitability of vegetation as a bank stabilization method was determined.

The area of catchment was regarded as a Lowveld zone with a flat to moderate relief; the earth comprises shallow black, brown or red clayey soils. The river is 40 m wide and slow flowing (River Health Programme, 2001).

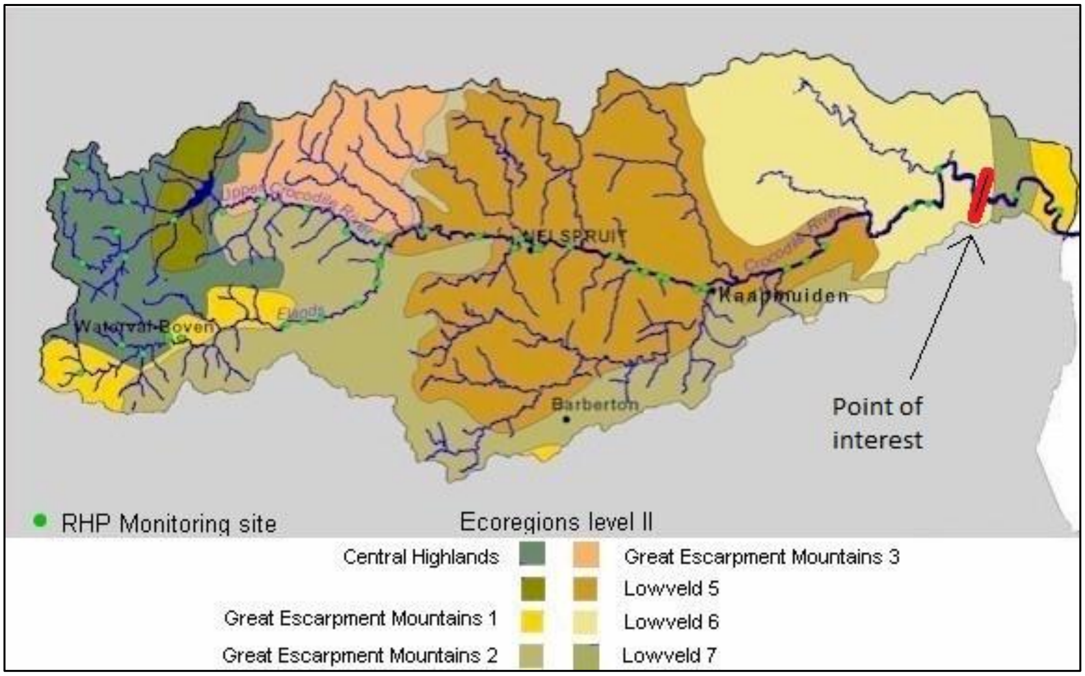

Figure 5.25: The Crocodile River system (after DWS, 2001)

The HRU design storm and synthetic unit hydrograph method was used to develop the flood hydrograph for the river. The flood hydrograph for the Crocodile River, as shown in Fig. 5.26, along with the relevant rating curve was used to obtain the rate of rise (flood duration) and the rate of drawdown (drawdown rate). The calculations are included in Appendix I. The rate of rise during the flood was calculated as 0.95 m/h and the drawdown rate was 0.33 m/h.

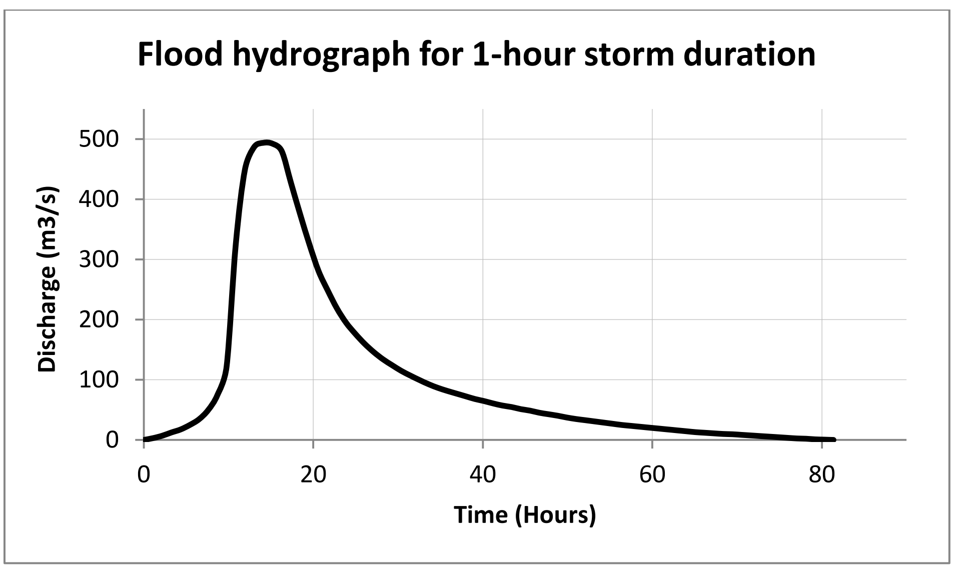

Figure 5.26: Flood hydrograph for point of interest on Crocodile River, 50 year return period and 1-hour storm duration

Specific data on the river cross section was unavailable (in practice this would need to be obtained using site-specific cross section capturing methods). Figure 5.27 shows the typical cross section of such a river profile. The river cross section at the point of interest was estimated to have the following characteristics:

- **Bank angle**: a steep slope of 2:1
- **Type of soil**: clay as described by the River Health Programme (2001), assuming the strength and permeability criteria as defined in section 4.2
- **Bank height**: a relatively high bank of 5 m

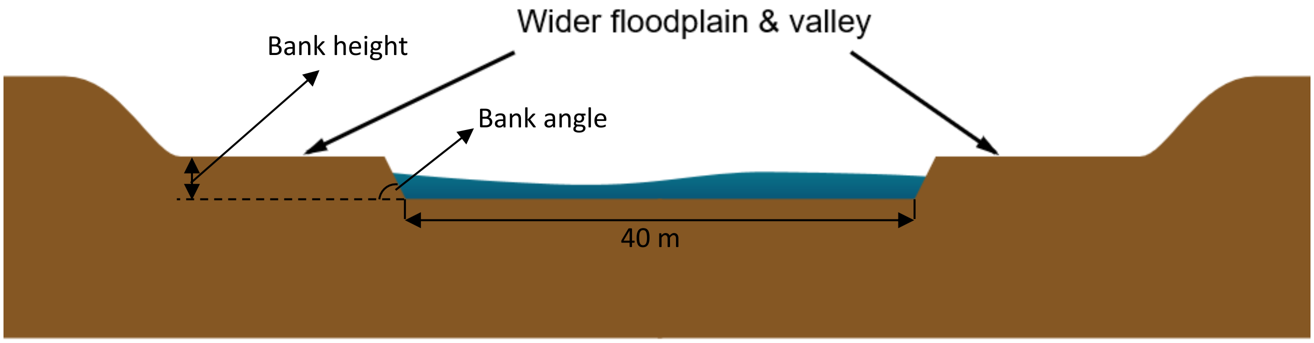

Figure 5.27: Approximate river cross section at Crocodile River point of interest (after Jackson, 2012)

The flood event corresponded closest to a short duration flood followed by rapid drawdown rate. For the assumed bank height and bank angle and using the design-aid in Table 5.1, the bank was classified as NV and hence was found to be in a stable state for this scenario and furthermore, vegetation stabilization was not considered.

5.4.2 Sabie-Sand River

Figure 5.28 shows the catchment outline for the Sabie-Sand River system, the point of interest as outlined refers to the location whereby the flow data is required and ultimately where the suitability of vegetation as a bank stabilization method must be determined.

The area of catchment was regarded as a Lowveld zone with mountainous regions and with a moderate relief; the earth comprises sandy, sandy loam, and clayey soils. The river is fairly narrow and has moderate flows (River Health Programme, 2001).

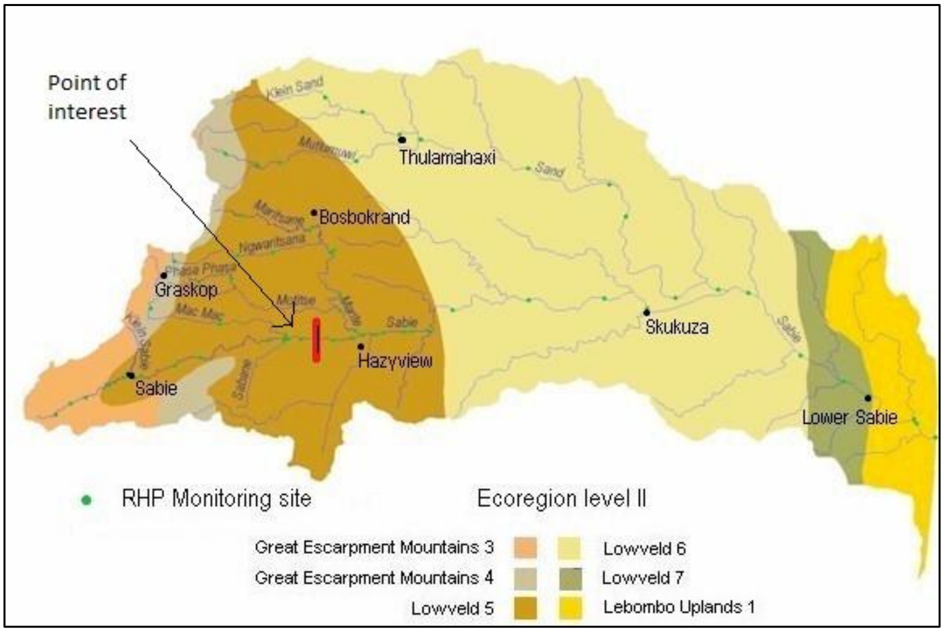

Figure 5.28: Sabie-Sand River system (after DWS, 2001)

The HRU design storm and synthetic unit hydrograph method was used to develop the flood hydrograph for the river. The flood hydrograph for the Sabie-Sand River, as shown in Fig. 5.29, along with the relevant rating curve was used to obtain the rate of rise and the rate of drawdown. The calculations are included in Appendix I. The rate of rise during the flood was calculated as 0.79 m/h and the drawdown rate was 0.18 m/h.

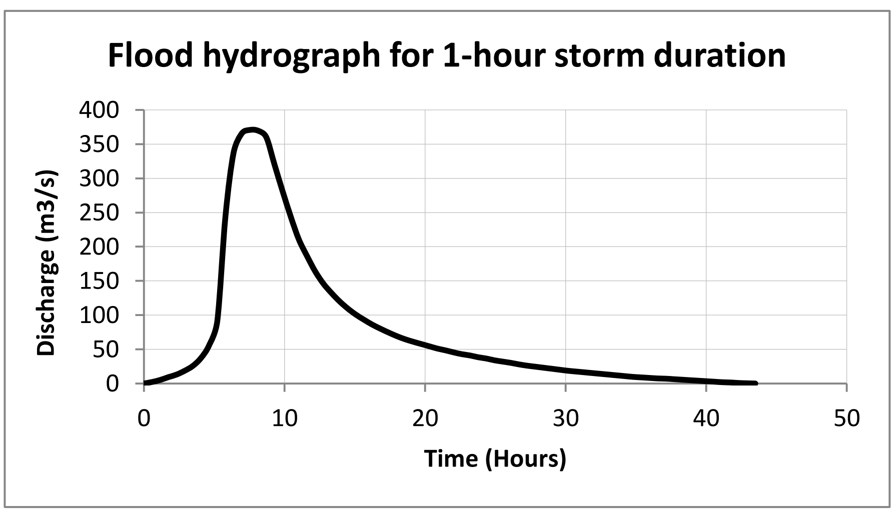

Figure 5.29: Flood hydrograph for point of interest on Sabie River, 100 year return period and 1-hour storm duration

Specific data on the river cross section was unavailable, as in the example of the Crocodile River, and in practice this would need to be obtained using site-specific cross section capturing methods. Figure 5.30 shows the typical cross section of the Sabie-Sands river profile. The river cross section at the point of interest was estimated to have the following characteristics:

- **Bank angle**: a moderate slope of 1:1
- **Type of soil**: loamy sand as described by the River Health Programme (2001), assuming strength and permeability criteria as defined in section 4.2
- **Bank height**: a low bank of 2 m

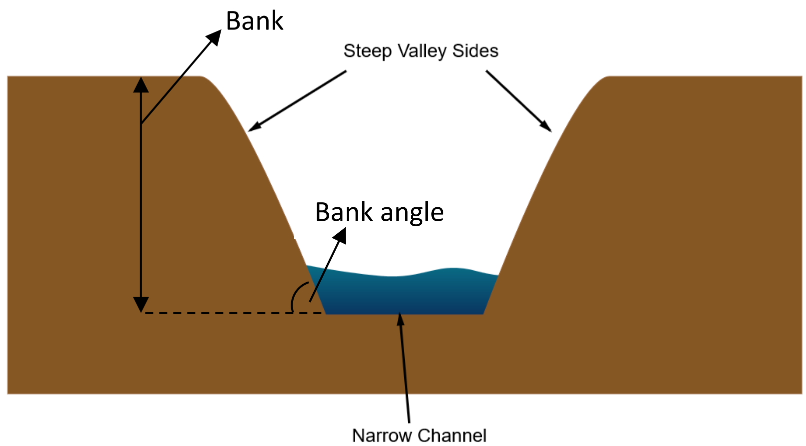

Figure 5.30: Approximate river cross section at Sabie River point of interest (after Jackson, 2012)

The flood event corresponded closest to a short duration flood followed by medium drawdown rate. For the assumed bank height and bank angle and using the design-aid in Table 5.1, the bank was classified as UV and hence was found to be suitable for vegetation stabilization.

When following the guideline as set out in Appendix H, it is recommended that the root functional traits required to stabilize the bank are: roots penetrating to a depth of at least 1.20 m below the slope face, providing a minimum additional cohesive strength of 18.33 kPa and a tensile strength of at least 16.96 MPa (Table H.2). These properties could be obtained by using conifer and broadleaved plant species, as documented by Danjon et al. (2008), with a high root density of 41 roots per sq. m and an average root diameter of 2.8 mm (providing a *RAR* of 0.025%).

Chapter 6 Conclusions

A procedure for determining the feasibility of vegetation use in bank stabilization for a number of soil types, bank angles, bank heights and flood conditions pertaining to South African riverbanks has been established. In the development of the procedure it was found that both the bank geometry and material permeability are significant factors in bank stability following flood events. It was also found that bank material strength provides an indication of the type of failure. Silt loam and loamy sand riverbanks are the most susceptible to instability caused by flooding events, due to material permeability. Loamy sand and gravel riverbanks are more suitable for vegetation stabilization, due to the lower cohesive strength, since these banks result in shallow slip failure i.e. in the zone of influence of plant roots. The additional cohesion due to vegetation is able to provide stability in these banks.

Since material permeability and material strength were identified as significant factors in bank stability and vegetation root suitability, the sensitivity of the soil-water characteristic curve to the main input parameters (air-entry value, grain size data and the saturated volumetric water content) was determined in SEEP/W using a sensitivity analysis. It was discovered that these input parameters are reliable within realistic ranges but the saturated volumetric water content should be identified with greater accuracy for soils of low permeability, for the guidelines presented to be used with greater confidence.

The analysis showed that the most significant root functional traits are root diameter, root density and root length. Subsequently, depending on the type of species, the most significant root strength properties are the pull out strength or root tensile strength (whichever is obtainable due to the fact that the pull out strength can be estimated from the tensile strength and vice versa) and the additional cohesion.

Therefore a guideline pertaining to the root functional traits required to stabilize the banks, for scenarios where bank stabilization would be appropriate, has been produced in section 5.3.

Finally, to demonstrate the use of the guidelines, hypothetical examples for the Crocodile and Sabie-Sand Rivers were presented. The examples provided a full assessment of the typical flood conditions at the points of interest, whether the use of vegetation roots was a suitable stabilization technique, and when suitable, which root functional traits would be able to provide stabilization.

Chapter 7 Recommendations

Data pertaining to the soil strata, bank height and bank slope are limited for South African rivers. It would be beneficial to survey actual river cross sections along South African rivers and develop guidelines that reflect which rivers, and at which locations along those rivers, would be expected to experience stability problems.

Further research is required to assess the degree of confidence necessary for the input data related to soil strength and permeability, such that the guideline may be used with a quantifiable level of reliability. It would also be useful to develop a guideline that can be used on site to diagnose which soil category the bank to be stabilized assigns to, so that the guideline provided in this report can be readily used. The bank heights and slopes can be physically measured in the field and the profiles can be developed along the river to assess where bank failure may be of concern. The steepest slopes should be prioritized as they will be most susceptible to bank failure. Determination of the flood conditions currently requires significant computational effort, as well as a site inspection of the river cross sectional information, and a desktop study may be carried out to determine regional information such as the length of the longest stream to the catchment boundary. However, the procedure suggested for determining the flood conditions in this study is based on a well-established methodology, and a simplification pertaining to the assessing of flood conditions can be done by developing code based algorithms and populating the program with existing relevant data for South African rivers. It is suggested that further research be carried out by making use of the guideline proposed in this research report together with the suggested coded program so that the end result would be similar to the ECO-SLOPES program, made relevant to the South African context.

Although a wide variety of plant species have been coupled with the root functional traits required to achieve bank stabilization, they were sourced from studies that were not specific to the South African environment. It is recommended that the database be refined by matching the required root functional traits and root strength properties to South African plant species. The database can be developed based on actual field measurements of root functional traits, which include the root diameter, root density and root length, all of which can be physically measured using a Vernier Caliper or similar instrumentation. This information can then be coupled with root strength properties (pull out strength/ root tensile strength and additional cohesion) which can be determined by field and laboratory tests. Once this database is developed the root properties can be linked to the root functional traits database developed for the Northern Hemisphere, making it possible to use Table 5.5 (Stabilizing root functional traits for scenarios where vegetation can be used to stabilize the bank) for the South African environment. Furthermore, for an improved design-aid, it would be beneficial to investigate the durability of these plant species with regards to various periods of inundation, wave action and erosion. It is necessary to determine how well plants grow in certain conditions and which conditions (climate, soil environments, north facing/south facing slope, drawdown conditions, river velocity and bank angle) would limit plant growth. The time taken for plant species to grow and to allow roots to reach the required depth must be taken into consideration and precautionary measures should be put in place until such time that the root properties are fully developed.

With regards to modelling in SLOPE/W and SEEP/W, it would be beneficial to determine the effect on riverbank stability for wider riverbank crests than those investigated in this study. Furthermore, the study could be extended to determining the effect of ponding on the riverbank plains on bank stability, as opposed to only considering the effect of flood events.

REFERENCES

Abernethy, B and Rutherfurd, I D (2001) The distribution and strength of riparian tree roots in relation to riverbank reinforcement, Hydrological Processes 15: 63-79.

Abernethy, B and Rutherfurd, I D (1999) Guidelines for Stabilizing Streambanks with Riparian Vegetation, Report no. 99/10, Cooperative Research Centre for Catchment Hydrology, Melbourne, Australia.

Abernethy, B and Rutherfurd, I D (1998) Where along a river's length will vegetation most effectively stabilize stream-banks?, Geomorphology, 23: 55-75.

Adamson P T (1981) South African Storm Rainfall, Pretoria: Department of Environment Affairs.

Adhikari, A R, Gautam, M R, Yu, Z, Imada, S and Acharya, K (2013) Estimation of root cohesion for desert shrub species in the Lower Colorado riparian ecosystem and its potential for streambank stabilization, Ecological Engineering 51: 33-44.

AIR/W (2012) Air flow modeling with AIR/W, GEO-SLOPE International, Calgary, Alta.

ASCE Task Committee on Hydraulics, Bank Mechanics, and Modeling of River Width Adjustment (1998) River width adjustment. I: Processes and mechanisms, Journal of Hydraulic Engineering 124(9): 881-902.

Aubertin, M, Ricard, J F and Chapius, R P (1998) A predictive model for the water retention curve: application to tailings from hard-rock mines, Canadian Geotechnical Journal, ProQuest Central 35: 55-69.

Baldwin, J P and Tinker, P B (1972) A method of estimating the length and spatial patterns of two interpenetrating root systems, Pl. Soil 37:209-213.

Beck, D L, Darrah, L L and Zuber, M S (1988) Relationship of root tensile strength to the vertical pulling resistance in maize, Crop Sci. 28: 571-573.

Bishop, A W (1955) The use of the slip circle in the stability analysis of slopes, Géotechnique 5: 7-17.

Blasio, F V D (2011) Friction, Cohesion and Slope Stability, Introduction to the Physics of Landslides: Lecture Notes on the Dunamics of Mass Wasting, Springer Science and Business Media.

Bowerman, T S (1999) Engineering Index Properties, Targhee National Forest Ecological Unit Inventory, U.S. Forest Service, Vol. 2, pp 630-648.

Brouwer, R (1964) Responses of bean plants to root temperature. 1. Root temperatures and growth in the vegetative stage, Jaarb. I.B.S, (Wageningen), 11-12.

Budhu, M and Gobin, R (1995) Seepage-induced slope failures on sandbars in Grand Canyon, Journal of Geotechnical Engineering 121(8): 601-609.

Burroughs, E R and Thomas, B R (1977) Declining root strength in Douglas-fir after felling, as a factor in slope stability, USDA Forest Service Research Paper no. INT-190.

Burylo, M, Rey, F, Mathys, N and Dutoit, T (2012) Plant root traits affecting the resistance of soils to concentrated flow erosion, Earth Surface Processes and Landforms 37: 1463-1470.

Burylo, M, Hudek, C and Rey, F (2010) Soil reinforcement by the root system of six dominant species on eroded mountainous marly slopes (Southern Alps, France), CATENA, Elsevier pp 45.

Caldwell, M M (1979) Root structure: the considerable cost of belowground function, In Topics in Plant Population Biology, O.T. Solbrig, S Jain, G B and P. H. Raven (Eds.), Columbia University Press, New York.

Calow, P and Petts, G E (1994) The Rivers Handbook, Blackwell Science, Vol. 2.

Cazzuffi, D, Corneo, A and Crippa, E (2006) Slope stabilisation by perennial “gramineae” in Southern Italy: plant growth and temporal performance, Journal og Geotechnical and Geological Engineering 24:429-447.

Chen, X and Huang, J (2011) Stability analysis of bank slope under conditions of reservoir impounding and rapid drawdown, Journal of Rock Mechanics and Geotechnical Engineering, 3: 429-437.

Coppin, N J, Barker, D H, Mogan, R P C and Rickson, R J (1990) Use of vegetation in civil engineering, CIRIA, London.

CSRA (Committee of State Road Authorities) (1994) Guide-lines for the hydraulic design and maintenance of river crossings, Volume 1, Hydraulics, Hydrology and Ecology, Committee of State Road Authorities, Pretoria.

CTRAN/W (2012) Contaminant modeling with CTRAN/W, GEO-SLOPE International, Calgary, Alta.

Danjon, F, Barker, D H, Drexhage, M and Stokes, A (2008) Using 3D plant root architecture in models of shallow-slope stability, Annals of Botany 101: 1281-1293.

Das, B M (2008) Fundamentals of Geotechnical Engineering, 3rd edn, Thomson Learning, Canada, pp 45.

Das, T K, Haldar, S K, Gupta, I D and Sen, S (2014) River bank erosion induced human displacement and its consequences, Living Reviews in Landscape Research 8: 1-35.

Davidson, R L (1969a) Effects of root/leaf temperature differentials on root/shoot ratios in some pasture grasses and clover, Ann. Bot, NS 33: 561-569.

Davidson, R L (1969b) Effects of soil nutrients and moisture on root/shoot ratios in Lolium perenne L and Trifolium repens L, Ann. Bot, NS 33: 571-577.

De Baets S, Poesen J, Reubens B, Wemans K, De Baerdemaeker J and Muys B (2008) Root tensile strength and root distribution of typical Mediterranean plant species and their contribution to soil shear strength, Plant Soil 305: 207-226.

Dias, A S, Pirone, M and Urciuoli (2017) Review on the Methods for Evaluation of Root Reinforcement in Shallow Landslides, In: M Mikoš, B Tiwari, Y Yin and K Sassa (Eds) Advancing culture of living with landslides, Vol. 2, Springer International Publishing, Switzerland.

Dietrich, W and Montgomery, D (1998) Slope stability model [Online] Available at: http://calm.geo.berkeley.edu/geomorph/shalstab/theory.htm [Accessed 6 February 2017].

Docker, B B, Hubble, T C T (2008) Quantifying the enhanced soil shear strength beneath four riparian tree species, Geomorphology 100: 400-418.

DWAF (Department of Water Affairs and Forestry) (2007) Berg River Baseline Monitoring Programme, G Ractliffe (Eds), DWAF, South Africa.

DWS (Department of Water and Sanitation) (2001) State of rivers report [Online] Available at: https://www.dwa.gov.za/iwqs/rhp/state_of_rivers/state_of_crocsabieolif_01/croc_eco.html [Accessed 6 December 2016].

Endo, T and Tsuruta, T (1969) On the effect of tree roots upon the shearing strength of soil, Annual report of the Hokkaido Branch, Forest Place Experimental Station, Sapporo, Japan, pp 167-183.

Fellenius, W (1936) Calculation of the Stability of Earth Dams, Proceedings of the Second Congress of Large Dams, Vol. 4, pp 445-463.

Fredlund, D G and Xing, A (1994) Equations for soil-water characteristic curve, Canadian Geotechnical Journal 31: 521-532.

Fredlund, M D, Fredlund D G, Houston S L and Houston, W B (2003) Assessment of unsaturated soil properties for seepage modeling through tailings and mine wastes, In Proceedings of the 10th International Conference on Tailings and Mine Wastes, Vail, Colorado, U.S.

Fuselier, T B H (2006) Evaluation of soil water characteristic curves and permeability functions for modeling of seepage in unsaturated soils, Master of Science thesis, Tufts University.

Gallage, C P K, Uchimura, T (2010) Effects of dry density and grain size distribution on soil-water characteristic curves of sandy soils. Soils Found. 50: 161–172.

Garcia, A C L (2004) Bank instability resulting from rapid flood recession along the Licking River, Kentucky, MSc research thesis, University of Cincinnati, Ohio.

GEO-SLOPE (2007) SEEP/W Version 7 Users Manual, GEO-SLOPE International, Calgary, Alta.

Geotechnical Design Manual (2015) Slope Stability Analysis, Oregon Department of Transportation 7: 1-3.

Geotechdata.info (2013) Soil void ratio [Online] Available at: http://geotechdata.info/parameter/soil-void-ratio.html [Accessed 8 August 2017].

Ghestem, M, Cao, K, Ma, W, Rowe, N, Leclerc, R, Gadenne, C and Stokes, A (2014) A Framework for Identifying Plant Species to Be Used as ‘Ecological Engineers’ for Fixing Soil on Unstable Slopes, PLoS ONE 9(8): e95876, doi:10.1371/journal.pone.0095876.

Goss, M J (1977) Effect of mechanical impedance on growth of seedlings, J. Exp. Bot. 28: 96-111.

Gray, D H and Barker, D H (2004) Root-soil mechanics and interactions, In: S J Bennett, A J C Collison and A Simons (Eds) Riparian vegetation and fluvial geomorphology: hydraulic, hydrologicand geotechnical interactions, Water Science and Application 8, American Geophysical Union, Washington, pp 125-139.

Gray, D H and Sotir, R B (1996) Biotechnical and Soil Bioengineering Slope Stabilization: A Practical Guide for Erosion Control, John Wiley & Sons, Canada.

Gray, D H, and Ohashi, H (1983) Mechanics of fiber reinforcement in sand, Journal of Geotechnical Engineering, 109: 335–353. doi:10.1061/(ASCE)0733-9410(1983)109:3(335).

Gray D H and Leiser A J (1982) Biotechnical Slope Protection and Erosion Control, Van Nostrand Reinhold, New York.

Green, S J (1999) Drawdown and river bank stability, MSc research thesis, Department of Civil and Environmental Engineering, University of Melbourne.

Greenway, D (1987) Vegetation and slope stability, In Slope Stability, M G Anderson and K S Richards (Eds), John Wiley & Sons, New York, pp 187-230.

Greenwood, J R (2006) SLIP4EX- A program for routine slope stability analysis to include the effects of vegetation, reinforcement and hydrological changes, Geotechnical and Geological Engineering 24: 449-465.

Greenwood, J R, Norris, J E and Wint, J (2004) Assessing the contribution of vegetation to slope stability, Geotechnical Engineering 157: 199-208.

Greenwood, J R (1985) Wedge analysis of embankment instability during construction of the M25 Motorway, In Proceedings of the ICE International Symposium on Earthworks Failures, pp 403- 405.

Gurdal, T, Benson, C and Albright, W (2003) Hydraulic properties of final cover soils from the Alternative Cover Assessment Program, Geo Engineering Rep. No. 03-02, Geo Engineering Program, University of Wisconsin-Madison, Madison, Wis.

Habibah, L, Avani, N and Bibalani, G H (2013) Effects of Acaia mangium root properties on shallow landslide and slope stability, Journal of Life Sciences and Technologies, Vol. 1, No. 2, pp 127-131.

Heshmati, A A and Motahari, M R (2012) Identification of key parameters on Soil Water Characteristic Curve, Life Science Journal 9(3): 1532-1537.

Hengchaovanich, D and Nilaweera, N S (1996) An assessment of strength properties of vetiver grass roots in relation to slope stabilization, Proc. First International Vetiver Conf. Thailand pp. 153-8.

Hey, R D, Heritage, G L, Tovey, N K, Boar, R R, Grant, A and Turner, R K (1991) Streambank Protection in England and Wales, R & D Note 22, National Rivers Authority, London.

Hill, K E (1941) Factors affecting the use of gravel in oil wells, API Drill. Prod. Pract., pp 134-143.

Hong, W T, Jung, Y S, Kang, S and Lee, J S (2016) Estimation of soil-water characteristic curves in multiple-cycles using membrane and TDR system, Materials, School of Civil, Environmental and Architectural Engineering, Korea University.

Hudek, C (2013) Efficiency of vegetation roots for protection against surface erosion in mountainous areas: the case of Mahonia aquifolium, Utrecht Studies in Earth Sciences.

Hubble, T C T (2010) Improving the stream of consciousness: A nomenclature for describing the factor of safety in river bank stability analysis, Ecological Engineering 36: 1765-1768.

Hydrological Research Unit (1972) Design flood determination in South Africa, Johannesburg: University of the Witwatersrand Dept. of Civil and Environmental Engineering.

Jaksa, M, Hubblet, T, Kuoy, L, De Carli, E and Liang, C (2013) Goyder Institute Research Project: E1.8 Riverbank Collapse in the Lower Murray River- Literature Review and Knowledge Gap Analysis, Goyder Institute for Water Research Technical Report Series 13/15, Adelaide, South Australia.

Jackson, A (2012) Geography AS notes. [Online] Available at:
https://geographyas.info/rivers/long-and-cross-profiles/ [Accessed 7 December 2016].

Janbu, N (1973) Slope stability computations in embankment dam engineering, Casagrande Memorial Volume, Wiley, New York, pp 47-86.

Kleinendorst, A and Brouwer, R (1965) Effect of temperature on two different clones of ryegrass, Jaarb. I.B.S., 29-39.

Kobayashi, H (1977) Studies of physical interaction of forage roots on grassland soil: 1. Roots system distribution and mechanical strength of forage grass roots, J. Jpn. Soc. Grassi. Sci. 23:135-139.

Kosiw M, Parks K and Besley S (2008) Solutions to riverbank erosion: A summary of current shoreline stabilization techniques for the Gull River in Minden, Ontario.

Kunberger, T M K (2007) Remediation of soil- Sorbed Cesium through the process of clay fines dispersion and piping, Releigh, North Carolina, pp 137.

Li, X, Li, J H and Zhang, L M (2014) Predicting bimodal soil water characteristic curves and permeability functions using physically based parameters, Computers and Geotechnics 57:85-96.

Manoli, G, Bonetti, S, Domec, J C, Putti, M, Katul, G and Marani, M (2014) Tree root systems copeteing for soil moisture in 3D soil-plant model, Advances in Water Resources 66: 32-42.

Mao, Z, Bourrier, F, and Fourcaud, T (2014) Evaluation of root reinforcement models using numerical modelling approaches, Plant Soil 381: 249-270.

Mattia, C, Bischetti, G B and Gentile, F (2005) Biotechnical characteristics of root systems of typical Mediterranean species, Plant Soil 278: 23-32.

McGill, B J, Enquist, B J, Weiher, E and Westoby, M (2006) Rebuilding community ecology from functional traits, Trends Ecol. Evol. 21: 178-185.

Mickovski, S B, Stokes, A, van Beek, R, Ghestem, M, Fourcaud, T (2011) Simulation of direct shear tests on rooted and non-rooted soil using finite element analysis, Ecological Engineering 37: 1523-1532.

Mickovski, S B and van Beek, L P H (2006) A decision support system for the evaluation of eco-engineering strategies for slope protection, Geotechnical and Geological Engineering 24: 483-498.

Mitchell, R L (1969) Rooting habits of soybeans: Root Growth, ed. Whittington W J, Butterworths, London, 399.

Moolman, J, Kleynhans, C J and Thirion, C (2002) Channel slopes in the Olifants, Crocodile, and Sabie river catchments, Pretoria: Department of Water Affairs and Forestry.

Morgenstern, N R and Price, V E (1965) The analysis of the stability of general slip surfaces, Geotechnique 15(1): 79-93.

Mulder, H F H M (1991) Assessment of Landslide Hazard, Utrecht, University of Utrecht 149.

Naghdi, R, Maleki, S, Abdi, E, Mousavi, R and Nikooy, M (2013) Assessing the effect of Alnus roots on hillslope stability in order to use in soil bioengineering, Journal of Forest Science 59(11): 417-423.

Neilson, K F and Cunningham, R K (1964) The effect of soil temperature and form and level of N on growth and chemical composition of Italian ryegrass, Proc. Soc. Soil Sci. Am., 28: 213-218.

Nicoll, B C, Berthier, S, Achim, A, Gouskou, K, Danjon, F and van Beek, L P H (2006) The architecture of *Picea sitchensis* structural root systems on horizontal and sloping terrain, Trees-Struct Func 20: 701-712.

Nilaweera, N S (1994) Effect of tree roots on slope stability: the case of Khao Luang Mountain area, southern Thailand, Doc. of Tech. Sci. thesis, Asian Institute of Technology, Bangkok, Thailand.

Norris, J E, Stokes, A, Mickovski, S B, Cammeraat, E, van Beek, R, Nicoll BC and Achim, A (Eds) (2008) Slope stability and erosion control: Ecotechnical solitions, Springer, The Nertherlands.

Norris, J E and Greenwood, J R (2006) Assessing the role of vegetation on soil slopes in urban areas, The Geological Society of London, IAEG, Paper number 744.

Norris, J E (2005a) Root mechanics applied to slope stability, PhD thesis, Nottingham Trent University, Nottingham, UK.

Norris J E (2005b) Root reinforcement by hawthorn and oak roots on a highway cut-slope in Southern England, Plant Soil 278: 43-53.

Norris, J E and Greenwood, J R (2000) In-Situ shear and pull-out testing to demonstrate the enhanced shear strength of root reinforced soil, In Proceedings of the 8th International Symposium on Landslides, Cardiff, UK, Vol. 3, pp 1125-1128.

Nyambane, O S and Mwea, S K (2011) Root tensile strength of 3 typical plant species and their contribution to soil shear strength; case study: Sasumua Backslope, Nyandarua District, Kenya, Journal of Civil Engineering Research and Practice, Vol. 8, No.1, pp 57-73.

Operstein, V and Frydman, S (2000) The influence of vegetation on soil strength. Ground Improv. 4: 81-89.

Osman, N, Abdullah, M N and Abdullah, C H (2011) Pull-out and tensile strength properties of two selected tropical trees, Sains Malaysiana, 40(6), 577-585.

Oya, A, Bui, H H, Hiraoka, N, Fujimonto, M and Fukagawa, R (2015) Seepage flow-stability analysis of the riverbank of Saigon river due to river water level fluctuation, Graduate School of Science and Engineering, Ritsumeikan University, Japan.

Palanikumar, M (2013) Soil Mechanics, Technology and Engineering, pp 305.

Perry, J (1989) A survey of slope condition on motorway earthworks in England and Wales, Transport and Road Research Laboratory, Research Report No. 199, pp 49.

Pinthus, M J (1967) Spread of the root system as indicator for evaluating lodging resistance of wheat, Crop Sci 7: 107-110.

Pollen, N and Simon, A (2005) Estimating the mechanical effects of riparian vegetation on stream bank stability using fiber bundle model, Water Resour. Res. 41, W07025.

Preti, F and Giadrossich, F (2009) Root reinforcement and slope bioengineering stabilization by Spanish Broom (*Spartium junceum* L.), Hydrology and Earth System Sciences 13: 1713-1726.

Price, P and Lovett, S (2002) Streambank stability, Fact Sheet 2, Land and Water Australia, Canberra.

QUAKE/W (2014) Dynamic modeling with QUAKE/W, GEO-SLOPE International, Calgary, Alta.

Rahardjo, H, Satyanaga, A and Mercer, K (2014) Application of unsaturated soil mechanics to open pit slope stability, Australian Centre for Geomechanics, Nanyang Technological University, Singapore.

Raper, C D and Barber, S A (1970) Rooting systems of soybeans, 1. Differences in root morphology among varieties, Agron. J., 62: 581-584.

Rawls, W J, Brakensiek, D L and Saxton, K E (1982) Estimation of Soil Water Properties, Trans. ASAE 25:1316-1320.

Reubens, B, Poesen, J, Danjon, F, Geudens, G and Muys, B (2007) The role of fine and coarse roots in shallow slope stability and soil erosion control with a focus on root system architecture: a review, Trees-Struct, 21(4): 385-402.

Ridley, A M, Dineen, K, Burland, J B and Vaughan, P R (2003) Soil matrix suction: some examples of its measurement and application in geotechnical engineering, Geotechnique 53(2): 241-253.

Riestenberg, M M and Sovonick-Dunford, S (1983) The role of woody vegetation on stabilizing slopes in the Cincinnati area, Geological Society of America Bulletin, 94: 504-519.

Rinaldi, M and Darby, S E (2008) Modelling river-bank-erosion processes and mass failure mechanisms: progress towards fully coupled simulations, in Gravel-Bed Rivers VI: From Process Understanding to River Restoration H. Habersack, H Piégay and M Rinaldi (Eds), Elsevier.

Russel, S R (1977) Plant Root Systems: Their function and interaction with the soil, McGraw-Hill, London.

River Health Programme (2001) State of the Rivers Report; Crocodile, Sabie-Sand and Olifants River Systems, Pretoria: Water Research Commission, Pretoria.

SANRAL (The South African National Roads Agency) (2013) Drainage Manual, 6th ed., The South African National Roads Agency, Pretoria.

SANRAL (The South African National Roads Agency) (2006) Drainage Manual, The South African National Roads Agency, Pretoria.

SEEP/W (2007) A software package for groundwater seepage analysis, Ver. 7. GEO-SLOPE International, Calgary, Alta.

SIGMA/W (2013) Stress-deformation modeling with SIGMA/W, GEO-SLOPE International, Calgary, Alta.

SLOPE/W (2007) A software package for slope stability analysis, Ver. 7. GEO-SLOPE International, Calgary, Alta.

Sieben, E J J (2000) The riparian vegetation of the Hottentots Holland Mountains, Ph.D. Thesis, Stellenbosch University, Matiland, ZA.

Simon A, Pollen N, Langendoen E (2006) Influence of two woody riparian species on critical conditions for streambank stability: upper Truckee river, California. J Am Water Resour. Assoc. 42: 99-113.

Simon, A, Thomas, R E, Curini, A and Shields J F D (2002) Case study: Channel stability of the Missouri river, Eastern Montana, Journal of Hydraulic Engineering, ASCE 28(10): 880-890.

Simon, A , Curini, S E, Darby and Langendoen, E J (2000) Bank and near-bank processes in an incised channel, Geomorphology 35(3-4): 193-217.

Sivakugan, N (2000) Soil Classification, Chapter 3, James Cook University, Available at: http://eng1.jcu.edu.au/research/compgeo/classify.pdf [Accessed 15 November 2016].

Smithers, J C (2012) Methods for design flood estimation in South Africa, Water SA 38(4): 633-646.

Smithers, J C and Schulze, R E (2002) Design rainfall and flood estimation in South Africa, Pietermaritzburg: University of Natal.

Sonwabile, A (2017) ‘Erosion concerns’, Randburg Sun, 8 December, pp 3.

Sonwabile, A (2017) ‘Crumbling away’, Randburg Sun, 23 November, pp 1.

Spencer, E E (1967) A method of analusis of the stability of embankments assuming parallel inter-slice forces, Géotechnique 17: 11-26.

State of Rivers Report (2001) Letaba and Luvuvhu river systems, WRC report no: TT165/01, Water Research Commission, Pretoria, ISBN no: 1868458253.

Steele, D P, MacNeil, D J, McMahon, W and Barker, D H (2004) The use of live willow poles for stabilising highway slopes, TRL Report 619, TRL Limited, Crowthorne.

Stokes, A, Atger, C, Bengough, A G, Fourcaud, T and Sidle, R C (2009) Desirable plant root traits for protecting natural engineering slopes against landslides, Plant Soil 324: 1-30.

Stokes, A, Mattheck, C (1996) Variation of wood strength in tree roots, J Exp. Bot. 47: 693-699.

Suriya, P, Jayalakshmi, R and EswarSudharsan, C (2015) Factors influences the soil water characteristic curve and its parameters, International Journal of Engineering Research and General Science, Vol. 3, ISSN: 2091-2730.

Swanston, D N (1970) Mechanics of debris avalanching in shallow till soils of southeast Alaska, U.S. Forest Service, Research Paper PNW-103, Pacific and Northwesr and Range Experimental Station, Portland, Oregon.

Thoma, M J, Barrash, W, Cardiff, M, Bradfprd, J and Mead, J (2013) Estimating Unsaturated Hydraulic Functions for Coarse Sediment from Field-Scale Infiltration Experiment, Soil science Society of America.

Thomas, R E and Pollen-Bankhead, N (2010) Modeling root-reinforcement with a fiber-bundle model and Monte Carlo simulation, Ecological Engineering 36:47-61.

Thorne, C R, Reed, S and Doornkamp, J C (1996) A Procedure for Assessing River Bank Erosion Problems and Solutions, R&D Report 28, National Rivers Authority, Bristol, United Kingdom.

Thorne, C R (1990) Effects of vegetation on riverbank erosion and stability, Chapter 10 in Vegetation and Erosion, J B Thornes (Ed.), John Wiley & Sons, Chichester.

Tiwari, R C, Bhandary, N P, Yatabe, R and Bhat, D R (2011) Simulation of Root-reinforcement effect in natural slopes based on progressive failure in soil-root interaction, Int. J. of GEOMATE, Vol. 1, No. 1, pp 32-38.

Toll, D G and Barr R J (2001) A decision support system for geotechnical applications, Computers and Geotechnics 28: 575-590.

VADOSE/W (2014) Vadose zone modeling with VADOSE/W, GEO-SLOPE International, Calgary, Alta.

Vandamme, J and Zou, Q (2013) Investigation of slope stability induced by seepage and erosion by a particle method, Computers and Geotechnics 48: 9-20.

Van De Wiel, M J and Darby, S E (2007) A new model to analyse the impact of woody riparian vegetation on the geotechnical stability of riverbanks, Earth Surface Processes and Landforms 32(14): 2185-2198.

Vanapalli, S K and Fredlund, D G (1997) Interpretation of undrained shear strength of unsaturated soils in terms of stress state variables, Department of Civil Engineering, University of Saskatchewan, Saskatoon, Canada.

van Genuchten, M Th, Leij, F J and Yates, S R (1991) The RETC code for quantifying the hydraulic functions of unsaturated soils, U.S. Department of Agriculture, Agriculture Research Service, Report EPA/600/2-91/065.

van Genuchten, M Th (1980) A closed-form equation for predicting the hydraulic conductivity of unsaturated soils. Soil Science Society of America Journal 44: 892-898.

Waisel, Y, Eshel, A and Kafkafi, U (1991) Plant Roots: The Hidden Half, Dekker.

Waldron, L J and Dakessian, S (1982) Effect of grass, legume and tree roots on soil shearing resistance, J. Soil Sci. Am., 46: 894-899.

Waldron, L (1977) The shear resistance of root-permeated homogeneous and stratified soil, Soil Sci. 41: 843-849.

Walker, J M (1969) One-degree increments in soil temperature affect maize seedling growth, Proc. Soc. Soil Sci. Am., 33: 889-896.

Ward, A L (2007) Geotechnical, Hydrological, and Vegetation Data Package for 200-UW-1 Waste Site Engineered Surface Barrier Design, PNNL-17134, Pacific Northwest National Laboratory, Richland, Washington.

Watson, A and Loughlin, C L (1990) Structural root morphology and biomass of three age-classes of Pinus radiata, New Zealand Journal of Forestry Science 20(1): 97-110.

Weaver J E and Clements F E (1938) Plant ecology, Mc Graw-Hill, New York.

Weaver, J E (1926) Root Development of Field Crops, McGraw-Hill, New York.

White, W A (1949) Atterberg plastic limits of clay minerals, Am. Mineral, Vol. 34, pp 508-512.

Wu, T H (2013) Root reinforcement of soil: review of analytical models, test results, and applications to design, Canadian Geotechnical Journal 50: 259-274.

Wu, T H (2007) Root reinforcement: analyses and experiments, In Eco-and Ground Bio-Engineering: The Use of Vegetation to Improve Slope Stability, A, Stokes, I, Spanos, J E, Norris and E, Cammeraat (Eds.), Development in Plant and Soil Sciences, Vol. 103, Springer, Dordrecht.

Wu, T H, Mckinnell, W P and Swanston D N (1979) Strength of tree roots and landslides on Prince of Wales Island, Alaska, Geotechnical Engineering Report no. 5, Department of Civil Engineering, Ohio State University.

Wynn, T and Mostaghimi, S (2006) The effects of vegetation and soil type on streambank erosion, southwestern Virginia, Journal of the American Water Resources Association 42(1): 69-82.

APPENDIX A

Sensitivity Results for each input parameter (plant root functional traits and root strength properties) using SLIP4EX

Sensitivity of FOS to root diameter

Figure A1 provides a graphical representation of the FOS obtained using the SLIP4EX program for a range of fine roots and coarse roots.

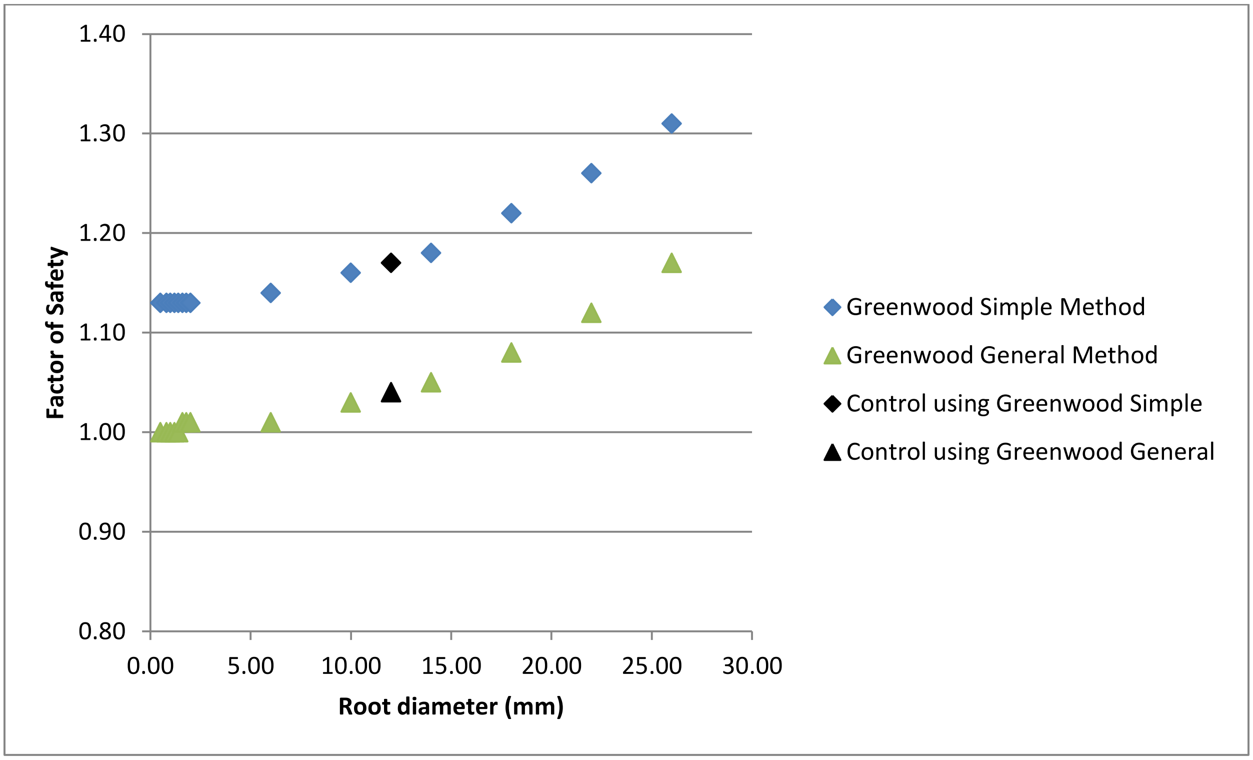

Figure A1: Sensitivity of FOS to root diameter

Figure A1 indicates that the FOS increases with increase in root diameter which is not true according to Gray and Sotir (1996) who found that finer roots have higher tensile strength as well as pullout resistances. It is clear (from Figure A1 above, as well as in the requirement of using a larger root diameter when varying the pull out strength and root density variables in SLIP4EX, to render meaningful changes in FOS) that SLIP4EX is less sensitive to fine roots in its method for calculating the reinforcement force on a slice. This suggests that for fine roots some or all of the other factors (additional cohesion due to vegetation, the increase in weight of slice due to vegetation and change in height of the free water surface due to suction) may be more significant in influencing the FOS. In addition, Fig. A1 suggests that determination of the FOS becomes more sensitive with increased root diameter.

The Greenwood General Method results in the same trend as the Greenwood Simple Method but produces lower FOS values.

Sensitivity of FOS to pull out strength

Figure A2 shows the sensitivity of FOS, in the SLIP4EX program, to variation in pull out strength.

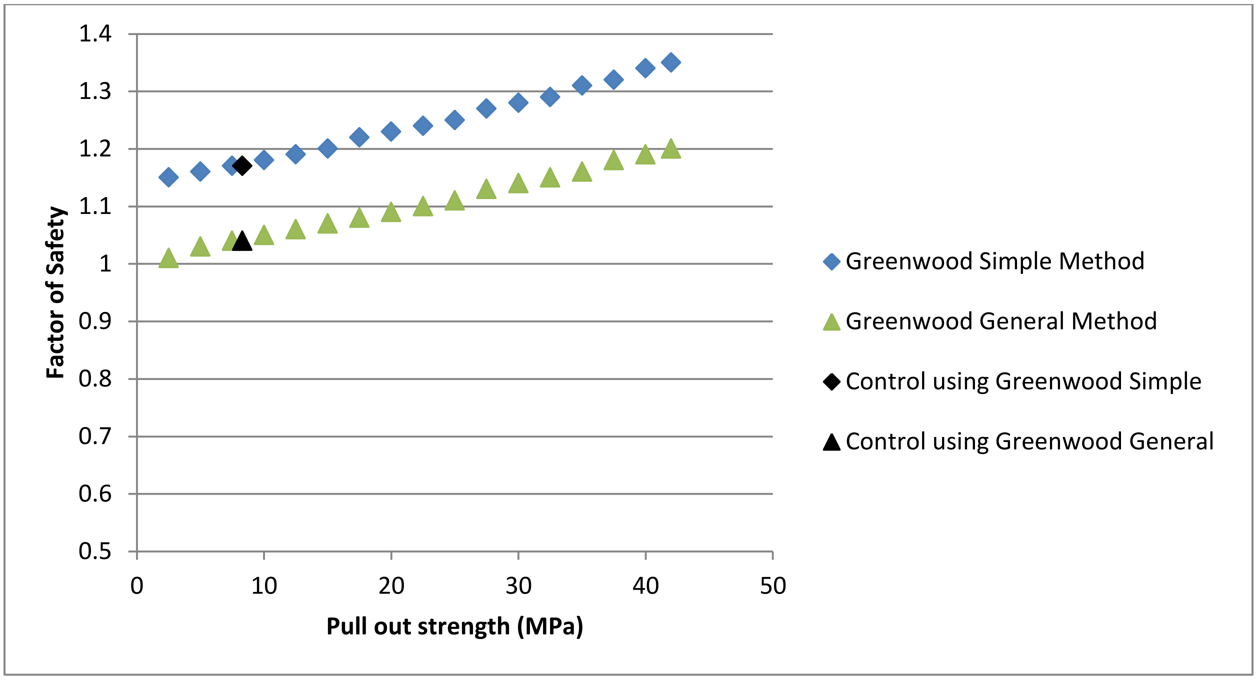

Figure A2: Sensitivity of FOS to pull out strength

The FOS is directly proportional and linearly related to the pull out strength as seen in Fig. A2. The magnitude of the change is small, an increase in pull out strength of 2.5MPa results in an average increase of 1% in the FOS. The linear relationship also indicates that the FOS may be easily predicted if the pull out strength is known.

Sensitivity of FOS to additional cohesion due to vegetation

Figure A3 provides a graphical representation of the FOS for a range of cohesion values, due to the additional cohesion provided by roots. A fine root diameter of 0.012 mm was used.

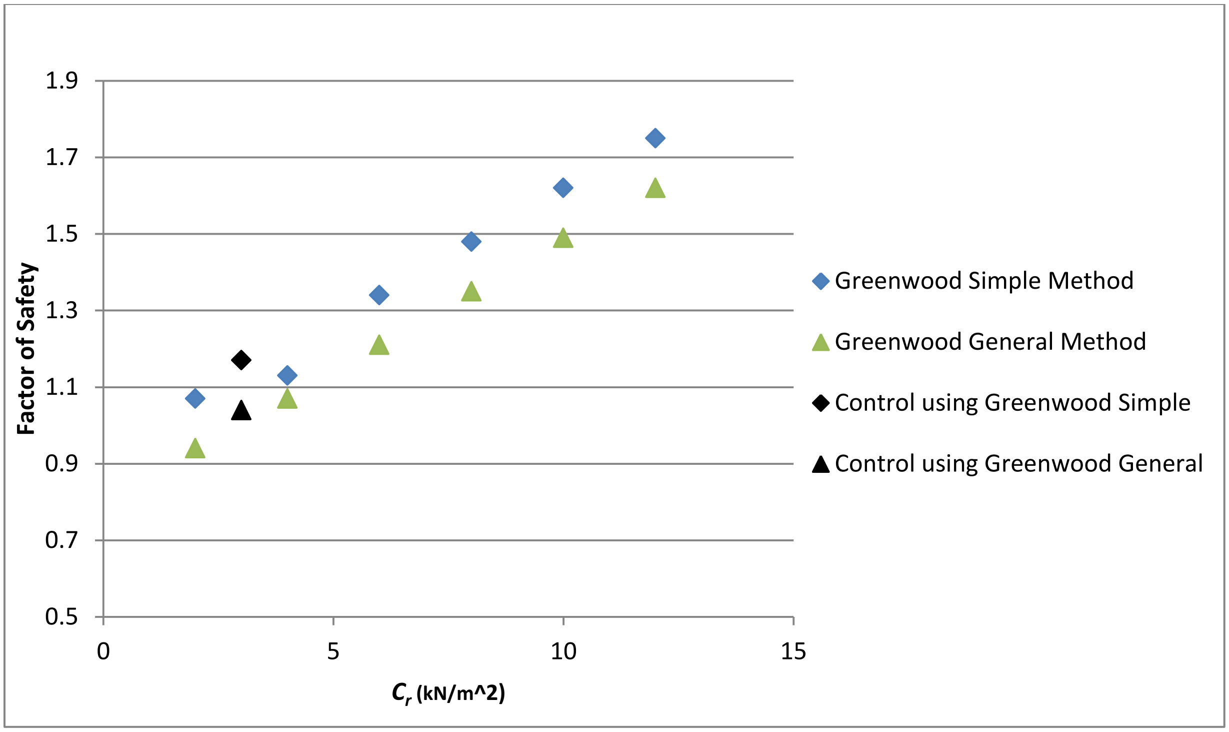

Figure A3: Sensitivity of FOS to additional cohesion due to vegetation (C_r)

Figure A3, similar to Fig. A2, displays a positive, linear relationship between the FOS and soil cohesion. However, the magnitude of the change is more significant, an increase in additional cohesion of 2 kN/m^2 results on average in a 14% increase in the FOS. The ability to determine this sensitivity using a fine root diameter confirms the hypothesis from Fig. A1, that for fine roots, the additional cohesion from vegetation would contribute more significantly to the FOS than the reinforcement force on a slice due to the vegetation. Again, the linear relationship suggests that the FOS may be easily predicted from the additional effective cohesion due to vegetation.

Sensitivity of FOS to root density

Figure A4 displays a graphical representation of the sensitivity in the FOS for a range of number of roots per square metre of soil.

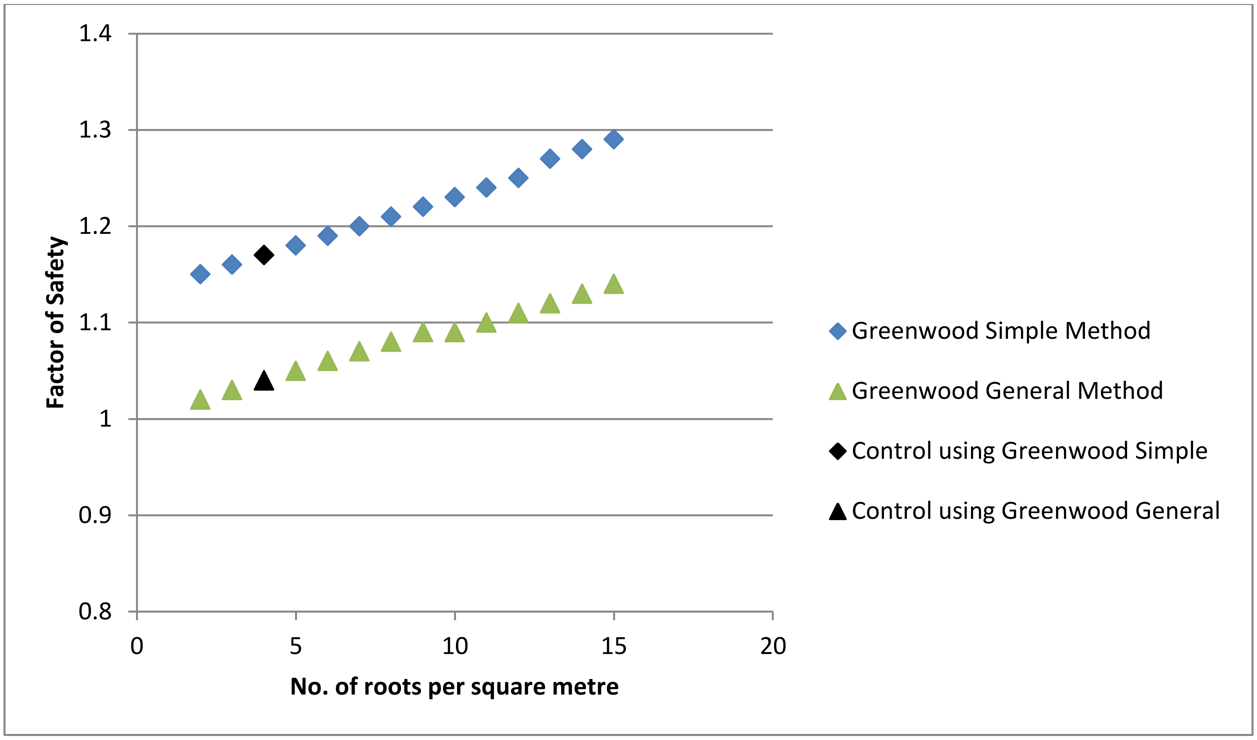

Figure A4: Sensitivity of FOS with the number of roots per square metre

Figure A4 also presents positive linear relationships with a low gradient, indicating the low sensitivity of the FOS to the number of roots per square metre of soil. An increase of one root per square metre of soil results, on average, in a 1% increase in the FOS.

Sensitivity of FOS with ϑ

Figure A5 provides the sensitivity of the FOS to a range of the angle between the root and the slip surface obtained from SLIP4EX.

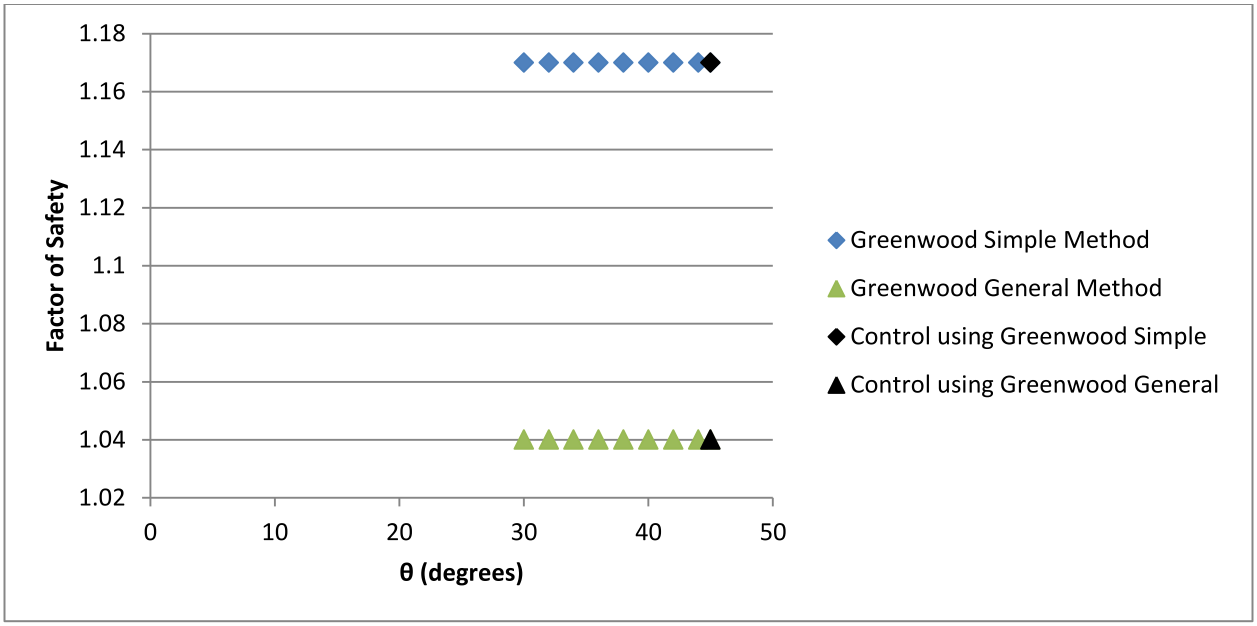

Figure A5: Sensitivity of FOS to the angle between the root and the slip surface (ϑ)

The FOS remains practically constant for the range of angles investigated. This indicates that the FOS is insensitive to the angle between the root and the slip surface. This suggests that the 45° angle assumed by Adhikar et al. (2013), De Baets et al. (2008) and other authors is a reasonable assumption.

Sensitivity of FOS to Δh_w

Figure A6 provides a graphical representation of the sensitivity of the FOS to change in depth of the piezometric head, where this depth is used as an indicator for the position of the phreatic surface.

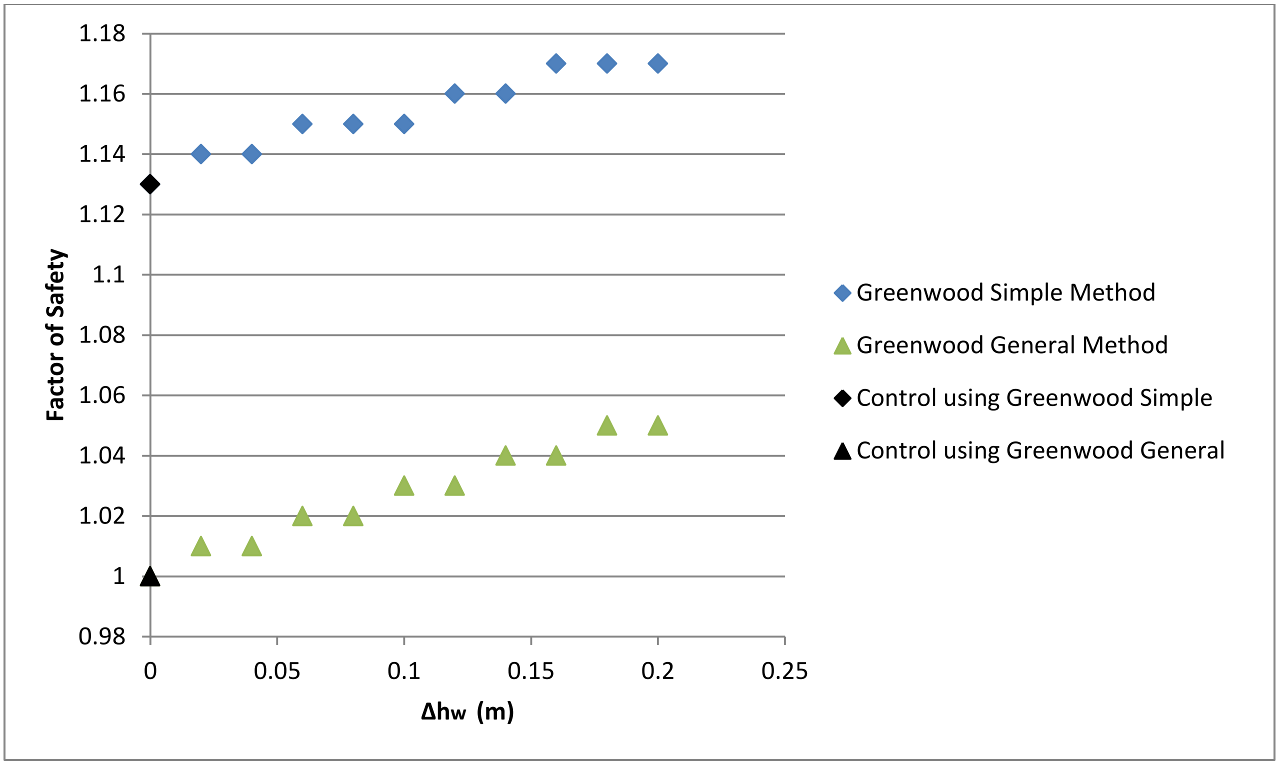

Figure A6: Sensitivity of FOS with the increase in average piezometric head at base of slice (Δh_w)

Figure A6 shows the significant sensitivity to the change in depth of the piezometric head. The FOS increases with increased depth of the piezometric head below the ground surface. The relationships are approximately linear. There is approximately a 2% increase in the FOS for every 100 mm reduction in the height of the piezometric head. This representation clearly shows that increased soil suction due to the presence of vegetation produces a stabilizing effect on the bank.

Sensitivity of FOS to surcharge load due to vegetation

Figure A7 represents the change in the FOS with the change in surcharge weight of vegetation. The sensitivity in the range of surcharge weight as specified in Table 3.2 was done for the control model. The changing surcharge weight was applied over the entire slope of the bank for this analysis, as shown by the green shaded area in Fig. 5.23.

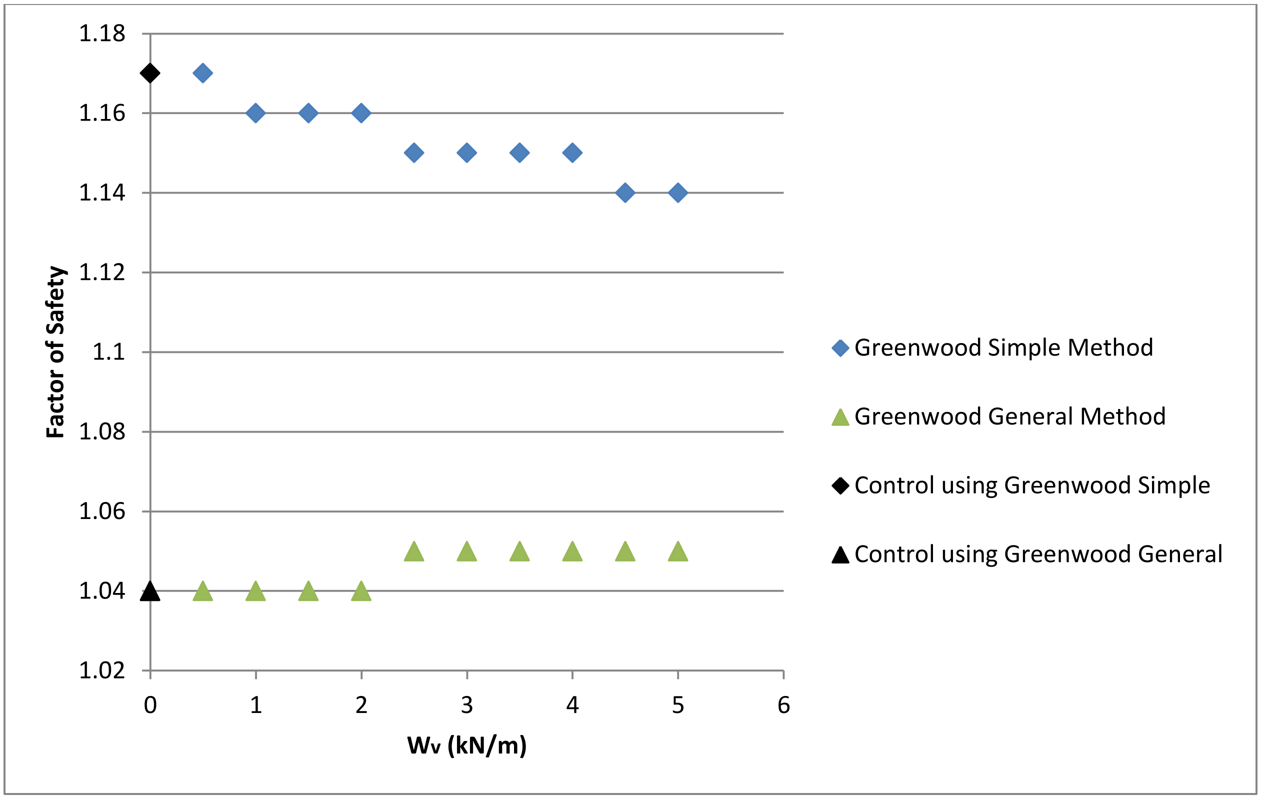

Figure A7: Sensitivity of FOS to surcharge load due to vegetation

The trend for the Greenwood Simple method is considerably different to the trend of the Greenwood General method. The trend of the Greenwood Simple method suggests that increased surcharge weight due to vegetation destabilizes the slope, as the FOS reduces. However, the trend of the Greenwood General method suggests that the increased surcharge due to vegetation mildly stabilizes the bank. The methods differ because they each sum the interslice forces differently, due to the different way in which they consider the water surface. In the Greenwood General equation the water surface is parallel to the slip surface and more continuous and hence more realistically accounts for the water surface. In the Greenwood Simple method there is a consistent horizontal water surface across the slice. The step change in water surface between each slice of soil in the Greenwood Simple method results in greater variability in the FOS. In the Greenwood General method, the difference is gradually accumulated (owing to the parallel, continuous water surface) and hence there is a step change in the FOS when the weight of the soil increases to a particular value. For the range of surcharge investigated (a realistic estimate according to Tiwari et al. (2011)), the stabilizing effect is small, at most a 1% increase or decrease in the FOS for the Greenwood General method and the Greenwood Simple method respectively.

Sensitivity of FOS to position of vegetation along the bank

In order to investigate whether SLIP4EX is able to account for the position of vegetation along the bank, the vegetation functional traits were initially only included in the first three slices (soil slices at the toe of the slope) while the remaining slices remained empty (zero effect of vegetation). The root functional traits were then included in the next three slices, positioned closer to the bank crest, while all other slices remained empty. The process was continued until the last three slices, adjacent to the bank crest, were used to include the root functional traits and all other slices were left empty.

Figure A8 shows the change in FOS with change in position of vegetation along the slope.

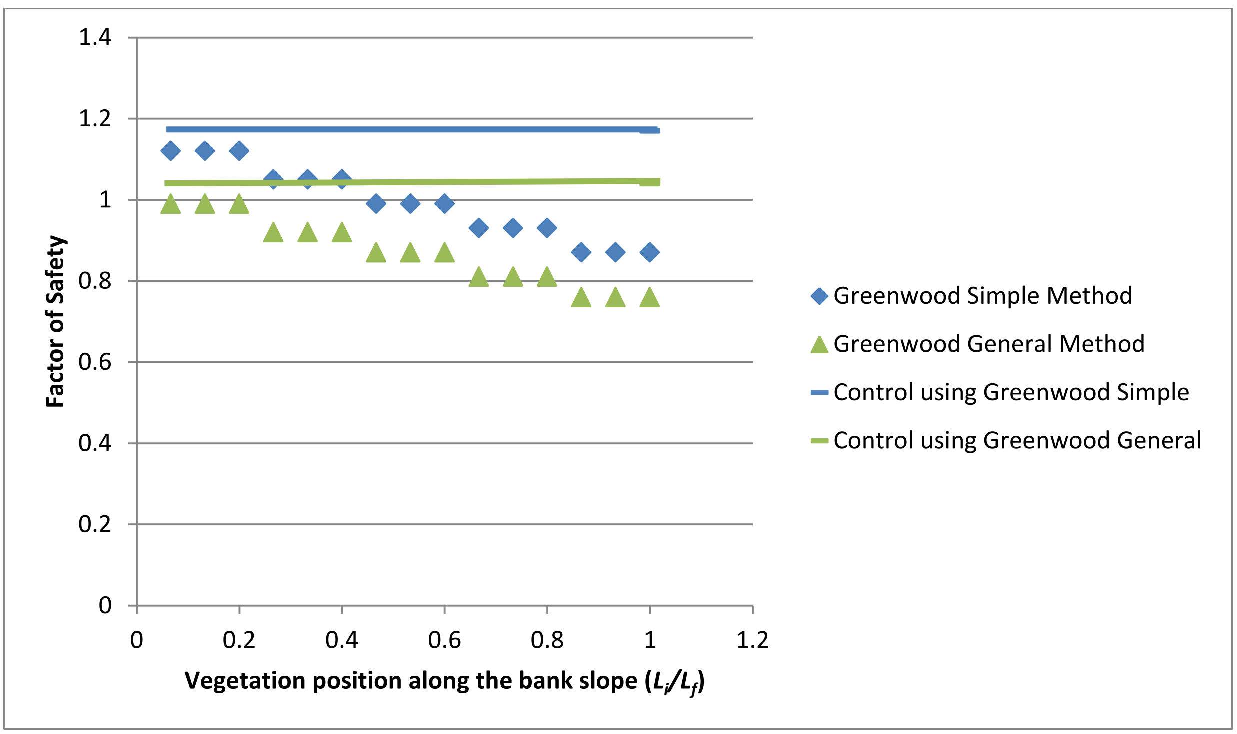

Figure A8: Sensitivity of FOS to the position of vegetation along the bank

The FOS clearly decreases for the surcharge weight of 5 kN/m as the vegetation is positioned closer to the bank crest. There is significant change in FOS with change in position of the vegetation along the bank, on average there is a 6% decrease in FOS with one incremental change in position up the bank. The results are consistent with Van De Wiel and Darby (2007) who found that the stabilizing effects of vegetation are maximized at the bank toe, in their investigation using the Wu et al. (1979) perpendicular model in analyzing banks for planar failure. It is clear from Fig. A8 that vegetation position is critical in bank stabilization.

APPENDIX B

Modeled flood hydrographs for bank heights between 1.0 m to 10.0 m

Table B.1: Flood hydrographs for 1.0 m high banks

Short flood, rapid drawdown		Short flood, medium drawdown		Short flood, slow drawdown		Medium flood, rapid drawdown		Medium flood, medium drawdown	
Time (sec)	**Water level (m)**	**Time (sec)**	**Water level (m)**	**Time (sec)**	**Water level (m)**	**Time (sec)**	**Water level (m)**	**Time (sec)**	**Water level (m)**
0	3.33	0	3.33	0	3.33	0	3.33	0	3.33
2700	4.0	2700	4.0	2700	4.0	10800	4.0	10800	4.0
5400	4.0	5400	4.0	5400	4.0	21600	4.0	21600	4.0
11610	3.33	16200	3.33	113400	3.33	27810	3.33	32400	3.33
Medium flood, slow drawdown		**Long flood, rapid drawdown**		**Long flood, medium drawdown**		**Long flood, slow drawdown**			
Time (sec)	**Water level (m)**	**Time (sec)**	**Water level (m)**	**Time (sec)**	**Water level (m)**	**Time (sec)**	**Water level (m)**		
0	3.33	0	3.33	0	3.33	0	3.33		
10800	4.0	64800	4.0	64800	4.0	64800	4.0		
21600	4.0	129600	4.0	129600	4.0	129600	4.0		
129600	3.33	135810	3.33	140400	3.33	237600	3.33		

Table B.2: Flood hydrographs for 2.0 m high banks

Short flood, rapid drawdown		Short flood, medium drawdown		Short flood, slow drawdown		Medium flood, rapid drawdown		Medium flood, medium drawdown	
Time (sec)	**Water level (m)**	**Time (sec)**	**Water level (m)**	**Time (sec)**	**Water level (m)**	**Time (sec)**	**Water level (m)**	**Time (sec)**	**Water level (m)**
0	3.67	0	3.67	0	3.67	0	3.67	0	3.67
5400	5.0	5400	5.0	5400	5.0	21600	5.0	21600	5.0
10800	5.0	10800	5.0	10800	5.0	43200	5.0	43200	5.0
23400	3.67	30960	3.67	244080	3.67	55800	3.67	63360	3.67
Medium flood, slow drawdown		**Long flood, rapid drawdown**		**Long flood, medium drawdown**		**Long flood, slow drawdown**			
Time (sec)	**Water level (m)**	**Time (sec)**	**Water level (m)**	**Time (sec)**	**Water level (m)**	**Time (sec)**	**Water level (m)**		
0	3.67	0	3.67	0	3.67	0	3.67		
21600	5.0	138240	5.0	138240	5.0	138240	5.0		
43200	5.0	276480	5.0	276480	5.0	276480	5.0		
276480	3.67	289080	3.67	296640	3.67	509760	3.67		

Table B.3: Flood hydrographs for 3.0 m high banks

Short flood, rapid drawdown		Short flood, medium drawdown		Short flood, slow drawdown		Medium flood, rapid drawdown		Medium flood, medium drawdown	
Time (sec)	**Water level (m)**	**Time (sec)**	**Water level (m)**	**Time (sec)**	**Water level (m)**	**Time (sec)**	**Water level (m)**	**Time (sec)**	**Water level (m)**
0	4.0	0	4.0	0	4.0	0	4.0	0	4.0
8100	6.0	8100	6.0	8100	6.0	30600	6.0	30600	6.0
16200	6.0	16200	6.0	16200	6.0	61200	6.0	61200	6.0
35190	4.0	46800	4.0	318600	4.0	80190	4.0	91800	4.0

Medium flood, slow drawdown		Long flood, rapid drawdown		Long flood, medium drawdown		Long flood, slow drawdown	
Time (sec)	**Water level (m)**	**Time (sec)**	**Water level (m)**	**Time (sec)**	**Water level (m)**	**Time (sec)**	**Water level (m)**
0	4.0	0	4.0	0	4.0	0	4.0
30600	6.0	207360	6.0	207360	6.0	207360	6.0
61200	6.0	414720	6.0	414720	6.0	414720	6.0
363600	4.0	433710	4.0	445320	4.0	717120	4.0

Table B.4: Flood hydrographs for 4.0 m high banks

Short flood, rapid drawdown		Short flood, medium drawdown		Short flood, slow drawdown		Medium flood, rapid drawdown		Medium flood, medium drawdown	
Time (sec)	**Water level (m)**	**Time (sec)**	**Water level (m)**	**Time (sec)**	**Water level (m)**	**Time (sec)**	**Water level (m)**	**Time (sec)**	**Water level (m)**
0	4.33	0	4.33	0	4.33	0	4.33	0	4.33
10800	7.0	10800	7.0	10800	7.0	41400	7.0	41400	7.0
21600	7.0	21600	7.0	21600	7.0	82800	7.0	82800	7.0
46800	4.33	63000	4.33	479520	4.33	108000	4.33	124200	4.33

Medium flood, slow drawdown		Long flood, rapid drawdown		Long flood, medium drawdown		Long flood, slow drawdown	
Time (sec)	**Water level (m)**	**Time (sec)**	**Water level (m)**	**Time (sec)**	**Water level (m)**	**Time (sec)**	**Water level (m)**
0	4.33	0	4.33	0	4.33	0	4.33
41400	7.0	285120	7.0	285120	7.0	285120	7.0
82800	7.0	570240	7.0	570240	7.0	570240	7.0
540720	4.33	595440	4.33	611640	4.33	1028160	4.33

Table B.5: Flood hydrographs for 5.0 m high banks

Short flood, rapid drawdown		Short flood, medium drawdown		Short flood, slow drawdown		Medium flood, rapid drawdown		Medium flood, medium drawdown	
Time (sec)	**Water level (m)**	**Time (sec)**	**Water level (m)**	**Time (sec)**	**Water level (m)**	**Time (sec)**	**Water level (m)**	**Time (sec)**	**Water level (m)**
0	4.67	0	4.67	0	4.67	0	4.67	0	4.67
13500	8.0	13500	8.0	13500	8.0	52200	8.0	52200	8.0
27000	8.0	27000	8.0	27000	8.0	104400	8.0	104400	8.0
58500	4.67	79200	4.67	519480	4.67	135900	4.67	156600	4.67

Medium flood, slow drawdown		Long flood, rapid drawdown		Long flood, medium drawdown		Long flood, slow drawdown	
Time (sec)	**Water level (m)**	**Time (sec)**	**Water level (m)**	**Time (sec)**	**Water level (m)**	**Time (sec)**	**Water level (m)**
0	4.67	0	4.67	0	4.67	0	4.67
52200	8.0	319680	8.0	319680	8.0	319680	8.0
104400	8.0	639360	8.0	639360	8.0	639360	8.0
596880	4.67	670860	4.67	691560	4.67	1131840	4.67

Table B.6: Flood hydrographs for 6.0 m high banks

Short flood, rapid drawdown		Short flood, medium drawdown		Short flood, slow drawdown		Medium flood, rapid drawdown		Medium flood, medium drawdown	
Time (sec)	**Water level (m)**	**Time (sec)**	**Water level (m)**	**Time (sec)**	**Water level (m)**	**Time (sec)**	**Water level (m)**	**Time (sec)**	**Water level (m)**
0	5.0	0	5.0	0	5.0	0	5.0	0	5.0
19800	9.0	19800	9.0	19800	9.0	63000	9.0	63000	9.0
39600	9.0	39600	9.0	39600	9.0	126000	9.0	126000	9.0
73890	5.0	102600	5.0	644400	5.0	160290	5.0	189000	5.0

Medium flood, slow drawdown		Long flood, rapid drawdown		Long flood, medium drawdown		Long flood, slow drawdown	
Time (sec)	**Water level (m)**	**Time (sec)**	**Water level (m)**	**Time (sec)**	**Water level (m)**	**Time (sec)**	**Water level (m)**
0	5.0	0	5.0	0	5.0	0	5.0
63000	9.0	401760	9.0	401760	9.0	401760	9.0
126000	9.0	803520	9.0	803520	9.0	803520	9.0
730800	5.0	837810	5.0	866520	5.0	1408320	5.0

Table B.7: Flood hydrographs for 7.0 m high banks

Short flood, rapid drawdown		Short flood, medium drawdown		Short flood, slow drawdown		Medium flood, rapid drawdown		Medium flood, medium drawdown	
Time (sec)	Water level (m)	Time (sec)	Water level (m)	Time (sec)	Water level (m)	Time (sec)	Water level (m)	Time (sec)	Water level (m)
0	5.33	0	5.33	0	5.33	0	5.33	0	5.33
18810	10.0	18810	10.0	18810	10.0	73800	10.0	73800	10.0
37620	10.0	37620	10.0	37620	10.0	147600	10.0	147600	10.0
81810	5.333	115020	5.333	741780	5.333	191790	5.333	225000	5.333
Medium flood, slow drawdown		Long flood, rapid drawdown		Long flood, medium drawdown		Long flood, slow drawdown			
Time (sec)	Water level (m)	Time (sec)	Water level (m)	Time (sec)	Water level (m)	Time (sec)	Water level (m)		
0	5.33	0	5.33	0	5.33	0	5.33		
73800	10.0	461376	10.0	461376	10.0	461376	10.0		
147600	10.0	922752	10.0	922752	10.0	922752	10.0		
851760	5.333	966942	5.333	1000152	5.333	1626912	5.333		

Table B.8: Flood hydrographs for 8.0 m high banks

Short flood, rapid drawdown		Short flood, medium drawdown		Short flood, slow drawdown		Medium flood, rapid drawdown		Medium flood, medium drawdown	
Time (sec)	Water level (m)	Time (sec)	Water level (m)	Time (sec)	Water level (m)	Time (sec)	Water level (m)	Time (sec)	Water level (m)
0	5.67	0	5.67	0	5.67	0	5.67	0	5.67
21600	11.00	21600	11.00	21600	11.00	84600	11.00	84600	11.00
43200	11.00	43200	11.00	43200	11.00	169200	11.00	169200	11.00
93690	5.67	127800	5.67	820800	5.67	219690	5.67	253800	5.67
Medium flood, slow drawdown		Long flood, rapid drawdown		Long flood, medium drawdown		Long flood, slow drawdown			
Time (sec)	Water level (m)	Time (sec)	Water level (m)	Time (sec)	Water level (m)	Time (sec)	Water level (m)		
0	5.67	0	5.67	0	5.67	0	5.67		
84600	11.00	561600	11.00	561600	11.00	561600	11.00		
169200	11.00	1123200	11.00	1123200	11.00	1123200	11.00		
946800	5.67	1173690	5.67	1207800	5.67	1900800	5.67		

Table B.9: Flood hydrographs for 9.0 m high banks

Short flood, rapid drawdown		Short flood, medium drawdown		Short flood, slow drawdown		Medium flood, rapid drawdown		Medium flood, medium drawdown	
Time (sec)	Water level (m)	Time (sec)	Water level (m)	Time (sec)	Water level (m)	Time (sec)	Water level (m)	Time (sec)	Water level (m)
0	6.0	0	6.0	0	6.0	0	6.0	0	6.0
24210	12.0	24210	12.0	24210	12.0	95400	12.0	95400	12.0
48420	12.0	48420	12.0	48420	12.0	190800	12.0	190800	12.0
105300	6.0	143820	6.0	955620	6.0	247680	6.0	286200	6.0

Medium flood, slow drawdown		Long flood, rapid drawdown		Long flood, medium drawdown		Long flood, slow drawdown	
Time (sec)	Water level (m)	Time (sec)	Water level (m)	Time (sec)	Water level (m)	Time (sec)	Water level (m)
0	6.0	0	6.0	0	6.0	0	6.0
95400	12.0	596160	12.0	596160	12.0	596160	12.0
190800	12.0	1192320	12.0	1192320	12.0	1192320	12.0
1098000	6.0	1249200	6.0	1287720	6.0	2099520	6.0

Table B.10: Flood hydrographs for 10.0 m high banks

Short flood, rapid drawdown		Short flood, medium drawdown		Short flood, slow drawdown		Medium flood, rapid drawdown		Medium flood, medium drawdown	
Time (sec)	Water level (m)	Time (sec)	Water level (m)	Time (sec)	Water level (m)	Time (sec)	Water level (m)	Time (sec)	Water level (m)
0	6.33	0	6.33	0	6.33	0	6.33	0	6.33
27000	13.0	27000	13.0	27000	13.0	106200	13.0	106200	13.0
54000	13.0	54000	13.0	54000	13.0	212400	13.0	212400	13.0
117180	6.33	160200	6.33	1064880	6.33	275580	6.33	318600	6.33

Medium flood, slow drawdown		Long flood, rapid drawdown		Long flood, medium drawdown		Long flood, slow drawdown	
Time (sec)	Water level (m)	Time (sec)	Water level (m)	Time (sec)	Water level (m)	Time (sec)	Water level (m)
0	6.33	0	6.33	0	6.33	0	6.33
106200	13.0	665280	13.0	665280	13.0	665280	13.0
212400	13.0	1330560	13.0	1330560	13.0	1330560	13.0
1223280	6.33	1393740	6.33	1436760	6.33	2341440	6.33

APPENDIX C

Factor of safety and maximum depth to the critical slip surface for various riverbank heights and flood scenarios

Notes:

Abbreviations

dd	-	drawdown
FOS	-	factor of safety
Max. depth to css	-	maximum depth to critical slip surface

Shaded regions

The shaded region in the factor of safety tables indicates values that are below the factor of safety of 1.3 that represents stable conditions.

The shaded region in the tables with depth to critical slip surface indicates values that are beyond the depth of influence of vegetation roots.

Depth measurements are given in m

Table C.1: Factor of safety for various riverbank heights and flood conditions for silt loam soil, 1:1 slope angle

Bank Height (m)	Initial Conditions	Short flood, rapid dd	Short flood, medium dd	Short flood, slow dd	Medium flood, rapid dd	Medium flood, medium dd	Medium flood, slow dd	Long flood, rapid dd	Long flood, medium dd	Long flood, slow dd
4	1.71	1.65	1.67	1.69	1.66	1.66	1.69	1.67	1.67	1.69
5	1.54	1.46	1.48	1.51	1.49	1.47	1.51	1.53	1.43	1.51
6	1.41	1.34	1.35	1.38	1.32	1.34	1.38	1.23	1.24	1.38
7	1.34	1.25	1.27	1.29	1.23	1.26	1.29	1.09	1.10	1.29
8	1.27	1.19	1.2	1.22	1.17	1.19	1.22	0.98	0.99	1.26
10	1.15	1.09	1.09	1.13	1.06	1.08	1.12	0.83	0.83	1.12

Table C.2: Max. depth to css for various riverbank heights and flood conditions for silt loam soil, 1:1 slope angle

Bank Height (m)	Short flood, rapid dd	Short flood, medium dd	Short flood, slow dd	Medium flood, rapid dd	Medium flood, medium dd	Medium flood, slow dd	Long flood, rapid dd	Long flood, medium dd	Long flood, slow dd
5	Stable, FOS >1.3								
6	Stable, FOS>1.3						2.30	2.27	Stable
7	2.46	2.53	2.57	2.42	2.47	2.43	2.55	2.51	2.45
8	2.86	2.86	2.82	2.83	2.83	3.13	2.89	2.90	3.36
10	Critical slip surface >> than 2 m								

Table C.3: Factor of safety for various riverbank heights and flood conditions for silt loam soil, 1:2 slope angle

Bank Height (m)	Initial Conditions	Short flood, rapid dd	Short flood, medium dd	Short flood, slow dd	Medium flood, rapid dd	Medium flood, medium dd	Medium flood, slow dd	Long flood, rapid dd	Long flood, medium dd	Long flood, slow dd
4	2.35	2.19	2.22	2.33	2.19	2.22	2.29	2.23	2.23	2.29
6	1.98	1.83	1.86	1.91	1.80	1.83	1.91	1.68	1.80	1.91
8	1.80	1.65	1.67	1.71	1.62	1.65	1.71	1.35	1.36	1.71
9	1.73	1.58	1.61	1.65	1.54	1.58	1.66	1.25	1.26	1.64
10	1.68	1.53	1.55	1.59	1.49	1.52	1.58	1.18	1.19	1.57

Table C.4: Max. depth to css for various riverbank heights and flood conditions for silt loam soil, 1:2 slope angle

Bank Height (m)	Short flood, rapid dd	Short flood, medium dd	Short flood, slow dd	Medium flood, rapid dd	Medium flood, medium dd	Medium flood, slow dd	Long flood, rapid dd	Long flood, medium dd	Long flood, slow dd
4	Stable, FOS >1.3								
6	Stable, FOS >1.3								
8	Stable, FOS >1.3								
9	Stable, FOS >1.3						4.03	4.07	Stable
10	Stable, FOS >1.3						4.16	4.07	Stable

Table C.5: Factor of safety for various riverbank heights and flood conditions for silt loam soil, 2:1 slope angle

Bank Height (m)	Initial Conditions	Short flood, rapid dd	Short flood, medium dd	Short flood, slow dd	Medium flood, rapid dd	Medium flood, medium dd	Medium flood, slow dd	Long flood, rapid dd	Long flood, medium dd	Long flood, slow dd
3	1.56	1.49	1.51	1.54	1.53	1.52	1.48	1.54	1.52	1.52
4	1.29	1.24	1.24	1.26	1.21	1.22	1.24	1.23	1.18	1.18
5	1.13	1.06	1.05	1.07	1.08	1.07	1.08	1.07	1.08	1.07
6	1.05	0.99	1.02	1.02	1.01	1.01	1.01	0.95	0.95	1.01
7	0.96	0.88	0.90	0.90	0.97	0.93	0.90	0.86	0.87	0.94
8	0.91	0.84	0.84	0.86	0.86	0.85	0.84	0.77	0.77	0.9
9	0.86	0.85	0.85	0.84	0.85	0.86	0.84	0.70	0.70	0.84
10	0.83	0.78	0.79	0.80	0.77	0.78	0.80	0.65	0.65	0.8

Table C.6: Max. depth to css for various riverbank heights and flood conditions for silt loam soil, 2:1 slope angle

Bank Height (m)	Short flood, rapid dd	Short flood, medium dd	Short flood, slow dd	Medium flood, rapid dd	Medium flood, medium dd	Medium flood, slow dd	Long flood, rapid dd	Long flood, medium dd	Long flood, slow dd
3	Stable, FOS >1.3								
4	1.61	1.52	1.55	1.59	1.60	1.56	1.55	1.56	1.59
5	1.91	1.97	1.97	1.97	1.99	1.98	1.98	1.99	1.90
6	1.62	1.70	1.74	1.67	1.54	1.74	2.23	2.28	1.76
7	2.11	2.14	2.05	2.43	2.00	2.12	2.47	2.49	2.01
8	2.17	2.23	2.19	2.38	2.26	2.22	2.37	2.12	3.73
9	2.39	2.27	2.63	2.27	2.31	2.34	2.24	2.11	2.31
10	2.45	2.44	2.38	2.48	2.45	2.49	2.19	2.19	2.50

Table C.7: Factor of safety for various riverbank heights and flood conditions for loamy sand soil, 1:1 slope angle

Bank Height (m)	Initial Conditions	Short flood, rapid dd	Short flood, medium dd	Short flood, slow dd	Medium flood, rapid dd	Medium flood, medium dd	Medium flood, slow dd	Long flood, rapid dd	Long flood, medium dd	Long flood, slow dd
1	1.08	1.03	1.04	1.08	1.03	1.04	1.07	0.98	0.99	1.05
2	0.84	0.76	0.77	0.79	0.75	0.76	0.79	0.63	0.62	0.78
3	0.75	0.66	0.66	0.68	0.62	0.63	0.68	0.54	0.54	0.68
4	0.70	0.6	0.61	0.62	0.60	0.60	0.62	0.53	0.53	0.62

Table C.8: Max. depth to css for various riverbank heights and flood conditions for loamy sand, 1:1 slope angle

Bank Height (m)	Short flood, rapid dd	Short flood, medium dd	Short flood, slow dd	Medium flood, rapid dd	Medium flood, medium dd	Medium flood, slow dd	Long flood, rapid dd	Long flood, medium dd	Long flood, slow dd
1	0.32	0.33	0.3	0.32	0.32	0.3	0.32	0.32	0.32
2	0.53	0.7	0.54	0.53	0.53	0.53	0.53	Unstable	0.53
3	0.75	0.75	0.74	0.77	0.76	0.7	Unstable, FOS<0.63		0.76
4	Unstable, FOS<0.63								

Table C.9: Factor of safety for various riverbank heights and flood conditions for loamy sand soil, 1:2 slope angle

Bank Height (m)	Initial Conditions	Short flood, rapid dd	Short flood, medium dd	Short flood, slow dd	Medium flood, rapid dd	Medium flood, medium dd	Medium flood, slow dd	Long flood, rapid dd	Long flood, medium dd	Long flood, slow dd
1	1.55	1.43	1.45	1.49	1.42	1.44	1.48	1.35	1.38	1.47
2	1.29	1.15	1.16	1.19	1.12	1.13	1.18	0.99	0.97	1.14
3	1.18	1.03	1.03	1.06	0.99	1.00	1.04	0.81	0.80	1.03
4	1.13	0.96	0.96	1.00	0.90	0.92	0.98	0.74	0.74	0.98
5	1.09	0.90	0.90	0.95	0.84	0.86	0.94	0.79	0.79	0.93
6	1.07	0.86	0.86	0.92	0.79	0.81	0.91	0.72	0.72	0.90
7	1.05	0.84	0.84	0.89	0.84	0.78	0.89	0.68	0.72	0.89
8	1.04	0.81	0.82	0.87	0.74	0.75	0.87	0.66	0.66	0.87
9	1.03	0.78	0.79	0.86	0.70	0.72	0.86	0.64	0.66	0.86
10	1.02	0.78	0.77	0.85	0.70	0.71	0.85	0.64	0.66	0.85

Table C.10: Max. depth to css for various riverbank heights and flood conditions for loamy sand, 1:2 slope angle

Bank Height (m)	Short flood, rapid dd	Short flood, medium dd	Short flood, slow dd	Medium flood, rapid dd	Medium flood, medium dd	Medium flood, slow dd	Long flood, rapid dd	Long flood, medium dd	Long flood, slow dd
1	Stable, FOS >1.3								
2	0.84	0.84	0.84	0.83	0.84	0.83	0.74	0.74	0.84
3	0.15	0.17	0.15	0.17	0.17	0.16	0.91	0.89	1.17
4	1.16	1.24	1.23	1.18	1.17	1.25	1.01	0.67	1.26
5	1.62	1.60	1.61	1.61	1.62	1.63	1.28	1.29	1.65
6	1.58	1.61	1.78	1.37	1.55	1.63	1.22	1.22	1.74
7	1.61	1.62	2.16	1.66	1.63	2.15	1.35	1.21	1.99
8	1.34	1.34	2.20	1.28	1.30	2.19	1.12	1.09	1.99
9	2.40	2.09	2.31	1.42	1.34	2.18	1.13	1.18	2.35
10	2.05	2.37	2.19	1.30	1.32	2.24	1.20	1.99	2.19

Table C.11: Factor of safety for various riverbank heights and flood conditions for loamy sand soil, 1:3 slope angle

Bank Height (m)	Initial Conditions	Short flood, rapid dd	Short flood, medium dd	Short flood, slow dd	Medium flood, rapid dd	Medium flood, medium dd	Medium flood, slow dd	Long flood, rapid dd	Long flood, medium dd	Long flood, slow dd
2	1.68	1.49	1.49	1.53	1.46	1.47	1.52	1.29	1.28	1.47
3	1.57	1.36	1.36	1.38	1.30	1.31	1.37	1.09	1.06	1.34
4	1.52	1.29	1.29	1.32	1.24	1.24	1.31	0.94	0.94	1.29
5	1.49	1.22	1.24	1.27	1.13	1.17	1.25	1.07	1.08	1.23
6	1.46	1.13	1.18	1.23	1.06	1.12	1.22	1.01	0.78	1.21
7	1.44	1.13	1.15	1.20	1.03	1.08	1.19	0.95	0.97	1.18
8	1.43	1.08	1.10	1.17	1.00	1.03	1.16	0.69	0.70	1.15
9	1.42	1.07	1.08	1.15	0.99	0.99	1.14	0.66	0.87	1.14
10	1.41	1.04	1.06	1.13	0.95	1.00	1.12	0.77	0.86	1.12

Table C.12: Max. depth to css for various riverbank heights and flood conditions for loamy sand, 1:3 slope angle

Bank Height (m)	Short flood, rapid dd	Short flood, medium dd	Short flood, slow dd	Medium flood, rapid dd	Medium flood, medium dd	Medium flood, slow dd	Long flood, rapid dd	Long flood, medium dd	Long flood, slow dd
2	Stable, FOS>1.3						0.98	1.11	Stable
3	Stable, FOS>1.3						0.88	0.75	Stable
4	1.64	1.64	Stable, FOS>1.3	1.45	1.47	Stable	1.17	0.98	1.62
5	1.64	1.82	1.94	1.45	1.72	2.02	1.7	1.56	1.77
6	1.72	1.9	2.55	1.56	1.56	2.48	1.53	1.89	2.42
7	1.66	1.66	2.10	1.49	1.59	2.07	2.11	1.57	2.11
8	1.80	1.75	2.27	1.54	1.56	2.31	2.35	0.86	2.32
9	1.66	1.68	2.27	1.62	1.86	2.22	2.64	1.39	2.02
10	1.77	1.79	2.04	1.61	1.63	2.33	2.69	2.45	2.09

Table C.13: Factor of safety for various riverbank heights and flood conditions for clay soil, 1:1 slope angle

Bank Height (m)	Initial Conditions	Short flood, rapid dd	Short flood, medium dd	Short flood, slow dd	Medium flood, rapid dd	Medium flood, medium dd	Medium flood, slow dd	Long flood, rapid dd	Long flood, medium dd	Long flood, slow dd
2	3.03	2.89	2.93	2.98	2.98	2.89	2.96	2.59	2.97	2.99
4	1.89	1.79	1.80	1.81	1.76	1.78	1.81	1.73	1.73	1.78
6	1.49	1.41	1.42	1.41	1.38	1.40	1.41	1.33	1.33	1.38
7	1.36	1.29	1.29	1.30	1.26	1.27	1.29	1.21	1.23	1.27
8	1.28	1.21	1.21	1.21	1.17	1.19	1.20	1.13	1.13	1.18
10	1.15	1.07	1.08	1.08	1.05	1.06	1.07	0.99	0.99	1.05

Table C.14: Max. depth to css for various riverbank heights and flood conditions for clay soil, 1:1 slope angle

Bank Height (m)	Short flood, rapid dd	Short flood, medium dd	Short flood, slow dd	Medium flood, rapid dd	Medium flood, medium dd	Medium flood, slow dd	Long flood, rapid dd	Long flood, medium dd	Long flood, slow dd
2	Stable, FOS>1.3								
4	Stable, FOS>1.3								
6	Stable, FOS>1.3								
7	2.66	2.86	Stable	2.78	2.79	3.2	2.99	3.16	2.95
8	2.99	3.04	3.22	3.06	3.11	3.19	3.27	3.25	3.29
10	Critical slip surface >> than 2 m								

Table C.15: Factor of safety for various riverbank heights and flood conditions for clay soil, 1:2 slope angle

Bank Height (m)	Initial Conditions	Short flood, rapid dd	Short flood, medium dd	Short flood, slow dd	Medium flood, rapid dd	Medium flood, medium dd	Medium flood, slow dd	Long flood, rapid dd	Long flood, medium dd	Long flood, slow dd
4	2.49	2.34	2.36	2.38	2.30	2.32	2.38	2.26	2.26	2.33
6	2.02	1.89	1.90	1.91	1.86	1.87	1.91	1.80	1.80	1.87
8	1.77	1.66	1.68	1.50	1.62	1.64	1.66	1.55	1.55	1.62
10	1.62	1.51	1.53	1.52	1.48	1.50	1.51	1.40	1.40	1.47

Table C.16: Factor of safety for various riverbank heights and flood conditions for clay soil, 2:1 slope angle

Bank Height (m)	Initial Conditions	Short flood, rapid dd	Short flood, medium dd	Short flood, slow dd	Medium flood, rapid dd	Medium flood, medium dd	Medium flood, slow dd	Long flood, rapid dd	Long flood, medium dd	Long flood, slow dd
1	4.86	4.71	4.71	4.7	4.69	4.68	4.74	4.68	4.69	4.69
4	1.56	1.49	1.48	1.37	1.49	1.49	1.47	1.46	1.48	1.49
5	1.32	1.31	1.32	1.29	1.24	1.30	1.29	1.28	1.30	1.24
6	1.14	1.12	1.14	1.11	1.14	1.14	1.13	1.10	1.10	1.09
8	0.96	0.92	0.91	0.91	0.89	0.92	0.91	0.87	0.90	0.90
10	0.82	0.79	0.81	0.80	0.81	0.79	0.80	0.75	0.74	0.77

Table C.17: Max. depth to css for various riverbank heights and flood conditions for clay soil, 2:1 slope angle

Bank Height (m)	Short flood, rapid dd	Short flood, medium dd	Short flood, slow dd	Medium flood, rapid dd	Medium flood, medium dd	Medium flood, slow dd	Long flood, rapid dd	Long flood, medium dd	Long flood, slow dd
1	Stable, FOS>1.3								
4	Stable, FOS>1.3								
5	Stable, FOS>1.3		2.18	3.06	Stable	2.36	3.04	Stable	3.13
6	2.86	2.82	2.96	2.83	2.89	2.87	2.96	2.97	2.91
8	Critical slip surface >> than 2 m								
10	Critical slip surface >> than 2 m								

Table C.18: Factor of safety for various riverbank heights and flood conditions for gravel, 1:1 slope angle

Bank Height (m)	Initial Conditions	Short flood, rapid dd	Short flood, medium dd	Short flood, slow dd	Medium flood, rapid dd	Medium flood, medium dd	Medium flood, slow dd	Long flood, rapid dd	Long flood, medium dd	Long flood, slow dd
1	0.63	0.61	0.61	0.61	0.62	0.61	0.62	0.62	0.62	0.62

Table C.19: Factor of safety for various riverbank heights and flood conditions for gravel, 1:2 slope angle

Bank Height (m)	Initial Conditions	Short flood, rapid dd	Short flood, medium dd	Short flood, slow dd	Medium flood, rapid dd	Medium flood, medium dd	Medium flood, slow dd	Long flood, rapid dd	Long flood, medium dd	Long flood, slow dd
1	1.21	1.17	1.18	1.19	1.17	1.18	1.22	1.21	1.21	1.20
2	1.20	1.19	1.19	1.19	1.19	1.19	1.19	1.20	1.20	1.19
3	1.20	1.19	1.19	1.19	1.19	1.19	1.19	1.20	1.20	1.19
4	1.20	1.19	1.19	1.19	1.19	1.19	1.17	1.20	1.20	1.19
10	1.20	1.18	1.18	1.18	1.19	1.19	1.17	1.20	1.20	1.19

Table C.20: Max. depth to css for various riverbank heights and flood conditions for gravel, 1:2 slope angle

Bank Height (m)	Short flood, rapid dd	Short flood, medium dd	Short flood, slow dd	Medium flood, rapid dd	Medium flood, medium dd	Medium flood, slow dd	Long flood, rapid dd	Long flood, medium dd	Long flood, slow dd
1	0.12	0.12	0.12	0.11	0.12	0.11	0.03	0.14	0.11
2	0.12	0.19	0.20	0.19	0.14	0.12	0.14	0.15	0.12
3	0.27	0.21	0.21	0.25	0.26	0.27	0.24	0.24	0.18
4	0.26	0.40	0.30	0.25	0.26	0.28	0.28	0.27	0.33
10	0.33	0.41	0.29	0.64	0.82	0.38	0.94	0.91	0.76

Table C.21: Factor of safety for various riverbank heights and flood conditions for gravel, 1:3 slope angle

Bank Height (m)	Initial Conditions	Short flood, rapid dd	Short flood, medium dd	Short flood, slow dd	Medium flood, rapid dd	Medium flood, medium dd	Medium flood, slow dd	Long flood, rapid dd	Long flood, medium dd	Long flood, slow dd
1	1.80	1.70	1.70	1.80	1.70	1.70	1.80	1.80	1.80	1.80
3	1.80	1.70	1.70	1.70	1.70	1.70	1.80	1.80	1.80	1.80
10	1.80	1.70	1.60	1.60	1.70	1.70	1.70	1.80	1.80	1.70

APPENDIX D

Models of flood events for various bank angles, bank heights and soil types- only considering when vegetation roots are a suitable bank stabilization technique

APPENDIX E

Models that include root functional traits required to stabilize banks for various flood events, bank angles, bank heights and soil types.

APPENDIX F

Sensitivity of the soil-water characteristic curves and factor of safety with air-entry value, saturated volumetric water content and grain size data

Sensitivity of SWCC to the air-entry value

Figure F1 shows the SWCCs for the range of AEV for the silt loam riverbank. The results are more sensitive for the silt loam soil but are similar for the clay, loamy sand and gravel riverbanks which can be found at the end of this Appendix.

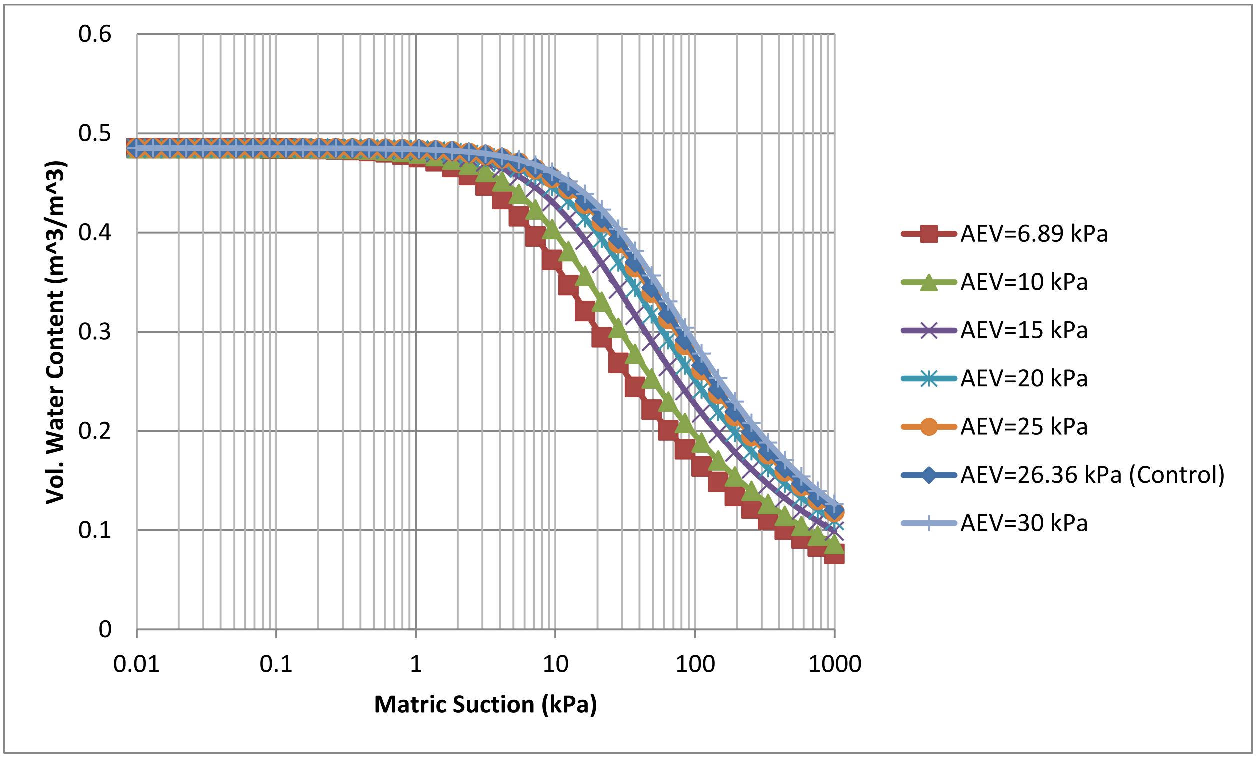

Figure F1: Sensitivity of SWCC with AEV for silt loam bank

The AEV of 26.36 kPa was the original value used in section 5.2, and lies within the range suggested in Table 5.2. Increasing the air-entry appears to steepen the SWCC. The steeper functions relate to a more uniform nature of pores within the soil, which means that the pores drain over a small range of negative pore-water pressures (Geo-Slope, 2007).

For clays, the pores between the individual particles are small which makes it difficult to identify a specific air-entry value since water is able to drain from the system over a wide range before air enters the pores. Furthermore, the slope of the function in the positive pore-water region is usually steeper due to the compressible nature of clays and it is suggested that this parameter should be considered in saturated seepage analyses (Geo-Slope, 2007).

Sensitivity of Factor of Safety to the air-entry value

Figure F2 shows the factor of safety results for the range of air-entry values and volumetric water content function from Fig.F1, for the silt loam riverbank.

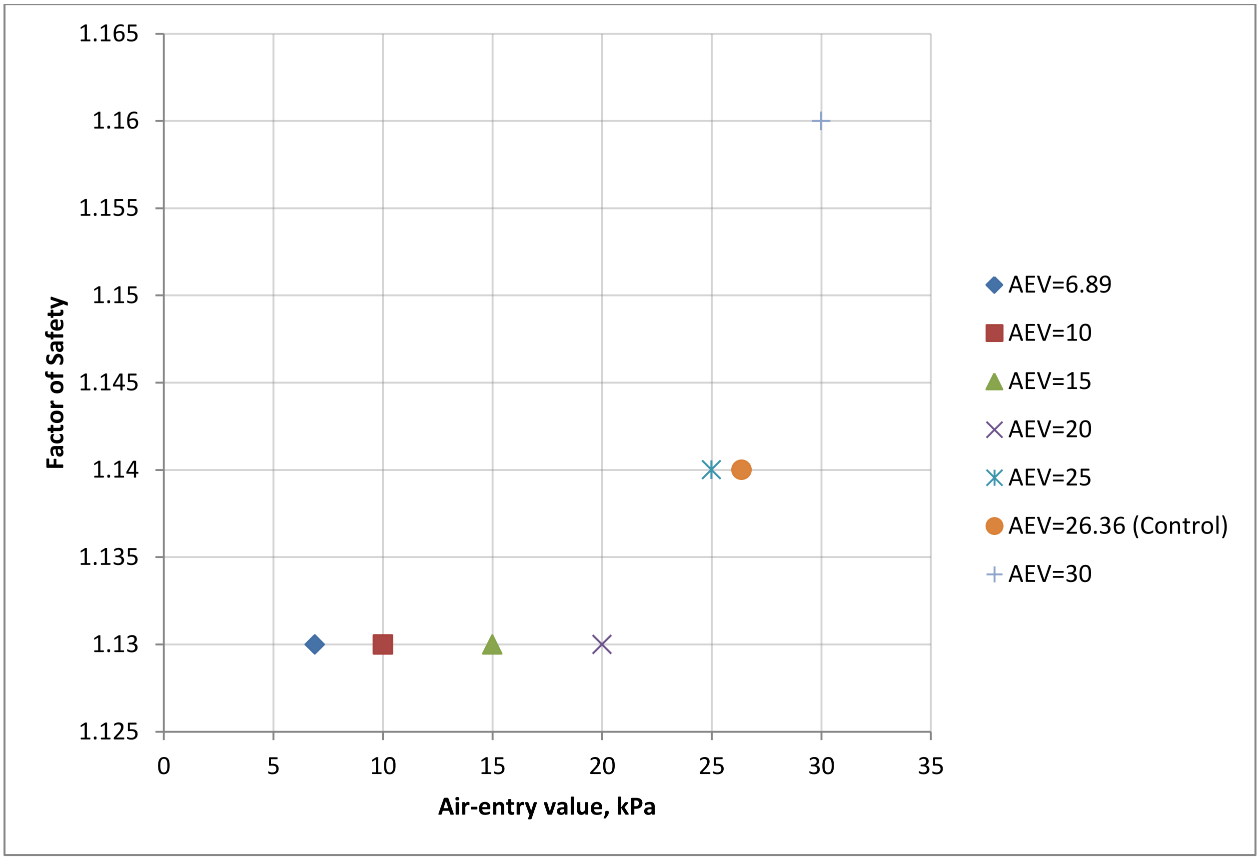

Figure F2: Sensitivity of FOS with AEV for silt loam bank

Although the silt loam riverbank was found to yield the most sensitive results, a difference in AEV of 23 kPa resulted in a minimal difference of 0.03 in the factor of safety. The change in the factor of safety occurred at the upper bounds of the AEV range where the SWCCs are steeper and there is increased drainage over a small range of negative pore-water pressures. The increase in factor of safety is a result of the increased drainage properties of the soil which allows the phreatic surface in the soil to recede at a faster rate. In addition, an increase in air-entry value relates to an increase in suction and correspondingly an increase in the cohesive strength of the soil. The silt loam soil has the largest range of air-entry values and so offers the greatest difference in the factor of safety values. There is similarly little sensitivity in the factor of safety for the clay, loamy sand and gravel soil riverbanks for the range of air-entry values investigated. For the gravel banks, there is no change in the safety factor for the range of air-entry values investigated as gravel naturally has high permeability and drains rapidly, as investigated in chapter 5.

Sensitivity of SWCC to the saturated volumetric water content

The sensitivity of the SWCC to the saturated volumetric water content (θ_s) for silt loam soil as shown in Fig. F3. The sensitivity for the other riverbanks; clay, loamy sand and gravel, is contained at the end of this Appendix.

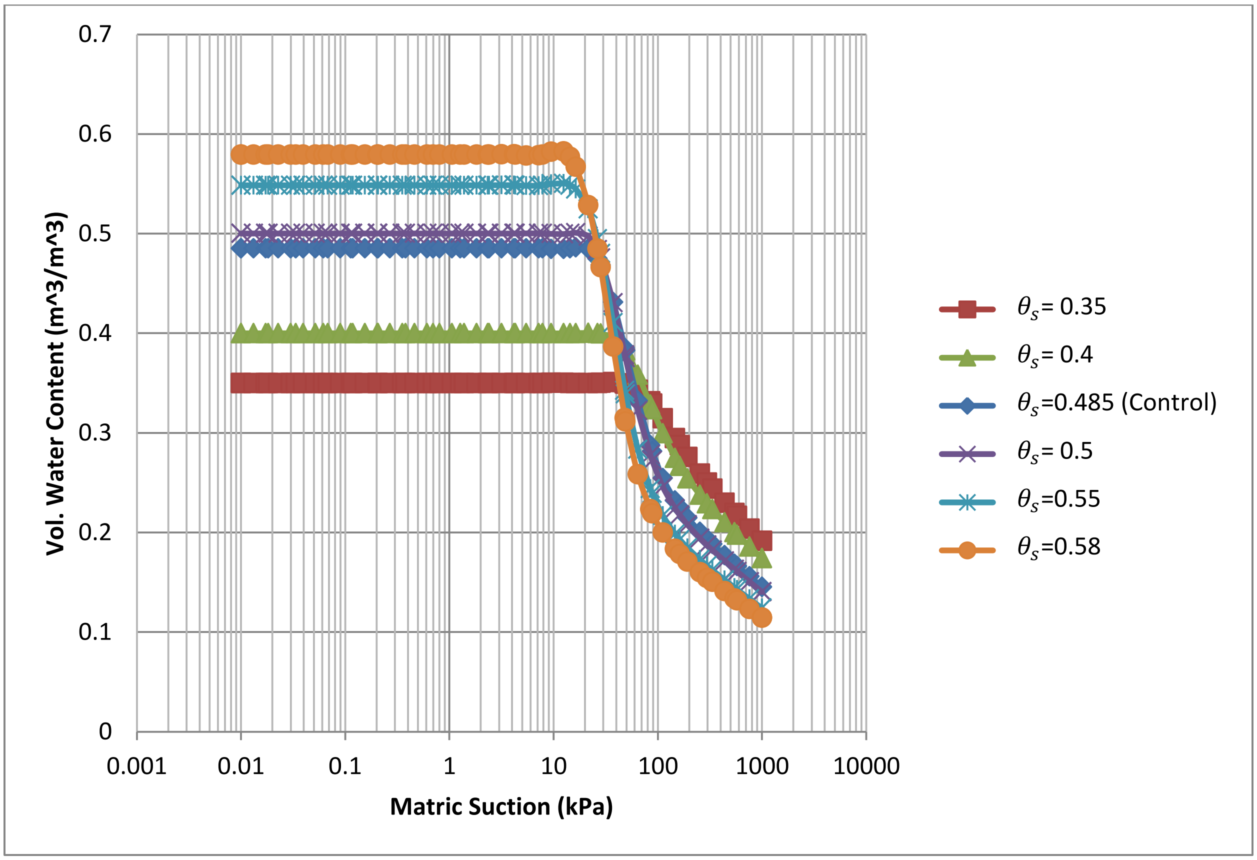

Figure F3: Sensitivity of SWCC with θ_s for silt loam bank

Figure F3 shows that the volumetric water content increases along with the increase in saturated volumetric water content. The saturated volumetric water content and the residual water content is less for high density samples (Suriya et al., 2015).

Sensitivity of Factor of Safety to the saturated volumetric water content

Figure F4 shows the factor of safety results for the range of saturated volumetric water content values investigated for the silt loam riverbank. The factor of safety is most sensitive to the saturated volumetric water content for the silt loam riverbank. The sensitivity for the clay, loamy sand and gravel riverbank is contained at the end of this Appendix.

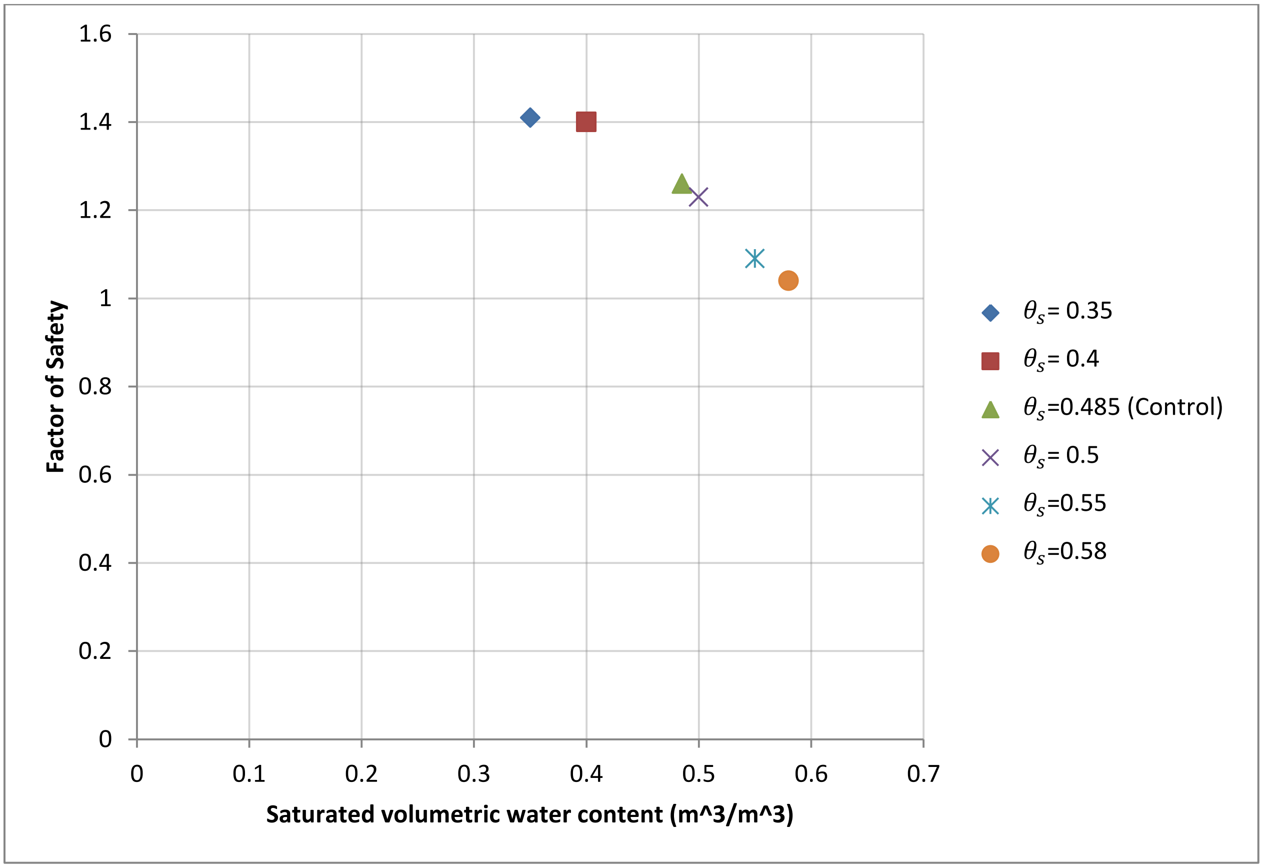

Figure F4: Sensitivity of FOS with θ_s for silt loam bank

A difference in saturated volumetric water content of 0.23 corresponds to a 0.37 change in the factor of safety for the silt loam soil. When the lower bound of the saturated volumetric water content range is used, the bank is unstable with a factor of safety less than 1.3 and when the upper bound of the saturated volumetric water content range is used, the bank is stable with a factor of safety value above 1.3. The factor of safety is relatively sensitive to the saturated volumetric water content for the silt loam soil but not significantly sensitive to the other soil bank types. Geo-Slope (2007) clarifies that in a saturated soil, all the voids are filled with water and the volumetric water content of the soil is equal to the porosity of the soil. As the porosity of the soil increases, it has a greater water holding capacity, and thereby delays the infiltration of water into the bank. Thus slope failure is delayed with increased soil porosity.

Sensitivity of SWCC to D_{10}

Figure F5 shows the SWCCs for the range of D_{10} values for the silt loam riverbank. The SWCC depends on the pore-size distribution of the soil, and so is directly related to the grain-size distribution. Furthermore, many empirical methods have been developed to predict the SWCC from the grain-size distribution of the soil (Gallage and Uchimura, 2010).

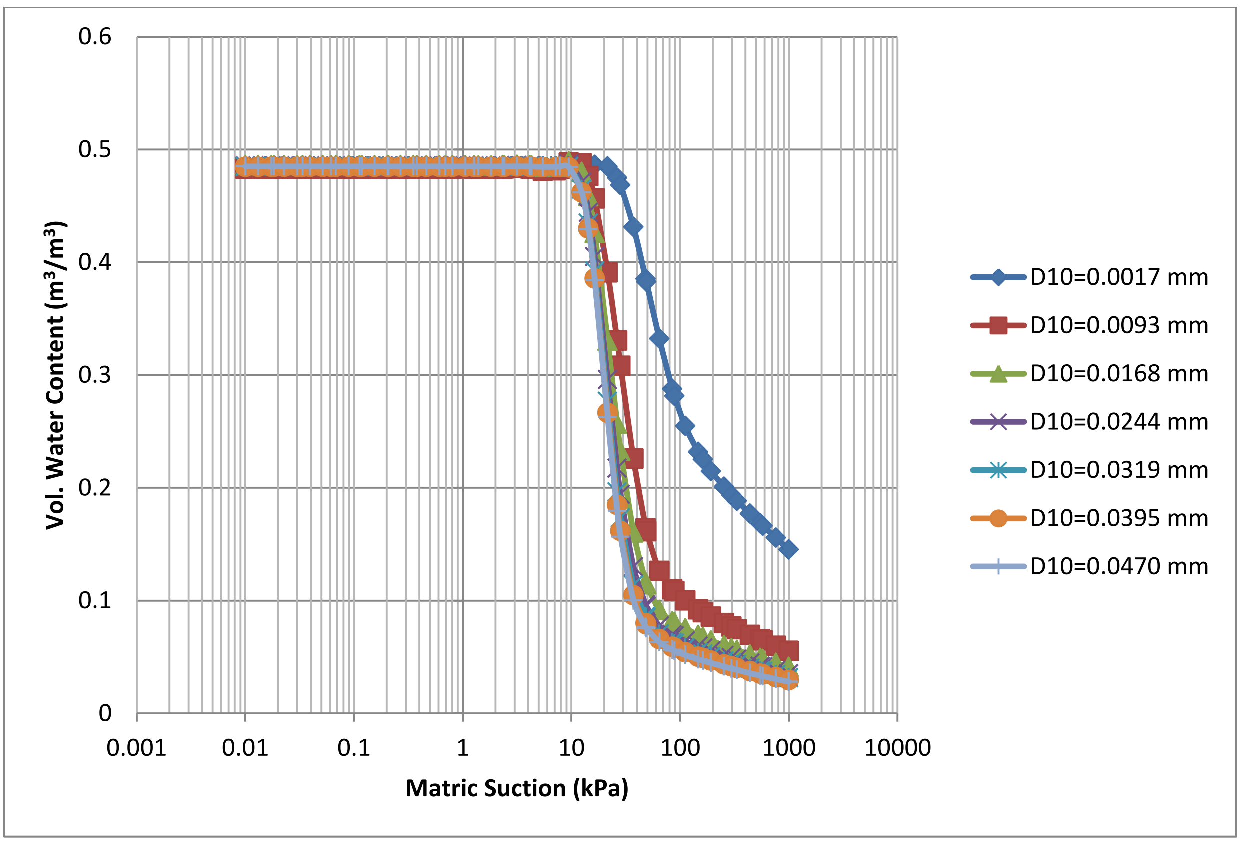

Figure F5: Sensitivity of SWCC with D_{10} for silt loam bank

For decreasing D_{10} values (pertaining to an increased volume of the fine content of the soil), there is an increase in the residual water content and a flattened desorption curve because the flow of the pore-water decreases in the smaller pore-sized soil. Soils with increased fines content tend to have greater adhesive binding properties and so release water at lower potentials, while soils with a lower volume of fines will release most of the water at higher potentials. The water retaining capacity of a soil is due to the porosity of the soil and the nature of the bonding in the soil (Hong et al., 2016).

For soils that consist of large uniform particles, such as sands and gravels, water is able to drain easily under small negative pore-water pressures, which makes the slope of the function steeper than in other soils (Geo-Slope, 2007). Figure F17 and Figure F23 display a steep slope in the SWCC for the loamy sand and gravel bank respectively.

Sensitivity of Factor of Safety to D_{10}

Figure F6 shows the factor of safety results for the range of D_{10} values investigated in the case of the silt loam riverbank.

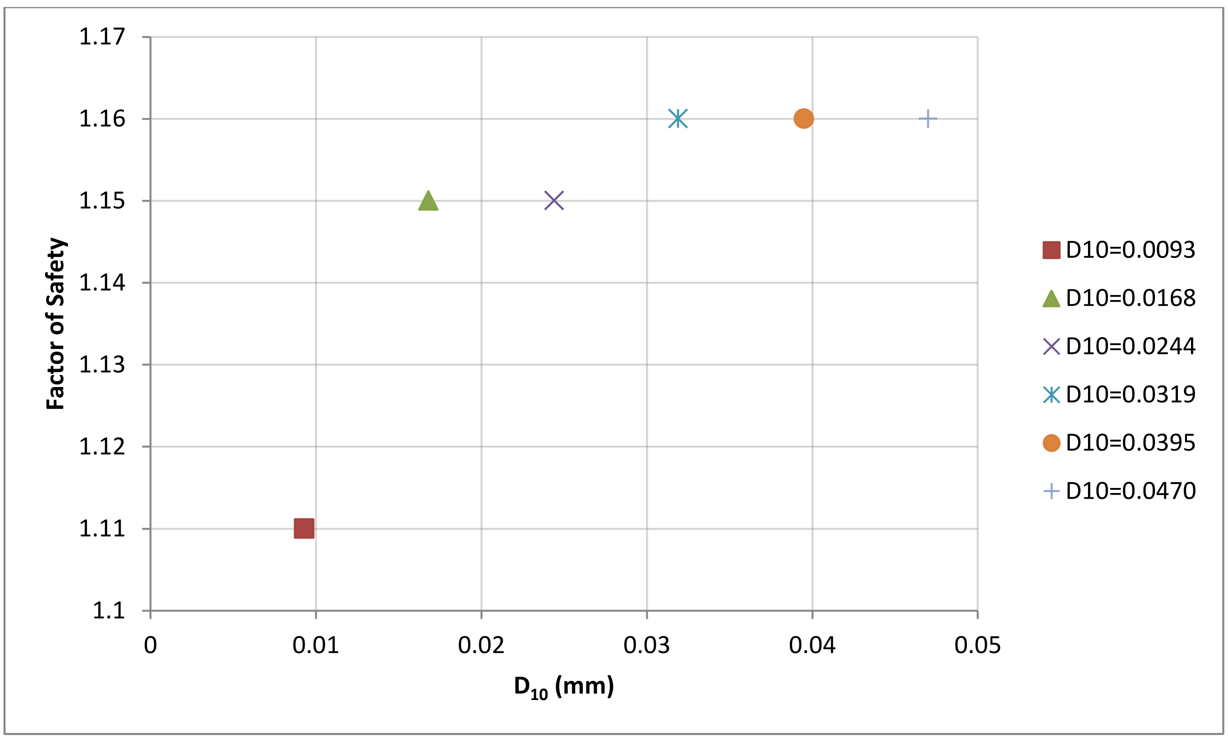

Figure F6: Sensitivity of FOS with D_{10} for silt loam bank

There is an increase in the factor of safety with an increase in the D_{10} values, however the effect is minimal as a change in D_{10} over a range of 0.04 mm results in a change in the factor of safety of 0.05 and further there is no change in the stability conditions. The trend of the result is expected as a greater D_{10} value corresponds to a lower volume in the fines content of the soil and hence the pore-water is able to flow out of the bank at a greater rate than in a soil with greater fines content. This reduces the effect of maintaining an elevated phreatic surface in the bank, and increases the bank stability. The change in the factor of safety with D_{10} is less for the clay, loamy sand, and gravel soils. In the case of the loamy sand soil, the factor of safety increases with a reduced volume of fines in the soil, as the adhesive properties are less in a sandy soil.

Results for sensitivity of SWCC for clay, loamy sand and gravel riverbanks

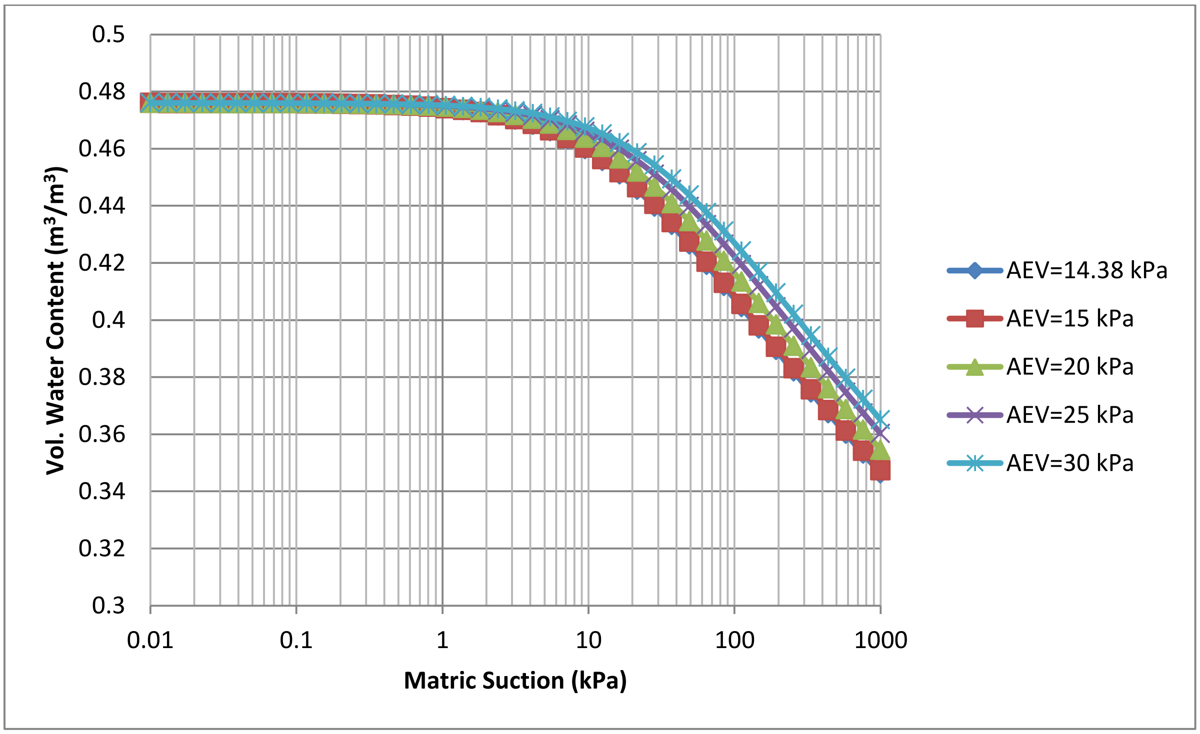

Figure F7: Sensitivity of SWCC with AEV for clay bank

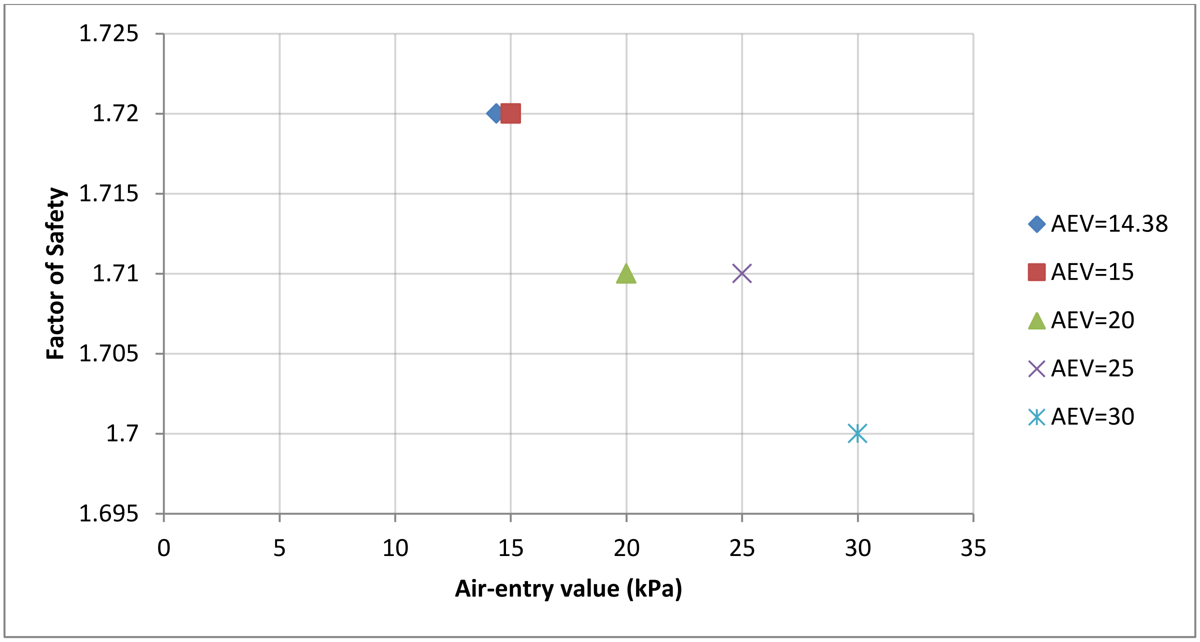

Figure F8: Sensitivity of FOS with AEV for clay bank

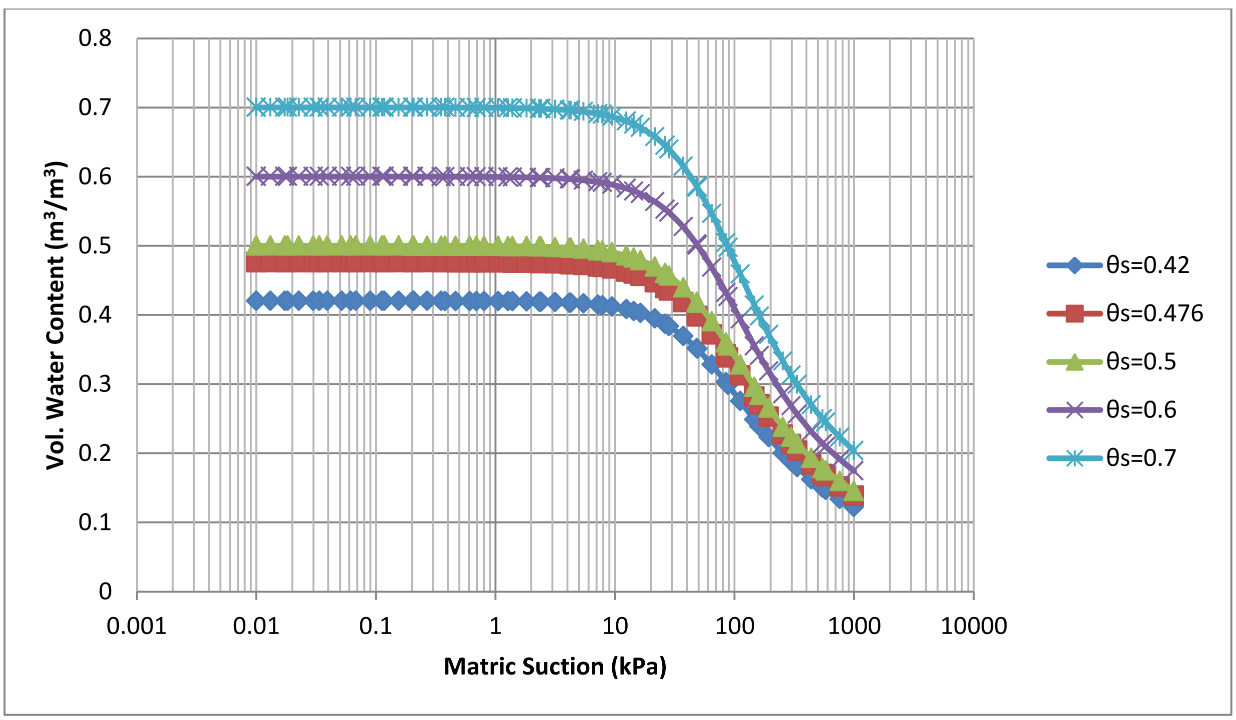

Figure F9: Sensitivity of SWCC with θ_s for clay bank

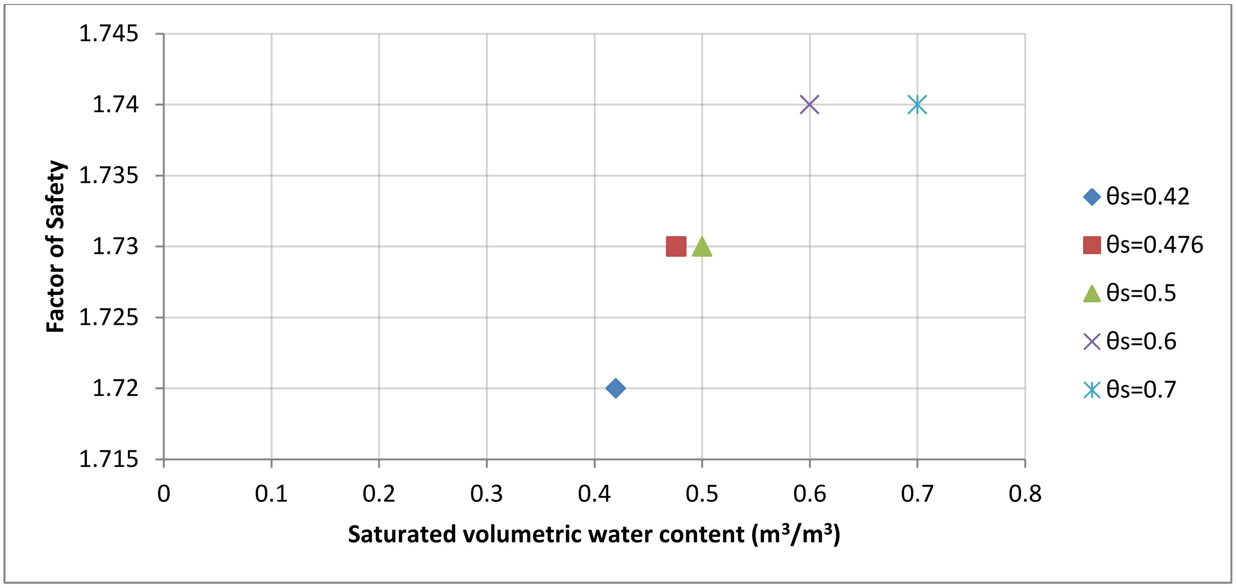

Figure F10: Sensitivity of FOS with θ_s for clay bank

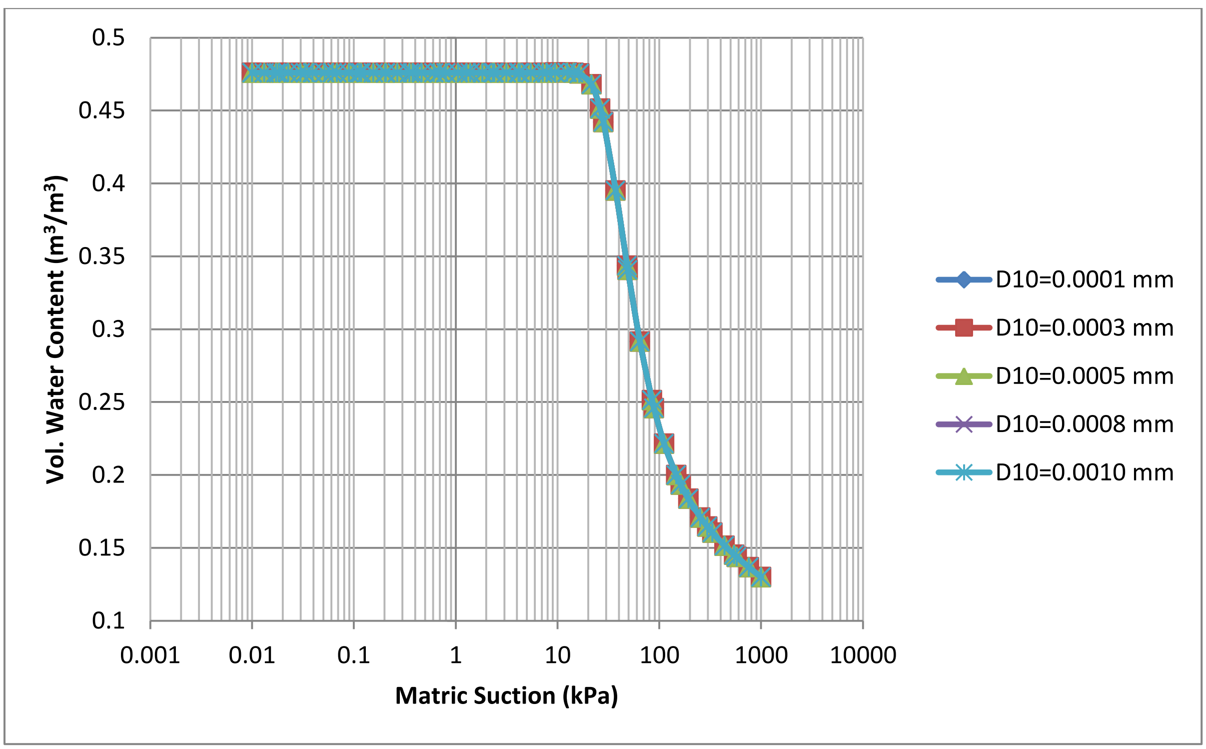

Figure F11: Sensitivity of SWCC with D_{10} for clay bank

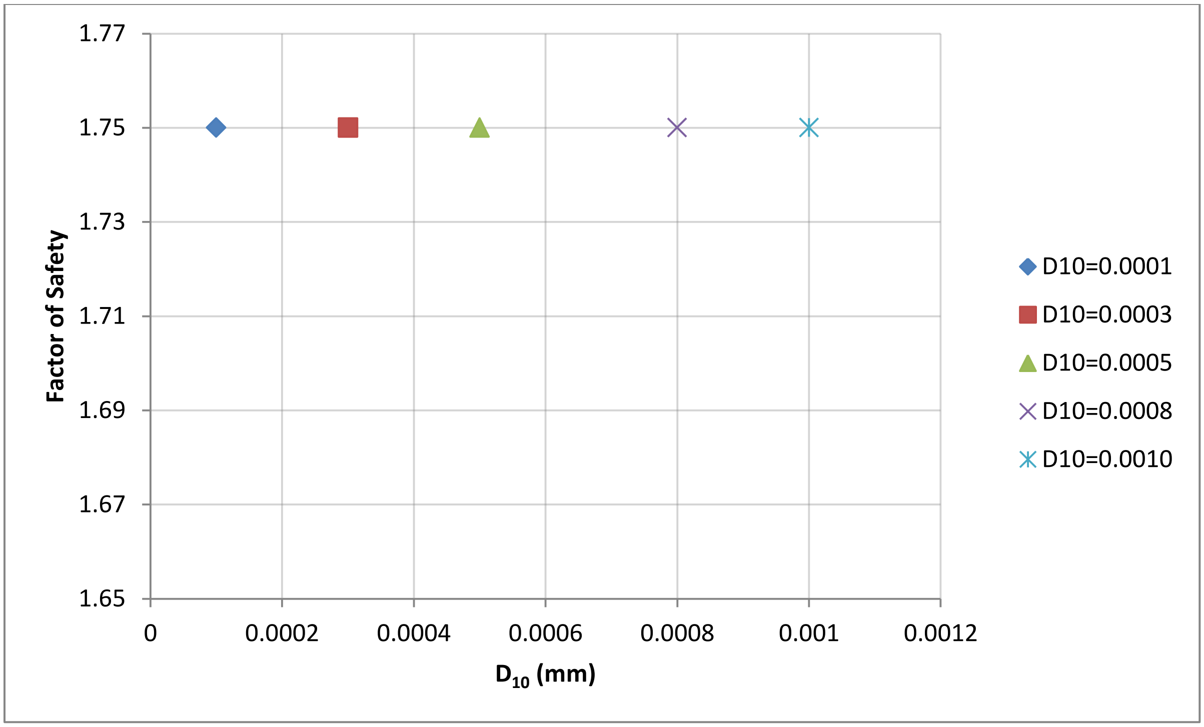

FigureF12: Sensitivity of FOS with D_{10} for clay bank

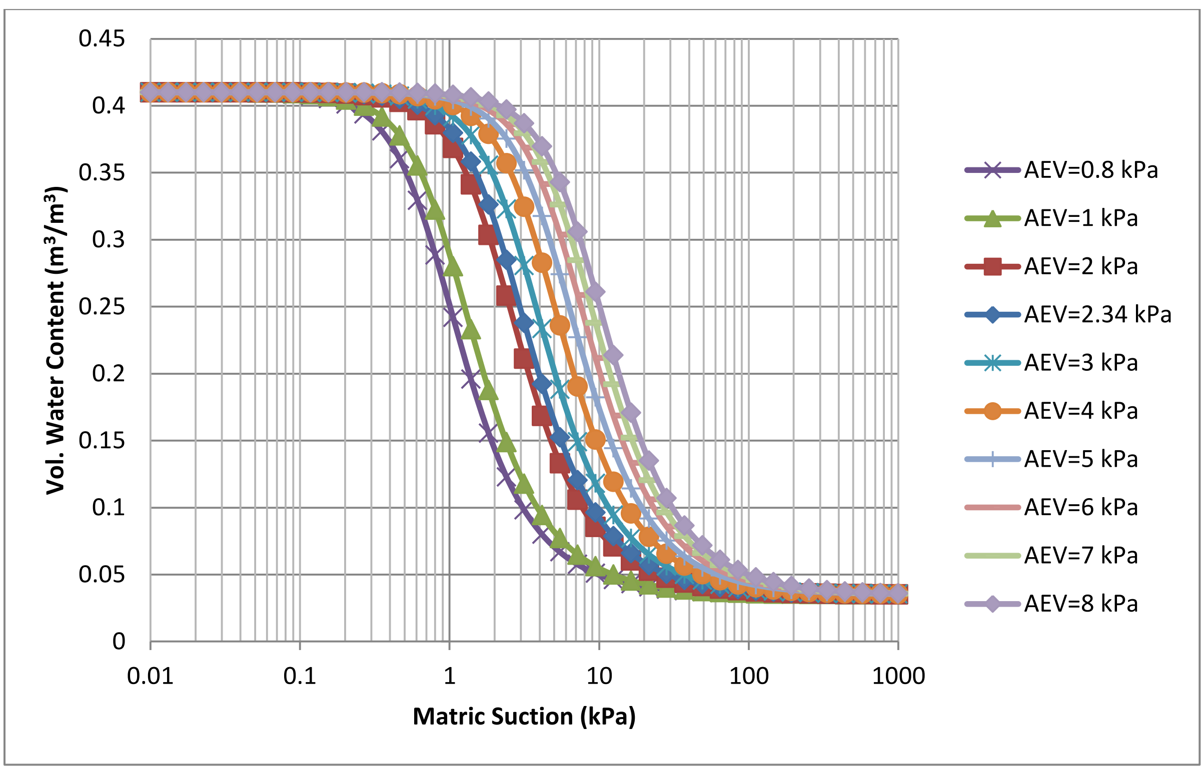

Figure F13: Sensitivity of SWCC with AEV for loamy sand bank

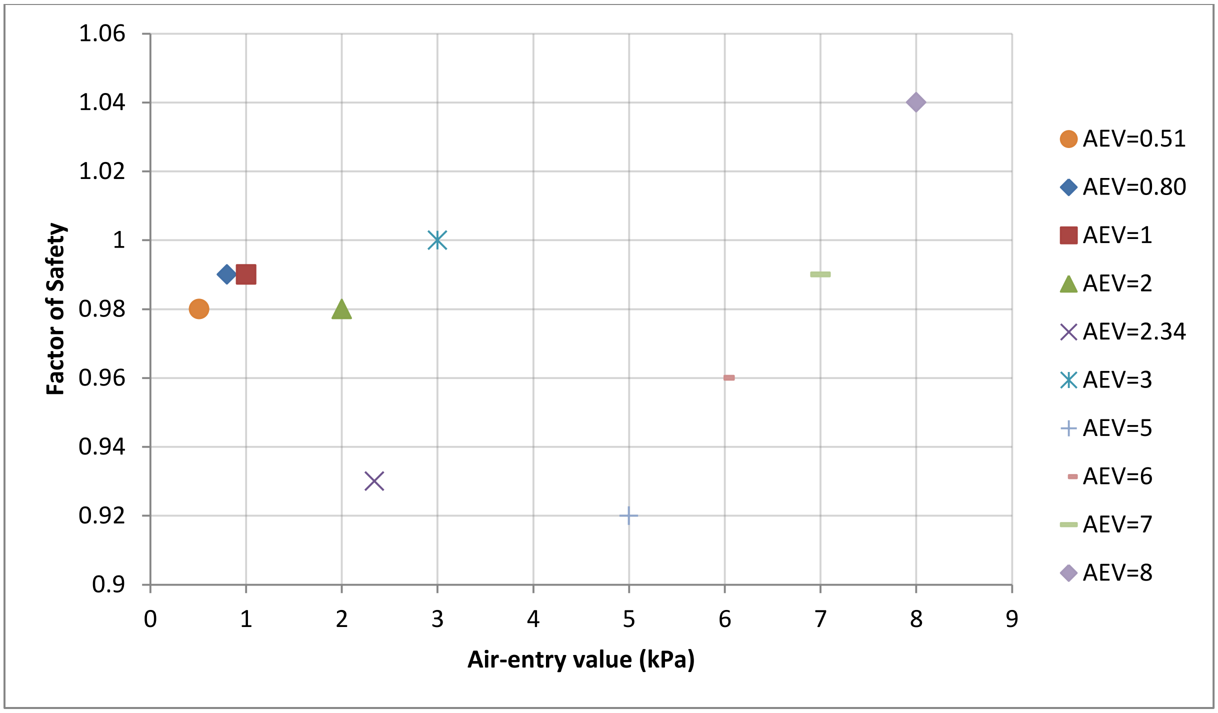

Figure F14: Sensitivity of FOS with AEV for loamy sand bank

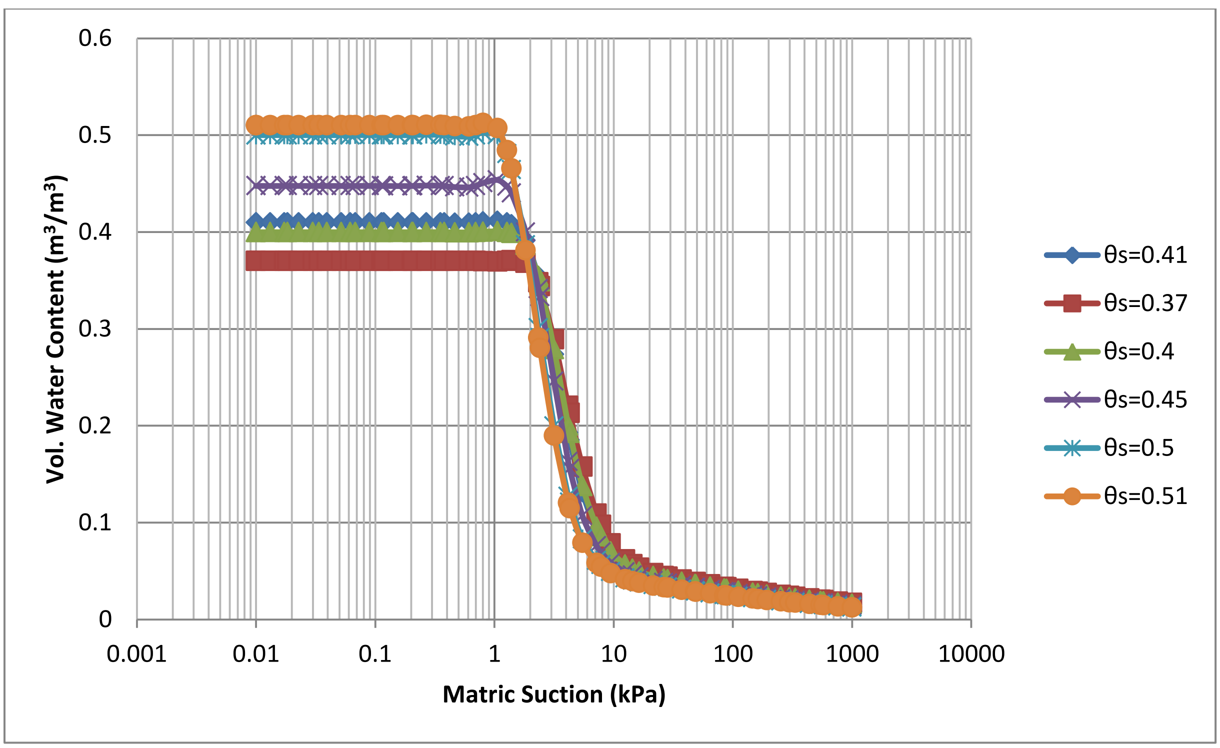

Figure F15: Sensitivity of SWCC with θ_s for loamy sand bank

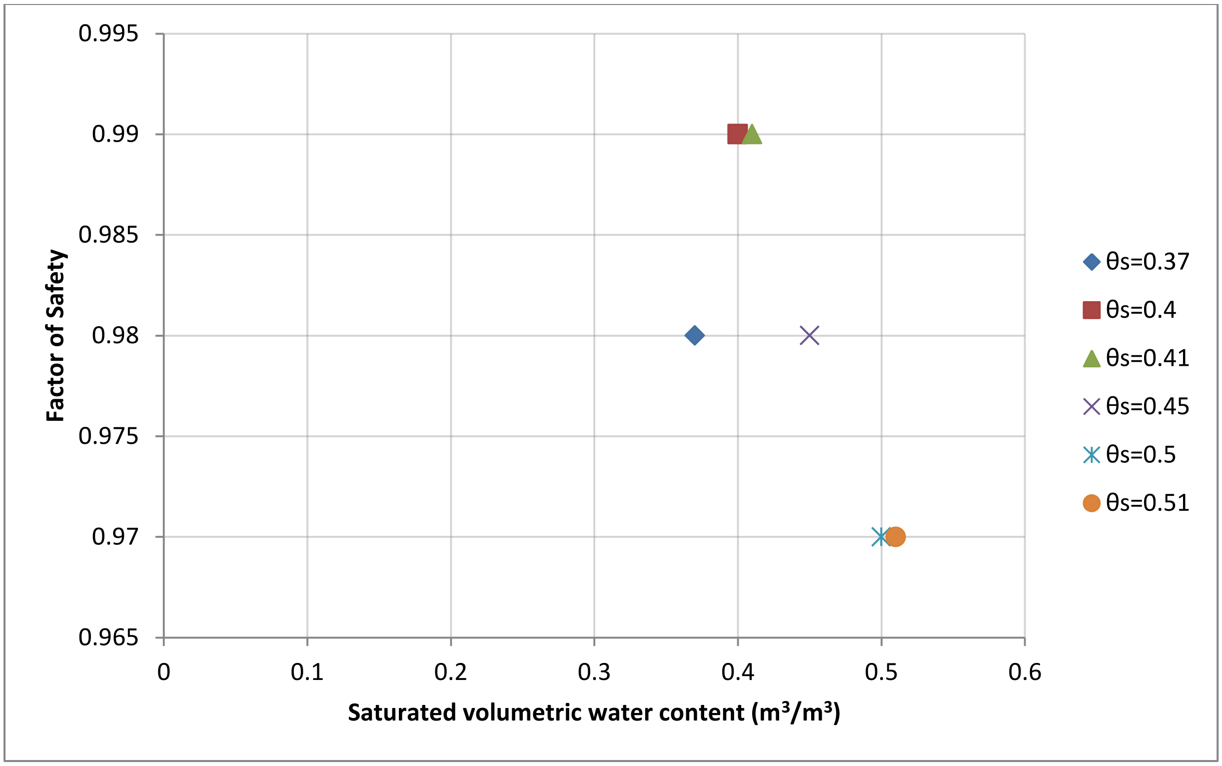

Figure F16: Sensitivity of FOS with θ_s for loamy sand bank

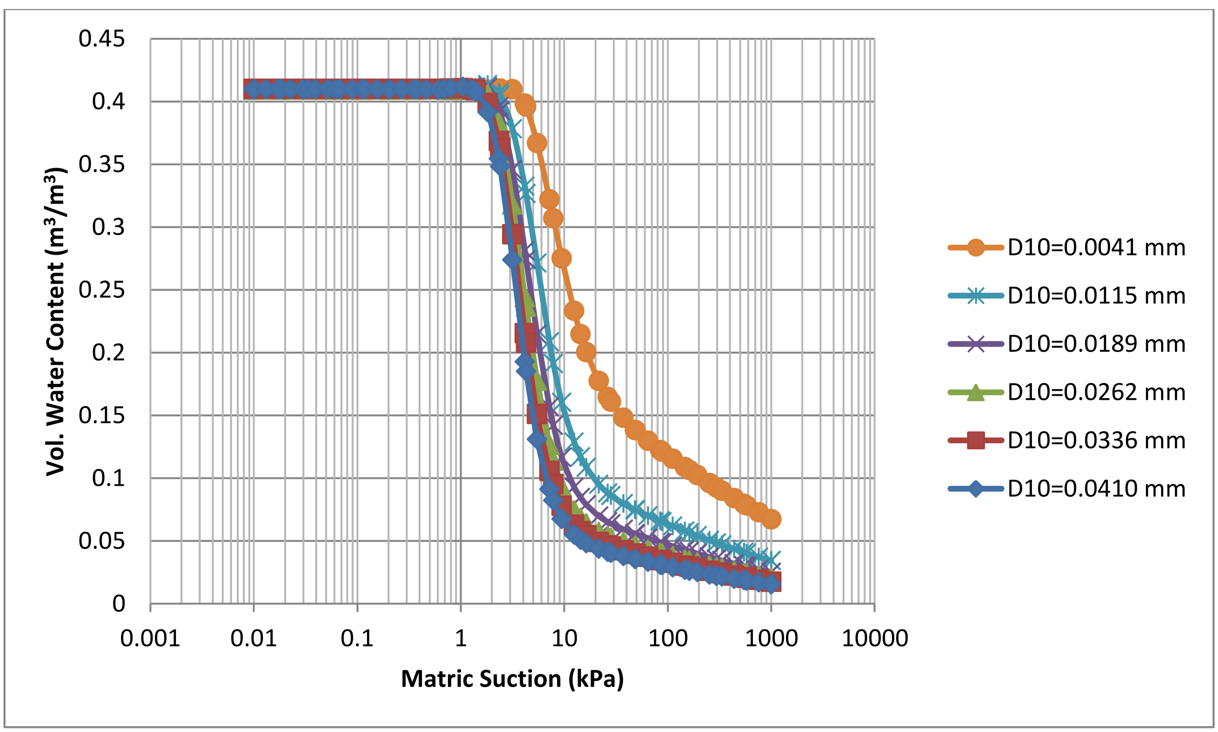

Figure F17: Sensitivity of SWCC with D_{10} for loamy sand bank

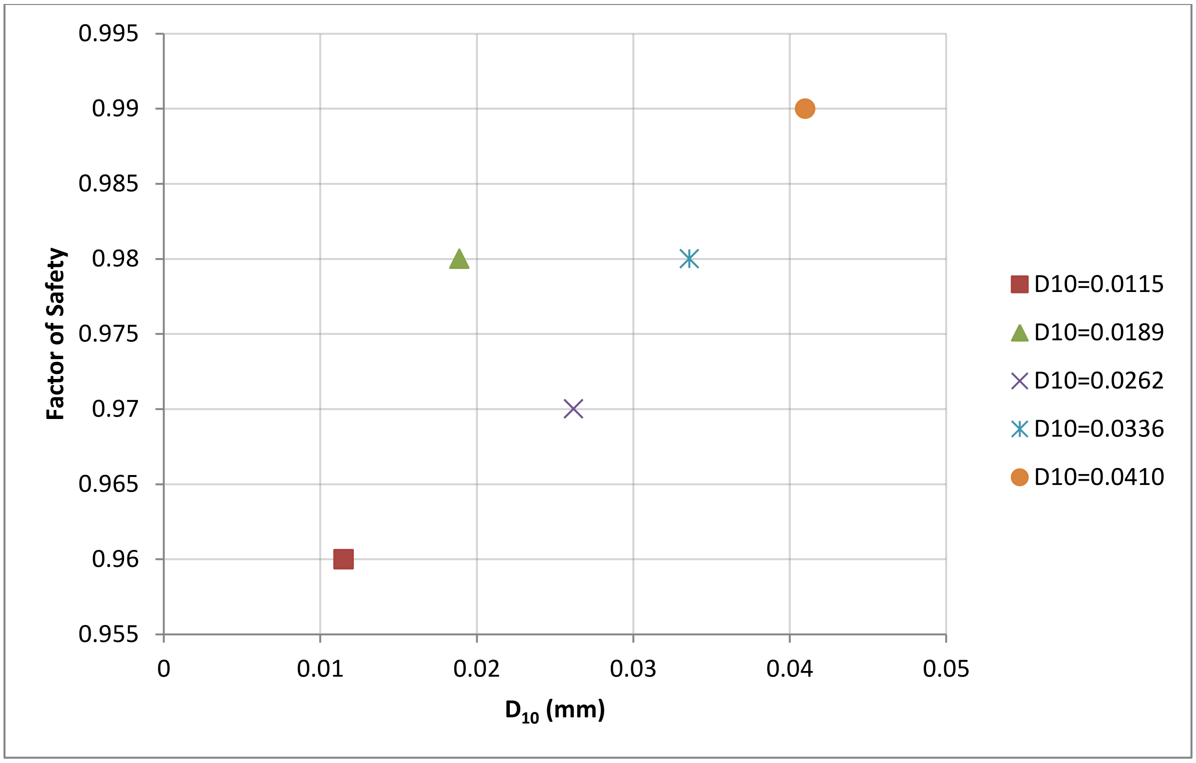

Figure F18: Sensitivity of FOS with D_{10} for loamy sand bank

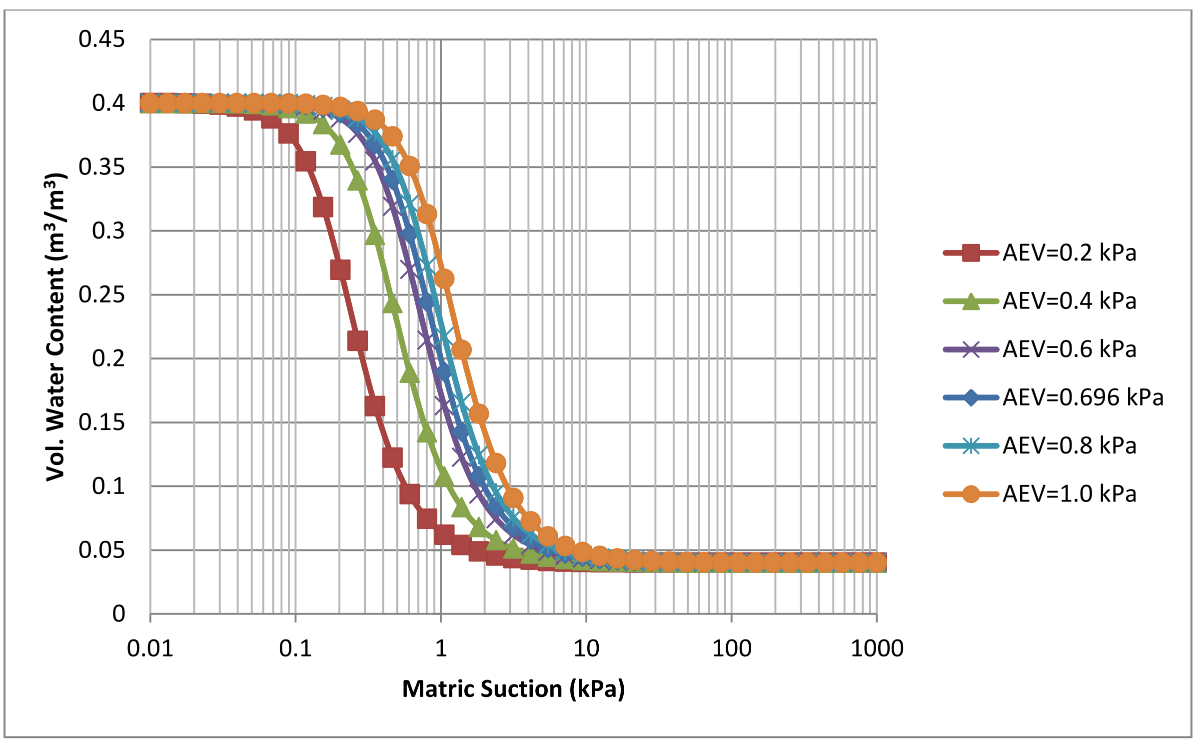

Figure F19: Sensitivity of SWCC with AEV for gravel bank

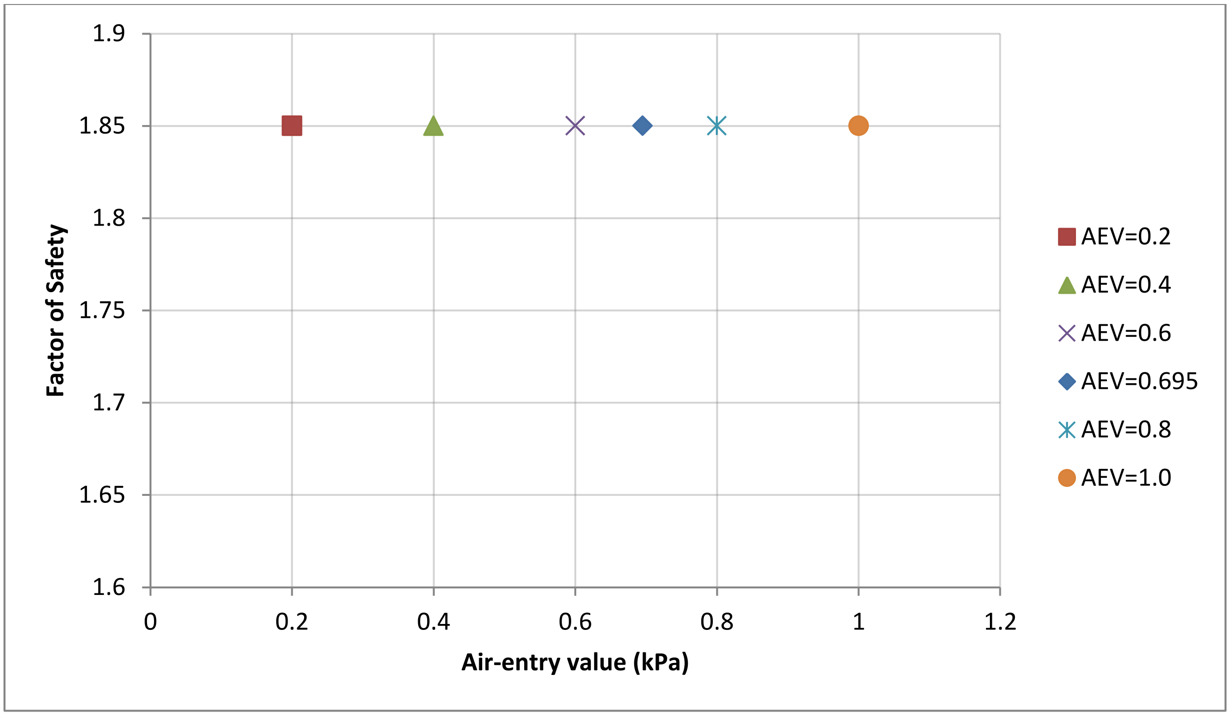

Figure F20: Sensitivity of FOS with AEV for gravel bank

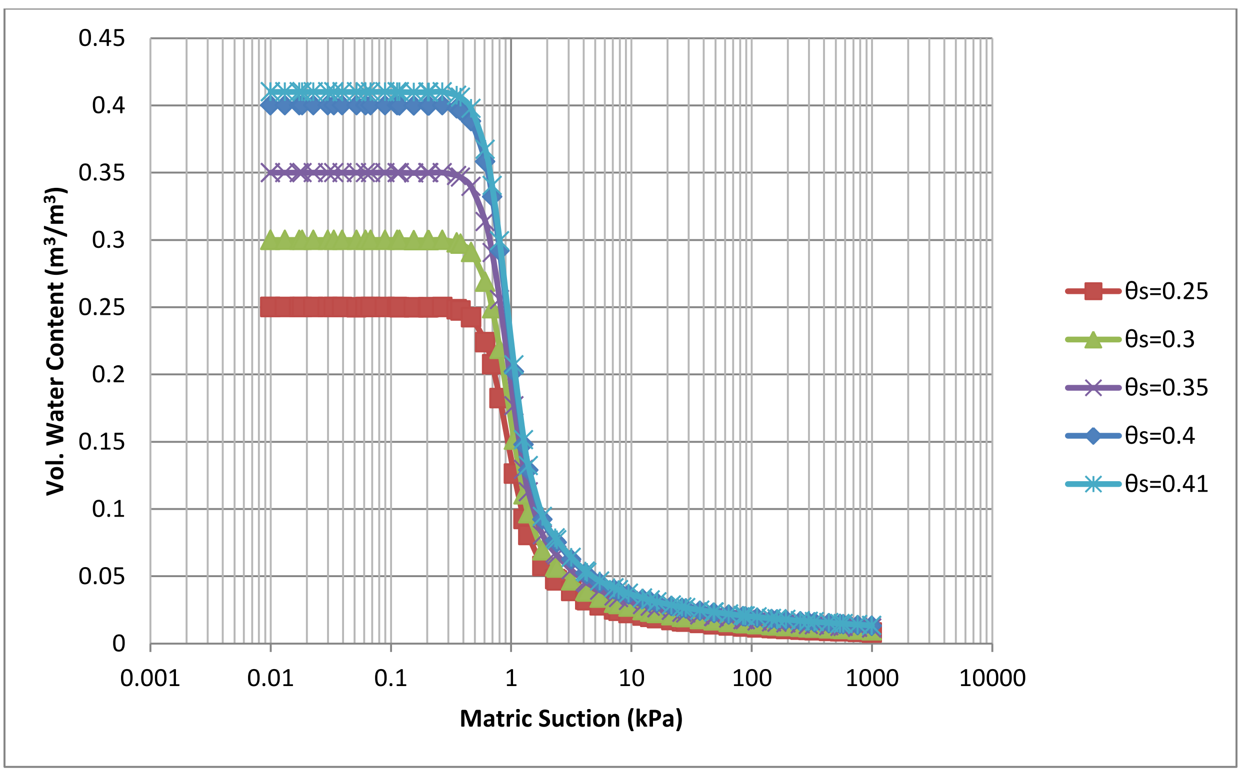

Figure F21: Sensitivity of SWCC with θ_s for gravel bank

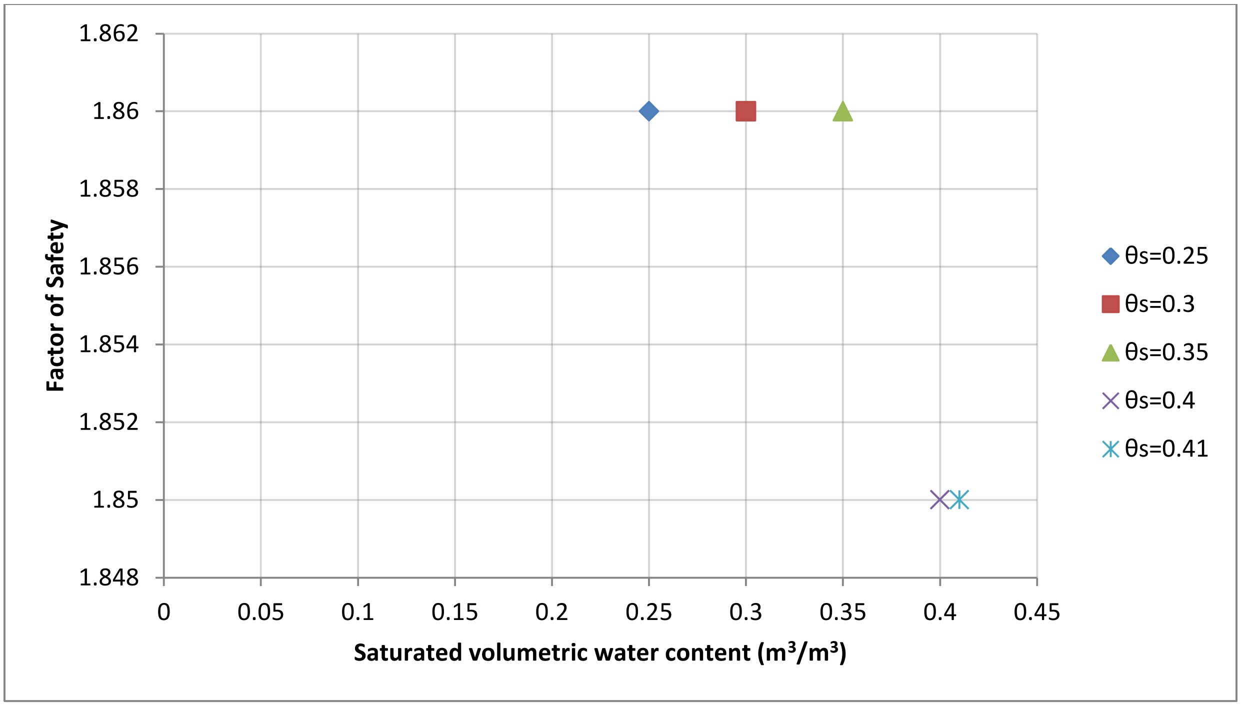

Figure F22: Sensitivity of FOS with θ_s for gravel bank

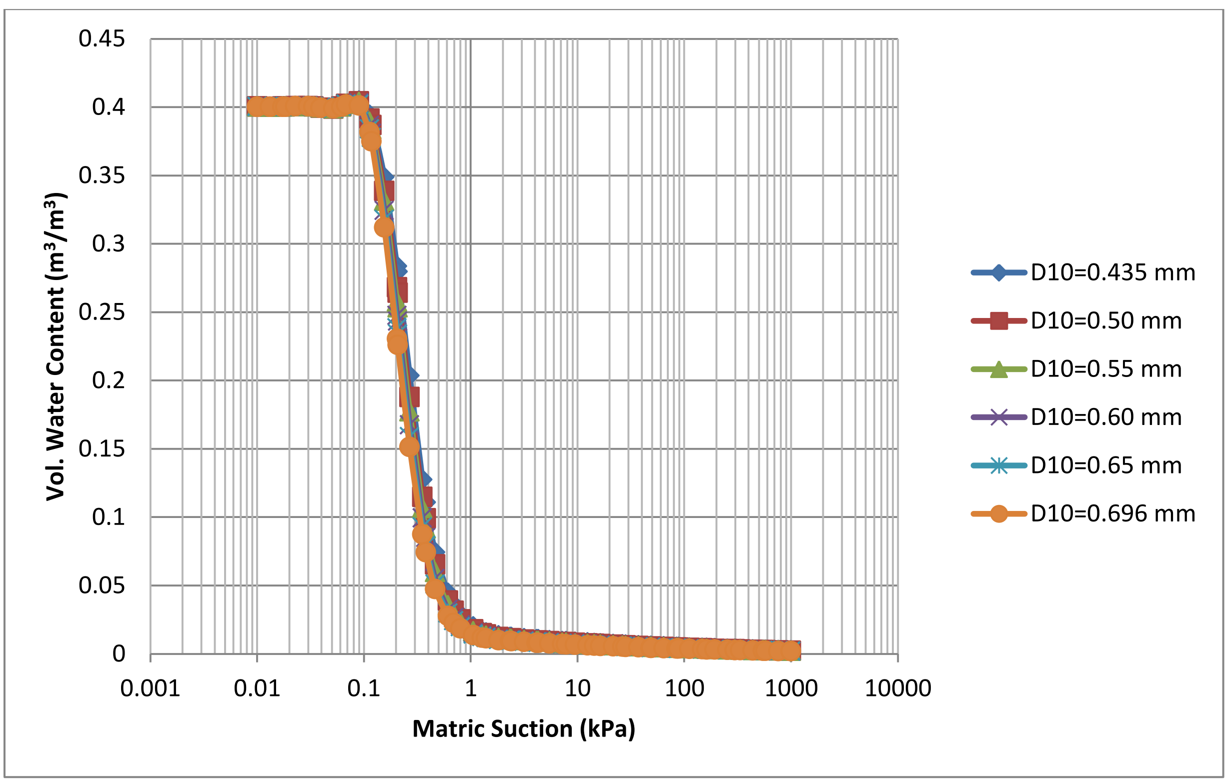

Figure F23: Sensitivity of SWCC with D_{10} for gravel bank

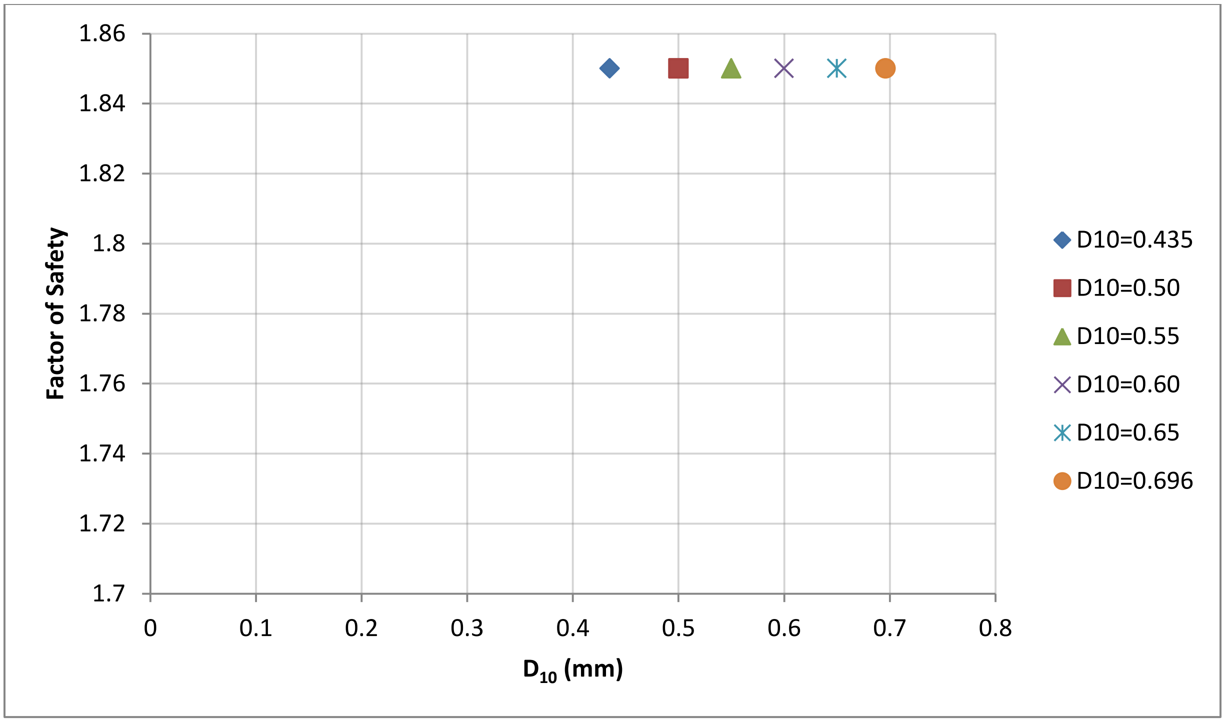

Figure F24: Sensitivity of FOS with D_{10} for gravel bank

APPENDIX G

T_R-*D* models and guideline for additional cohesion due to vegetation, for various plant species found in literature.

Notes:

Abbreviations

Ref. no. - Reference number

The reference numbers are used in Appendix H to list the appropriate plant species.

Ref. no.	Vegetation type	Diameter range (mm)	$T_R = \alpha . D^{\beta}$ (from source)	Maximum rooting depth (m)	Source	C_r (kPa) with depth (m) according to source	T_R (MPa) with diameter (mm) according to source
	Shrub	1.20-6.00 2.40-5.20 2.20-4.50 2.20-5.10	$T_R = 49.21. D^{-1.45}$ $T_R = 38.87. D^{-0.76}$ $T_R = 38.49. D^{-0.63}$ $T_R = 46.05. D^{-1.17}$	0.5	Nyambane and Mwea (2011)	C_r= 25 at d= 0.50	T_R= 35 at *D*= 1.20; T_R= 17 at *D*= 2.00; T_R= 5-10 at *D*= 4.00-5.00; T_R= 4 at *D*= 6.00
1	Shrub, *Atriplex halimus*	0.23-4.68	$T_R = 45.59. D^{-0.56}$	0.50	De Baets et al. (2008)	C_r= 10 at d= 0.45; C_r= 15 at d= 0.35; C_r= 35 at d= 0.25; C_r= 50 at d= 0.10	T_R= 120 at *D*= 0.20; T_R= 60 at *D*= 1.00; T_R= 30 at *D*= 2.00; T_R= 25 at *D*= 4.00; T_R= 20 at *D*= 4.68
2	Shrub, *Atriplex halimus*	0.50-4.30	$T_R = 73.00. D^{-0.60}$	0.50	Mattia et al. (2005)	C_r= 1 at d= 0.5; C_r= 1.5 at d= 0.4; C_r= 4 at d= 0.2; C_r= 5 at d= 0.10	T_R= 60 at *D*= 0.50; T_R=18 at *D*= 0.50
3	Shrub, *Salsola genistoides*	0.30-3.84	$T_R = 44.23. D^{-0.51}$	0.50	De Baets et al. (2008)	C_r=8 at d=0.45; C_r= 15 at d= 0.35;	T_R= 30 at *D*= 2.00; T_R = 25 at *D*= 4.00;

						C_r=25 at d=0.2	T_R= 20 at D=4.68
4	Shrub, *Thymelaea hirsuta*	0.18-2.70	$T_R = 33.31. D^{-0.64}$	0.5	De Baets et al. (2008)	C_r= 0 at d= 0.45; C_r= 10 at d= 0.25; C_r = 15 at d= 0.15; C_r = 20 at d= 0.10	*No data available*
5	Shrub, *Artemisia barrelieri*	0.16-2.15	$T_R = 30.12. D^{-0.61}$	0.5	De Baets et al. (2008)	C_r = 10 at d= 0.25; C_r = 15 at d= 0.15; C_r =80 at d=0.05	*No data available*
6	Shrub, *Fumana thymifolia*	0.19-2.43	$T_R = 15.71. D^{-0.66}$	0.5		*No data available*	
7	Shrub, *Dorycnium pentaphyllum*	0.27-4.35	$T_R = 16.32. D^{-0.62}$	0.5		C_r = 0 at d= 0.45; C_r = 5 at d= 0.35; C_r = 10 at d= 0.25; C_r = 15 at d= 0.15; C_r = 18 at d= 0.05	
8	Shrub, *Teucrium capitatum*	0.22-2.60	$T_R = 18.72. D^{-0.42}$	0.5		*No data available*	
9	Shrub, *Dittrichia viscosa*	0.30-5.50	$T_R = 18.94. D^{-0.45}$	0.50		C_r = 10 at d= 0.25; C_r =22 at d=0.15;	

						C_r = 40 at d= 0.05	
10	Shrub, *Thymus* zygis	0.12-2.88	$T_R = 19.31. D^{-0.73}$	0.5	De Baets et al. (2008)	*No data available*	*No data available*
11	Shrub, *Rosmarinus officinalis*	0.16-3.60	$T_R = 12.89. D^{-0.77}$	0.5		C_r= 5 at d= 0.25; C_r =15 at d= 0.15; C_r =18 at d=0.05	*No data available*
12	Shrub, *Rosmarinus officinalis*	0.16-3.60	$T_R = 34.66. D^{-0.78}$	0.5	Operstein and Frydman (2000)	*No data available*	*No data available*
13	Shrub, *Nerium oleander*	0.09-4.11	$T_R = 4.41. D^{-1.75}$	0.5	De Baets et al. (2008)	*No data available*	T_R= 120 at D= 0.20; T_R= 60 at D= 1.00; T_R =30 at D=2.00; T_R= 25 at D= 4.00; T_R= 20 at D= 4.48
	Grass	1.30-2.30 1.20-2.90 1.10-2.90 1.60-3.90 1.30-2.90	$T_R = 22.45. D^{-1.55}$ $T_R = 25.53. D^{-0.87}$ $T_R = 44.08. D^{-1.28}$ $T_R = 25.53. D^{-1.23}$ $T_R = 36.72. D^{-0.87}$	0.50	Nyambane and Mwea (2011)	C_r= 25-75 at d= 0.3	T_R =17-45 at D= 1.20; T_R= 12-20 at D= 2.00; T_R =10-12 at D= 3.00; T_R = 6 at D= 4.00
14	Grass, *Brachypodium retusum*	0.10-1.45	$T_R = 45.05. D^{-0.61}$	0.25	De Baets et al. (2008)	C_r= 20 at d= 0.15; C_r = 240 at d= 0.05	T_R= 210 at D= 0.20; T_R= 50 at D= 1.00; T_R= 25 at

							D= 1.5
15	Grass, *Stipa tenacissima*	0.43-1.34	$T_R = 24.34. D^{-0.61}$	0.50	De Baets et al. (2008)	*No data available*	T_R = 50 at *D*= 0.20; T_R = 45 at *D*= 1.00
16	Grass, *Lygeum spartum*	0.26-2.72	$T_R = 19.28. D^{-0.68}$	0.50	De Baets et al. (2008)	*No data available*	T_R = 120 at *D*= 0.50; T_R = 80 at *D*= 0.80; T_R = 10 at *D*= 2.00
17	Grass, *Lygeum spartum*	0.30-2.00	$T_R = 60.70. D^{-1.30}$	0.50	Mattia et al. (2005)	C_r= 5 at d= 0.40; C_r= 15 at d= 0.25; C_r = 35 at d= 0.25; C_r = 45 at d= 0.1	T_R = 58 at *D*= 1.00; T_R= 40 at *D*= 1.50; T_R= 20 at *D*= 2.00
18	Grass, *Helictotrichon filifolium*	0.34-1.22	$T_R = 14.51. D^{-1.08}$	0.50	De Baets et al. (2008)	*No data available*	*No data available*
19	Grass, *Piptatherum miliaceum*	0.10-0.64	$T_R = 11.49. D^{-1.77}$	0.25	De Baets et al. (2008)	C_r = 15 at d= 0.15; C_r = 90 at d= 0.05	T_R= 270 at *D*= 0.20
20	Grass, *Avenula bromoides*	0.15-0.32	$T_R = 4.77. D^{-1.52}$	0.50	De Baets et al. (2008)	C_r= 50 at d= 0.15; C_r= 190 at d= 0.05	T_R= 90 at *D*= 0.20; T_R= 20 at *D*= 0.30
	Tree fern	1.40-2.40 1.80-3.20 1.40-3.00 1.50-4.30	$T_R = 30.50. D^{-1.53}$ $T_R = 39.29. D^{-0.88}$ $T_R = 55.86. D^{-1.44}$ $T_R = 42.66. D^{-1.22}$	0.70	Nyambane and Mwea (2011)	C_r= 20 at d= 0.65	T_R= 12-20 at *D*= 2.00; T_R= 10-15 at *D*= 3.00; T_R =10 at *D*= 3.50

21	Tree, *Tamarix canariensis*	0.10-4.80	$T_R = 31.74. D^{-0.89}$	0.65	De Baets et al. (2008)	C_r= 5 at d= 0.65; C_r= 20 at d= 0.45; C_r= 50 at d= 0.05	T_R= 260 at *D*= 0.20; T_R= 10 at *D*= 2.00; T_R= 20 at *D*= 4.00; T_R= 10 at *D*= 4.80
22	Rush, *Juncus acutus*	0.18-1.10	$T_R = 23.23. D^{-0.89}$	0.35		C_r= 5 at d= 0.35; C_r= 50 at d= 0.25; C_r =25 at d=0.10	T_R= 120 at *D*= 0.20; T_R= 25 at *D*= 1.00; T_R =10 at *D*=2.00
23	Reed, *Phragmites australis*	0.10-7.91	$T_R = 34.29. D^{-0.78}$	0.50		*No data available*	T_R= 200 at *D*= 0.20; T_R= 10 at *D*= 6.00; T_R= 2 at *D*= 8.00
24	Herb, *Limonium supinum*	0.34-3.90	$T_R = 33.82. D^{-0.85}$	0.30		C_r= 5 at d= 0.15; C_r=20 at d=0.05	T_R= 120 at *D*= 1.00; T_R =40 at *D*=2.00; T_R= 5 at *D*= 4.00
25	Herb, *Plantago albicans*	0.21-2.55	$T_R = 16.75. D^{-0.52}$	0.30		C_r= 20 at d= 0.15; C_r= 50 at d= 0.05	*No data available*
26	*Alnus* roots	0.17-3.12	$T_R = 11.361D^{-0.758}$	1.00	Naghdi et al. (2013)	C_r= 10 at d= 0.7; C_r= 17 at d= 0.2m 9 roots at	T_R= 115 at *D*= 0.2; T_R= 20 at *D*= 0.50;

26	*Alnus* roots	0.17-3.12	$T_R = 11.361D^{-0.758}$	1.00	Naghdi et al. (2013)	0.8 m depth and 22 at 3.3 m depth	T_R= 10 at *D*= 2.00; T_R= 5 at *D*= 3.20
27	*Spanish Broom*	0.65-9.90	$T_R = 37.605D^{-0.306}$	0.70	Preti and Giadrossich (2009)	C_r= 0.5 at d= 0.70; C_r= 0.2-45 at d= 0.35; C_r= 60-180 at d= 0.15; C_r= 80-210 at d= 0.10 20 roots at 0.15 m depth (*D*= 5-10)	T_R= 31.9 at *D*= 0.70-9.90; T_R= 30.3 at *D*= 0.65-9.35; T_R =44.6 at *D*= 0.44-2.68
28	Conifer and broadleaved species	2.00-20.00	$T_R = 28.97D^{-0.52}$	1.20	Danjon et al. (2008)	40 roots at 0.9 m depth C_r= 26-94	*No data available*
29	Vetiver grass roots	0.20-2.20	$T_R = 59.80D^{-0.5785}$	3.50	Hengchaovanich and Nilaweera (1996)	C_r= 4.96 at d= 1.50; C_r= 5.45 at d= 1.25; C_r =4.73 at d= 0.50 Cazzuffi et al. (2006) report C_r= 15	T_R =75 at *D*=0.70-0.80
30	*Bauhinia championii*	0.20-2.00	$T_R = 26.05D^{-0.64}$	1.00	Ghestem et al. (2014)	*No data available*	T_R =80 at *D*= 0.50; T_R =20 at *D*=1.00 T_R =10 at *D*=2.00

APPENDIX H

Results of the root functional traits required to stabilize the suitable banks, coded UV in Table 5.1

Notes:

Abbreviations

B. championii, - *Bauhinia championii*

The numbers in brackets in the furthest right column are the reference numbers that correlate to Appendix G. The furthest right column lists the plant species that possess the root strength properties required for the functional root traits listed in the central columns.

Table H.1: Stabilizing root functional traits for silt loam bank, 2:1 slope angel

			Root Functional Traits				Root Strength Properties			
Bank height (m)	Drawdown rate	FOS without roots	Root Diameter (mm)	No. of roots per sq. m	RAR (%)	Root Length (m)	T_r (MPa)	C_r (kPa)	FOS with roots	Suitable vegetation type [Ref. no. from guideline doc., Appendix G]
4	Short duration, rapid drawdown	1.24	1.60	34	0.0068	0.50	24.15-45.56	6.29-11.86	1.30-1.37	Grass, shrubs, Vetiver grass roots, [1-4, 12, 17, 23, 27 and 29]
	Short duration, medium drawdown	1.24	1.60	32	0.0064	0.50	24.15-55.06	5.57-12.70	1.30-1.46	Grass, shrubs, *Atriplex halimus* (2), [1-5, 12, 17, 23, and 27-30]
	Short duration, slow drawdown	1.26	1.50	30	0.0053	0.50	26.23-57.24	4.67-10.20	1.30-1.44	Grass, shrubs, *Atriplex halimus* (2), [1-4, 12, 17, 27 and 29]
	Medium duration, rapid drawdown	1.21	1.90	36	0.0102	0.50	19.38-31.82	7.98-13.10	1.31-1.45	Grass, shrubs, *Atriplex halimus* (1), [1-5, 12, 17, 23, and 27-29]
	Medium duration, medium drawdown	1.22	1.75	32	0.0077	0.50	21.54-33.32	5.94-9.19	1.30-1.39	Grass, shrubs, *Atriplex halimus* (1), [1-5, 12, 17, 23 and 27-29]
	Medium duration, slow drawdown	1.24	1.70	34	0.0077	0.50	22.35-33.87	6.57-9.95	1.32-1.44	Grass, shrubs, *Atriplex halimus* (1), [1-4, 12, 17, 23, 27 and 29]
	Long duration, rapid drawdown	1.23	1.70	34	0.0077	0.50	22.35-33.87	6.57-9.95	1.31-1.42	Grass, shrubs, *Atriplex halimus* (1), [1-4, 12, 17, 23, 27 and 29]
	Long duration, medium drawdown	1.18	1.75	32	0.0077	0.50	21.54-33.32	5.94-9.19	1.30-1.38	Grass, shrubs, *Atriplex halimus* (1), [1-5, 12, 17, 23 and 27-29]
	Long duration, slow drawdown	1.18	1.75	32	0.0077	0.50	21.54-33.32	5.94-9.19	1.31-1.41	Grass, shrubs, *Atriplex halimus* (1), [1-5, 12, 17, 23 and 27-29]
5	Short duration, rapid drawdown	1.06	2.00	39	0.0123	1.00	16.72-20.20	8.95-10.81	1.31-1.34	*B. championii*, vetiver grass, conifer and broadleaf species
	Short duration, medium drawdown	1.05	2.00	38	0.0119	1.00	16.72-20.20	8.49-10.27	1.31-1.32	*B. championii*, vetiver grass, conifer and broadleaf species

5	Short duration, slow drawdown	1.07	2.00	37	0.0116	1.00	16.72-20.20	8.05-9.73	1.31-1.33	*B. championii,* vetiver grass, conifer and broadleaf species
	Medium duration, rapid drawdown	1.08	1.60	22	0.0044	1.50	45.56	4.97	1.31	Vetiver grass roots
	Medium duration, medium drawdown	1.07	1.60	22	0.0044	1.50	45.56	4.97	1.30	Vetiver grass roots
	Medium duration, slow drawdown	1.08	1.60	21	0.0042	1.50	45.56	4.53	1.31	Vetiver grass roots
	Long duration, rapid drawdown	1.07	1.75	22	0.0053	1.50	43.26	5.64	1.31	Vetiver grass roots
	Long duration, medium drawdown	1.08	1.75	22	0.0053	1.50	43.26	5.64	1.30	Vetiver grass roots
	Long duration, slow drawdown	1.07	1.70	20	0.0045	1.50	44.00	4.47	1.30	Vetiver grass roots
6	Short duration, rapid drawdown	0.99	1.70	25	0.0057	2.50	43.99	6.99	1.31	Vetiver grass roots
	Short duration, medium drawdown	1.02	1.70	25	0.0057	2.50	43.99	6.99	1.31	Vetiver grass roots
	Short duration, slow drawdown	1.02	1.70	24	0.0054	2.50	43.99	6.44	1.31	Vetiver grass roots
	Medium duration, rapid drawdown	1.01	1.70	25	0.0057	2.50	43.99	6.99	1.30	Vetiver grass roots
	Medium duration, medium drawdown	1.01	1.70	25	0.0057	2.50	43.99	6.99	1.31	Vetiver grass roots
	Medium duration, slow drawdown	1.01	1.70	24	0.0054	2.50	43.99	6.44	1.33	Vetiver grass roots
	Long duration, slow drawdown	1.01	1.70	24	0.0054	2.50	43.99	6.44	1.31	Vetiver grass roots

Table H.2: Stabilizing root functional traits for loamy sand, 1:1 slope angle

			Root Functional Traits				Root Strength Properties			
Bank height (m)	Drawdown rate	FOS without roots	Root Diameter (mm)	No. of roots per sq. m	RAR (%)	Root Length (m)	T_r (MPa)	C_r (kPa)	FOS with roots	Suitable vegetation type [Ref. no. from guideline doc., Appendix G]
1	Short duration, rapid drawdown	1.03	1.20	14	0.0016	0.50	37.77-65.44	0.86-1.51	1.30-1.35	Shrubs, *Atriplex halimus*(2), [1-3, 12, 17, 27 and 29]
	Short duration, medium drawdown	1.04	1.10	14	0.0013	0.50	39.02-68.94	0.75-1.34	1.30-1.36	Grass, shrubs, *Atriplex halimus* (2), [1-3, 17, and 29]
	Short duration, slow drawdown	1.08	1.40	12	0.0018	0.50	28.65-59.65	0.66-1.38	1.31-1.38	Grass, shrubs, *Atriplex halimus* (2), [1-3,17, 27 and 29]
	Medium duration, rapid drawdown	1.03	1.45	14	0.0023	0.50	28.71-58.41	0.97-1.97	1.30-1.38	Shrubs, *Atriplex halimus* (2), [1-3, 17, 27 and 29]
	Medium duration, medium drawdown	1.04	1.20	14	0.0016	0.50	34.91-65.44	0.79-1.51	1.30-1.35	Grass, *Atriplex halimus* (2), [1-3, 17, 27 and 29]
	Medium duration, slow drawdown	1.07	1.10	13	0.0012	0.50	39.02-68.94	0.65-1.16	1.30-1.36	Grass, shrubs, *Atriplex halimus* (2), [1-3, 17 and 29]
	Long duration, rapid drawdown	0.98	2.00	12	0.0038	0.35	18.01-48.16	0.85-2.27	1.30-1.44	Grass, shrubs, *Atriplex halimus* (2), [1-5, 12, 17, 23, 24 and 27-29]
	Long duration, medium drawdown	0.99	2.00	16	0.0050	0.50	18.15-48.16	1.52-4.04	1.30-1.39	Grass, shrubs, *Atriplex halimus* (2), [1-5, 12, 17, 23, and 27-29]
	Long duration, slow drawdown	1.05	1.35	13	0.0019	0.50	30.02-60.97	0.75-1.54	1.31-1.37	Grass, shrubs, *Atriplex halimus* (2), [1-3, 17, 27 and 29]
2	Short duration, rapid drawdown	0.76	0.85	28	0.0016	1.50	65.70	3.05	1.36	Vetiver grass roots
	Short duration, medium drawdown	0.77	2.80	41	0.0253	1.20	16.96	18.33	1.30	Conifer and broadleaved species
	Short duration, slow drawdown	0.79	2.80	41	0.0253	1.20	16.96	18.33	1.30	Conifer and broadleaved species

2	Medium duration, rapid drawdown	0.75	0.85	32	0.0018	1.50	65.70	3.99	1.32	Vetiver grass roots
	Medium duration, medium drawdown	0.76	1.80	19	0.0048	1.50	42.56	4.08	1.32	Vetiver grass roots
	Medium duration, slow drawdown	0.79	2.80	41	0.0253	1.20	16.96	18.33	1.30	Conifer and broadleaved species
	Long duration, rapid drawdown	0.63	1.28	24	0.0031	1.80	51.84	4.01	1.30	Vetiver grass roots
	Long duration, slow drawdown	0.78	1.10	25	0.0024	1.50	56.59	3.51	1.32	Vetiver grass roots
3	Short duration, rapid drawdown	0.66	1.25	30	0.0037	2.30	52.56	6.06	1.31	Vetiver grass roots
	Short duration, medium drawdown	0.66	1.26	30	0.0037	2.30	52.32	6.10	1.30	Vetiver grass roots
	Short duration, slow drawdown	0.68	1.05	34	0.0029	2.30	58.14	6.08	1.30	Vetiver grass roots
	Medium duration, medium drawdown	0.63	1.54	28	0.0052	2.50	46.58	7.10	1.31	Vetiver grass roots
	Medium duration, slow drawdown	0.68	1.53	28	0.0051	2.30	46.76	7.04	1.30	Vetiver grass roots
	Long duration, slow drawdown	0.68	1.53	28	0.0051	2.30	46.76	7.04	1.30	Vetiver grass roots

Table H.3: Stabilizing root functional traits for loamy sand, 1:2 slope angle

			Root Functional Traits				Root Strength Properties			
Bank height (m)	**Drawdown rate**	**FOS without roots**	**Root Diameter (mm)**	**No. of roots per sq. m**	**RAR (%)**	**Root Length (m)**	T_r **(MPa)**	C_r **(kPa)**	**FOS with roots**	**Suitable vegetation type [Ref. no. from guideline doc., Appendix G]**
2	Short duration, rapid drawdown	1.15	2.00	32	0.0101	0.85	6.72-20.20	2.26-6.79	1.31-1.39	*Alnus* roots, conifer and broadleaved species, [29 and 30]
	Short duration, medium drawdown	1.16	2.00	30	0.0094	0.85	6.72-20.20	1.98-5.96	1.31-1.40	*Alnus* roots, conifer and broadleaved species, [29 and 30]
	Short duration, slow drawdown	1.19	2.00	26	0.0082	0.85	6.72-20.20	1.49-4.48	1.31-1.41	*Alnus* roots, conifer and broadleaved species, [29 and 30]
	Medium duration, rapid drawdown	1.12	1.90	35	0.0099	0.85	6.98-20.75	2.53-7.52	1.30-1.37	*Alnus* roots, conifer and broadleaved species, [29 and 30]
	Medium duration, medium drawdown	1.13	2.40	30	0.0014	0.85	5.85-18.38	2.49-7.81	1.30-1.37	*Alnus* roots, Conifer and broadleaved species, [29 and 30]
	Medium duration, slow drawdown	1.18	1.70	28	0.0064	0.85	7.60-21.98	1.41-4.08	1.30-1.40	*Alnus* roots, conifer and broadleaved species, [29 and 30]
	Long duration, rapid drawdown	0.99	2.45	35	0.0165	0.90	18.18	10.96	1.30	Conifer and broadleaved species
	Long duration, medium drawdown	0.97	2.00	30	0.0094	1.00	20.20-40.05	5.96-11.82	1.30-1.32	Vetiver grass roots, conifer and broadleaved species
	Long duration, slow drawdown	1.14	1.75	35	0.0084	0.85	7.43-21.66	2.29-6.66	1.31-1.38	*Alnus* roots, conifer and broadleaved species, [29 and 30]
3	Short duration, rapid drawdown	1.03	0.85	34	0.0019	1.50	65.70	4.50	1.30	Vetiver grass roots

3	Short duration, medium drawdown	1.03	0.85	34	0.0019	1.50	65.70	4.50	1.30	Vetiver grass roots
	Short duration, slow drawdown	1.06	0.90	31	0.0020	1.50	63.56	4.06	1.30	Vetiver grass roots
	Medium duration, rapid drawdown	0.99	1.15	32	0.0033	1.50	55.16	6.12	1.30	Vetiver grass roots
	Medium duration, medium drawdown	1.00	1.30	28	0.0037	1.50	51.38	5.58	1.30	Vetiver grass roots
	Medium duration, slow drawdown	1.04	0.90	32	0.0020	1.50	63.56	4.32	1.30	Vetiver grass roots
	Long duration, rapid drawdown	0.81	1.45	30	0.0050	2.00	48.23	7.48	1.30	Vetiver grass roots
	Long duration, medium drawdown	0.80	1.40	32	0.0049	2.00	49.22	8.10	1.30	Vetiver grass roots
	Long duration, slow drawdown	1.03	1.10	30	0.0029	1.50	56.59	5.05	1.30	Vetiver grass roots
4	Short duration, rapid drawdown	0.96	1.45	30	0.0050	2.00	48.23	7.48	1.30	Vetiver grass roots
	Short duration, medium drawdown	0.96	1.35	32	0.0046	2.00	50.27	7.69	1.30	Vetiver grass roots
	Short duration, slow drawdown	1.00	1.45	30	0.0050	2.00	48.23	7.48	1.30	Vetiver grass roots
	Medium duration, rapid drawdown	0.90	1.75	28	0.0067	2.20	43.26	8.51	1.30	Vetiver grass roots
	Medium duration, medium drawdown	0.92	1.70	28	0.0064	2.20	43.99	8.17	1.30	Vetiver grass roots
	Medium duration, slow drawdown	0.98	1.75	28	0.0067	2.00	43.26	8.51	1.30	Vetiver grass roots

4	Long duration, rapid drawdown	0.74	1.35	20	0.0028	2.20	50.27	3.00	1.37	Vetiver grass roots
	Long duration, medium drawdown	0.74	Note: There is no suitable model for tensile strength and additional cohesion from literature for a root reinforcing deeper than 2.5 m.							
	Long duration, slow drawdown	0.98	1.50	24	0.0042	2.50	47.30	5.03	1.31	Vetiver grass roots
5	Short duration, rapid drawdown	0.90	Note: There is no suitable model for tensile strength and additional cohesion from literature for a root reinforcing deeper than 2.5 m.							
	Short duration, medium drawdown	0.90	Note: There is no suitable model for tensile strength and additional cohesion from literature for a root reinforcing deeper than 2.5 m.							
	Short duration, slow drawdown	0.95	Note: There is no suitable model for tensile strength and additional cohesion from literature for a root reinforcing deeper than 2.5 m. vegetation							
	Medium duration, rapid drawdown	0.84	Note: There is no suitable model for tensile strength and additional cohesion from literature for a root reinforcing deeper than 2.5 m.							
	Medium duration, medium drawdown	0.86	Note: There is no suitable model for tensile strength and additional cohesion from literature for a root reinforcing deeper than 2.5 m.							
	Medium duration, slow drawdown	0.94	Note: There is no suitable model for tensile strength and additional cohesion from literature for a root reinforcing deeper than 2.5 m.							
	Long duration, rapid drawdown	0.79	Note: There is no suitable model for tensile strength and additional cohesion from literature for a root reinforcing deeper than 2.5 m.							
	Long duration, medium drawdown	0.79	Note: There is no suitable model for tensile strength and additional cohesion from literature for a root reinforcing deeper than 2.5 m.							
	Long duration, slow drawdown	0.93	Note: There is no suitable model for tensile strength and additional cohesion from literature for a root reinforcing deeper than 2.5 m.							
6-10	All	0.91-0.70	Note: There is no suitable model for tensile strength and additional cohesion from literature for a root reinforcing deeper than 2.5 m.							

Table H.4: Stabilizing root functional traits for loamy sand, 1:3 slope angle

			Root Functional Traits				Root Strength Properties			
Bank height (m)	**Drawdown rate**	**FOS without roots**	**Root Diameter (mm)**	**No. of roots per sq. m**	**RAR (%)**	**Root Length (m)**	T_r **(MPa)**	C_r **(kPa)**	**FOS with roots**	**Suitable vegetation type [Ref. no. from guideline doc., Appendix G]**
2	Long duration, rapid drawdown	1.29	0.60	25	0.0007	0.50	27.29-80.36	0.50-1.48	1.31-1.37	*Lygeum spartum,*vetiver grass and [1-5, 10, 12,15-17, 21, 23 and 30]
	Long duration, medium drawdown	1.28	0.60	25	0.0007	0.50	16.73-80.36	0.31-1.48	1.31-1.36	*Alnus* roots,vetiver grass and [1-12,15-19,21-25 and 30]
3	Long duration, rapid drawdown	1.09	1.50	35	0.0062	1.00	20.10-23.46	4.54-5.30	1.32-1.33	*B. championii,* conifer and broadleaved species
	Long duration, medium drawdown	1.06	1.60	65	0.0070	1.20	19.28-22.69	4.96-5.83	1.30-1.30	*B. championii,* conifer and broadleaved species
4	Short duration, rapid drawdown	1.29	0.60	25	0.0007	0.50	27.29-80.36	0.50-1.48	1.30-1.30	*Lygeum spartum,*vetiver grass and [1-5, 10, 12,15-17, 21, 23 29, and 30]
	Short duration, medium drawdown	1.29	0.60	25	0.0007	0.50	27.29-80.36	0.50-1.48	1.30-1.31	*Lygeum spartum,*vetiver grass and [1-5, 10, 12,15-17, 21, 23 and 30]
	Medium duration, rapid drawdown	1.24	1.10	30	0.0029	1.00	24.51-56.59	2.19-5.05	1.31-1.33	*B. championii,* vetiver grass, conifer and broadleaf species
	Medium duration, medium drawdown	1.24	1.10	30	0.0029	1.00	24.51-56.59	2.19-5.05	1.31-1.34	*B. championii,* vetiver grass, conifer and broadleaf species
	Long duration, rapid drawdown	0.94	1.10	30	0.0029	2.00	56.59	5.05	1.31-	Vetiver grass roots
	Long duration, medium drawdown	0.94	1.00	34	0.0027	2.00	59.80	5.67	1.30	Vetiver grass roots

4	Long duration, slow drawdown	1.29	0.70	32	0.0012	0.50	24.57-73.50	1.01-3.02	1.30-1.31	*Lygeum spartum,*vetiver grass and [1-5, 10, 12,15-17, 21, 23, 27, 29 and 30]
5	Short duration, rapid drawdown	1.22	1.55	27	0.0051	1.00	19.68-46.41	2.82-6.66	1.30-1.31	*B. championii,* vetiver grass, conifer and broadleaf species
	Short duration, medium drawdown	1.24	1.55	28	0.0053	1.00	19.68-46.41	3.04-7.17	1.30-1.31	*B. championii,* vetiver grass, conifer and broadleaf species
	Short duration, slow drawdown	1.27	1.15	24	0.0025	1.00	23.82-55.15	1.49-3.45	1.30-1.32	*B. championii,* vetiver grass, conifer and broadleaf species
	Medium duration, rapid drawdown	1.13	1.70	25	0.0057	1.50	43.99	6.52	1.31	Vetiver grass roots
	Medium duration, medium drawdown	1.17	1.50	24	0.0042	1.50	47.30	5.02	1.31	Vetiver grass roots
	Long duration, rapid drawdown	1.07	1.60	29	0.0058	2.00	45.56	8.04	1.30	Vetiver grass roots
	Long duration, medium drawdown	1.08	1.65	26	0.0056	2.00	44.76	6.75	1.30	Vetiver grass roots
	Long duration, slow drawdown	1.23	2.0	30	0.0094	1.00	20.20	5.96	1.30	Conifer and broadleaf species
6	Short duration, rapid drawdown	1.13	2.0	15	0.0047	2.00	40.05	2.96	1.31	Vetiver grass roots
	Short duration, medium drawdown	1.18	1.65	16	0.0034	2.00	44.76	2.56	1.30	Vetiver grass roots
	Medium duration, rapid drawdown	1.06	1.80	22	0.0056	2.50	42.56	5.47	1.30	Vetiver grass roots
	Medium duration, medium drawdown	1.12	1.70	25	0.0057	2.00	43.99	6.52	1.30	Vetiver grass roots

6	Long duration, rapid drawdown	1.01	Note: There is no suitable model for tensile strength and additional cohesion from literature for a root reinforcing deeper than 2.5 m.							
	Long duration, medium drawdown	0.78	Note: There is no suitable model for tensile strength and additional cohesion from literature for a root reinforcing deeper than 2.5 m.							
7	Short duration, rapid drawdown	1.13	1.65	20	0.0043	2.00	44.76	4.00	1.30	Vetiver grass roots
	Short duration, medium drawdown	1.15	1.60	22	0.0044	2.00	45.56	4.63	1.30	Vetiver grass roots
	Medium duration, rapid drawdown	1.03	Note: There is no suitable model for tensile strength and additional cohesion from literature for a root reinforcing deeper than 2.5 m.							
	Medium duration, medium drawdown	1.08	1.75	28	0.0067	2.50	43.26	8.52	1.30	Vetiver grass roots
	Long duration, medium drawdown	0.97	Note: There is no suitable model for tensile strength and additional cohesion from literature for a root reinforcing deeper than 2.5 m.							
8	Short duration, rapid drawdown	1.08	1.70	28	0.0064	2.50	44.00	8.17	1.30	Vetiver grass roots
	Short duration, medium drawdown	1.10	1.70	28	0.0064	2.50	44.00	8.17	1.30	Vetiver grass roots
	Medium duration, rapid drawdown	1.00	Note: There is no suitable model for tensile strength and additional cohesion from literature for a root reinforcing deeper than 2.5 m.							
	Medium duration, medium drawdown	1.03	Note: There is no suitable model for tensile strength and additional cohesion from literature for a root reinforcing deeper than 2.5 m.							
	Long duration, medium drawdown	0.70	Note: There is no suitable model for tensile strength and additional cohesion from literature for a root reinforcing deeper than 2.5 m.							
9-10	All	0.87-1.06	Note: There is no suitable model for tensile strength and additional cohesion from literature for a root reinforcing deeper than 2.5 m.							

Table H.5: Stabilizing root functional traits for gravel banks, 1:3 slope angle

			Root Functional Traits				**Root Strength Properties**			
Bank height (m)	**Drawdown rate**	**FOS without roots**	**Root Diameter (mm)**	**No. of roots per sq. m**	**RAR (%)**	**Root Length (m)**	T_r **(MPa)**	C_r **(kPa)**	**FOS with roots**	**Suitable vegetation type [Ref. no. from guideline doc., Appendix G]**
1	All	1.17-1.20	0.90	25	0.0016	0.20	12.31-38.84	0.56-1.77	1.30-1.44	*Alnus* roots, *Spanish Broom*, [1-12, 14-18, 21-27, 29 and 30]
2	All	1.19-1.20	1.10	20	0.0019	0.40	39.02-42.86	1.70-1.87	1.30-1.33	Grass, Shrubs, [1-3, 17 and 29]
3	All	1.19-1.20	1.10	20	0.0019	0.40	39.02-42.86	1.70-1.87	1.30-1.31	Grass, Shrub, [1-3, 17 and 29]
4	All	1.17-1.20	1.30	28	0.0037	0.50	31.51-33.64	3.77-4.02	1.32	Grass, Shrub, [1-3, 17 and 27-30]
5-10	All	1.17-1.20	1.20	24-26	0.0030	1.50	53.81	4.03-4.73	1.30-1.47	Vetiver grass

APPENDIX I

Calculations for the determination of flood duration and drawdown rate, using the HRU design storm and synthetic unit hydrograph method, for the Crocodile and Sabie-Sand river systems

CALCULATIONS: FLOOD DURATION AND DRAWDOWN RATE FOR THE CROCODILE RIVER

Determination of the 1-hour unit hydrograph for the catchment:

The catchment occurs in veld type zone number 8: Bushveld, according to Hydrological Research Unit (1972). The dimensionless 1-hour unit hydrograph for this zone is displayed below.

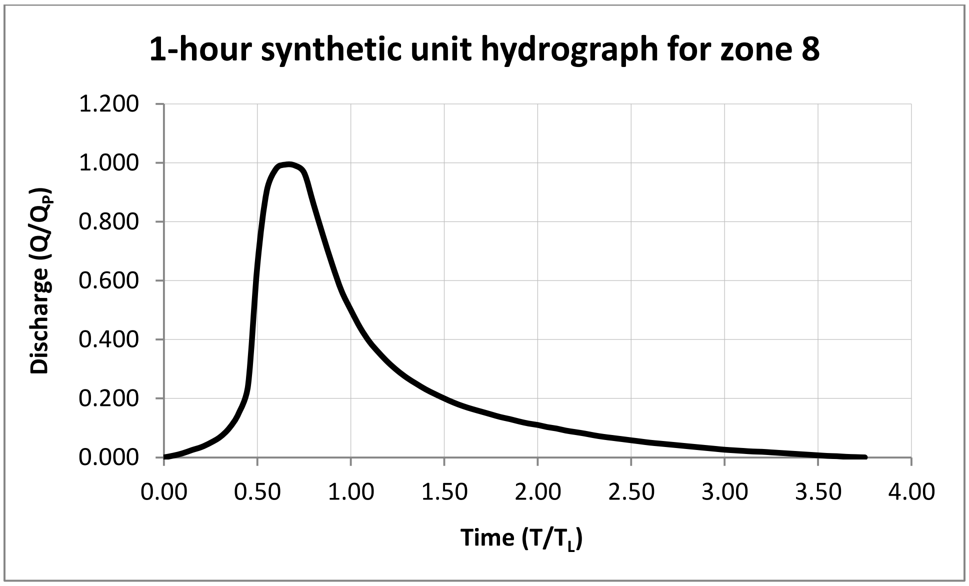

Figure I1: Synthetic unit hydrograph (after the Hydrological Research Unit, 1972)

C_T is taken as: 0.19 for zone 8 (Hydrological Research Unit, 1972)

L is taken as: 270 km (Moolman et al., 2002)

L_C is taken as: 160 km (Moolman, et al., 2002)

S is determined from equation 4.8.

$H_{0.85L}$ is taken as: 1600 m

$H_{0.1L}$ is taken as: 200 m

Equation 4.8: $S = \frac{1600-200}{0.75(270000)}$ and so S is taken as: <u>6.91x10^{-3}</u>

Equation 4.7: $T_L = 0.19 \times (\frac{270\times160}{\sqrt{6.91E-3}})^{0.36}$ and so T_L is taken as: <u>21.7 hours</u>

The information on stream length and elevation is crucial and is as taken from Figure I2 below:

Note: The catchment boundary is adjusted to account for only the proportion of catchment above the point of interest.

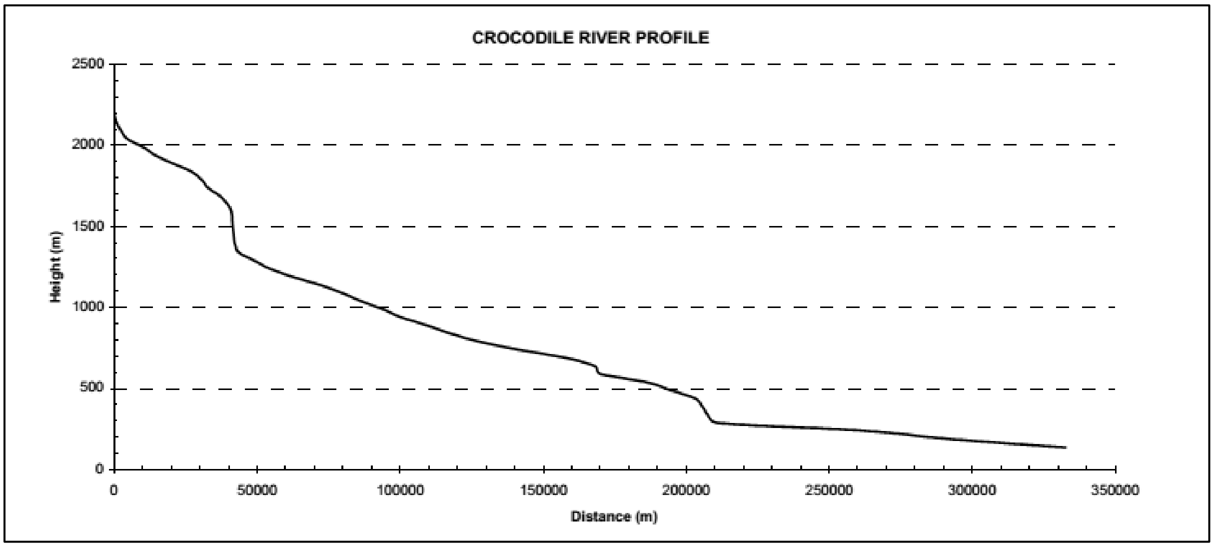

Figure I2: Crocodile River stream profile (after Moolman et al., 2002)

The peak discharge is as calculated from equation 4.9.

K_U is obtained as: 0.367 for zone 8 (Hydrological Research Unit, 1972)

A is approximated as: 10 200 km^2 (River Health Programme, 2001)

Equation 4.9: $Q_P = 0.367 \times \frac{10200}{21.7}$ and so Q_P is taken as: 172.5 m^3/s

The synthetic unit hydrograph above is then made dimensional by multiplying each x-ordinate by T_L and each y-ordinate by Q_P. The resulting dimensional 1-hour unit hydrograph for the catchment is as shown in Figure I3.

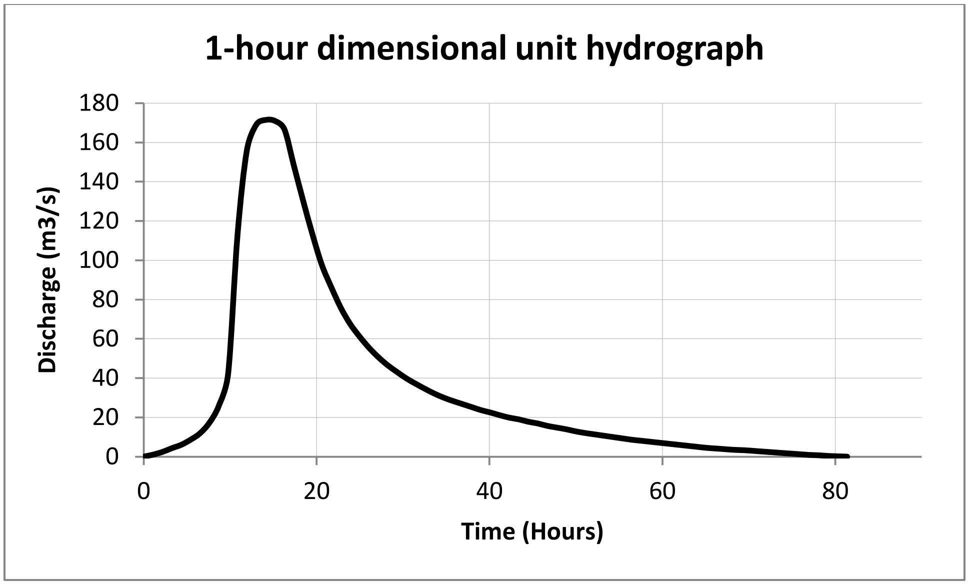

Figure I3: Dimensional 1-hour unit hydrograph, obtained from HRU method

Determination of the design storm for the catchment:

For this example a recurrence interval of 50 years is selected and a storm duration of 1 hour is used.

In order to use Figure 4.4 to determine the storm point rainfall the region is selected as being coastal and the mean annual precipitation is selected from Figure 4.5 as 900 mm. Reading from the coaxial plot in Figure 4.4 the storm point rainfall is: 80 mm. The rainfall intensity is then 80/1 = 80 mm/h.

Figure 4.6 is then used to determine the average rainfall intensity over the catchment area. Using the catchment area and the storm duration selected, the reduction factor may be taken as 40% so that the average rainfall intensity is 80 x 0.4 = 32 mm/h.

Finally the storm losses are determined from Figure 4.7 in order to calculate the total excess rainfall that occurs and thus that which becomes direct runoff. The veld zone and catchment area is used to determine the percentage of storm runoff, which in this case is 9% and this means that the total effective rainfall for the design storm event is 32 x 0.09 = 2.88 mm/h.

Due to the fact that the storm duration is 1 hour, there is no need to utilise the S-curve technique to change the duration of the unit hydrograph, each y-ordinate of the dimensional unit hydrograph in Figure I3 can simply be multiplied by the excess rainfall intensity of 2.88 mm/h in order to obtain the storm hydrograph. The flood hydrograph is shown in Figure I4.

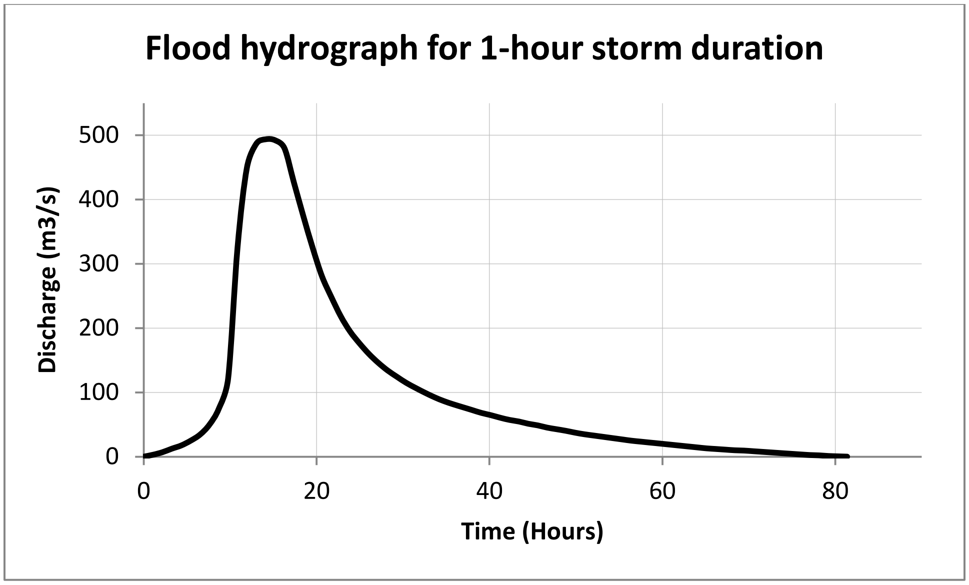

Figure I4: Flood hydrograph for point of interest on Crocodile River, 50 year return period and 1-hour storm duration

If the worst flood hydrograph for the given return period is required then the above design storm method must be repeated for two more storm durations in order to determine the worst storm duration and effective rainfall which may then be combined with the same duration unit hydrograph (obtained from the S-curve method being applied to the 1-hour unit hydrograph).

Determination of the flood duration and drawdown rate using the relevant rating curve with the flood hydrograph:

Figure I5 represents the rating curve for the Crocodile River profile.

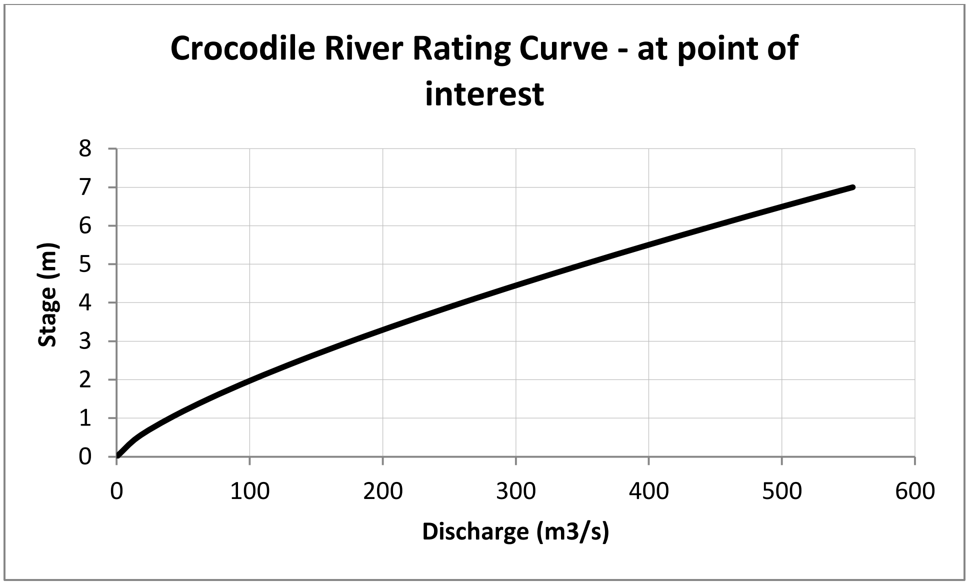

Figure I5: Hypothetical rating curve for point of interest on Crocodile River

Using the flood hydrograph in Figure I4 in conjunction with the rating curve above provides a means for determining the rate of rise and drawdown at the point of interest. From the hydrograph the rising limb of the flood begins at approximately 9.8 hours with a flow of 121.70 m^3/s, and ends at approximately 14.1 hours with a flow of 493.80 m^3/s. From the rating curve this means that in 4.3 hours the water level rises from 2.20 m to 6.30 m, and as such the rate of rise is 0.95 m/h. The steepest section of the falling limb of the hydrograph ends at 23.9 hours with a flow rate of 195.70 m^3/s, and from the rating curve the corresponding stage is 3.10 m. As such the water level falls from 6.30 m to 3.10 m in 9.8 hours and thus the drawdown rate is 0.33 m/h.

CALCULATIONS: FLOOD DURATION AND DRAWDOWN RATE FOR THE SABIE-SAND RIVER

Determination of the 1-hour unit hydrograph for the catchment:

The catchment occurs in veld type zone number 8: Bushveld, according to Hydrological Research Unit (1972). The dimensionless 1-hour unit hydrograph for this zone is displayed below.

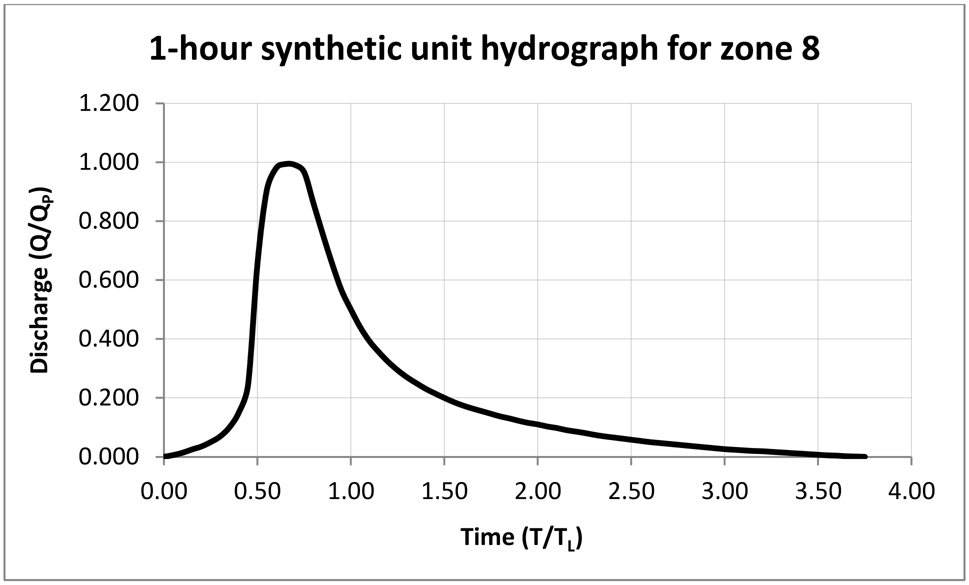

Figure I6: Synthetic unit hydrograph (after the Hydrological Research Unit, 1972)

The lag time for the catchment is calculated as per equation 4.7.

C_T is taken as: 0.19 for zone 8 (Hydrological Research Unit, 1972)

L is taken as: 47.5 km (Moolman et al., 2002)

L_C is taken as: 19 km (Moolman, et al., 2002)

S is determined from equation 4.8.

$H_{0.85L}$ is taken as: 1150 m

$H_{0.1L}$ is taken as: 800 m

Equation 4.8: $S = \frac{1150-800}{0.75(47500)}$ and so S is taken as: <u>9.82x10^{-3}</u>

Equation 4.7: $T_L = 0.19 \times (\frac{47.5\times 19}{\sqrt{9.82E-3}})^{0.36}$ and so T_L is taken as: <u>11.6 hours</u>

The information on stream length and elevation is as taken from the Figure I7:

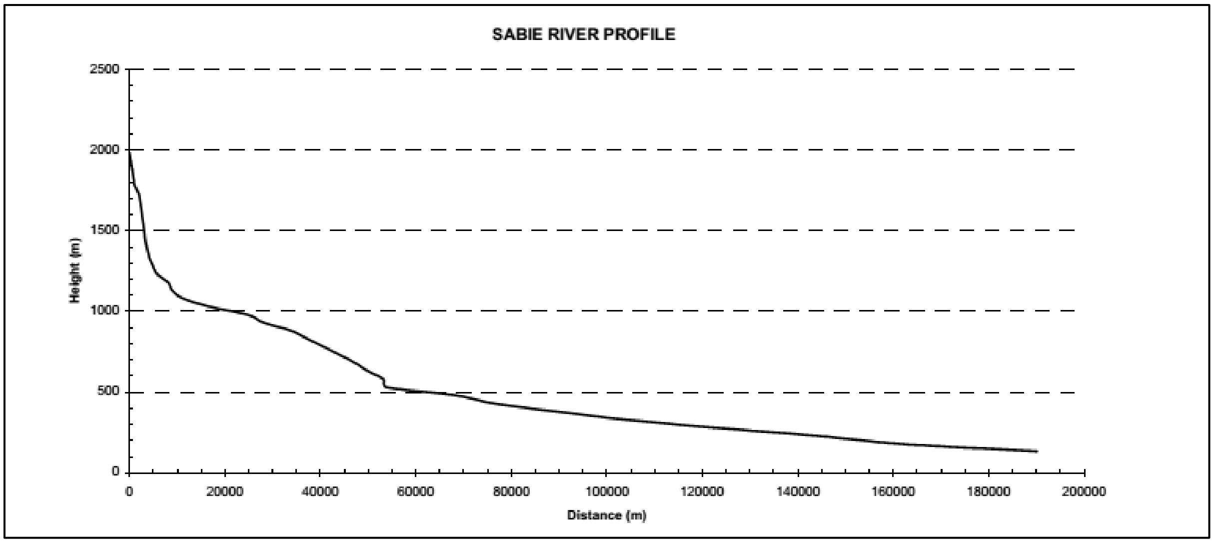

Figure I7: Sabie River stream profile (after Moolman et al., 2002)

The peak discharge is as calculated from equation 4.9.

K_U is obtained as: 0.367 for zone 8 (Hydrological Research Unit, 1972)

A is approximated as: 820 km^2 (River Health Programme, 2001)

Equation 4.9: $Q_P = 0.367 \times \frac{820}{11.6}$ and so Q_P is taken as: 25.9 m^3/s

The synthetic unit hydrograph above is then made dimensional by multiplying each x-ordinate by T_L and each y-ordinate by Q_P. The resulting dimensional 1-hour unit hydrograph for the catchment is as shown in Figure I8.

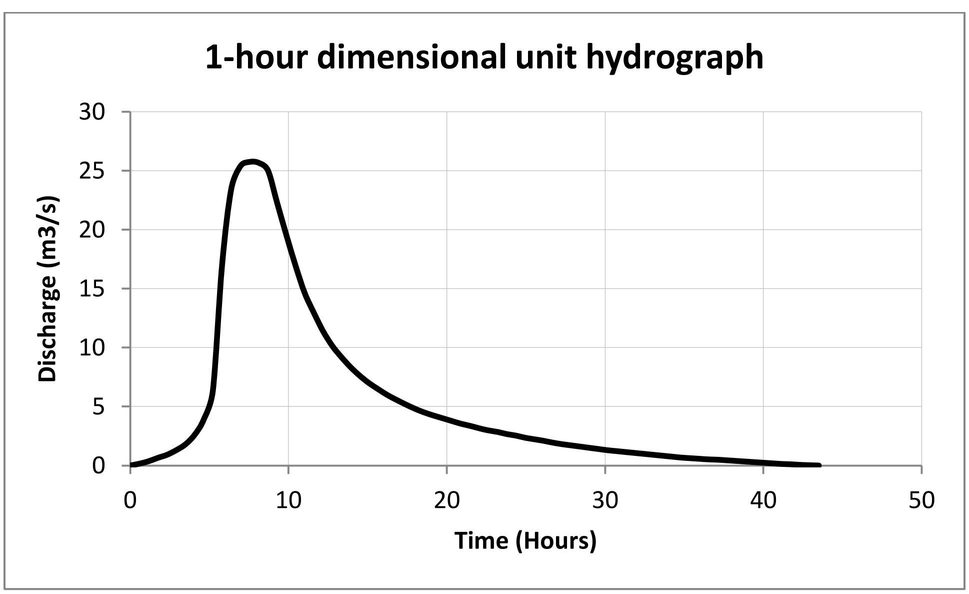

Figure I8: Dimensional 1-hour unit hydrograph, obtained from HRU method

Determination of the design storm for the catchment:

For this example a recurrence interval of 100 years is selected and again a storm duration of 1 hour is used.

In order to use Figure 4.4 to determine the storm point rainfall the region is selected as being inland and the mean annual precipitation is selected from Figure 4.5 as 700 mm. Reading from the coaxial plot in Figure 4.4 the storm point rainfall is 105 mm. The rainfall intensity is then 105/1 = 105 mm/h.

Figure 4.6 is then used to determine the average rainfall intensity over the catchment area. Using the catchment area and the storm duration selected, the reduction factor may be taken as 72% so that the average rainfall intensity is 105 x 0.72 = 75.6 mm/h.

Finally the storm losses are determined from Figure 4.7 in order to calculate the total excess rainfall that occurs and thus that which becomes direct runoff. The veld zone and catchment area is used to determine the percentage of storm runoff, which in this case is 19% and this means that the total effective rainfall for the design storm event is 75.6 x0.19 = 14.4 mm/h.

Due to the fact that the storm duration is 1 hour, there is no need to utilise the S-curve technique to change the duration of the unit hydrograph, each y-ordinate of the dimensional unit hydrograph in Figure I8 can simply be multiplied by the excess rainfall intensity of 14.4 mm/h in order to obtain the storm hydrograph. The flood hydrograph is shown in Figure I9.

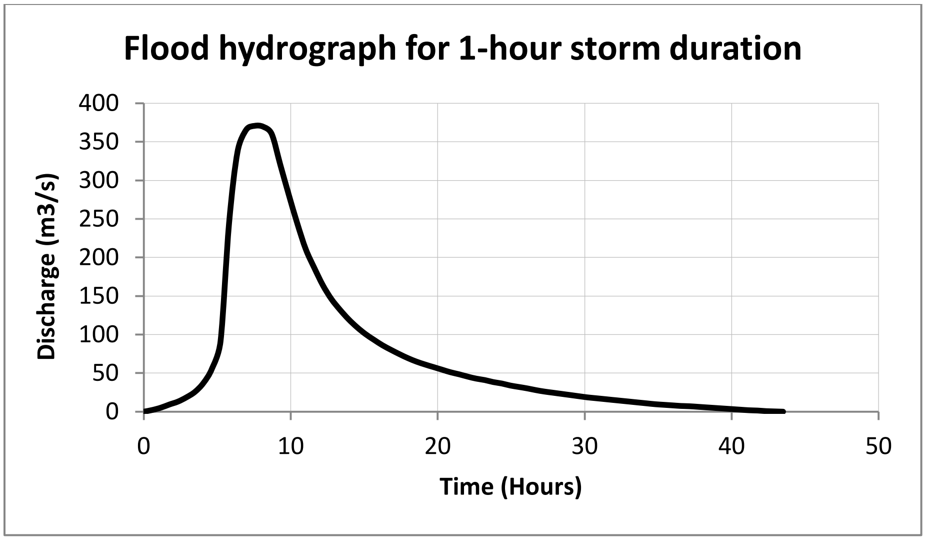

Figure I9: Flood hydrograph for point of interest on Sabie River, 100 year return period and 1-hour storm duration

As with the previous example, a 1-hour storm may not be the storm duration that produces the worst flood hydrograph for a 100 year return period at this point of interest. If the worst storm duration is required then the same procedure as described for the previous example may be carried out.

Determination of the flood duration and drawdown rate using the relevant rating curve with the flood hydrograph:

Figure I10 represents the rating curve for the Sabie-Sand River

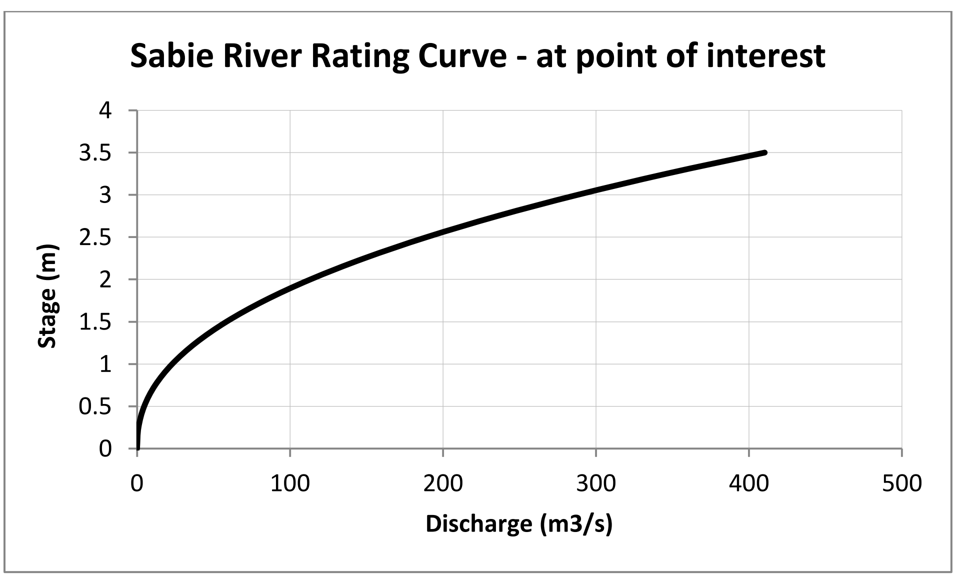

Figure I10: Hypothetical rating curve for point of interest on Sabie River

Using the flood hydrograph in Figure I9 in conjunction with the rating curve above provides a means for determining the rate of rise and drawdown at the point of interest. From the hydrograph the rising limb of the flood begins at approximately 4.6 hours with a flow of 55.90 m^3/s, and ends at approximately 7 hours with a flow of 365.50 m^3/s. From the rating curve this means that in 2.4 hours the water level rises from 1.4 m to 3.3 m, and as such the rate of rise is 0.79 m/h. The steepest section of the falling limb of the hydrograph ends at 15.7 hours with a flow rate of 93.2 m^3/s, and from the rating curve the corresponding stage is 1.7 m. As such the water level falls from 3.3 m to 1.7 m in 8.7 hours and thus the drawdown rate is 0.18 m/h.